



**Characterization of Synapsin, Tubulin-Binding
Chaperone E-like, And Their Putative Interactions With
Synapse Associated Protein Of 47 kDa In
*Drosophila melanogaster***

Dissertation zur Erlangung des
naturwissenschaftlichen Doktorgrades
der Bayerischen Julius-Maximilians-Universität Würzburg

vorgelegt von

Tulip Nuwal

aus Indore, India

Würzburg, 2010

Eingereicht am:

Mitglieder der Promotionskommission:

Vorsitzender: Prof. Dr. Thomas Dandekar

Gutachter: Prof. Dr. Erich Buchner

Gutachter: Prof. Dr. Georg Krohne

Tag des Promotionskolloquiums:

Doktorurkunde ausgehändigt am:

INDEX

Chapter	Page
1. INTRODUCTION	9
1.1 Cytoskeletal architecture of the neuron	10
1.1.1 Microtubules	10
1.1.1.1 GTP cap model for dynamic instability	11
1.1.1.2 MT destabilizing proteins	11
1.1.1.3 MT stabilizing proteins	13
1.1.1.4 Effects of specific drugs on MT stability	13
1.1.1.5 Motor proteins associated with MT	14
1.1.1.6 Chaperone mediated MT formation	15
1.1.1.6.A Cofactor A (TBCE)	16
1.1.1.6.B Cofactor B (TBCEB)	16
1.1.1.6.C Cofactor C (TBCEC)	16
1.1.1.6.D Cofactor D (TBCECD)	16
1.1.1.6.E Cofactor E (TBCEE)	17
1.2 TBCE plays a role in neurodegenerative disorders	17
1.2.1 Mutation in human <i>Tbce</i> causes hypoparathyroidism, mental retardation and facial dysmorphism and Kenny–Caffey syndrome symptoms	17
1.2.2 Mutation of mouse <i>Tbce</i> causes progressive motor neuropathy (<i>pmn</i>) symptoms	18
1.3 Yeast <i>Tbce</i> (<i>pac2</i>)	20
1.4 <i>Drosophila Tbce</i> gene (<i>CG7861</i>)	20
1.4.1 <i>Drosophila</i> TBCE is essential for MT formation and synaptic transmission at the NMJ synapses	21
1.5 Tubulin binding chaperone E-Like (E-like or TBCEL)	22
1.5.1 <i>In vitro</i> and <i>in vivo</i> functions of TBCEL	23

1.6 Molecular architecture of the synapse	24
1.6.1 Electrical synapse	24
1.6.2 Chemical synapse	25
1.7 Synapsins	29
1.7.1 The <i>Syn</i> gene locus is highly conserved in different species	29
1.7.2 Structural analysis of synapsin	31
1.7.3 Biochemical properties of vertebrate synapsins	31
1.7.4 Role of vertebrate synapsins at the synapse	32
1.7.4.1 Phosphorylation dependent interaction and function of vertebrate synapsin	33
1.7.4.2 Phosphorylation dependent interaction of vertebrate synapsins with synaptic vesicles and components of the cytoskeleton	34
1.7.5 Other PTMs in vertebrate synapsin	37
1.7.6 Analysis of <i>Synapsin</i> null mutants	38
1.7.7 Synapsin related human disorders	38
1.7.8 <i>Drosophila</i> synapsin	39
1.8 Synapse associate protein of 47 kDa (SAP47)	42
1.9 Tools used in investigating genes and proteins of <i>Drosophila</i>	44
1.9.1 Gal4-UAS system for transgene expression	44
1.9.2 Microarray technique for transcriptome analysis	45
1.9.3 Mass spectrometry for analysis of posttranslational modifications (PTMs)	46
2. MATERIALS	49
2.1 Fly rearing	49
2.2 Fly strains	49
2.3 Buffers and reagents	50
2.3.1 DNA and RNA analysis	50
2.3.1.1 Primers	50
2.3.1.2 Reagents for RT-PCR	51

2.3.2 Protein analysis	51
2.3.2.1 SDS-PAGE and Western blotting	51
2.3.2.2 Buffers and reagents for Blum silver staining (modified for mass spectrometry)	53
2.3.2.3 Buffers and reagents for 2D-PAGE	54
2.3.2.4 Buffers and reagents for Native PAGE	55
2.3.2.5 Buffer and reagents for Enzyme Linked Immunosorbent Assay (ELISA)	55
2.3.2.6 Buffers and reagents for Immunohistochemistry	56
2.4 Proteins and Inhibitors	57
2.5 Ladders	57
2.6 Antibodies	58
2.7 Kits	58
3. METHODS	59
3.1 Protein analysis	59
3.1.1 1D-SDS-PAGE analysis	59
3.1.1.1 Non-pre-cast SDS-PAGE system	59
3.1.1.2 Pre-cast SDS-PAGE (from Invitrogen)	60
3.1.2 Western blotting	60
3.1.2.1 Wet blotting	61
3.1.2.2 Semi-dry blotting	62
3.1.3 Coomassie staining	63
3.1.4 Silver staining	64
3.1.5 2D-SDS-PAGE analysis	65
3.1.5.1 Sample preparation for 2D-SDS-PAGE	65
3.1.5.2 First dimension: Isoelectric focussing	66
3.1.5.3 Second dimension: SDS-PAGE	66
3.1.6 Native PAGE analysis	67
3.1.6.1 Blue native-PAGE	67
3.1.6.2 Blue native-SDS-PAGE	68

3.2	Immunochemistry procedures	69
3.2.1	Immunoprecipitation	69
3.2.1.1	Small scale lysate preparation	70
3.2.1.2	Large scale lysate preparation	70
3.2.1.2.1	IP protocol without cross-linking of antibody to beads	71
3.2.1.2.2	IP protocol with cross-linking of antibody to beads	71
3.2.2	Enzyme Linked Immunosorbent Assay (ELISA)	72
3.2.3	Cryosections and dissections of adult <i>Drosophila</i> tissues	73
3.3	Peptide analysis by nano-LC-ESI-MS/MS	74
3.3.1	In-gel trypsin digestion of proteins for MS analysis	74
3.3.2	In-gel alkaline phosphatase treatment for MS analysis	75
3.4	Generation of anti-TBCEL antiserum	77
3.4.1	Cloning of <i>Tbcel</i> cDNA in pET expression vector	77
3.4.2	Expression of His-tagged TBCEL in <i>E.coli</i> and immunisation of Guinea pigs for antiserum production	78
3.5	DNA analysis	78
3.5.1	Isolation and purification of genomic DNA	78
3.5.1.1	Large scale genomic DNA isolation	78
3.5.1.2	Single fly genomic DNA isolation	79
3.5.2	Polymerase chain reaction	79
3.5.3	PCR product purification and gel extraction	80
3.6	RNA analysis	80
3.6.1	RNA isolation	80
3.6.2	Reverse transcription	81
3.6.3	Microarray analysis	81
3.6.4	Quantitative PCR	82
3.7	Behavioural assays	84
3.7.1	Negative geotaxis	84
3.7.2	Longevity assay	84

3.7.3 Fertility assay	84
4. RESULTS	85
4.1 Analysis of SAP47 and synapsin protein interactions	85
4.1.1 Higher phospho-synapsin in <i>Sap47</i> null mutant flies	85
4.1.2 Partial rescue of synapsin phosphorylation in <i>Sap47</i> null mutants	89
4.1.3 <i>Syn</i> transcript levels in <i>Sap47^{156CS}</i> and <i>CS</i>	91
4.1.4 Investigating direct protein interactions of SAP47 and synapsin by co-immunoprecipitation experiments	92
4.1.4.1 Competitive elution of immunoprecipitated SYN	93
4.1.5 Blue-native PAGE analysis of synapsins	94
4.2 Functional interaction between <i>Sap47</i> and <i>Syn</i> genes	97
4.2.1 Generation of the <i>Sap47</i> and <i>Syn</i> double mutants <i>NS17</i> and <i>NS62</i>	97
4.3 Behavioural analysis of <i>Syn^{97CS}</i> , <i>Sap47^{156CS}</i> and double null mutants	100
4.3.1 Locomotor assays	100
4.3.2 Longevity assay	102
4.4 Characterization of synapsin PTMs	103
4.4.1 Analysis of synapsins by 2D-PAGE	103
4.4.2 IP of synapsin from head homogenate and analysis by silver staining	104
4.4.3 nano-LC-ESI-MS/MS analysis of synapsins	105
4.5 Genome wide transcript analysis of <i>Syn^{97CS}</i> , <i>Sap47^{156CS}</i> and double null mutants	114
4.6 Analysis of Tubulin binding chaperone E-Like	117
4.6.1 TBCE and TBCEL have conserved domains	117
4.6.2 Generation of anti-TBCEL antiserum	119
4.6.3 Analysis of NP4786 and G18151 P-insertion stocks	120
4.6.3.1 Transcript analysis of NP4786 stock	121
4.6.3.2 Protein analysis of NP4786 and G18151 stocks	123

4.6.4 Expression of TBCEL in <i>Drosophila</i> testes	126
4.6.4.1 Expression and localization of TBCEL in adult <i>Drosophila</i> testis	127
4.6.4.2 Overexpression of TBCEL in testis	129
4.6.4.3 Expression of gal4 in adult brain and testis of the NP enhancer trap line	131
4.6.5 Fertility assay	133
4.6.6 P-element mutagenesis of <i>Tbcel</i> gene	134
4.6.6.1 First attempt	135
4.6.6.2 Second attempt	136
5. DISCUSSION	140
5.1 Up-regulated and hyper-phosphorylated synapsin in <i>Sap47</i> null mutants	140
5.2 Functional genetic interaction between <i>Sap47</i> and <i>Syn</i> genes	142
5.3 Posttranslational modifications of synapsin and their implications	143
5.4 Whole genome microarray analysis of <i>Syn</i> ^{97CS} , <i>Sap47</i> ^{156CS} and double null mutants <i>V2</i> and <i>V3</i>	149
5.5 <i>Drosophila</i> TBCEL expression in adult testis and brain	150
5.6 P-element mutagenesis of <i>Tbcel</i> gene	154
6. SUMMARY	156
7. ZUSAMMENFASSUNG	159
8. APPENDIX	162
9. BIBLIOGRAPHY	170
10. ACKNOWLEDGEMENTS	194
11. PUBLICATIONS	195
12. CURRICULUM VITAE	196
13. ERKLÄRUNG	198

1. INTRODUCTION

In the past few decades *Drosophila melanogaster* (fruit fly) has been widely used as a model organism for investigating the nervous system, and this research has got impetus from the complete sequencing of the *Drosophila* genome (Adams et al., 2000). Generating *Drosophila* mutants by several approaches like Ethyl Methyl Sulfonate (EMS) and X-ray treatment, P-element jump-out mutagenesis for targeted gene disruption and many other techniques have elucidated the role of genes and proteins in different cellular and molecular pathways occurring in different subsets of cells in a fly. In this thesis I have used *Drosophila* as a model system for analyzing functions of synaptic proteins synapsin and SAP47, as well as a putative SAP47 interaction partner TBCE-Like which have direct or indirect role in neurotransmission.

In the nervous system of vertebrates and invertebrates several neuronal cells connect together by means of synaptic connections (chemical synapses) or physical contacts (in case of gap junctions) to faithfully transmit a signal from one part of the body to another. Neuronal cells have polarized structure and function, namely: (i) a signal input domain represented by dendrites and the cell body which receives inputs from other neurons via synaptic connections; (ii) a signal assimilation domain represented by the initial segment of the axon which integrates the several inputs into an electrical impulse; (iii) a transfer domain represented by axons transfers signals called action potentials (electrical impulses) rapidly and without loss to the terminal; (iv) finally, the nerve terminals form the transmission domain, which convert the action potential to a chemical signal by releasing neurotransmitters via a controlled exocytosis of vesicles containing chemical neurotransmitters into the synaptic cleft. The postsynaptic receptors bind to the neurotransmitters and respond to it in a way such that the downstream signal transduction can occur.

Proteins that participate in neurotransmission can be classified into two major groups:

- A. **Cytoskeletal and associated proteins.** These proteins form the inner scaffold of a neuron and provide the basis for transport of substances in retro- and anterograde directions.
- B. **Synaptic proteins (pre- and postsynaptic).** These proteins function in the regulated release (exocytosis) or uptake (endocytosis) of synaptic vesicles (presynaptic proteins) or are involved in signal transduction cascade at the postsynaptic side (postsynaptic proteins).

1.1 Cytoskeletal architecture of the neuron

The cytoskeleton determines the shape of a neuron and is responsible for the asymmetric distribution of organelles within the cytoplasm. It contains three main filamentous structures:

- A. Actin microfilaments,
- B. Neurofilaments (called intermediate filaments in non-neuronal cells), and
- C. Microtubules

The role and function of microtubules and associated proteins is discussed in detail.

1.1.1 Microtubules

Microtubules (MTs) are cytoskeletal structures made of 13 protofilaments of tandem α - and β -tubulin heterodimers. The staggered assembly of protofilaments yields a helical arrangement of tubulin heterodimers in the form of a hollow cylinder (Fig. 1). The orientation of α - and β -tubulin in the polymer confers polarity to MTs, with β -tubulin at the 'plus' end and α -tubulin at the 'minus' end. MTs play a major role in providing cell shape and division, structural conformity, flagellar movement, sperm and cellular motility and many other similar functions. In neurons, MTs serve as tracks for transporting variety of cargo in anterograde (towards the synaptic terminal) and retrograde (towards the soma) directions by motor proteins like kinesin and dynein, respectively. In axons, MTs are

uniformly oriented with their 'plus' ends directed towards the axon terminals whereas in dendrites both the orientations are observed.

MTs under *in vivo* and *in vitro* conditions, undergo continuous growth and shrinkage from the plus and minus ends, respectively (Fig. 1). This property of MTs is referred to as dynamic instability (Desai and Mitchison, 1997). The non-equilibrium nature of MT dynamics is dependent on several tubulin and MT binding proteins and also on the hydrolysis state of the bound GTP (Mitchison and Kirschner, 1984a, b).

1.1.1.1 GTP cap model for dynamic instability

Mitchison et al., in 1984 proposed that MTs are constantly growing and shrinking and this is due to the hydrolysis or uptake of GTP molecules. Each tubulin monomer at the either end can bind to a single molecule of GTP. The GTP bound to α -tubulin does not hydrolyze whereas the GTP bound to β -tubulin is hydrolyzed to GDP and this GDP is later exchanged for GTP to confer stability (formation of GTP cap) or continue the growth of MTs. The MT end with exposed GDP bound tubulin subunits is highly unstable and is depolymerized at least 100 times faster than GTP bound tubulin end, also known as the GTP cap. The presence and absence of this 'cap' determines the polymerization and depolymerization rates of MTs. The stability of MTs is also dependent on several cofactors and proteins which regulate the capping process or the assembly/disassembly of tubulin subunits (McNally, 1996; Desai and Mitchison, 1997).

The dynamics of MTs are largely governed by the presence of two classes of proteins namely:

1.1.1.2 MT destabilizing proteins

These are a family of proteins which promote disassembly of intact microtubules under *in vivo* and *in vitro* conditions (Cassimeris and Spittle, 2001). These proteins have a regulatory role on MT dynamics by mechanisms which include inhibition of MT formation, by quenching of nascent tubulin heterodimers or by promoting disassembly of

already formed MTs. For example, Op18/stathmin proteins cause hydrolysis of GTP at the plus end and promote formation of unstable GDP-MTs and in the case of XKCM1 (Xenopus kinesin-related protein) and X/mKIF2 (Xenopus or mouse kinesin-related protein with high similarity to XKCM1) the destabilization is caused by binding and altering the ends of the MTs (Belmont et al., 1996; Belmont and Mitchison, 1996; Walczak and Mitchison, 1996; Walczak et al., 1996; Desai et al., 1999; Kline-Smith and Walczak, 2002). MTs are also destabilized by the action of AAA ATPases like katanins, which function by assembling on MT surface and then undergoing conformational change by ATP hydrolysis and phosphorylation subsequently destabilizing the tubulins in the protofilaments (Quarmby, 2000).

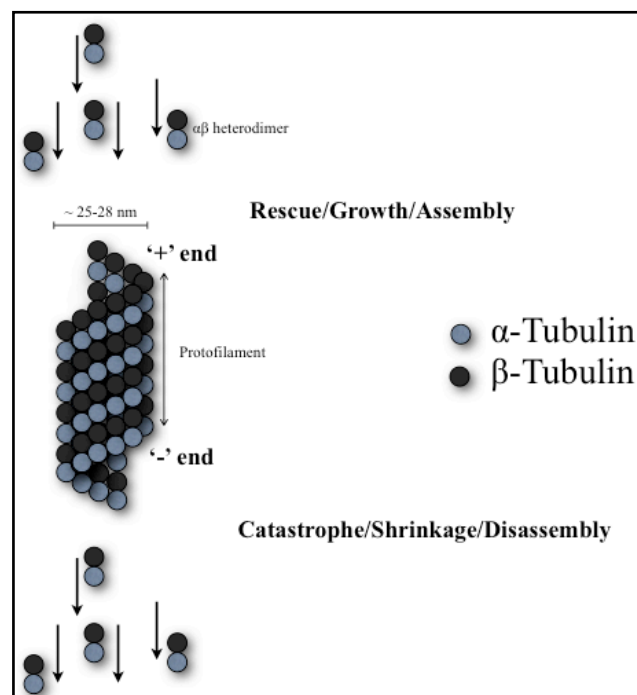


Fig. 1: Microtubule structure and dynamics: The heterodimers of α - and β -tubulin form 13 protofilaments which form the microtubule. The growth is faster at the ‘plus’ end relative to the ‘minus’ end (compiled from Nogales, 2000).

1.1.1.3 MT stabilizing proteins

Microtubule stabilizing proteins also known as the microtubule associated proteins (MAPs), are a large family of proteins that have functional and regulatory roles in MT assembly and disassembly (Maccioni, 1986; Rose et al., 1993; Schoenfeld and Obar, 1994). MAPs are involved in stabilizing and controlling MT dynamics by interacting with MTs via the C-terminal tubulin domains. MAPs play a central role in forming and stabilizing interactions of MT with other cytoskeletal components like actin (Griffith and Pollard, 1978; Margolis and Wilson, 1978; Margolis et al., 1978; Danowski, 1989; Cross et al., 1993). The MAPs family is comprised of MAP-1(A to C), MAP-2 and 2C, MAP-4 and tau.

1.1.1.4 Effects of specific drugs on microtubule stability

- MT polymerization inhibition: Drugs like colchicine, colcemid, and nocadazole inhibit polymerization by binding to tubulin and preventing its addition to the plus ends.
- MT depolymerization: Drugs like vinblastine and vincristine aggregate tubulin and lead to microtubule depolymerization.
- MT stabilization: Drugs like taxol, epothilone and tiscodermolide stabilizes microtubules by binding to MT polymer.

1.1.1.5 Motor proteins associated with MTs

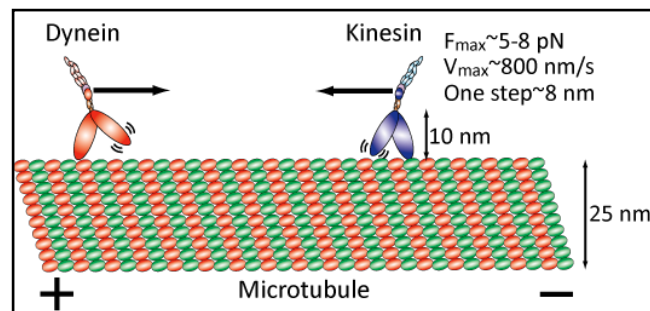


Fig. 2: Motor proteins: Kinesin and dynein move along the MTs accompanied with hydrolysis of ATP. The directed motion of both the proteins is shown. (Image source: <http://www.ksys.me.kyoto-u.ac.jp/ry/e/index.php?Research>, with permission from Ryuji Yokokawa, (Sheetz et al., 1987; Vale, 1987; Yokokawa, 2004; Yokokawa et al., 2008))

There are two motor proteins associated with MTs: (1) The kinesins transport the cargo towards the plus end, for example they transfer synaptic vesicle proteins and precursors from cell body to axon terminals or transfer receptors to dendrite terminals (anterograde transport)(Vale et al., 1985a; Okada et al., 1995; Setou et al., 2000; Zhao et al., 2001; Wong et al., 2002; Guillaud et al., 2003). (2) The dyneins transport the axonal cargo from peripheral arborizations to the cell body (retrograde transport)(Vale et al., 1985b; Schnapp et al., 1986; Vale, 1987). Both these proteins have head regions that are ATPase motors that bind to MTs and ATP (Vale et al., 1985a; Porter et al., 1987). The tail domain binds the cargo (organelle). ATP hydrolysis is needed for both binding and movement (Porter et al., 1987) (Fig. 2).

Apart from the different proteins mentioned in 1.1.1.2, 1.1.1.3 and 1.1.1.5 which alter the state and dynamics of MTs there is another group of proteins known as the MT associated cofactors or chaperones. These proteins function by binding and stabilizing the monomers or the heterodimers of tubulin thus regulating the rate of MT formation.

1.1.1.6 Chaperone mediated microtubule formation

First step in the proper folding of nascent tubulin involves the interaction with prefoldin. Prefoldin is a heterohexameric chaperone that captures nascent tubulin and actin and transfers them to the cytosolic chaperonin (CCT or c-cpn)(Lewis et al., 1996; Geissler et al., 1998; Vainberg et al., 1998).

Chaperonin in an ATP dependent manner facilitates the proper folding and formation of tertiary structure of α - and β -tubulin subunits (Gao et al., 1992; Gao et al., 1993; Gao et al., 1994; Kubota et al., 1994). The properly folded tubulin subunits bind to a series of tubulin binding cofactors (TBCE to TBCE). The β -tubulins bind to TBCD or to TBCE and the α -tubulins bind to TBCE or TBCB. The properly folded and stabilized tubulin monomers are then joined together by a complex formation between TBCE/ α -tubulin and TBCD/ β -tubulin. Finally, the heterodimers of α - and β -tubulins are released in the presence of TBCC (Lewis et al., 1997)(Fig. 3).

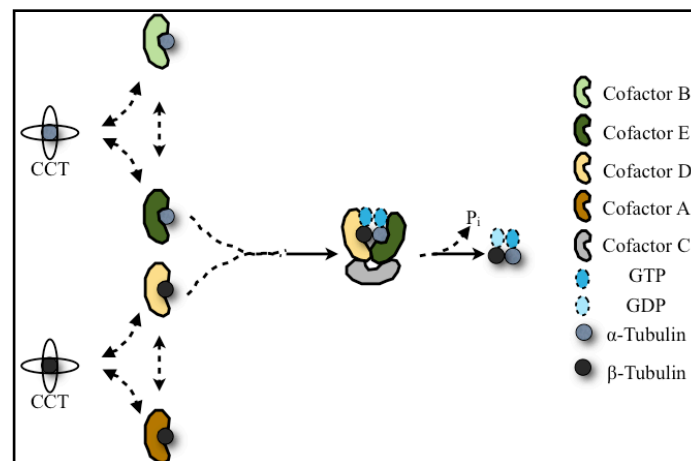


Fig. 3: Chaperonin (CCT) and cofactors mediated α - and β -tubulin folding. The interaction with chaperonin is ATP-dependent. Post-chaperonin quasi-stable polypeptide is acted upon by several chaperones to produce stable $\alpha\beta$ heterodimers in a GTP dependent manner (modified from Tian et al., 1996; Lewis et al., 1997).

1.1.1.6.A Cofactor A (TBCA)

TBCA is a 38-40 kDa protein that exists in a monomeric and at times partially dimeric state. It was first discovered in bovine testes and subsequently in pig and human testes (Gao et al., 1994; Melki et al., 1996). TBCA binds to β -tubulin under *in vitro* and *in vivo* conditions (Campo et al., 1994). In *S. pombe*, TBCA is required for growth, polarity and stability of MTs (Radcliffe et al., 2000b). Studies done in mouse have shown that TBCA is highly enriched in testis tissues and is involved in β -tubulin processing during spermatogenesis (Fanarraga et al., 1999).

1.1.1.6.B Cofactor B (TBCB)

TBCB is a 38 kDa protein which was first isolated from bovine testes (Lewis et al., 1997; Tian et al., 1997). TBCB binds to α -tubulin under *in vivo* and *in vitro* conditions (Feierbach et al., 1999; Radcliffe et al., 2000a; Radcliffe et al., 2000b). TBCB has a cytoplasmic linker (CLIP-170) domain that is also present in most of the MAPs and mediates the interaction with MTs (Lewis et al., 1997; Feierbach et al., 1999).

1.1.1.6.C Cofactor C (TBCC)

TBCC binds to TBCD/TBCE/ α - and β -tubulin heterodimer complex and releases $\alpha\beta$ tubulin heterodimers from the complex (Zabala and Cowan, 1992). TBCC is a 40 kDa protein and functions as a quality controller in the MT polymerization pathway (Lewis et al., 1996; Tian et al., 1996).

1.1.1.6.D Cofactor D (TBCD)

TBCD is a 300 kDa dimeric protein associated with β -tubulin (Zabala and Cowan, 1992; Fontalba et al., 1993; Tian et al., 1996; Lewis et al., 1997). TBCD has high affinity for β -tubulin and hence under *in vivo* and *in vitro* conditions it specifically binds to β -tubulin in the tubulin heterodimer and disrupts the dimer and subsequently the MT. Thus, TBCD is also termed as a MT destabilizing protein (Martin et al., 2000). The binding of

TBCD to β -tubulin is regulated by proteins of the Arl family which are ADP ribosylation factors. These proteins prevent the formation of a TBCD- β -tubulin complex by preventing GTP hydrolysis required for this reaction (Fontalba et al., 1993).

1.1.1.6.E Cofactor E (TBCE)

TBCE is a 60 kDa protein that binds to α -tubulin under *in vivo* and *in vitro* conditions (Lewis et al., 1996; Tian et al., 1996). TBCE has three conserved domains: a glycine rich cytoskeletal associated protein domain CAP-Gly; a leucine-rich protein-protein interaction domain LRR; and an ubiquitin-like domain UBL (Parvari et al., 2002; Grynberg et al., 2003; Bartolini et al., 2005). It is largely present in the cytosolic fraction of spinal cord and brain tissue homogenates but is also observed in crude membrane fractions (Bhamidipati et al., 2000; Tian et al., 2006; Schaefer et al., 2007). Overexpression of TBCE leads to disruption of MTs by binding to the α -tubulin subunits and altering the conformation of the $\alpha\beta$ -tubulin heterodimer (Bhamidipati et al., 2000).

1.2 TBCE plays a role in neurodegenerative disorders

1.2.1 Mutation in human *Tbce* causes hypoparathyroidism, mental retardation and facial dysmorphism (HRD) and Kenny–Caffey syndrome (AR-KCS) symptoms

Parvari et al (2002) have reported that a 12 bp mutation in human homologue of *Tbce* gene which maps to chromosome 1q42.3 causes autosomal recessive disorder HRD (hypoparathyroidism, mental retardation and facial dysmorphism)/Sanjad-Sakati/Richardson-Kirk syndrome and autosomal recessive Kenny-Caffey syndrome (AR-KCS) in mostly Middle Eastern populations (Richardson and Kirk, 1990; Richardson and Kirk, 1991; Sanjad et al., 1991; Hershkovitz et al., 1995). It was observed that the amount of α -tubulin incorporated into MTs was lowered in diseased cells and the polarity and the density of the MTs was irregular (Parvari et al., 2002) (Fig. 4).

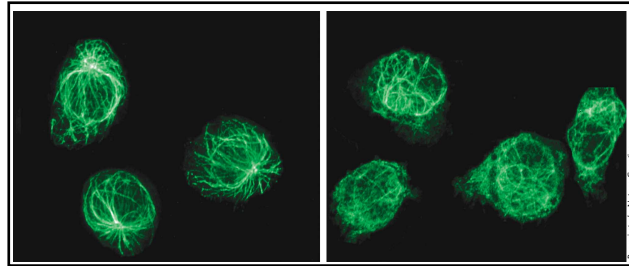


Fig. 4: Individuals with AR-KCS have disorganized tubulin (shown in lymphoblastoid cells). Left, Organized tubulin in cells of a healthy individual. Right, Disorganized tubulin in cells from an affected individual (Reprinted by permission from Macmillan Publishers Ltd: Nature genetics (Lewis and Cowan, 2002), copyright (2002)).

HRD patients show symptoms of enophthalmos (deep set eyes), hypoparathyroidy, small foot and hand, thin lips, teeth anomalies, depressed nasal bridge, beaked nose tip and external ear anomalies like thick ear lobe along with mental retardation and severe intrauterine and postnatal growth retardation (Richardson and Kirk, 1990; Richardson and Kirk, 1991; Sanjad et al., 1991; Hershkovitz et al., 1995; Kelly et al., 2000).

AR-KCS patients have stunted growth, small and thin bones, thickened cortex of the long bones, hypocalcemia, hyperphosphatemia, and ocular abnormalities. Unlike HRD, AR-KCS patients have normal intelligence (Bergada et al., 1988; Franceschini et al., 1992; Diaz et al., 1998; Parvari et al., 2002).

1.2.2 Mutation of mouse *Tbce* causes progressive motor neuropathy (*pnn*) symptoms

Bömmel et al., (2002) have shown that a point mutation (Trp524Gly) in the *Tbce* gene causes progressive motor neuropathy (*pnn*). The missense mutation in *Tbce* gene destabilizes the protein and targets it for degradation causing a reduction of TBCE protein levels in the system (Martin et al., 2002). The *pnn* mouse serves as a model for human spinal muscular atrophy (SMA) (Bömmel et al., 2002; Martin et al., 2002). It is also

noteworthy that the *pmn* mouse has defects in spermatogenesis (Schmalbruch et al., 1991).

Degeneration of motoneurons in *pmn* mutant mouse in early postnatal period is similar to the observation in SMA patients (Bommel et al., 2002; Martin et al., 2002). It is also observed that in isolated motoneuron cultures from wild-type and *pmn* mutant mouse, the length and survival of axonal processes is significantly reduced, they have axonal swellings and varicosities (Bommel et al., 2002). The *pmn* mutant mouse dies within 6 weeks after birth and also shows axonal degeneration in the sciatic and phrenic nerves (Bommel et al., 2002).

Mutations of both human and mouse *Tbce* gene cause reduced number of MTs whereas most of the other manifestations are distinct and specific to the organism under study. However, a human individual with the same mutation as the *pmn* mouse (Replacement of C-terminal penultimate amino acid W to G) has not been reported.

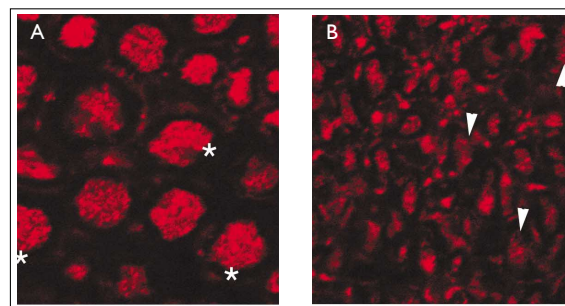


Fig. 5: Analysis of α -tubulin levels in (A) wild-type and (B) *pmn* mutant mouse sciatic nerves. Asterisks mark the α -tubulin staining in cross-sections of sciatic nerve from 4 weeks old wild-type mouse and arrowheads point to the same region in *pmn* homozygous mutant mouse with disrupted and reduced α -tubulin staining (Reprinted by permission from Macmillan Publishers Ltd: Nature genetics (Martin et al., 2002), copyright (2002)).

1.3 Yeast homologue of *Tbce* (*pac2*)

The yeast TBCE protein, also known as Pac2, has the three conserved domains CAP-Gly, leucine rich repeats and ubiquitin like domain (Verma et al., 2000) and is involved in several interactions:

- A. with α -tubulin and MTs via the CAP-Gly domain,
- B. with regulatory core of the proteosomal degradation machinery namely Rpn1 and Rpn10 via the LRR and the UBL domain, respectively (Voloshin et al., 2010).
- C. Pac2 interacts with the UBL domain of TBCB to maintain the quality and turnover of MTs and
- D. Pac2 also interacts with the Skp1-Cdc53-F-box (SCF) ubiquitin ligase complex for ubiquitylation and targeting for proteosomal degradation (Voloshin et al., 2010).

1.4 *Drosophila* *Tbce* gene (*CG7861*)

The orthologous protein for mammalian TBCE in *Drosophila* is coded by *CG7861* gene (flybase.org). The high sequence similarity between *Drosophila* TBCE and human form are suggestive of the fact that the protein is evolutionarily conserved and thus may have similar function across species (Jin et al., 2009). The null mutants of *Tbce* are embryonic lethal with few escapers as was verified by two independent null mutations generated by Jin et al (2009). One of the mutants (*Z0241*) has a nonsense mutation in the 5' coding region and the other mutant (*LH15*) has a deletion spanning the first three exons and an exon of the neighboring gene *CG14591* (disruption of *CG14591* does not cause any obvious defects). In *Drosophila*, TBCE expression was detected in the central nervous system (CNS) and TBCE was also localized to the neuromuscular junctions (NMJs) suggesting that it has a nervous system specific function. It was also shown that TBCE is present in the perinuclear region of muscle cells and epidermal cells (Jin et al., 2009) but the specificity of the signal was not verified by immunostaining of null mutants.

1.4.1 *Drosophila* TBCE is essential for MT formation and synaptic transmission at the NMJ synapses

The homozygous null mutants of *Tbce* (escapers from *Z0241*) have disrupted MT network, a phenotype which is also observed in flies with RNAi mediated TBCE knockdown. As a consequence, the structure of axons is disrupted in *Tbce* mutants. The observation is similar to the presence of degenerate axons in *pnn* mutant mouse (Bommel et al., 2002). Overexpression of TBCE by the Gal4-UAS system (Brand and Perrimon, 1993) facilitates the recovery and formation of stable MTs from nocodazole treated and disrupted MTs. TBCE has a regulatory function at synapses of the NMJ, knockdown of TBCE by RNAi mechanism causes increased synaptic branchings along with large numbers of small sized boutons. It is interesting to note that the overexpression of TBCE in the presynaptic compartment has a mild or no effect on the development of NMJ synapses but causes an increase in miniature excitatory junction potentials (mEJPs), excitatory junction potentials (EJPs) and quantal content. The knockdown of TBCE at the presynapse also causes an increase in mEJP and EJP amplitude along with an increase in mEJP frequency (Jin et al., 2009).

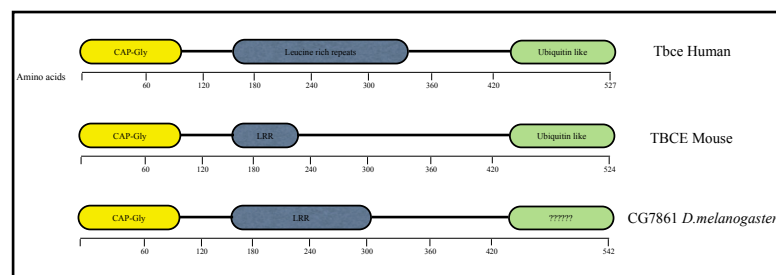


Fig. 6: Conserved domains in TBCE protein. CAP-Gly is a glycine rich domain involved in attachment to the cytoskeletal structure, LRR is a leucine rich domain involved in protein-protein interaction (modified from Riehemann and Sorg, 1993; Grynberg et al., 2003).

1.5 Tubulin binding chaperone E-Like (E-like or TBCEL)

TBCE-Like/E-like/TBCEL, as the name suggests, is a protein with high sequence similarity to TBCE. It has been studied in vertebrates by Bartolini et al., (2005). TBCEL is conserved across several species (Fig. 7).

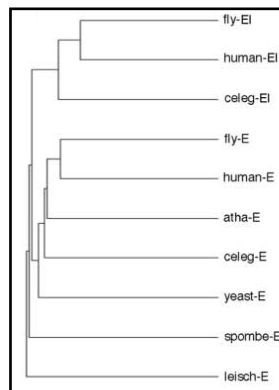


Fig. 7: TBCEL is conserved across several species. *Drosophila* and Human TBCE and E-like are closely related (Reproduced with permission from Development- (Bartolini et al., 2005), copyright (2005)).

TBCEL has UBL and LRR domains but no CAP-Gly domain (Fig. 8). Human TBCEL is present in several tissues but specifically enriched in the testis (Fig. 9).

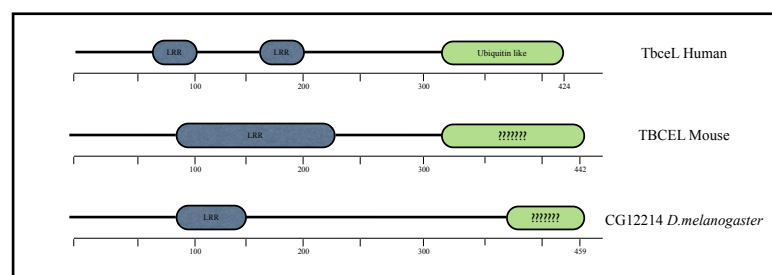


Fig. 8: Conserved domains in TBCEL protein. There is no CAP-Gly domain in TBCEL which is found in TBCE.

1.5.1 *In vitro* and *in vivo* functions of TBCEL

TBCEL affects the unpolymerized $\alpha\beta$ -tubulin heterodimers by rapidly degrading the α - and subsequently β -tubulin subunits by proteosomal degradation pathway (Bartolini et al., 2005). This way TBCEL is similar to TBCE (Tian et al., 1997).

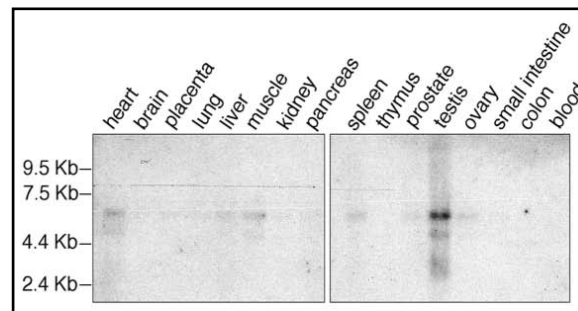


Fig. 9: Northern blot reveals TBCEL transcript is abundant in testis and also present at lower levels in different tissues (Reproduced with permission from Development-(Bartolini et al., 2005), copyright (2005)).

However, in several aspects TBCE and TBCEL are functionally distinct even though they have high sequence similarity. TBCE and TBCEL are both localized to the cytoplasm of the cell but TBCEL is also present in the nucleus. Equal amounts or 10 times the amount of TBCEL relative to TBCE cannot substitute for TBCE function in MT polymerization under *in vitro* conditions suggesting that they have distinct functions. TBCEL does not directly bind to the MTs but binds to the freely available $\alpha\beta$ -tubulin heterodimers and prevents the formation of MTs. Overexpression of TBCEL in HeLa cells causes severe MT depolymerization and disruption of Golgi membrane, causing the Golgi apparatus to be mislocalized to several peripheral sites through out the cytoplasm of the cell. Also, TBCEL does not substitute for TBCE's function of enhancing the activity of TBCC and TBCD (Bartolini et al., 2005).

On expression of TBCEL-specific small interfering RNA (siRNA) in HeLa cells the debilitating effects of TBCEL on MTs was suppressed and the number of stable MTs increased in the perinuclear region of the cell. Also, TBCEL knockdown in HeLa cells

resulted in clustering of endocellular membrane around the microtubule-organizing center (MTOC). Bartolini et al., (2005) have concluded from their experiments that TBCEL plays a significant role in regulation of MT stability and in the organization of endocellular membranes.

1.6 Molecular architecture of the synapse

British physiologist Charles S. Sherrington coined the term “Synapse” (from the Greek term “tighten together”). There are two types of synapses- (1) Chemical synapses, which represents the most common mechanism for signaling between neurons and involves release of neurotransmitter from synaptic vesicles into the synaptic cleft. (2) Electrical synapses are formed from specialized structures called gap junctions that allow ionic current to flow directly between neurons for faster and simpler signaling.

1.6.1 Electrical Synapse

First evidence for the existence of electrical synapses was obtained from studies in crayfish and shrimp neurons (Furshpan and Potter, 1957; Watanabe, 1958) subsequently electrical synapses were also discovered in vertebrate nervous system (Bennett et al., 1959).

In electrical synapses, groups of channels containing connexin link the two neurons by aligning the channels in the post- and presynaptic membranes to form pores and thus electrically coupling the two cells (Wolburg and Rohlmann, 1995; Evans and Martin, 2002; Bruzzone and Dermietzel, 2006; Mese et al., 2007). These gap junction pores allow ions, secondary messengers and metabolites to flow from one side to the other by diffusion or electrophoresis. Important consequences of ionic current flow through electrical synapse is that the transmission is usually bidirectional and is extraordinarily fast; as passive current flow across the gap junction is virtually instantaneous, communication can occur without the delay that is characteristic of chemical synapses.

In invertebrates like *Drosophila* and *C. elegans*, there is no homologous protein for connexin but they have a family of gap junction coding proteins totally unrelated to vertebrate connexins called innexins (invertebrate connexins)(Landesman et al., 1999; Phelan and Starich, 2001). Recently, innexin-like genes were discovered in mammals called pannexins (Px)(Panchin et al., 2000). The function of pannexins in mammals is currently unknown.

1.6.2 Chemical Synapse

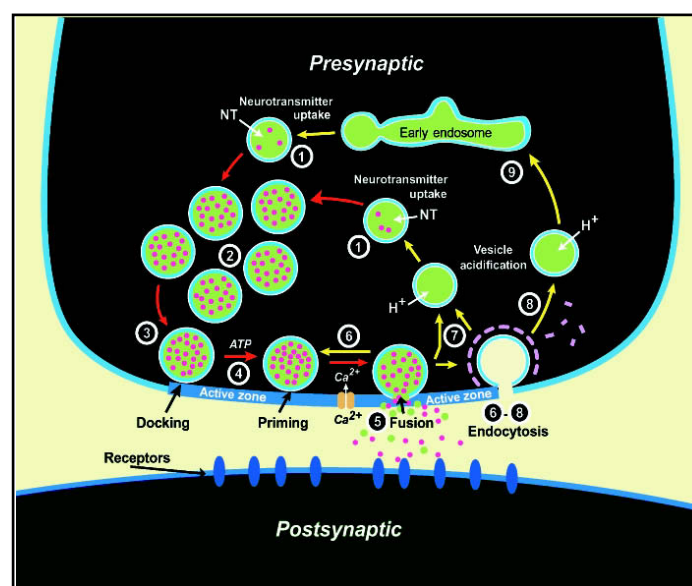


Fig. 10: Neurotransmission in a chemical synapse (permission obtained by University of Wuerzburg (from review Sudhof, 2004)).

Several steps are involved in successful neurotransmission through a chemical synapse (Fig. 10):

- Synthesis, transport and filling of synaptic vesicles: Vesicle synthesis begins with the synthesis of lipids and associated proteins in the cell body of the neuron, specifically in the endoplasmic reticulum (ER). The proteins and lipids are then modified in the Golgi apparatus and subsequently integral membrane proteins are incorporated into the vesicles. The vesicles are transported to the synaptic terminals by MT-associated

motor proteins like kinesins. Neurotransmitter uptake into mature synaptic vesicles (SVs) occurs at the nerve terminal and involves different mechanisms, namely: (1) A H^+ ATPase pump, establishes a proton gradient across the SV membrane. (2) The proton gradient drives specific transporter which cause transmitter uptake against a concentration gradient (Buckley and Kelly, 1985; Fykse and Fonnum, 1988; Hell et al., 1988; Bajjalieh et al., 1992; Parsons et al., 1993) (3) ion channels (for example chloride channel)(Rahamimoff et al., 1988), and in some cases, electron transporters allow for charge compensation or provide reduction equivalents (for example cytochrome b561)(Beers et al., 1986).

- B. The next step is the arrival of an action potential at the presynaptic terminal and depolarization of the cell. Neurotransmitter release is initiated within 400 μ s after the arrival of the action potential (see review Sudhof, 2004).
- C. Depolarization of the pre-synaptic terminal causes voltage-gated Ca^{2+} channels to open. In vertebrate synapses the release is stimulated by Ca^{2+} influx through P/Q- ($Ca_v2.1$) or N-type Ca^{2+} channels ($Ca_v2.2$)(Olivera et al., 1994; Dunlap et al., 1995).
- D. Rapid influx of Ca^{2+} ions through the voltage gated Ca^{2+} channels occurs due to the concentration gradient across the membrane (the external Ca^{2+} concentration is approximately 10^{-3} M, whereas the internal Ca^{2+} concentration is approximately 10^{-6} M).
- E. The sudden influx of Ca^{2+} causes the concentration of Ca^{2+} in the vicinity to reach approximately 10 μ M (threshold for exocytosis of SV) and subsequently the maximal activation concentration of 50 μ M (Llinas et al., 1992; Smith et al., 1993; Stanley, 1997; Schneggenburger and Neher, 2000).
- F. SNARE proteins: The Ca^{2+} ion sensor protein synaptotagmin and other intracellular proteins involved in feedback regulation of the channels and Ca^{2+} dependent proteins and kinases involved in synaptic plasticity are activated. The SNARE proteins are localized near the Ca^{2+} channels by having a direct interaction with an intracellular

domain of the channel, the synaptic protein interaction (synprint) site on the N-type Ca^{2+} channels ($\text{Cav}2.2$) (Sheng et al., 1994; Sheng et al., 1997) (Cohen et al., 1991; Westenbroek et al., 1992; Westenbroek et al., 1995; Catterall, 2000) and thus they instantaneously respond to the Ca^{2+} influx and initiate vesicle exocytosis. The SNARE proteins are classified into two categories- (1) v-SNARE or vesicle associated SNARE, like VAMP (or synaptobrevin) and (2) t-SNARE or target membrane associated SNARE, like syntaxin and SNAP-25 (see Fig. 10). Only the t-SNARE proteins syntaxin-1A and SNAP-25 interact with the Ca^{2+} channels at synprint sites (Sheng et al., 1994; Sheng et al., 1997). Syntaxin interacts with Ca^{2+} -bound synaptotagmin and triggers the SNARE complex to fuse vesicles with the pre-synaptic membrane which causes the release of neurotransmitters into the synaptic cleft (Sheng et al., 1994; Sheng et al., 1996; Sheng et al., 1997).

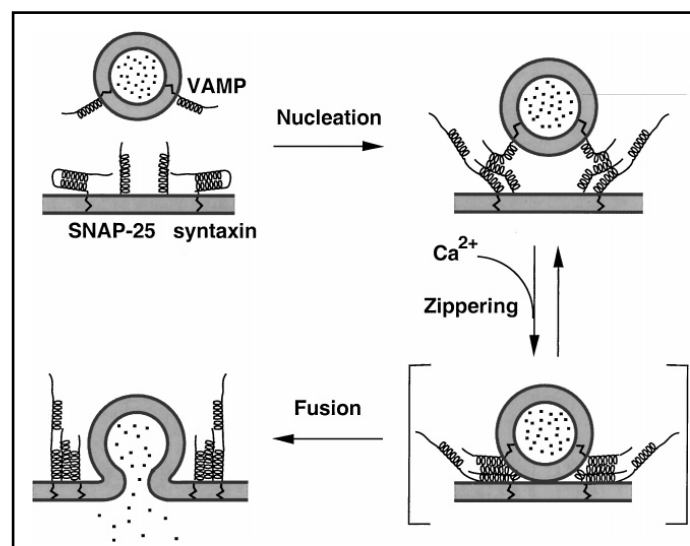


Fig. 11: SNARE proteins mediated vesicle exocytosis. Ca^{2+} bound synaptotagmin interacts with syntaxin, which then interact with v-SNAREs and cause the ‘zippering’ and fusion of SVs to the presynaptic membrane (permission obtained by University of Wuerzburg (Lin and Scheller, 2000), copyright (2002)).

G. The transmitters bind to the receptors on the postsynaptic side which cause the opening or closing of postsynaptic channels or activation of secondary messengers mediated signaling pathways, thereby altering the excitability of the postsynaptic cell.

H. Phosphorylation of proteins like synapsin by Ca^{2+} dependent kinases causes the vesicles at the reserve pool to move towards the active zone for replenishing the readily releasable pool of SVs (see Fig. 10 and 12). Properties of the different SV pools are summarized in Table 1.

Table. 1: Characteristics of different vesicle pools at the synapse (modified from Rizzoli and Betz, 2005).

Pools	Readily releasable pool (RRP)	Recycling pool	Reserve pool
Size (% of total vesicles)	~1-2 %	~10-20 %	~80-90 %
Location	Docked	Scattered	Scattered
Recycling	Fast (Seconds)	Fast(Seconds)	Slow (minutes)
Mixing with other pools	Fast mixing with recycling pool	Slow mixing with reserve pool	Slow mixing with all other pools
Mobility at the terminals	Docked (No mobility)	High	None or low

I. Finally, the vesicle membranes are retrieved from the plasma membranes by clathrin mediated endocytosis and are sent back into the cycle (Fig. 12).

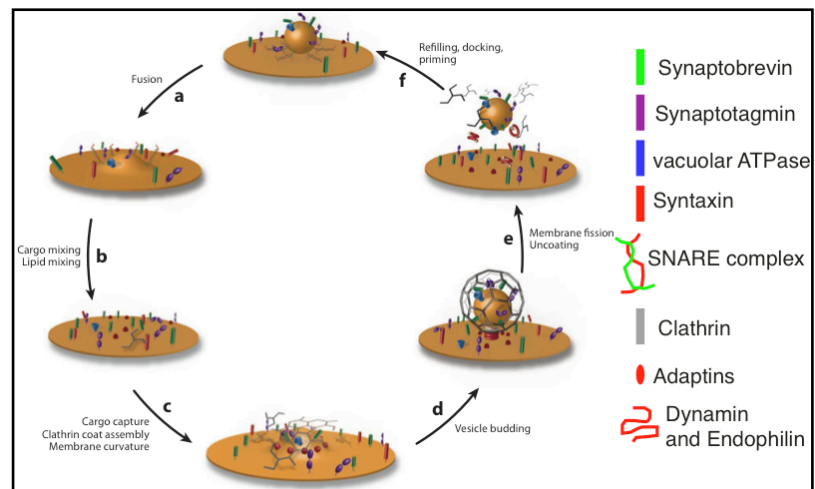


Fig. 12: Synaptic vesicle cycle. The vesicles are retrieved from the synaptic cleft via endocytosis, filled with neurotransmitters and recycled back to different vesicle pools based on requirement (modified from review Dittman and Ryan, 2009) (Permission obtained by University of Wuerzburg).

The process of transmitter release is a result of concerted interactions between several signaling pathways activated sequentially or in parallel. The main components of these pathways are the presynaptic proteins, both vesicle associated and non-associated. In section 1.7 and subsections I will discuss in detail the functions of two presynaptic proteins of particular interest with respect to this thesis synapsin and synapse associated protein of 47 kDa (SAP47).

1.7 Synapsins

1.7.1 The *synapsin* gene locus is highly conserved in different species

Synapsins are a family of presynaptic phosphoproteins associated with synaptic vesicles (SVs) (Fig. 13) where they constitute approximately 10% of the total SV protein (Navone et al., 1984; De Camilli and Greengard, 1986; Sudhof et al., 1989; Greengard et al., 1993) and approximately 0.4% of the total protein content in a mammalian brain (Goelz et al., 1981). Synapsins are evolutionarily conserved proteins and are abundant at the presynaptic terminals in most neuronal cells but are absent in cells with ribbon

synapses which are generally found in neuronal population involved in sensory transduction (see review Cesca et al., 2010). The *synapsin* gene locus in several species has a nested tissue inhibitor of metalloproteinases gene (*Timp*). In vertebrates, three genes (*synapsin I, II, and III*) code for at least six isoforms (De Camilli et al., 1983a; Sudhof et al., 1989; Esser et al., 1998; Hosaka and Sudhof, 1998a, b; Kao et al., 1998; Hosaka et al., 1999; Hosaka and Sudhof, 1999).

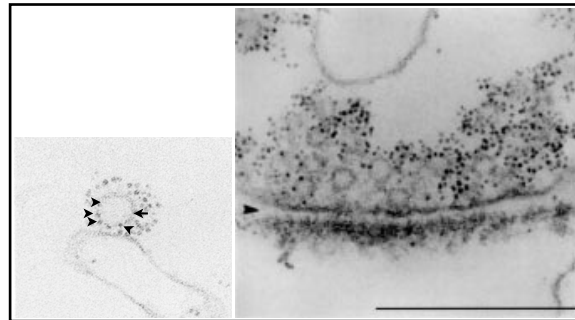


Fig. 13: Localization of synapsins on synaptic vesicle surface in a vertebrate synapse by immunoferritin labeling. In the left image, arrow heads mark the synapsins and arrow points to the vesicle and in the right image, dark spots mark the synapsin and the arrowhead marks the synaptic cleft. Scale bar on the right image 0.37 μm . (modified from De Camilli et al., 1983b)

In humans, the *synapsin III* gene locus codes for at least 6 different transcripts (*synapsin IIIa–III f*) by alternative splicing (Porton et al., 1999). The *synapsin* isoforms IIIa–III d are brain specific and the III d isoform is only expressed in the human fetal brain (Porton et al., 1999). The *synapsin* isoforms III e and III f are expressed only in non-neuronal tissues by the presence of an alternative promoter in an intron of the *synapsin III* gene locus (Porton et al., 1999).

Recently, vertebrate synapsins have also been found in non-neuronal cells, e.g. chromaffin cells, pancreatic β cells, epithelial cells etc. (see review Cesca et al., 2010).

1.7.2 Structural analysis of synapsins

All the different isoforms of vertebrate synapsins have a highly conserved central domain known as the C-domain and a fairly conserved NH₂-terminal A-domain and a COOH-terminal E-domain (Sudhof et al., 1989; Kao et al., 1999) (Fig. 14). The domain E is present in 'a'-type synapsin isoforms (Ia, IIa and IIIa) but not in the 'b'-type isoforms (Ib and IIb) (Sudhof et al., 1989; Kao et al., 1999). Domain D is composed of basic and neutral non-polar residues like glycine and proline (see review De Camilli et al., 1990).

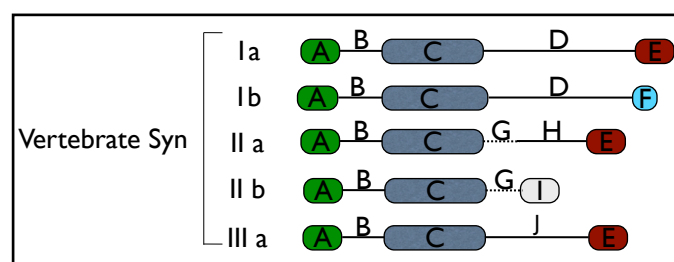


Fig. 14: Conserved domains of vertebrate synapsins. Domains A, C and E are highly conserved across different isoforms.

Human synapsin IIIa has A, B, C, J and E domains whereas IIIb and IIIc have only the A, B and C- domains and the IIIe isoform has A, B, C and a short J-domain. The isoforms IIIe and IIIf have no conserved domains (Porton et al., 1999).

1.7.3 Biochemical properties of vertebrate synapsins

In vitro experiments with different isoforms of vertebrate synapsins demonstrate that the central C-domain of synapsins binds to ATP with high affinity and with different prerequisites, synapsin I-ATP interaction is dependent on Ca²⁺; for synapsin II, interaction with ATP is independent of Ca²⁺ and for synapsin III, presence of Ca²⁺ is inhibitory for interaction with ATP (Esser et al., 1998; Hosaka and Sudhof, 1998a, b). Structural analysis of recombinant protein consisting of domain C of vertebrate synapsin I has revealed that it has high structural similarities to ATPase enzymes like glutathione

synthetase. These enzymes breakdown ATP to ADP and in the process release orthophosphate and energy which drives other biochemical reactions.

Isoforms of vertebrate synapsins form multimers by interacting through their C and E domains (Hosaka and Sudhof, 1999; Monaldi et al., 2009). The formation of synapsin I, II and III heteromultimers is essential for synapsin III protein stability and in the *synapsin I/II* double knock-out mouse the levels of synapsin III is reduced by 50% (Hosaka and Sudhof, 1999). *In vitro* analysis of recombinant synapsin domain E containing peptide demonstrates their involvement in interaction with synapsin isoforms I and II and formation of dimers (Monaldi et al., 2010).

Vertebrate synapsins have an isoelectric point around 6 to 8 (basic) (John et al., 2007; Kang et al., 2009).

1.7.4 Role of vertebrate synapsins at the synapse

In vertebrates, it has been demonstrated that synapsins are required for constant release of vesicles during conditions of high neuronal activity, a mechanism related to short-term plasticity (Pieribone et al., 1995). It was shown by video-microscopy that dephosphorylated synapsins anchor synaptic vesicles to the actin-based cytoskeleton thereby maintaining a reserve pool of vesicles near the release sites (Ceccaldi et al., 1995). Synapsins have also been implicated in other forms of short-term plasticity, such as post-tetanic potentiation (Rosahl et al., 1995; Humeau et al., 2001), and in modulating a post-docking step of the release process (Hilfiker et al., 1998; Humeau et al., 2001). Vertebrate synapsin I is preferentially expressed in inhibitory synapses whereas synapsin II is mainly expressed in excitatory synapses (Mandell et al., 1992). Vertebrate synapsin I is exclusively found on the surface of small SVs but absent from the surface of large dense core vesicles (De Camilli et al., 1983b; Huttner et al., 1983; Navone et al., 1984).

Vertebrate synapsins have been shown to bind lipid and protein components of synaptic vesicles in a phosphorylation-dependent manner (Schiebler et al., 1986; Benfenati et al., 1989a; Benfenati et al., 1989b). Synapsins also bind to various

cytoskeletal proteins, including actin, spectrin, and microtubules (see review Cesca et al., 2010; Baines and Bennett, 1985; Bennett et al., 1985; Baines and Bennett, 1986; Bennett et al., 1986; Bahler and Greengard, 1987; Petrucci and Morrow, 1987; Benfenati et al., 1992; Hurley et al., 2004). Biochemical approaches have shown that domains C and E bind to a presynaptic actin scaffold and thus maintain a synaptic vesicle pool in the periphery of the plasma membrane, whereas the domain A regulates neurotransmitter release in a phosphorylation-dependent manner (Hilfiker et al., 2005).

Phosphorylation of vertebrate synapsin I changes its confirmation and plays a role in synapsin function as vesicle tethering proteins (Benfenati et al., 1990). Synapsin I interacts with Rab3A, an effect that is weakly dependent on phosphorylation by PKA or MAPK/Erk at site 1 and sites 4-6, respectively. The interaction stimulates GTP binding, GTPase activity and association of Rab3A with synaptic vesicles (Giovedi et al., 2004a; Giovedi et al., 2004b). Rab3A on the other hand, inhibits the interactions of synapsin I with actin and the synapsin-induced phospholipid vesicle aggregation (Giovedi et al., 2004a; Giovedi et al., 2004b).

1.7.4.1 Phosphorylation dependent interaction and function of vertebrate synapsin

Synapsin is a substrate for several protein kinases like PKA, CaMKs, Src, cdk and MAPK/Erk, which modulate its biochemical properties. One of the first reported substrate of Ca²⁺/Calmodulin dependent protein kinase was synapsin I (Schulman and Greengard, 1978). Protein kinase A (PKA) and Ca²⁺-calmodulin-dependent protein kinase-I or IV (CaMK-I/IV) phosphorylate at Ser-9 in domain A of rat, mouse and human synapsin I, II (Ser-10) and III (P-site 1; Hosaka et al., 1999; Fiumara et al., 2007). CaMK-II phosphorylates Ser-566 and Ser-603 (P-sites 2 and 3) in domain D of rat synapsin I. Synapsin II is phosphorylated only at P-site 1 and not at P-site 2 and 3 as it does not possess the consensus motif (Sudhof et al., 1989). P-sites 4 and 5 (Ser-62 and Ser-67 respectively) in domain B of rat, human and mouse synapsin I are phosphorylated by extracellular signal-regulated kinases Erk-1(p44) and Erk-2(p42) of the mitogen-activated protein kinase (MAPK) superfamily (Jovanovic et al., 1996). P-site 6 (Ser-549 in rat synapsin I or Ser-551 in mouse, human and bovine synapsin I) in domain D is

phosphorylated by MAPK, as well as by cyclin-dependent kinase cdk-1 and cdk-5 (Jovanovic et al., 1996). P-site 7 (Ser-551) in domain D is phosphorylated only by cdk-5 (Jovanovic et al., 1996). P-site 8 (Tyr-301) in domain C of human, rat and bovine synapsin I is phosphorylated by Src kinase (Onofri et al., 2007). P-site 9 in domain E of rat synapsin Ia is phosphorylated by phosphoinositide 3-kinase, ATM (Li et al., 2009) (see Fig. 15a, b and c). Phosphorylation sites apart from the ones discussed above have been identified and verified in large scale proteome analyses by mass spectrometry (Ballif et al., 2004; 2006; 2008; Trinidad et al., 2005; 2006; 2008; Munton et al., 2007; Tweedie-Cullen et al., 2009). As a general scheme, the phosphorylation sites were identified from tissue homogenates of mouse, rat or bovine samples by MS and subsequently verified by treating the samples with alkaline phosphatase and again performing MS to determine a shift in mass equivalent to that of a phosphate group (79 Da).

1.7.4.2 Phosphorylation dependent interaction of vertebrate synapsins with synaptic vesicles and components of the cytoskeleton

Vertebrate synapsin I interacts with protein components of the vesicles via domain C and this interaction is susceptible to phosphorylation (Benfenati et al., 1989a). It also interacts in an phosphorylation dependent manner with several components of the cytoskeleton like F-actin and microtubules (Bahler and Greengard, 1987; Petrucci and Morrow, 1987, 1991). Phosphorylation of synapsin I at sites 1, 2 and 3 causes complete dissociation of synapsin I from actin whereas dephosphorylation at site 2 and 3 causes strong interaction and bundling of F-actin (Petrucci and Morrow, 1987). Synapsin I mediated G-actin polymerization and bundling of actin filaments is altered by MAP kinase-dependent phosphorylation of synapsin I (Jovanovic et al., 1996).

Phosphorylation specifically at site 2 and 3 and not at site 1 causes conformational changes in synapsin I (Benfenati et al., 1990) and reduces the affinity of synapsin towards synaptic vesicles by approximately 5 fold whereas phosphorylation at site 1 reduces the affinity only slightly (Schiebler et al., 1986). Biochemical and optical studies suggest that dephosphorylated synapsins cage synaptic vesicles and prevent the release of neurotransmitter, while synapsin phosphorylation initiates vesicle mobilization and

priming (Greengard et al., 1993; Chi et al., 2001). Phosphorylation at site 8 (Y301) of synapsin I by Src kinase increases synapsin dimer formation and the interactions with SVs and actin are also enhanced (Messa et al., 2010).

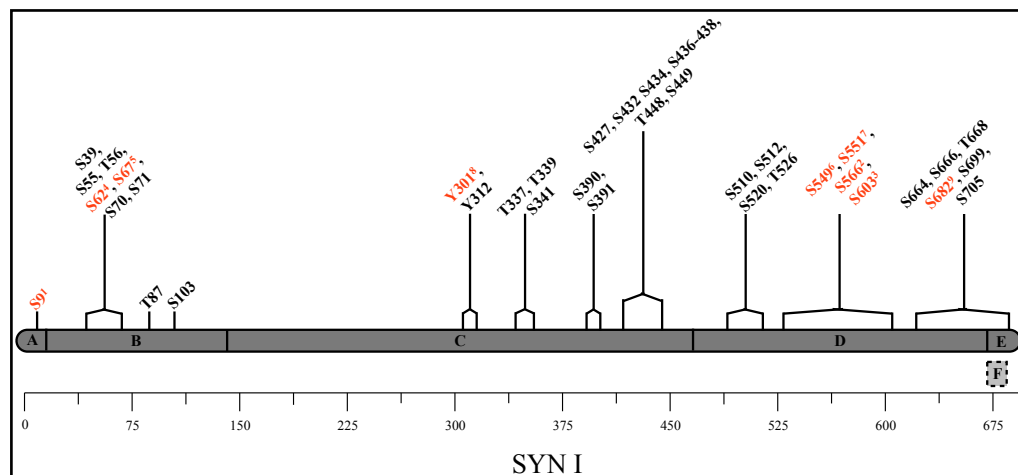


Fig. 15a: Mammalian synapsin I has 9 characterized phosphorylation sites as shown in red, the superscripts refer to the order of identification and characterization of these sites (see review Cesca et al., 2010). By mass spectrometry (MS) 30 more sites have been identified (Ballif et al., 2004; 2006; 2008; Trinidad et al., 2005; 2006; 2008; Munton et al., 2007; Tweedie-Cullen et al., 2009).

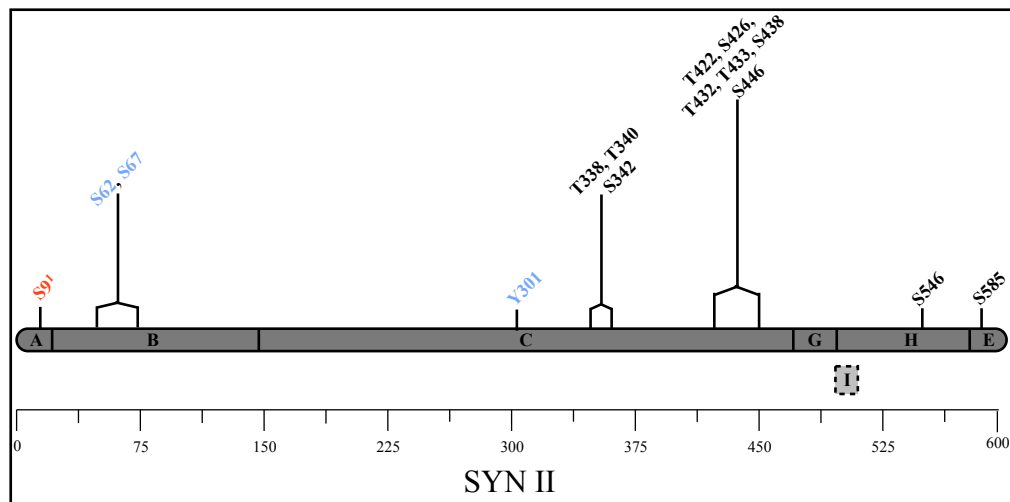


Fig. 15b: Mammalian synapsin II has 1 characterized phosphorylation site, as shown in red. The 3 sites shown in blue are uncharacterized and inferred from sequence similarity with synapsin I. The rest 11 sites have been identified by MS (Hosaka et al., 1999; Trinidad et al., 2006; 2008; John et al., 2007; Onofri et al., 2007).

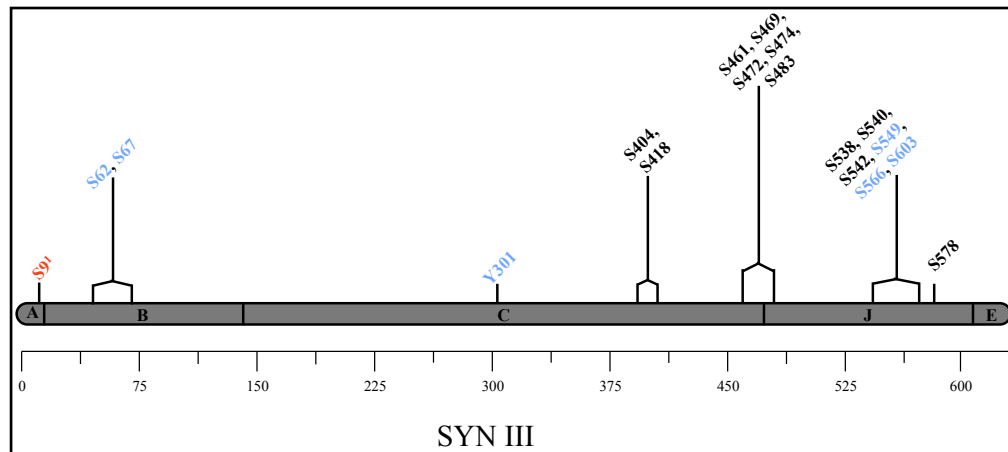


Fig. 15c: Mammalian synapsin III has only 1 phosphorylation site characterized so far, as shown in red. The 6 sites shown in blue are uncharacterized and inferred from sequence similarity with synapsin I. The rest 11 sites have been identified by MS. Synapsin III is demonstrated to have 6 different isoforms but only isoforms a-d are expressed in neuronal cells (Kao et al., 1998; Hosaka et al., 1999; Porton et al., 1999; 2004; Ballif et al., 2006; Trinidad et al., 2006; 2008; Munton et al., 2007).

Phosphorylation at sites 1-3 in vertebrate synapsin is selectively dephosphorylated by phosphatase PP2A. The sites 4-7 are dephosphorylated by PP2B or calcineurin. The influx of Ca^{2+} causes the inactivation of PP2A but activation of PP2B. Phosphorylation at sites 1-3 rapidly increases upon Ca^{2+} influx on depolarization. It has been suggested that the dephosphorylation at sites 4-7 can play a role in SV endocytosis as the situation is comparable to the phosphorylation/dephosphorylation cycle of dynamin I, synaptojanin and amphiphysin I and II proteins which are involved in SV endocytosis (see review Cesca et al., 2010).

1.7.5 Other PTMs in vertebrate synapsin

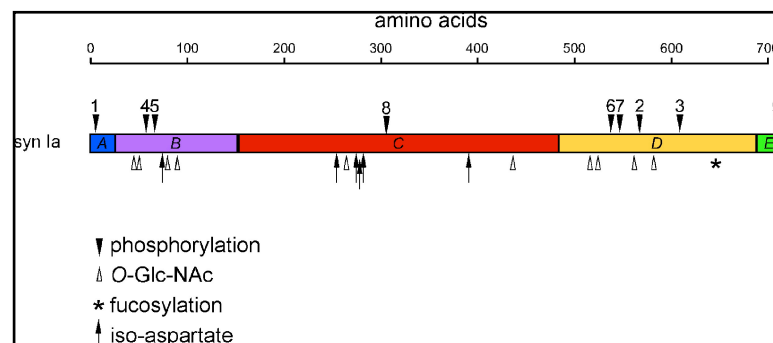


Fig. 16: PTMs in vertebrate synapsin (see review Cesca et al., 2010).

Vertebrate synapsin I and II are shown to contain several other PTMs apart from phosphorylation. The second major PTM of vertebrate synapsin I and II after phosphorylation is O-linked N-Acetylglucosamine which is usually clustered around the serine and threonine residues which are phosphorylated. Fucosylation is another PTM observed in vertebrate synapsin Ia and Ib. Isoaspartate formation is spontaneous and ubiquitous process, this PTM is kept under check by the action of 1-Isoaspartyl Methyltransferase (PIMT). Mouse homozygous mutants of PIMT have increased amount of isoaspartate synapsin and a selective expression of PIMT in neuronal cells rescues this phenotype (Fig. 16) (see review Cesca et al., 2010).

1.7.6 Analysis of *synapsin* mutants

Loss or disruption of *synapsin* I function in mouse increases synaptic depression, indicating that synapsins are required to sustain neurotransmitter release during high levels of neuronal activity (Li et al., 1995; Rosahl et al., 1995; Takei et al., 1995; Hilfiker et al., 1998; Chi et al., 2001; Humeau et al., 2001; Gitler et al., 2008). *Synapsin* I KO also decreases the number of vesicles in the periphery of the active zone, suggesting that synapsins participate in transmitter release by regulating a reserve pool of synaptic vesicles. *Synapsin* I KO mouse show increased propensity for epileptic seizures (Li et al., 1995). *Synapsin* II KO and *synapsin* I and II double KO have normal paired pulse facilitation (PPF) and lowered potentiation after tetanic stimulation (PTP) whereas only *synapsin* I KO have increased PPF but normal PTP (Silva et al., 1996). *Synapsin* II KO and *synapsin* I, II double KO mice have impaired learning and short term plasticity in fear conditioning experiments (Silva et al., 1996). Also, the levels of synaptotagmin (I and II), synaptophysin I, synaptoporin II, synaptobrevin II, SV2 and synapsin II are reduced significantly in *synapsin* I and *synapsin* I/II double KO mouse. In *synapsin* II KO only the levels of synaptophysin I, synaptobrevin II, SV2 and synapsin I are reduced (Rosahl et al., 1995). The levels of Rab5a are increased significantly in *synapsin* I, II and double KO mice (Rosahl et al., 1995). Rab3A deletion rescues epileptic-like seizures in mouse, typical for *synapsin* II KO animals, as observed in a double KO mouse for *synapsin* II and Rab3A (Coleman and Bykhovskaia, 2010).

1.7.7 Synapsin related human disorders

Synapsin I content is altered in hippocampus of Alzheimer patients (Perdahl et al., 1984; Qin et al., 2004). In patients with bipolar disorder and schizophrenia a reduction in levels of synapsins II and III in hippocampus is observed (Vawter et al., 2002). Polymorphisms in human *synapsin* III gene locus in certain population (from Italy) can lead to multiple sclerosis (MS) and has led to the speculation that synapsin III plays a role in MS (Liguori et al., 2004; Akkad et al., 2006). A family with history of epilepsy was found to have a nonsense mutation in the *synapsin* I gene which is likely to cause *synapsin* mRNA degradation (Garcia et al., 2004). The *synapsin* II gene locus is found to

be highly susceptible to variations in sporadic cases of epilepsy (Lakhan et al., 2010; Cavalleri et al., 2007).

1.7.8 *Drosophila* synapsin

In *Drosophila*, a single synapsin (*Syn*, CG3985) gene codes for at least 5 different isoforms which are divided into two groups: the shorter (70-80 kDa) and the longer isoforms (~143 kDa) (Klagges et al., 1996). The longer isoform which is generated with an efficiency of 20-25% by read through of an in-frame *amber* stop codon codes for a proline rich region (see Results section). As in vertebrate synapsin, the domains A, C and E are conserved with highest degree of conservation in the central C-domain (Fig. 17) (Klagges et al., 1996). Apart from the ubiquitous expression in the larval and adult brain, synapsin is localized in type I but not in type II and III synaptic boutons at larval neuromuscular junctions (Godenschwege et al., 2004).

In mammals and other vertebrates the domain 'A' of synapsin contains the P-site 1 (consensus amino acid sequence RRXS) that has been identified as a target site for PKA/CaMK-I/IV. In *Drosophila*, this motif is encoded in the genome, but the enzyme adenosine deaminase acting on RNA (ADAR) edits the majority of RNAs such that the conserved kinase recognition motif in domain 'A' is modified (Diegelmann et al., 2006). ADAR catalyzes the conversion of a single base (A to G) and thus alters the predicted phosphorylation site to RGFS. In an *in vitro* phosphorylation experiment with an undecapeptide containing the genome-encoded motif (RRFS) is readily phosphorylated by bovine PKA but the edited motif (RGFS) is not (Diegelmann et al., 2006). The majority of synapsins in *Drosophila* is not phosphorylated by PKA in the 'A' domain. Whether a second RRXS site in *Drosophila* synapsin is accessible to PKA, and whether the protein is a substrate for other kinases is not known.

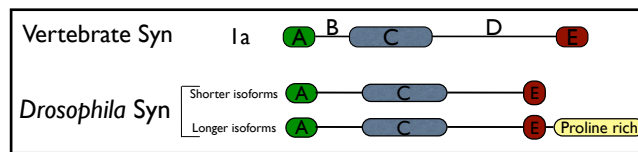


Fig. 17: Conserved domains of *Drosophila* synapsin. The shorter isoforms are around 70-80 kDa whereas the longer isoforms are ~143 kDa. The proline rich region is coded by *amber* codon read through (Klagges et al., 1996).

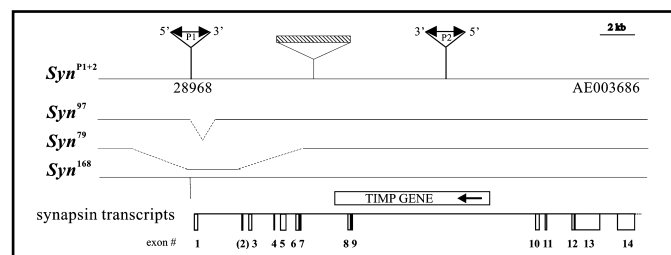


Fig. 18: *Syn* gene of *Drosophila*, comprises of 14 exons. The null alleles *Syn*⁹⁷ and *Syn*⁷⁹ were generated by mobilizing the P1 P-element (from Godenschwege et al., 2004).

As in vertebrates, the precise mode of action of synapsin is unknown in flies. The *Drosophila Syn*⁹⁷ null mutants were generated by remobilizing a P-element (P1, Fig. 18). The *Syn*⁹⁷ deletion obtained by this P-element mutagenesis does not affect the coding region but has a deletion of 1397 bp, which disrupts the predicted promoter and the transcription start site, the first exon (207 bp), and part of the first intron (841 bp) (Godenschwege et al., 2004). The *Syn*⁷⁹ deletion line has ~7 kb deletion which spans the first seven exons (Godenschwege et al., 2004). The *Syn*⁹⁷ null mutant adult flies do not show any immediately visible phenotypes but, adult locomotor activity and complex behavior like optomotor responses at high pattern velocities, wing beat frequency, and visual pattern preference are modified (Godenschwege et al., 2004). In *Drosophila* larvae, *Syn*⁹⁷ null mutants have ~50% reduced olfactory associative learning when compared to wild-type CS (Michels et al., 2005). Recently it has been shown that the anesthesia sensitive component of olfactory associative memory of adult *Syn*⁹⁷ mutants is impaired while the anesthesia resistant memory component is unaffected (Knapek et al., 2010).

The distribution and morphology of vesicles is unaltered in type I synaptic boutons of *Syn⁹⁷* null mutants (Godenschwege et al., 2004) (Fig. 19). A recent FM1-43 dye uptake study on third instar larval NMJs of *Drosophila Syn⁹⁷* and *Syn^{97CS}* (cantonized *Syn⁹⁷*, by outcrossing with *CS*) has revealed that stimulation of motor neuron by light K^+ concentration or 15 min electrical stimulation at 3 Hz, the dye taken up is homogeneously spread over the presynaptic bouton and not localized to the periphery as observed in WT boutons thus implying that the localization of vesicles in recycling pool at *Drosophila* presynaptic boutons of NMJs is disrupted in the absence of synapsin (Akbergenova and Bykhovskaia, 2007). When NMJ preparations were treated with cyclosporin A which increases endocytosis by inhibiting calcineurin the dye loading was not as prominent in *Syn⁹⁷* and *Syn^{97CS}* mutants as in WT suggesting that the quantity of vesicles in the reserve pool is diminished in the mutants (Akbergenova and Bykhovskaia, 2007).

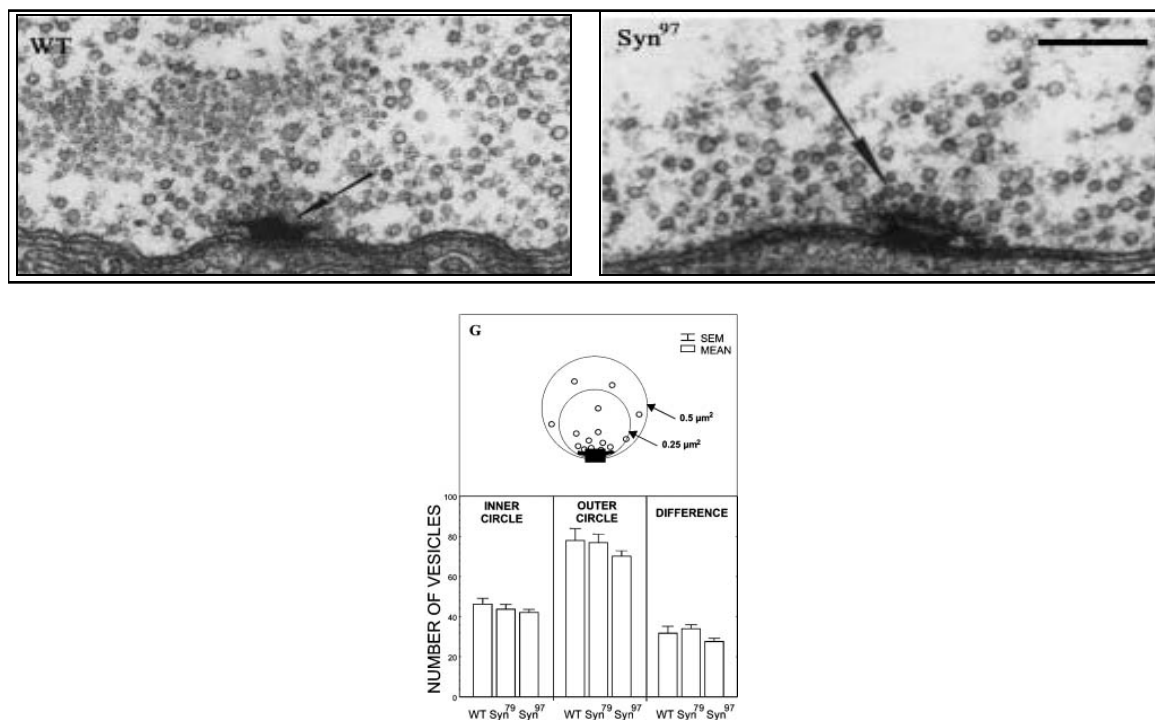


Fig. 19: The distribution of synaptic vesicles in wild type and *Syn* null mutant is not altered (Godenschwege et al., 2004). The EM image for *Syn⁷⁹* is not shown.

After bafilomycin treatment which blocks SV refilling, EPSPs from NMJs of *Syn⁹⁷* null mutants show faster depression when compared to WT, supporting the

conclusion that *Syn⁹⁷* null mutants have a smaller number of vesicles in the reserve pool to replenish the recycling pool (Akbergenova and Bykhovskaia, 2007).

1.8 Synapse associate protein of 47 kD (SAP47)

SAP47 is a novel conserved protein of unknown function which was identified by screening a *Drosophila* cDNA expression library with monoclonal antibody nc46 (Reichmuth et al., 1995). This antibody was selected from a hybridoma library generated by A. Hofbauer (Hofbauer, 1991; Hofbauer et al., 2009), because it binds to all synaptic terminals of the *Drosophila* nervous system. The MAB nc46 stains a prominent protein of 47 kD on Western blots (Fig. 21) and it recognizes a protein of similar size in various other diptera (Reichmuth et al., 1995). The gene was cloned and by comparing the encoded amino acid sequence with the protein databases SAP47 was found to be conserved among various species like mouse, *C.elegans* etc, but so far no strong homology has been observed to known proteins (Reichmuth et al., 1995). Thus, the primary structure of this novel brain protein gives no clue about its functions. The SAP47 protein does not contain any domains defined by Prosite patterns that could be indicative of a specific function or molecular interaction, however SAP47 shares a novel domain (termed BSD) with the transcription factors BTF2/TFB1 and DOS2-like proteins of various species (Doerks et al., 2002) but the role of this domain remains unclear.

The gene structure of the *Sap47* gene as given in flybase (released May 28th, 2010) is shown in Figure 20.

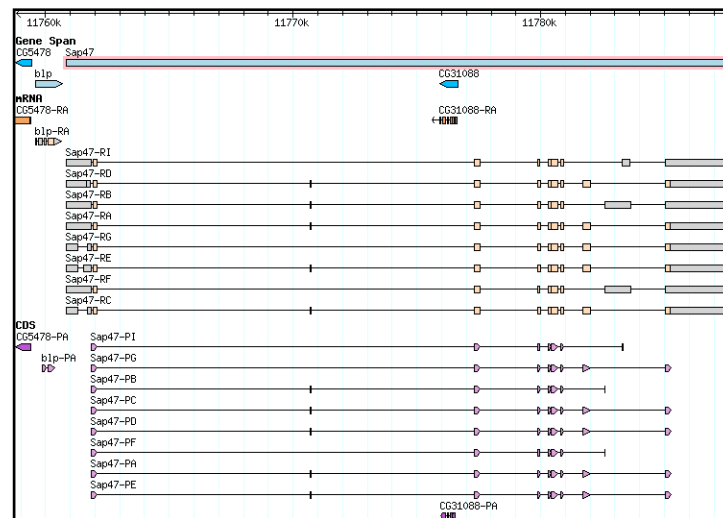


Fig. 20: *Sap47* gene (from flybase.org).

The process of alternative splicing produces 8 different mRNAs encoding five predicted proteins (Fig. 20). However, in Western blots at least 9 different isoforms are detected (see Fig. 21 Funk et al., 2004).

Using a P-element insertion line from the Berkeley Drosophila Genome Project the *Sap47*¹⁵⁶ null mutant was generated by jump-out mutagenesis. In this mutant the deletion comprises 110 base pairs in 3' UTR of the upstream adjacent gene black pearl (*blp*), 170 base pairs between *blp* and the *Sap47* transcription start site, the entire first exon including the 5' UTR and the translation start site, and 220 base pairs of the 1st intron of the *Sap47* gene (Funk et al., 2004). Two other alleles from the same mutagenesis, *Sap47*²⁰¹ and *Sap47*²⁰⁸, have not been analyzed in detail.

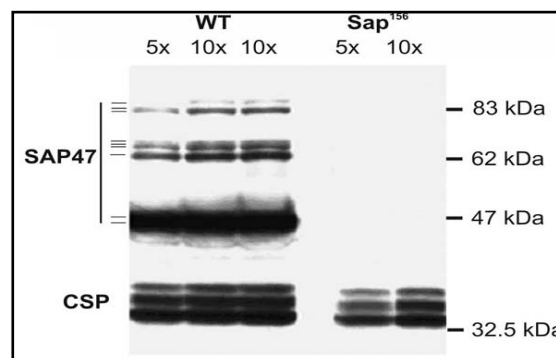


Fig. 21: Western blot with nc46 antibody (from Funk et al., 2004).

Sap47¹⁵⁶ null mutant flies are fertile and viable (Funk et al., 2004) but are impaired in associative olfactory learning behavior as studied at the larval stage (communication from Dr. B. Gerber).

1.9 Tools used in investigating genes and proteins of *Drosophila*

1.9.1 Gal4-UAS system for transgene expression

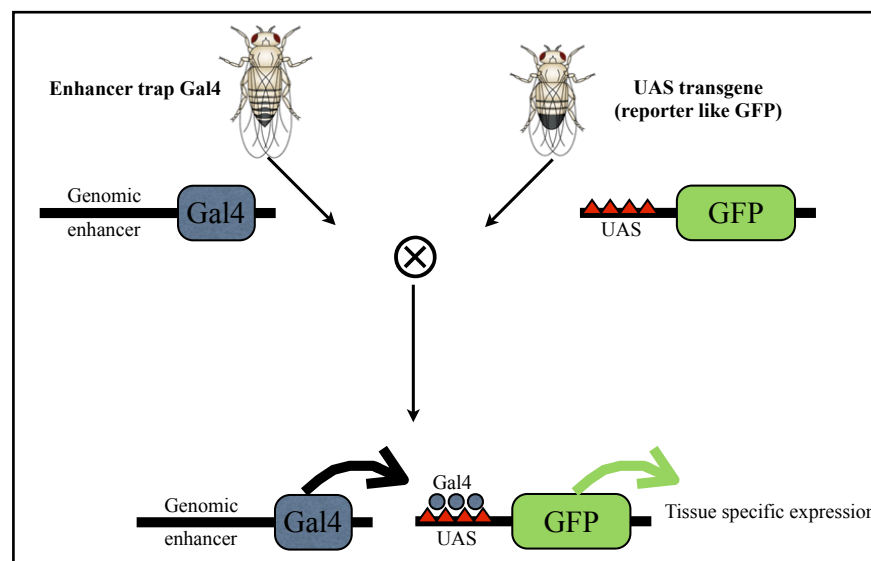


Fig. 22: GAL4-UAS system. Cell specific promoter/enhancer mediated expression of GAL4 yeast transcription factor is used for spatial (and in some cases temporal) control of transgene expression which is cloned downstream of the UAS sequence (modified from Brand and Perrimon, 1993).

GAL4 is a yeast transcription factor which selectively binds to cis-regulatory sites called upstream activating sequences (UAS) and enhances transcription of the downstream gene. This method of bipartite gene expression control has become a powerful method for the expression of transgenes in *Drosophila*. In *Drosophila*, the two components are cloned into separate lines to permit different combinations of expression. The 'driver' line carries a GAL4 gene expressing in specific tissues and the 'effector' line has a gene of interest, e.g. a reporter gene like GFP (see Fig. 22), cloned downstream and under control of the UAS sites (Brand and Perrimon, 1993). If the GAL4 gene is in a P-

element cassette which is inserted at specific regions in the genome, e.g. 5' UTR of a gene X, the genomic enhancer influencing the gene X promoter would also influence the GAL4 promoter (generally a weak promoter) in the P-element and cause the expression of GAL4 similar to gene X. The GAL4 traps the enhancer expression and reflects the endogenous gene expression pattern. These P-element insertion lines are known as enhancer trap lines. Two such lines, NP4786 and NP6285 are described in this thesis for investigating TBCEL expression in *Drosophila*.

1.9.2 Microarray technology for transcriptome analysis

DNA microarrays extend conventional hybridization techniques as large numbers of DNA fragments are attached to a substrate by an automated process and are then probed by sequences of interest for complementarity (see Fig. 23). The use of microarrays for gene expression profiling was first reported in 1995 (Schena et al., 1995). The complete genome of yeast was the first to be assembled on a microarray chip (Lashkari et al., 1997), this paved the way for developing genome chips of other organisms like mouse, *Drosophila* etc. In this thesis we have used short oligonucleotide arrays or gene chips from *Drosophila melanogaster* for analyzing differences in gene expression between synaptic protein null mutants and the wild-type with respect to the complete genome. Some facts about *Drosophila* gene chips obtained from (<http://www.affymetrix.com>) are given below:

- A. Number of transcripts: 18,953
- B. Number of probe sets: 18,880
- C. Feature size: 11 μ m
- D. Probe length: 25 nucleotides
- E. Probe pairs/gene: 14
- F. Hybridization controls: *bioB*, *bioC*, *bioD* from *E. coli* and *cre* from P1 bacteriophage
- G. Poly-A controls: *dap*, *lys*, *phe*, *thr*, *trp* from *B. subtilis*
- H. Housekeeping/Control genes: *Actin (Actin42A)*, *GAPDH (Glyceraldehyde 3 phosphate dehydrogenase 2)*, *Eif-4a (Eukaryotic initiation factor 4a)*

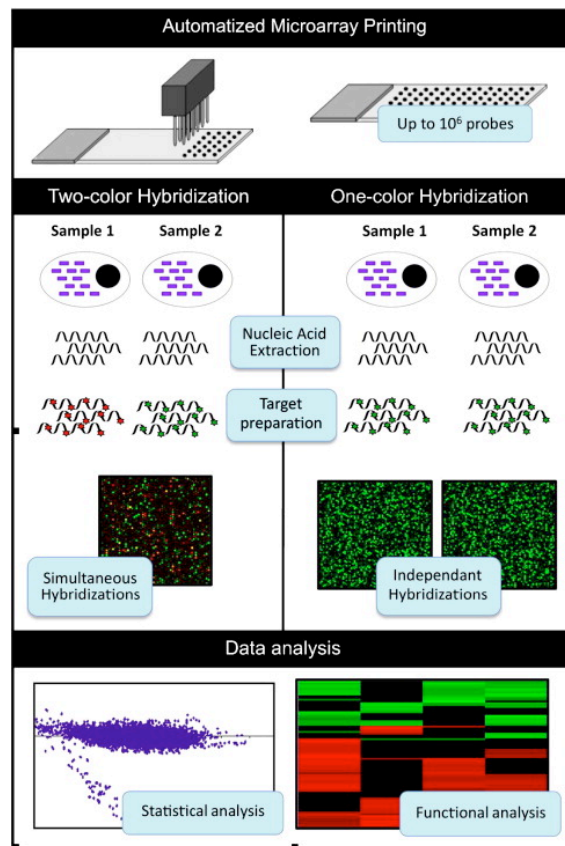


Fig. 23: Flow chart for a microarray experiment (from Leroy and Raoult, 2010). We used one color hybridization for our experiments and the two sets of samples were WT and mutants (in collaboration with S. Kneitz and N. Nuwal).

1.9.3 Mass spectrometry for analysis of posttranslational modifications (PTMs)

Prior to mass spectrometry, Edman degradation method was used for detection and verification of PTMs like phosphorylation. The process was very cumbersome and had limitations like-

- A. insolubility of the phosphoamino acid products and
- B. the necessity to obtain highly purified phosphopeptides.

Recent technological advances like coupling of HPLC with mass spectrometer/s for selective and controlled injection of complex peptide mixtures have made MS or tandem MS an ideal choice for detection and analysis of post-translational modifications

like phosphorylation. In a given protein or peptide mixture, the amount of proteins/peptides with a specific PTM like phosphorylation are lesser in quantity when compared to the total amount of protein/peptide. Thus, it becomes imperative to enrich the proteins/peptides with the desirable PTM or begin with a larger amount of crude sample.

Several approaches have been reported to enrich proteins/peptides with phosphorylated residues (Reinders and Sickmann, 2005) :

- A. Affinity enrichment of phosphorylated species, e.g., by immobilized metal-affinity chromatography (IMAC) on Fe^{3+} , ZrO_2 or TiO_2 matrices.
- B. P-Ser/P-Thr/P-Tyr antibodies can be used to enrich phosphorylated proteins by immunoprecipitation. However, for *Drosophila* phosphorylated residues specific antibodies do not work well.

In mass-spectrometric analysis, the protein sample is digested by an enzyme (e.g., Trypsin) or by a cocktail of several enzymes to produce short peptides (mass preferably lesser than 7-10 kD). The peptides are introduced into the MS in an ionized state and these ionic species are analyzed by the first analyzer and this produces the precursor ion spectrum. Through collision-induced dissociation (CID) with an inert gas like argon these ionic species are fragmented to produce product ions, which are analyzed using a second mass analyzer. Under these conditions, a phosphopeptide produces two types of product ions namely PO^{3-} and PO^{2-} with masses of 79 Da and 63 Da respectively. The presence of these phosphorylations is further verified by running the sample again but after treatment with alkaline phosphatase to remove all phosphorylation and thus in this sample we practically do not observe product ions at 79 Da and 63 Da (Annan et al., 2001; Steen et al., 2001; Zappacosta et al., 2002). The Figure 24 describes a nano-LC-MS/MS method (direct coupling of a high performance liquid-chromatography system to a mass spectrometer) for determining phosphorylation sites from a peptide mixture generated by in-gel digestion.

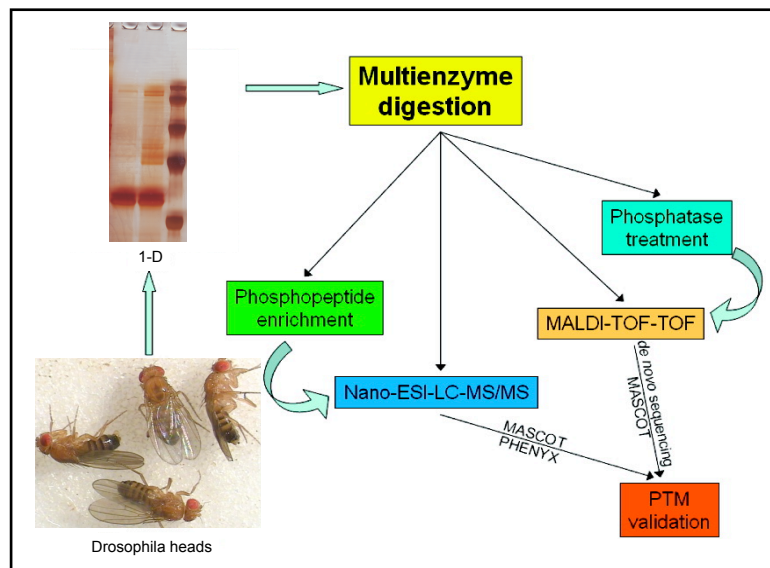


Fig. 24: LC-ESI MS/MS method for determining phosphorylation sites from a peptide mixture generated by in-gel digestion (modified from John et al., 2007). We performed the nano-LC-ESI-MS/MS after multienzyme digestion of gel extracted immunoprecipitated sample. The PTMs obtained were validated by MASCOT software.

2. MATERIALS

2.1 Fly rearing

The flies were grown in large or medium sized vials containing yeast, agar and corn meal media. The vials were maintained at 25°C, 60%-70% relative humidity, with a 14/10-h light/dark cycle.

Fly strains used for different experiments are as given below:

2.2 Fly strains

- Canton S In lab
- *w¹¹¹⁸*; +; + In lab
- *w⁻*; +; *Sap47¹⁵⁶ CS* Funk, N.
- *w⁻*; +; *Syn⁹⁷ CS* Funk, N.
- *w⁻*; +; *TM3/TM6* In lab
- *w⁻*; +; *Tri/Sap47¹⁵⁶ CS, Syn⁹⁷ CS* Funk, N.
- *w⁻*; +; *Sap47¹⁵⁶ CS-V, Syn⁹⁷ CS-V/Sap47¹⁵⁶ CS-V, Syn⁹⁷ CS-V* Albertowa, V.
(*V1, V2, V3*)
- *w⁻*; +; *Sap47¹⁵⁶ CS-NF, Syn⁹⁷ CS-NF/Sap47¹⁵⁶ CS-NF, Syn⁹⁷ CS-NF* Nuwal, T.
(*NS17, NS62*)
- *w⁻*; +; $\Delta 2-3^{ki}$ Bloomington
- *w⁻*; Actin-Gal4/CyO; + Bloomington
- *elav*-Gal4; +; + Sigrist, S.
- *w⁻*, *elav* Gal4; +; + (*Syn* null background) Godenschwege, T.
- *w¹¹¹⁸*; *Sco*/CyO; + Bloomington
- *w⁻*; UAS *CG12214* RNAi; + VDRC
- *w⁻*; +; UAS *Sap* RNAi Funk, N.
- *w¹¹¹⁸*; Df(2R) BSC350/CyO; + Bloomington
- *w¹¹¹⁸*; Df(2R) BSC281/CyO; + Bloomington
- *w⁻*; +; UAS *Syn* PKA1 non-edited, PKA2 mutated Virstyuk, O.

- *w⁻*; +; UAS *Syn* PKA1 and PKA2 mutated Virstyuk, O.
- *w⁻*; +; UAS *Syn* PKA1 non-edited, PKA2 WT Chen, Y.
- *w⁻*; +; UAS *Syn* cDNA PKA1 mutated, PKA2 WT Husse, J.
- *w⁻*, UAS DCR2; +; *elav* Gal4 Sigrist, S.
- *w⁻*; NP4786/*CyO*; + Kyoto
- *w⁻*; G18151/*CyO*; + Bloomington

2.3 Buffers and reagents

2.3.1 DNA and RNA analysis

2.3.1.1 Primers

- GH13040-not1-fw: 5'-CATT GCGGCCGC ATG CCT TCC CTT TTG G-3'
- GH13040-not1-rw: 5'-GATT GCGGCCGC TCA CTT CTT GGC ATC G-3'
- RpLP0 sense: 5'-CAG CGT GGA AGG CTC AGT A-3'
- RpLP0 antisense: 5'-CAG GCT GGT ACG GAT GTT CT-3'
- G6PD left: 5'-CGA GGC CCT GTA CTT TAA GAT G-3'
- G6PD right: 5'-GCC GGA GTA CTT GAA ATT GTT C-3'
- 1, 1r, 2f: 5'-CGA CGG GAC CAC CTT ATG TTA -3'
- 1f: 5'-CGT AAA GTC ATT GGG CAG GT-3'
- 5r: 5'-AAC CCC CAC AGC AGT CTA TCT-3'
- XP5': 5'-AAT GAT TCG CAG TGG AAG GCT-3'
- RB3': 5'-TGC ATT TGC CTT TCG CCT TAT-3'
- 4, 2r: 5'-CCA ACG TAA CGG CAC TTT AT-3'
- 3r: 5'-CGA GCG ACC TAC ACA CAA AA-3'
- 3f: 5'-TTT CAG GCT CAC ATT GAC CA-3'
- 2: 5'-CGT AAA GTC ATT GGG CAG GT-3'
- 3, 4r: 5'-CAA CCC CAG CAG TCT AT-3'
- 5: 5'-GAT CCA AAA CCA ATC CCA. TCT. A-3'
- 6: 5'-AAA TTC TTC AGC AGG GTA TCC A-3'
- 7: 5'-CTG CTC TAA AGA CCC TGC ATT T-3'

- 8: 5'-GTA GGT GAA CAG GAC CTT GAC C-3'
- 9, 4f: 5'-TCA CTG GCC AGA ACG TGA TA-3'

2.3.1.2 Reagents for RT-PCR

- First strand buffer (5x) Invitrogen
- Oligo(dT)18 Primer Fermentas
- dNTP set Bioline
- Homogenization buffer
 - 10 mM Tris (pH 8.2)
 - 1 mM EDTA
 - 25 mM NaCl
 - added ddH₂O upto 10ml
 - added Proteinase K before use.
- GelPilot Loading Dye, 5x QIAGEN
- TBE (10x)
 - 151.4 ml of Tris
 - 77.3 g of boric acid
 - 23.3 g of EDTA
 - dissolved in 2.5 l of ddH₂O.
- Agarose gel 1%
 - 4 g Agarose
 - 400 ml TBE buffer
 - added 20 µl of EtBr after the temperature reached 65 °C.
- PCR Master Mix Thermo Fisher and Finnzymes

2.3.2 Protein analysis

2.3.2.1 SDS-PAGE and Western blotting

Reagents for SDS-Polyacrylamide gel (1 large gel of dimension 20x15 cm)

Running gel

Reagents	8% (ml)	10%(ml)	12.5%(ml)
----------	---------	---------	-----------

30%Acrylamide bisacrylamide (29:1)	10.66	13.33	16.60
1.88 M Tris/HCl, pH 8.8	8.00	8.00	8.00
Distilled Water	13.10	10.44	7.30
0.5% SDS buffer	8.00	8.00	8.00
10% Ammonium persulfate (APS)	0.20	0.20	0.20
TEMED	0.05	0.05	0.05

Stacking gel

Reagents	5.0% (ml)
30%Acrylamide bisacrylamide (29:1)	1.60
0.635 M Tris/HCl, pH 6.8	2.00
Distilled Water	4.30
0.5% SDS buffer	2.00
10% Ammonium persulfate (APS)	0.06
TEMED	0.01

- SDS buffer (5X)
 - 30 g Tris
 - 144 g glycine
 - 5 g SDS
 - added 1 l of dH₂O, the pH was adjusted to 8.9 and stored at room temperature.
- Laemmli buffer (2X)
 - 1.25 ml Tris (125 mM, pH 6.8)
 - 0.6 ml glycerine (6.0%)
 - 1.0 ml SDS (2.0%)
 - 0.25 ml Bromophenol blue (0.025%)
 - 0.5 ml β-Mercaptoethanol (5.0%)
 - added 6.4 ml ddH₂O for final volume of 10 ml.
- Transfer buffer (1X)
 - 3.02 g Tris 25mM
 - 11.26 g glycine 150 mM
 - 100 ml methanol (10%)
 - added 900 ml of dH₂O,

- the pH was adjusted to 8.3 and stored at 4°C.
- Washing buffer (10X TBST)
 - 12.11 g Tris 100 mM
 - 87.66 g NaCl 1.5 M
 - 5.0 ml Tween-20 (0.5%)
 - added 1 l of dH₂O, the pH was adjusted to 7.6 and stored at room temperature.
 - Blocking buffer (5%)
 - 5 g Non fat dry milk powder dissolved in 100 ml of 1X TBST,
 - warmed the buffer to 50°C and cooled it back to room temperature prior to use.
 - MOPS SDS running buffer (20x)
 - 209.2 g MOPS 1.0 M
 - 121.2 g Tris base 1.0 M
 - 20 g SDS 69.3 mM
 - 6.0 g EDTA free acid 20.5 mM
 - ddH₂O for final volume of 1 l.
 - 1x buffer pH 7.7
 - MES SDS running buffer (20x)
 - 195.2 g MES 1.0 M
 - 121.2 g Tris base 1.0 M
 - 20 g SDS 69.3 mM
 - 6.0 g EDTA free acid 20.5 mM
 - added ddH₂O to 1 l.
 - 1x buffer pH 7.3
 - LDS Sample Buffer (4x)
 - Invitrogen
 - Sample Reducing Agent
 - Invitrogen
 - Antioxidant
 - Invitrogen

2.3.2.2 Buffers and reagents for Blum Silver staining (modified for Mass Spectrometry)

- Gel fixative
 - 80 ml ethanol (100 %)
 - 20 ml acetic acid (100%)
 - 100 ml ddH₂O

- Washing buffer
60 ml ethanol (99.8%)
140 ml ddH₂O.
- Sensitising solution
0.04 g Na₂S₂O₃
200 ml ddH₂O.
- Silver stain
0.4 g AgNO₃
40 µl formaldehyde 37%
200 ml ddH₂O.
- Developer
6.0 g Na₂CO₃
100 ml formaldehyde 37%
200 ml ddH₂O.
- 5% Acetic acid
2.5 ml acetic (100%)
50 ml ddH₂O.
- 1% Acetic acid
500 µl acetic acid (100%)
50 ml ddH₂O.

2.3.2.3 Buffers and reagents for 2D-PAGE

- Homogenisation buffer
303 µl protein solubilizer 1 or 2
(Invitrogen), 1 µl Tris base 1 M
3 µl protease inhibitor cocktail (100x)
3 µl DTT 2 M
6 µl ddH₂O.
- Reducing Solution
0.5 ml DTT (0.5 M)
4.5 ml 1x NuPAGE[®] LDS sample buffer
(Invitrogen).
- Alkylating Solution
28 µl N,N-Dimethylacrylamide
5 ml 1x NuPAGE[®] LDS sample buffer
(Invitrogen).
- Quenching Solution
50 µl DTT (0.5 M)
1 ml ethanol (100%)
4 ml 1x NuPAGE[®] LDS sample buffer
(Invitrogen).

2.3.2.4 Buffers and reagents for Native PAGE

- NativePAGE™ Running Buffer (20x) Invitrogen
- NativePAGE™ Anode Buffer (1x) 50 ml NativePAGE™ running buffer (20x)
950 ml ddH₂O.
- NativePAGE™ Cathode Buffer (1x) 10 ml NativePAGE™ running buffer (20x) (Invitrogen)
1 ml NativePAGE™ cathode additive (20x) (Invitrogen)
189 ml ddH₂O.
- NativePAGE Sample Buffer (4x) Invitrogen
- NuPAGE Transfer Buffer (20x) Invitrogen
- Coomassie staining 1.25 g Coomassie Brilliant blue R250
450 ml methanol
450 ml H₂O
100 ml acetic acid
filtered the solution after complete mixing.
- Destaining solution 30% methanol
10% acetic acid
made up to 1 l with ddH₂O.

2.3.2.5 Buffer and reagents for Enzyme Linked Immunosorbent Assay (ELISA)

- PBS (10X) 14.8 g Na₂HPO₄
4.3 g KH₂PO₄
72.0 g NaCl
added 1 l H₂O and adjusted the pH to 7.4.
- Blocking buffer (1X) 1.0 g Bovine Serum Albumin (BSA)
dissolved in 100 ml of 1X PBS
- Detection buffer (1X) 12.11 g Tris 100mM
0.2 g MgCl₂

added 1 l H₂O and adjusted the pH to 9.5.

2.3.2.6 Buffers and reagents for Immunohistochemistry

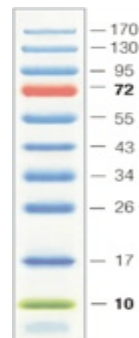
- Normal Saline (1x)
 - 4.08 g NaCl
 - 4.08 g MgCl₂ · 6 H₂O
 - 0.36 g KCl
 - 1.2 g HEPES
 - 0.84 g NaHCO₃
 - 39.2 g Sucrose
 - 40 ml EGTA (0.5 M)
 - added ddH₂O to 1 l.
- Fixative (4% PFA in PBS)
 - 4 g paraformaldehyde (PFA)
 - 20 µl 10N NaOH
 - 90 ml ddH₂O
 - heated to and held at 65°C for 15 min , add 10 ml PBS (10x).
- PBS (10x)
 - 80 g NaCl
 - 2 g KCl
 - 14.4 g NaHPO₄
 - 2.4 g NaH₂PO₄
 - ddH₂O to 1 l and pH to 7.4.
- Blocking solution
 - 0.2% Triton X-100
 - 5% Normal Horse Serum
 - 2% Bovine Serum Albumin (BSA)
 - dissolved in PBS.
- Washing buffer PBST (1x)
 - 10 ml PBS (10x)
 - 100 µl Triton X-100
 - ddH₂O to 1 l and pH to 7.3.

2.4 Proteins and Inhibitors

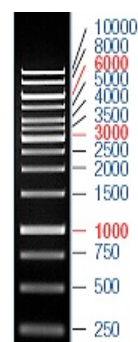
- Aprotinin Roche
- Leupeptin Roche
- Phenylmethylsulfonylfluorid (PMSF) Roche
- Pepstatin Roche
- Avidin-Alkaline Phosphatase Sigma
- Complete Mini, EDTA-free Roche
- DNase Roche
- Protein A-Agarose Roche
- Protein G-Agarose Roche
- Proteinase K Roche
- SuperScript® II Reverse Transcriptase Invitrogen
- RNase (DNase-free) Roche

2.5 Ladders

PageRuler™ Pre-stained Protein Ladder (Fermentas)



GeneRuler™ 1kb DNA Ladder (Fermentas)



2.6. Antibodies

- Mouse MAB nc46 A. Hofbauer
- Mouse MAB nb200 A. Hofbauer
- Mouse MAB 3C11 A. Hofbauer
- Mouse MAB ab49 A. Hofbauer
- Mouse MAB nc82 A. Hofbauer
- Polyclonal anti-TBCE-like T. Nuwal
- β -tubulin rabbit polyclonal IgG Santa Cruz Biotech
- IgG HRP conjugated (Mouse, Rabbit) Biorad
- Biotin conjugated (Mouse, Guinea pig) Biorad
- Rabbit HRP anti-guinea pig IgG Invitrogen
- Alexa Fluor 488
(Mouse, Guinea pig, Rabbit) Invitrogen
- Cy3 (Mouse, Guinea pig, Rabbit) Invitrogen
- Mouse MAB anti-GFP Invitrogen

2.7 Kits

- ECL Western blotting detection reagent Amersham, Millipore
- Alkaline Phosphatase Yellow (pNPP)
Liquid Substrate system for ELISA Sigma
- One-Step Complete Western Kit Genscript

3. METHODS

3.1 Protein analysis

3.1.1 1D-SDS-PAGE (Sodium Dodecyl Sulfate- Polyacrylamide Gel Electrophoresis) analysis

3.1.1.1 Non-pre-cast SDS-PAGE system

The glass plates and the spacers were washed thoroughly and dried prior to use. The running gel solution (10%) was prepared in a falcon tube (50 ml) by mixing the components described in the materials section. Prior to the addition of TEMED the glass plates were set up. The glass plates were clamped to each other with spacers at the bottom and the sides. To seal the bottom, 0.8% agarose was poured along the inner edges of the plates. The agarose was allowed to solidify (about 30 minutes). TEMED was added to the running gel solution and the mixture was vortexed. Immediately after, the solution was poured gently in between the plates from the top. The top surface of the gel was overlaid with layer of water to avoid oxidation of the topmost gel layer.

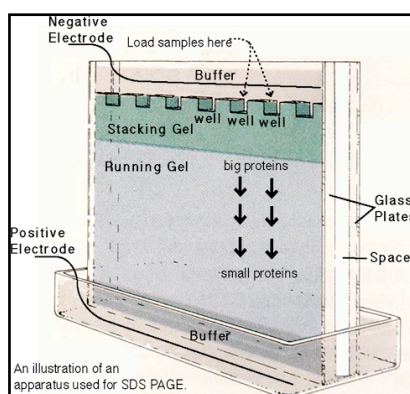


Fig. 25: SDS-PAGE setup and working (Source: World wide web)

The running gel was allowed to polymerise completely (~60 minutes). The stacking gel was prepared in a similar way as running gel but with minor changes (see Materials). After the polymerisation of running gel, the stacking gel solution was poured

on top of it and the comb was carefully placed to avoid any air bubbles in between and under the comb teeth. The gel was allowed to polymerize (~60-80 minutes). After polymerization, the clips clamping the glass plates and the bottom spacers were removed. The cassette (glass plates and gel) was then placed in the buffer as shown above. Proper electrical connections were made and the set up was placed in the 4°C room to dissipate the heat produced during the run. The sample was loaded (70 µl per well) after mixing with 2X Laemmli buffer (1:1 ratio) and boiling at 95°C for 5 minutes. The gel was run at 50 mA for 3 to 4 hours to get optimum resolution of proteins.

The protein ladder was observed as a reference. After achieving desired separation, the power supply was switched OFF and the cassette was carefully removed from the setup. The glass plates were separated and the gel was carefully removed to perform a Western blot (3.1.2) or a Coomassie staining procedure (3.1.3).

3.1.1.2 Pre-cast SDS-PAGE (from Invitrogen)

The samples were mixed with NuPAGE® LDS sample buffer (Invitrogen) and boiled at 70°C for 10 minutes before loading on a pre-cast gel placed in running buffer (MOPS-/MES-SDS buffer). The running conditions were: 200 V constant; 100-125 mA/gel (start), 60-80 mA/gel (end); 50 minutes (MOPS Buffer) or 35 minutes (MES Buffer) respectively. For further analysis, Western Blotting (3.1.2) or silver staining (3.1.4) techniques were performed.

3.1.2 Western blotting

The Western blot technique is an analytical method to transfer and identify proteins separated by SDS-polyacrylamide gel electrophoresis. “Blotting” is the actual transfer of polypeptides from the acrylamide gel to a nitrocellulose or polyvinylidene difluoride (PVDF) membrane in an electric field. The proteins are immobilised on the membrane through hydrophobic interactions. The membrane is then incubated with specific antibodies after appropriate blocking to detect proteins of interest.

Two types of blotting: A. Wet blotting

B. Semi-dry blotting

3.1.2.1 Wet blotting

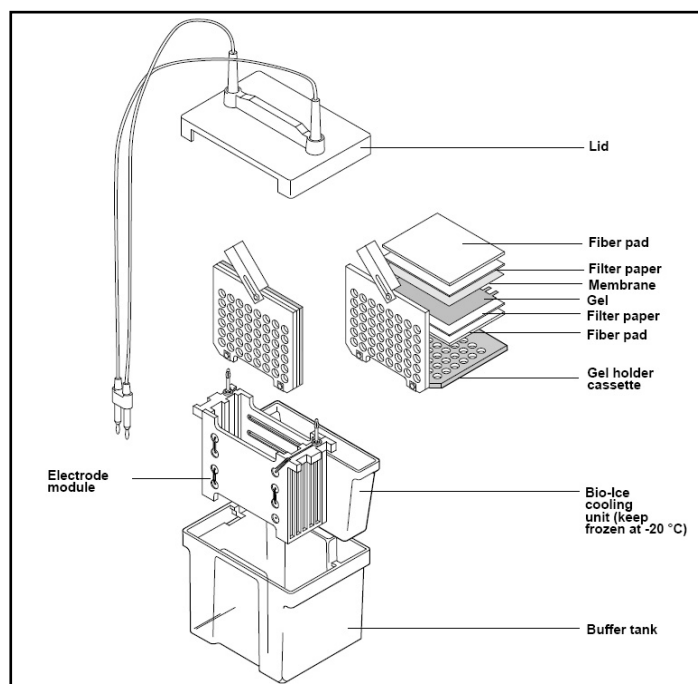


Fig. 26: Wet blotting procedure (Source: BioRad website)

Electric current is used to transfer the proteins from gel to the nitrocellulose membrane which is kept completely immersed in a chamber filled with transfer buffer. A transfer stack, as seen in Figure 26 was set up in a “Mini” trans-blot system (Bio-Rad). Sponges and Whatman filter paper were soaked in the transfer buffer and the membrane was placed between the gel and the cathode, the power supply was switched ON (100 V constant) and the protein samples due to the high negative charge (due to SDS binding) moved towards the cathode and on to the membrane.

3.1.2.2 Semi-dry blotting

On completion of SDS-PAGE, the gel was incubated in transfer buffer for 15 minutes to remove the salt and other traces of impurities. Filter papers and nitrocellulose membrane were cut according to the size of the gel. Filter papers and the membrane were soaked in transfer buffer for 10-15 minutes. Gel, filter papers and the membrane were arranged as shown in Figure 27.

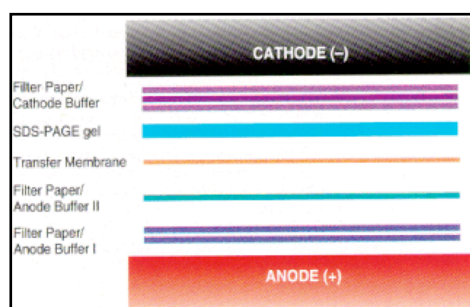


Fig. 27: Semi dry blot setup and working (Source: world wide web)

The electrophoretic transfer was done using semi-dry method. The power pack was adjusted so as to constantly deliver 4 W (400 mA and 10 V) of power. The transfer procedure took about 2-3 hours. After the completion of transfer, the membrane was incubated in 5% Non Fat Dry Milk (NFDM) in washing buffer (1X TBST) for 12 hours on a shaker at 4°C in order to block unspecific protein binding sites on the membrane.

On completion of membrane blocking, the membrane was then incubated with the primary antibody (3C11, nc46 etc) for 2 hours at room temperature. The primary antibody dilution was done in washing buffer (see Materials). The dilutions of various antibodies used in this thesis are as mentioned below:

Primary antibody	Dilution
3C11	1:50

nc46	1:200
nb200	1:50
ab49	1:50
Anti- β -Actin	1:3000
Anti-TBCEL	1:4000

On completion of Western blotting (end of 2 hours), the antibody solution from the membrane was removed and 3 washes (10 minutes each) with the washing buffer were performed on a shaker at room temperature, the membrane was then incubated with the secondary antibody (anti-mouse HRP-conjugated) diluted (1:7500) in the washing buffer, for 1 hour at room temperature. On completion, the antibody solution was removed and stored at 4°C. Non-specifically bound secondary antibody was removed by washing the membrane 3 times (10 minutes each) with washing buffer on a shaker at room temperature. The detection and visualisation of protein band was done using ECL (Enhanced Chemiluminescence) kit. The chemiluminescent reagents were mixed in the ratio 1:1 just prior to use. The nitrocellulose membrane was laid on a clean dry surface with the side with the bound antibody facing up. The chemiluminescent solution was poured over the membrane, covering it completely. The solution was allowed to stand on the membrane for 1 minute and then drained.

The membrane was covered with a thin plastic film and placed in a cassette. The membrane was then exposed to a X-Ray film in a dark room for 1-15 minutes and then the film was developed and fixed. Finally, the X-Ray film was washed with copious amounts of water and allowed to dry.

3.1.3 Coomassie Staining

This technique of protein detection and visualisation can detect upto 100 ng of proteins. After SDS-PAGE, the apparatus was disassembled and the gel was removed from the glass plates and soaked in water for 30 minutes. The water was drained and the

gel was covered with the colloidal coomassie stain. The proteins were fixed by incubating with fixative (see Materials) overnight at room temperature with gentle agitation. The gel was covered during this process to avoid contamination and to prevent the evaporation of the solution. The stain was then removed and the destaining solution was added to the gel. The destaining procedure was carried out till a sufficient contrast was observed between the background and the protein bands. The procedure was accelerated by adding kimwipe tissues to the destaining solution and allowing the gel to destain with gentle agitation, the kimwipes were changed several times to increase the effectiveness. The destaining was continued until the protein bands were seen with minimal background staining of the gel.

3.1.4 Silver staining

This technique of protein detection and visualisation can detect upto 5-10 ng of proteins. The SDS-PAGE was performed using 10% precast Bis-Tris gels at constant voltage of 200 V in a MOPS running buffer (Invitrogen, Germany). On completion of the run, the gel was transferred to a glass chamber for silver staining according to modified Blum silver staining protocol for mass spectrometry (Mortz et al., 2001). Briefly, the gel was fixed in a solution containing 40% ethanol, 10% acetic acid at room temperature for 1 hour on a shaker. The gel was washed with 30% ethanol for 20 min on a shaker and this step was repeated two more times with the final wash being with ultra pure water. Sensitisation of the gel was performed by incubation in 0.02% sodium thiosulfate (Sigma, Germany) for 1 min and the gel was immediately washed 3 times with ultra pure water for a total of 1 min. Cold staining solution containing 0.2% silver nitrate (Sigma, Germany) and 0.007% formalin (Sigma, Germany) was added and the gel was incubated at 4°C for 20 min on a shaker. The gel was washed with ultra pure water 4 times for a total of 1 min and then transferred to a new glass chamber. Briefly washed the gel for 1 min with ultra pure water and then proceeded to visualisation of signal. For visualisation of the proteins the gel was incubated with developer solution containing 3% sodium carbonate and 0.05% formalin until sufficient signal to background contrast was obtained. The reaction was terminated by addition of 5% acetic acid. The gel was washed and stored in 1% acetic acid until further analysis.

3.1.5 2D-SDS-PAGE analysis

The two-dimensional polyacrylamide gel electrophoresis is a method to separate mixtures of proteins according to their charge (pI) in the first dimension through isoelectric focusing (IEF) and according to their size (M) by SDS-PAGE in the second dimension (Fig. 28). The 2D PAGE was performed using the ZOOM® IPG runner system by Invitrogen.

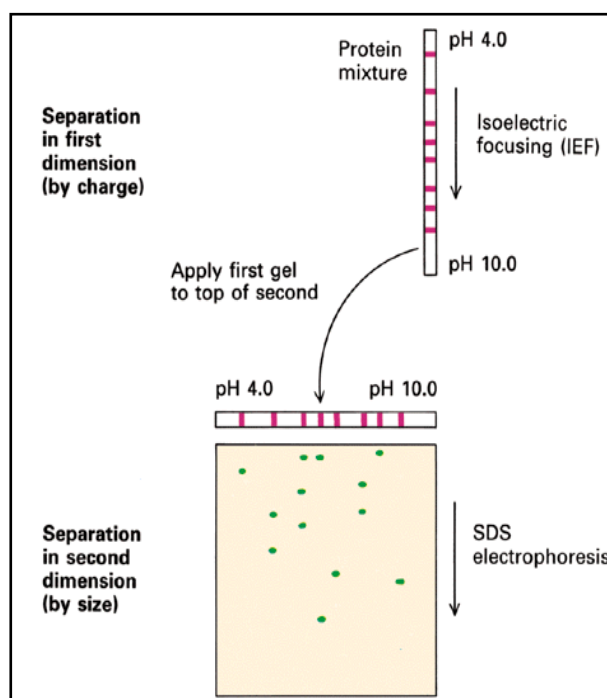


Fig. 28: 2D SDS-PAGE protocol (Source: world wide web)

3.1.5.1 Sample preparation for 2D-SDS-PAGE

12 fly heads of a given genotype were collected and homogenised in the sample buffer (303 μ l ZOOM 2D Protein solubilizer 1 or 2, 1 μ l Tris Base, 3 μ l Protease inhibitor cocktail, 3 μ l of 2 M DTT and 6 μ l ddH₂O).

The samples were incubated at room temperature for 15 minutes on a rotary shaker. Alkylation was carried out by adding 1.6 μ l Dimethylacrylamide (DMA) and incubating on a shaker at room temperature (RT) for 30 minutes. The excess DMA was

quenched by adding 3.5 μl of 2 M DTT and centrifugation at 13,000 rpm for 20 minutes at 4°C. The supernatants were transferred into fresh eppendorf tubes and centrifuged again for 10 minutes at 4°C. 140 μl of the supernatant from each sample was transferred to a clean tube and mixed with 15 μl ZOOM[®] 2D Protein solubiliser, 1 μl DTT (2 M), 1.6 μl of the ampholytes (3-10), 1.4 μl ddH₂O and trace amounts of bromophenol blue dye.

The IPG strips were incubated in the sample buffer prepared above in a special cassette from Invitrogen. The cassette was sealed using the provided sealing tape and left overnight at 18°C. On the next day, the sealing tape and the sample loading device were removed from the cassette. An electrode wick was first wet with 600 μl of water and placed at each end of the cassette over the adhesive using the black alignment marks to align the wicks. The cassette was then placed in a running chamber designed for isoelectric focussing (Invitrogen). The outer chamber was filled with 600 ml of deionized water without pouring any liquid into the inner chamber. The chamber was closed with the lid and connected to the power supply (ZOOM[®] Dual Power by Invitrogen).

3.1.5.2 First dimension: Isoelectric focussing

The isoelectric focussing was performed using the broad pH and the narrow pH range ZOOM[®] strips. Running conditions: 2000 V; 0.05 mA/strip; 0.1 W/strip; 1600 Vh.

3.1.5.3 Second dimension: SDS PAGE

On completion of isoelectric focussing the cassette was removed from the chamber and the gel strips were prepared for second dimension of the 2D PAGE as follows:

1. Reducing step (Incubated the strip in 0.05 M DTT at room temperature for 20 minutes).
2. Alkylating step (Incubated the strip in 125 mM iodoacetamide at room temperature for 20 minutes).

The buffer recipes for each step are provided in the materials section.

The plastic ends of the IPG strips were cut off and the strips were carefully placed in the wells of precast 4-12% Bis-Tris gels (Invitrogen). The strips were overlaid with 60 μ l of LDS sample buffer (1x) and the protein marker was loaded into the marker well. The chamber was filled with MOPS-/MES-SDS running buffer and 500 μ l of NuPAGE[®] antioxidant/ β -mercaptoethanol was added to the inner buffer chamber. The chamber was closed firmly and connected to the power supply. The running conditions were as follows: 200 V constant; 100-125 mA/gel (start), 60-80 mA/gel (end); 50 minutes (MOPS Buffer) or 35 minutes (MES Buffer) respectively.

On completion of the electrophoresis the gel was transferred on to a nitrocellulose membrane using the Western blot Protocol (see above).

3.1.6 Native PAGE analysis

3.1.6.1 BN-PAGE

The blue native polyacrylamide gel electrophoresis is a method for separation of native proteins and multiprotein complexes (MPCs) (Schagger and von Jagow, 1991; Swamy et al., 2006; Wittig and Schagger, 2008) (Fig. 29). It is highly useful in determination of the size, subunit composition, and relative abundance of different MPCs.

The blue native polyacrylamide gel electrophoresis relies on binding of the Coomassie blue G250 dye which provides the negative charge to the protein. In an electric field, during migration to the anode, protein complexes are separated according to molecular mass and/or size and high resolution is obtained by the decreasing pore size of the polyacrylamide gradient gel.

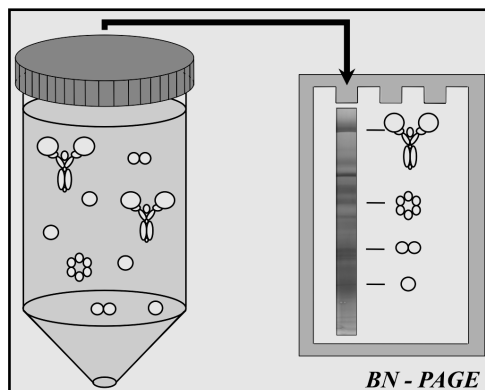


Fig. 29: BN-PAGE (modified from Eubel et al., 2005)

3.1.6.2 BN-SDS-PAGE

On completion of the gel electrophoresis under native condition the lanes which contained the sample were cut out of the gel using a sharp knife. The gel strips were prepared for the second dimension as described below:

1. Reduction (Incubated the gel strip in 4.5 ml of 1X LDS sample buffer with 0.5 M DTT at RT for 20 minutes).
2. Alkylation (Incubated the gel strip in 5 ml of 1X LDS sample buffer with 28 μ l of DMA at RT for 20 minutes).
3. Quenching (Incubated the gel strip in 4 ml of 1X LDS sample buffer with 1 ml of ethanol (100%) and 0.5 M DTT at RT for 15 minutes).

The gel strip was carefully placed in the well of a precast 4-12% Bis-tris gel (Invitrogen) (Fig. 30). Further steps were similar to second dimension of 2D-SDS-PAGE (3.1.5). On completion of the electrophoresis the gel was transferred on to a nitrocellulose membrane using the Western blot protocol (see above).

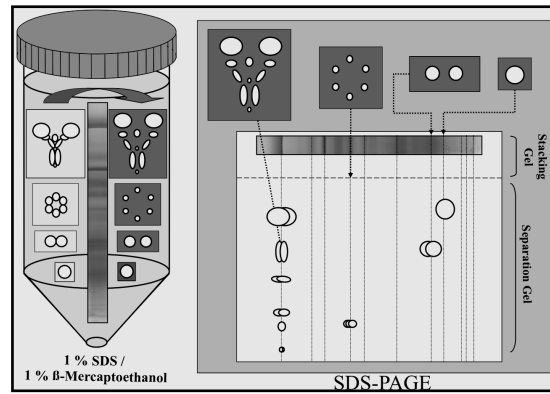


Fig. 30: BN-SDS-PAGE (modified from Eubel et al., 2005)

3.2 Immunochemistry procedures

3.2.1 Immunoprecipitation

Immunoprecipitation is a technique to enrich and isolate a protein of interest from a crude protein mixture. The protein specific antibody is coupled to a substrate or matrix by high affinity interaction or in some cases by formation of covalent bonds (e.g., Cross-linking of antibody by DSS cross linker). This matrix coupled antibody is added to and incubated with the crude protein mixture allowing specific protein to be bound to the antibody and subsequently enriched from the mixture. Either polyclonal or monoclonal antibodies from various animal species can be used in immunoprecipitation protocols and in our case the antibodies used (3C11, nc46 etc) were all mouse derived. Antibodies were bound non-covalently to immunoabsorbents such as protein A– or protein G–agarose (Fig. 31).

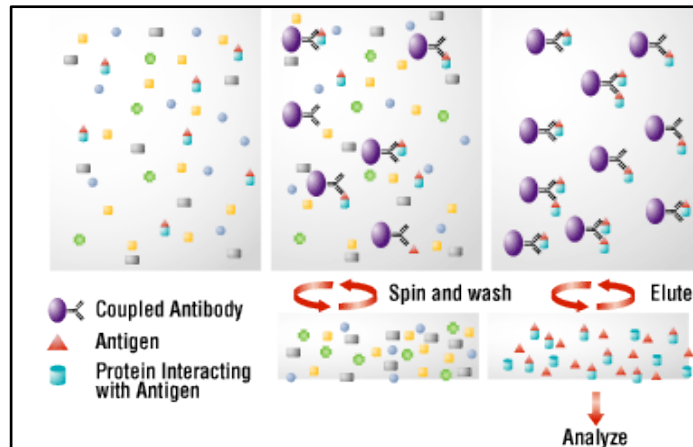


Fig. 31: Immunoprecipitation procedure (Source: world wide web)

3.2.1.1 Small scale lysate preparation

25-50 *Drosophila* heads of required genotypes were manually collected by severing adult *Drosophila* with surgical scalpel. The heads were transferred to fresh eppendorf tubes and 20 μ l of lysis buffer per head was added to the tubes. The homogenisation was done on ice using plastic or glass pestles and the homogenate was incubated at 4 °C for an hour. The tubes were centrifuged at 13,000 rpm for an hour at 4°C, the pellet was discarded and the supernatant was transferred to a fresh eppendorf tube. About 30-40 μ l of the supernatant was taken in a separate eppendorf and mixed with equal amount of (1:1) 2X Laemmli buffer and stored at -20°C to be used as a lysate control in SDS-PAGE analysis. Rest of the sample was used for immunoprecipitation by specific antibody.

3.2.1.2 Large scale lysate preparation

375 mg of *Drosophila* heads (approximately 2500 heads) were homogenised using pre-cooled glass homogenisers (Hartenstein, Germany) in homogenisation buffer consisting of 150 mM NaCl (chemicals from AppliChem, Germany, unless otherwise noted), 0.1 % Nonidet P-40 (NP-40), 20 mM Tris-HCl pH 7.6, 10 mM sodium fluoride (NaF), 10 mM β -glycerol phosphate, “mini”-EDTA free protease inhibitors (Roche, Switzerland), 2 tablets in 10 ml of buffer. The homogenate was cleared by centrifugation

at 16,000g at 4°C. The cleared homogenate was transferred to a fresh tube suitable for ultracentrifugation (Beckman, USA) and ultracentrifuged (L8-70M, Beckman, USA) at 100,000g for 60 min at 4°C. The final cleared lysate was transferred to fresh 15 ml falcon tubes and kept on ice until used for further analysis. After the collection and homogenisation of the fly heads, the buffers for the immunoprecipitation were prepared.

3.2.1.2.1 Immunoprecipitation protocol without cross-linking of antibody to beads

50 µl of protein G-agarose beads (Roche, Switzerland) were added to 2 ml of hybridoma supernatant in two polyethylene filter attached centrifuge columns (pore size 30 µm) and incubated on a rotator for 4 hours at 4° C. The columns were placed in a 15 ml falcon tube and centrifuged at 300g for 1 min to remove unbound antibody. The columns were washed 3 times with wash buffer containing 500 mM NaCl, 0.1 % NP-40, 20 mM Tris-HCl pH 7.6, 10 mM NaF, 10 mM β-glycerol phosphate, EDTA free protease inhibitors, 2 tablets in 10 ml of buffer. The wash buffer was completely removed from the columns by centrifugation at 300g for 5 min. The cleared lysate from *CS* and *Syn*⁹⁷ were added to the antibody-coupled beads in two columns and incubated overnight on a rotator at 4°C. The columns were centrifuged at 300g for 1 min and the flow-through was discarded. The columns were washed 7 times with 2 ml of wash buffer each. The columns were centrifuged at 300g for 1 min after each wash to remove the wash buffer and the centrifugation after the last wash was carried out for 5 min to remove any traces of the buffer. The beads were incubated in 50 µl of 4X LDS sample buffer (Invitrogen, Germany) for 30 min. The columns were centrifuged at 500g and the flow-through was collected in fresh Eppendorf tubes. To the tubes, 6 µl of 0.5 M DTT (Sigma, Germany) was added and the tubes were incubated in a heat block at 70°C for 10 min. The tubes were cooled on ice and 15 µl per lane were loaded on a 10 % precast Bis-Tris gels (Invitrogen, Germany) for further analysis.

3.2.1.2.2 Immunoprecipitation protocol with cross-linking of antibody to beads

The IP procedure mentioned above is modified to further limit antibody contamination in the sample by coupling the 3C11 antibody covalently to protein G-

agarose beads using disuccinimidyl suberate (DSS). The elution was performed competitively by using the 3C11 epitope containing peptide (60 µg/ml of the peptide was used for each elution).

Disuccinimidyl suberate (DSS) is a membrane permeable cross-linker. It contains amine-reactive N-hydroxysuccinimide (NHS) ester groups at both ends. NHS esters react with primary amines at pH 7-9 to form stable amide bonds. DSS was first dissolved in DMSO, then added to the aqueous cross-linking reaction mix containing the antibody (MAB 3C11) and the protein G-agarose beads. Antibody and protein G have several primary amines in the side chain of their lysine (K) residues that are cross-linked through the NHS-ester in DSS.

3.2.2 Enzyme Linked Immunosorbent Assay (ELISA)

The ELISA technique is widely used to detect antibody or antigen quantitatively and/or qualitatively as per the need. In this thesis the ELISA technique is used to detect the presence of antigen (protein) in *Drosophila* tissue homogenates (Fig. 32). The various steps involved in the technique are as follows: The antigen was obtained in PBS buffer by homogenizing the fly heads using mortar and pestle. About 50 µl of antigen was loaded in each well of the ELISA plate. The plate was kept at room temperature on a shaker for 2 hours. After 2 hours of incubation, the plate was washed once with water. Blocking solution (see Materials) was added to each well (300 µl/well). The plate was kept on a shaker for about 2 hours at room temperature. On completion of the blocking step the primary antibody was added to each well (100 µl / well) and incubated at 4°C on a shaker for 12 hours. The primary antibody solution was prepared by diluting the antibody in blocking solution.

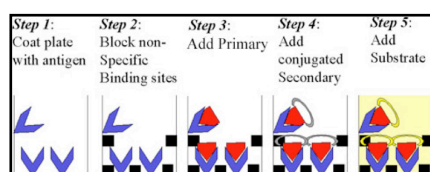


Fig. 32: ELISA procedure (Source: world wide web)

PBS washes (3 times) were performed for 10 minutes duration each. In the next step the secondary antibody (anti-mouse biotin conjugated, diluted in blocking solution (1:400)) was added to each well (100 µl/well) and the plate was incubated at room temperature for 2 hours. Three washes with PBS were performed for 10 minutes duration each. In the next step, avidin alkaline phosphatase (diluted in blocking solution (1:10000)) was added to each of the wells (100 µl/well) and the plate was incubated at room temperature for 1 hour. Two washes with PBS were performed for 10 minutes duration each followed by the third wash using detection buffer (Tris/HCl, MgCl₂ pH 9.5) for 10 minutes duration. The substrate (pNPP) was added (100 µl/well) and the plate was kept in the dark until colour development was observed. The developed colour was measured at 405 nm using the ELISA reader and the data was analysed using statistical software (Origin Version 7.5).

3.2.3 Cryosections and dissections of adult *Drosophila* tissues

Flies were anaesthetised and glued to a plastic stick with their thorax. The stick was dipped in freshly prepared ice cold fixative buffer containing 4% paraformaldehyde. Proboscis and air sacs were removed with the help of a tweezer and a sharp blade. Flies were fixed at 4°C for 3-4 hours and then the solution was replaced with *Drosophila* saline containing 25% sucrose and incubated overnight. Fly heads were immersed in 3% carboxymethylcellulose (CMC) gel on a peg and frozen in liquid nitrogen after orienting. Cryosections were collected on pre-chilled SuperFrost™ Plus (Menzel-Glaser GmbH) slides and left at -20°C for 20 minutes prior to drying them at RT. Slides were marked with a grease pen around the sections. Sections were blocked with normal serum (Vectastatin ABC kit, Vector laboratories) at RT. Primary antibody was applied for overnight incubation at 4°C. After washing in PBST 2 times, 10 minutes each, appropriately diluted secondary antibody (Vectastatin ABC kit, Vector laboratories) was added to the sections for 1 hour at 37°C.

ABC complex was added to the sections for 1 hour at 37°C after washing the secondary antibody away with PBST 2 times, 10 minutes each. After monitoring the colour development, and obtaining the desired staining, sections were washed with 1X

PBST and dH₂O to stop the reaction and were mounted in the vectashield mounting medium.

For whole mount stainings, adult *Drosophila* heads or testis were dissected in ice-cold calcium-free saline. The preparations were fixed in ice cold buffered 4% paraformaldehyde pH 7.4 for 30 min on ice. After fixation the preparations were washed 3 times for 10 minutes each in PBST (PBS containing 0.1% Triton-X 100) at room temperature. Non-specific binding was blocked by incubating with a blocking solution (2% BSA (Sigma-Aldrich), 5% normal serum (Vector Laboratories, Burlingame, USA) in PBST) for 2 hour at room temperature. Incubation with the primary antibody was performed over night at 4 °C. Before incubation with the secondary antibody, unbound primary antibody was removed by washing with PBST (5 times, 15 minutes each) at room temperature. Incubation with the fluorophore coupled secondary antibody was performed at room temperature in the dark for 1 h. Secondary antibodies were diluted 1:1000 in 1X PBST. Then unbound secondary antibody was removed by washing in PBST for 5 times, 20 minutes each in the dark. Finally, preparations were mounted in Vectashield (Vector Laboratories) mounting medium. Scans were performed with a confocal laser scanning microscope and the images were processed using ImageJ software.

3.3 Peptide analysis by nano-LC-ESI-(CID/ETD)-MS/MS (in collaboration with S. Heo and G. Lubec)

3.3.1 In-gel trypsin digestion of proteins and peptides for MS analysis

The gel pieces from SDS-PAGE gels were cut into small pieces and transferred to a 1.5 ml tube. They were incubated with 100 µl of destaining solution (50 mM potassium hexacyanoferrate/300 mM sodium thiosulfate) for 10 min with vortexing. Destained gel pieces were washed 4 times with washing solution (50% methanol/40% water/10% glacial acetic acid) for 5 min each with vortexing. The gel pieces were completely covered with 100 µl of 100% acetonitrile and incubated for 10 min. The gel pieces were dried completely using a SpeedVac concentrator. Cysteine residues were reduced by

treatment with a 10 mM dithiothreitol (DTT) solution in 100 mM ammonium bicarbonate pH 8.6 for 60 min at 56°C. To perform alkylation, the DTT solution was discarded and the same volume of a 55 mM iodoacetamide (IAA) solution in 100 mM ammonium bicarbonate buffer pH 8.6 was added and incubated in darkness for 45 min at 25°C. The IAA solution was replaced by washing buffer (50% 100 mM ammonium bicarbonate/50% acetonitrile) and washed twice for 15 min each with vortexing. Gel pieces were washed in 100% acetonitrile followed by drying in a SpeedVac.

The dried gel pieces were re-swollen by incubating for 16 h (overnight) at 37°C with 12.5 ng/μl trypsin (Promega, Germany) solution reconstituted in 25 mM ammonium bicarbonate. The supernatant was transferred to fresh 0.5 ml tubes, and the peptides were extracted with 50 μl of 0.5% formic acid / 20% acetonitrile for 20 min in a sonication bath, repeated the step three times. Samples in extraction buffer were pooled in 0.5 ml tubes and concentrated (SpeedVac concentrator). 15 μl HPLC grade water (Sigma, Germany) was added to approximately 15 μl of concentrated sample and proceeded to nano-LC-ESI-(CID/ETD)-MS/MS analysis (HCT; Bruker, Germany).

3.3.2 In-gel alkaline phosphatase treatment for MS analysis

Gel pieces spots were destained, reduced, alkylated and dried as described above. The dried gel pieces spots were incubated in a solution of 0.5 μl of calf intestine alkaline phosphatase (New England Biolabs, Ipswich, MA, USA) in the presence of 100 mM ammonium bicarbonate for 1 h at 37°C. Washed the gel pieces with washing solution (50% 100 mM ammonium bicarbonate/50% acetonitrile), dried in 100% acetonitrile and subsequently dried in a SpeedVac followed by in-gel digestion and extraction for nano-LC-ESI-(CID/ETD)-MS/MS analysis (HCT; Bruker, Germany).

Trypsin digested peptides were separated by biocompatible Ultimate 3000 nano-LC system (Dionex, Sunnyvale, CA, USA) equipped with a PepMap100 C-18 trap column (300 μm id × 5 mm long cartridge, from Dionex) and PepMap100 C-18 analytic column (75 μm id × 150 mm long, from Dionex). The gradient consisted of (A) 0.1% formic acid in water, (B) 0.08% formic acid in ACN: 8–25% B from 0 to 195 min, 80% B

from 195 to 200 min and 8% B from 200 to 205 min. An HCT ultra-PTM discovery system (Bruker Daltonics, Bremen, Germany) was used to record peptide spectra over the mass range of m/z 350–1500 Da, and MS/MS spectra in information-dependent data acquisition over the mass range of m/z 100–2800 Da. Repeatedly, MS spectra were recorded followed by three data-dependent collision induced dissociation (CID) MS/MS spectra and three electron transfer dissociation (ETD) MS/MS spectra generated from three highest intensity precursor ions. The voltage between ion spray tip and spray shield was set to 1500 V. Drying nitrogen gas was heated to 150°C and the flow rate was 10 l/min. The collision energy was set automatically according to the mass and charge state of the peptides chosen for fragmentation. Multiple charged peptides were chosen for MS/MS experiments due to their good fragmentation characteristics. MS/MS spectra were interpreted and peak lists were generated by DataAnalysis 4.0 (Bruker Daltonics).

Searches were performed by using the MASCOT v2.2.06 (Matrix Science, London, UK) against latest UniProtKB database for protein identification. Searching parameters were set as follows (i) MASCOT: enzyme selected as used with four maximum missing cleavage sites, species limited to *Drosophila*, a mass tolerance of 0.2 Da for peptide tolerance, 0.2 Da for MS/MS tolerance, fixed modification of carbamidomethyl (C) and variable modification of methionine oxidation (M) and phosphorylation (S, T, Y). Positive protein identifications were based on significant MOWSE scores. After protein identification, an error-tolerant search was performed to detect unspecific cleavage and unassigned modifications. Protein identification and modification information returned from MASCOT were manually inspected and filtered to obtain confirmed protein identification and modification lists of CID MS/MS and ETD MS/MS.

Posttranslational modification searches were done using Modiro v1.1 software (Protagen AG, Germany) with following parameters: enzyme selected as used with four maximum missing cleavage sites, species limited to drosophila, a peptide mass tolerance of 0.2 Da for peptide tolerance, 0.2 Da for fragment mass tolerance, modification 1 of carbamidomethyl (C) and modification 2 of methionine oxidation. Searches for unknown mass shifts, amino acid substitution and calculation of significance were selected on

advanced PTM explorer search strategies. A list of 172 common modifications including phosphorylation, methylation and hydroxylation was selected and added to virtually cleaved and fragmented peptides searched against experimentally obtained MS/MS spectra. Positive protein identification was first of all listed by spectra view and subsequently each identified peptide was considered significant based on the 0.2 Da delta value, ion-charge status of peptide, b- and y- ion fragmentation quality, ion score and significant scores. The Modiro software is complementary to the MASCOT software, using already identified sequences, and has the advantage that also unknown mass shifts can be handled. Protein identification and modification information returned were manually inspected and filtered to obtain confirmed protein identification and modification lists.

3.4 Generation of anti-TBCEL antiserum

The antisera for *Drosophila* TBCEL was generated by cloning the complete cDNA clone GH13040 (from BDGP Gold cDNAs collection) downstream of an in-frame His-tag in a pET 28a expression vector and expressing it in *E.coli* to generate large amount of His-TBCEL. The His-TBCEL was injected in Guinea pigs (in collaboration with G. Krohne) and the animal was sacrificed after sufficient antisera was produced against the immunised TBCEL and the serum was collected.

3.4.1 Cloning of *Tbcel* cDNA in expression vector

Not I restriction sites were linked to the GH13040 cDNA clone using GH13040-not1-fw and GH13040-not1-rw primers by a linker PCR (refer to Materials section). The PCR product and the vector was digested with Not I restriction enzyme (2-3 hours at recommended temperature). The fragments were ligated by incubating overnight at 18°C with DNA ligase enzyme. The presence of right insert in proper orientation was verified by restriction digestion with Sac I and Kpn I. Sac I and Kpn I cut in the vector and inserted fragment, respectively. The cloning was further verified by sequencing. The ligated product was used to transform competent *E.coli* cells.

3.4.2 Expression of protein in *E.coli* and immunisation of Guinea pig for antisera production (in collaboration with G. Krohne)

E.coli BL21 cells were transformed for expression of His-TBCEL. The transformed *E.coli* cells were used to inoculate 500 ml culture media for large scale production of His-TBCEL on induction by IPTG. The culture was monitored for growth at 37°C and after sufficient growth was obtained the cells were precipitated and the protein was extracted after lysis according to the protocol (Qiagen; Hilden; Germany). The His-TBCEL protein was purified by using nickel-chelate affinity chromatography following the protocol (Qiagen; Hilden; Germany). 1 µg of His-TBCEL in 50 µl urea buffer (8 M urea in PBS (137 mM NaCl, 70 mM Na₂HPO₄, 30 mM NaH₂PO₄)) was mixed with 600 µl ddH₂O and incubated on ice for 10 minutes. 700 µl of Freund's adjuvant was added to the above solution and thoroughly mixed. The mixture of Freund's adjuvant and His-TBCEL was used for immunising the guinea pigs. Incomplete Freund's adjuvant were used for subsequent booster dosages. Whole blood was collected after sacrificing the animal, and the serum was separated for antibody purification (in collaboration with G. Krohne).

3.5 DNA analysis

3.5.1 Isolation And Purification Of Genomic DNA

3.5.1.1 Large amount of genomic DNA isolation

The desired number of flies were collected and kept on ice. 50 flies/preparation were homogenised in 1 ml of homogenisation buffer (100 mM NaCl, 100 mM Tris 50 mM, EDTA (pH 8.0), 0.5% SDS). Homogenate was incubated at 68 °C for 30 minutes. The homogenate was then incubated on ice for 30 minutes after the addition of 125 µl of 8 M calcium acetate. A centrifugation for 10 minutes at 14,000 rpm followed this step and was repeated once after transferring the supernatant to a fresh tube. The DNA was precipitated with 2.5 volumes of 100% ethanol for 10 minutes at RT. The pellet was washed with 70% ethanol, dried and dissolved in the appropriate amount of 10mM Tris

pH- 8.0 or dH₂O. This procedure typically yields 15 µg DNA/100 µl. The DNA was stored at -20 °C in elution buffer.

3.5.1.2 Single fly genomic DNA isolation

One adult fly was homogenised in 50 µl of the homogenisation buffer with 0.5 µl Proteinase K pre-added. The homogenate was incubated for 30 min at 37°C to digest all proteins in the sample. The enzymatic activity of the Proteinase K was then inhibited by heating the sample for 2 minutes at 97°C.

3.5.2 Polymerase chain reaction (PCR)

PCR was used to amplify DNA (including cDNA) sequences by using specific primers. It was also used for linking restriction sites to sequences (linker PCR).

Primers were designed using primer3 software available online at (http://frodo.wi.mit.edu/cgi-bin/primer3/primer3_www.cgi). CG concentration was set at 50%. Melting temperatures of the primer pairs were adjusted to be similar within an interval of 1-2°C and primer length was usually restricted to 18–22 bases. Melting temperatures were kept around 57°C. Primer stocks (100 pmol/µl) were prepared by re-suspending lyophilised primer in ultrapure water. The primers were diluted 1:10 prior to usage. For linker PCR restriction sites were added to the primers along with few bases to have the restriction site ‘in’ the sequence and not at the terminal. Master mix with premixed buffer, dNTPs and DNA polymerase was added upto 50% of the total PCR reaction volume.

PCR Conditions

Denaturation: 5 minutes at 95°C for the first time and then 30 s denaturation at the beginning of each cycle.

Annealing : Annealing temperature was 3-5°C less than the average T_m of forward and reverse primer. Usually, a PCR with gradient temperature was performed to determine the optimum annealing temperature.

Extension: 1-2 minute (1 minute/1000 bp) at 72°C at the end of each cycle and then final extension for 10 minutes.

Number of cycles : Typically of 35 to 45 cycles yielded detectable amount of product for most of the reactions.

At the end of the PCR reaction the samples were mixed with 6X loading dye and kept at 4°C until further analysis.

3.5.3 PCR product purification and gel extraction

PCR and RT-PCR products were purified using commercially available silica gel based QIAquick PCR Purification Kit (QIAGEN). Purification procedure as recommended by the manufacturer was followed with slight modifications at the elution step. DNA was eluted in small amounts of ultrapure H₂O or elution buffer (10 mM Tris pH 8.5), columns were incubated at 68°C for 5 minutes and centrifuged for 2 minutes in a tabletop centrifuge at maximum speed. For gel extraction the DNA was fractionated on an agarose gel (using lowest possible concentration of agarose in the gel for the given species of DNA), visualised under UV light, excised with a clean blade and subjected to gel extraction using the QIAquick Gel Extraction Kit from QIAGEN.

3.6 RNA analysis

3.6.1 RNA isolation

RNeasy[®] Mini Kit (50) from QIAGEN was used for isolating RNA from *Drosophila* tissues (head and whole flies). Prior to isolation, the working place was thoroughly cleaned with 100% ethanol. Sterile filter tips were used to avoid contamination of the sample. 40 whole flies were homogenised on ice in 600 µl RLT buffer (QIAGEN, RNeasy[®] Mini Kit) with 6 µl β-Mercaptoethanol using sterile homogenizers. The homogenate was transferred to a fresh eppendorf tube. 1 µl of DNase was added to the tubes and incubated at 37°C for 45 minutes. The digestion process was stopped by heating the sample for 10 minutes at 95°C. Concentration and purity of the RNA was measured using spectrophotometer.

3.6.2 Reverse transcription

Reverse transcription is the mechanism of reverse transcribing RNA to cDNA using reverse transcriptase enzyme. The cDNA obtained can be amplified using routine PCR protocols.

11 μ l of total RNA (3.6.1) was incubated with 1 μ l of oligo-dT-primers and 1 μ l dNTPs for 5 minutes at 65°C. The sample is then incubated with 5 μ l of 5x first-strand buffer and 2 μ l of 0.1 M DDT for 2 minutes at 42°C. Immediately, 1 μ l of the superscript II (reverse transcriptase) was added to the reaction tube and incubated at 42°C for 90 min. The elongation step was performed by incubating the reaction tube at 70°C for 10 minutes. To remove the RNA template, 1 μ l of RNase was added to the tubes and incubated at 37°C for 30 minutes. Amplification of the cDNA was achieved by performing PCR (3.5.2) with sequence specific primers.

3.6.3 Microarray analysis (for detailed protocol refer to PhD thesis of N. Nuwal, 2010)

RNA was isolated from 400 adult *Drosophila* heads according the protocol mentioned in section 3.6.1. Purity of the isolated RNA was checked by running an aliquot on an agarose gel with formaldehyde, all subsequent steps were done by S. Kneitz. RNA was retested by Capillary electrophoresis (Bioanalyzer 2100; Agilent). An aliquot of highly pure RNA was used for reverse transcription and subsequently labelled by fluorescence dye (Cy3 or Cy5). This labelled cRNA was used for hybridisation to *Drosophila* genome arrays 2.0 from Affymetrix. The gene chips were scanned by GeneChip Scanner 3000 (IZKF, Wuerzburg). The signal intensities were normalised by variance stabilisation. Open source program 'R', bioconductor package of pre-compiled statistical analyses and limma (Linear Models for Microarray Analysis) package were used to test the quality of all data sets, and perform statistical analysis to select differentially expressed genes. Candidate genes from microarray analyses were confirmed by quantitative PCR of cDNA obtained from reverse transcription of poly-A⁺ RNA isolated from 400 adult *Drosophila* heads of WT and mutants.

3.6.4 Quantitative PCR (for detailed protocol refer to PhD thesis of N. Nuwal)

RNA was isolated from 400 adult *Drosophila* heads of WT and mutants, and reverse transcribed to cDNA (3.6). Transcript levels of RpLP0 (Ribosomal protein LP0) was used as an internal control or reference gene. The samples were run in triplicates. To perform the quantitative PCR the following reaction was set up in PCR tubes compatible with ROTOR Gene-Q (QIAGEN):

Component	Quantity
Template	~100 ng in 1 μ l
Master mix (Rotor-Gene Q SYBR Green)	10 μ l
Primers	1 μ l each sense and antisense
Total	H ₂ O to 20 μ l

The PCR conditions were as follows-

Step	Temperature	Time	Cycles
Hot start	95 °C	5 minutes	1
Denaturation	95 °C	10 seconds	45
Annealing	60 °C	15 seconds	45
Extension	72 °C	20 seconds	45
Melt	72 °C-95°C ramp		

In principle, the amount of amplified DNA is directly proportional to the SYBR green fluorescence as the dye fluoresces only on binding to double stranded DNA and thus the plot of fluorescence intensity (Y axis) against the number of cycles (X axis) reflects the exponential increase in transcript copy number. However, this is true only in

the low fluorescence range which avoids saturation phenomena, the intensities were plotted online by the Rotor Gene Q software (QIAGEN). C_t values (X-intercept) for transcript t were determined for each sample by setting a threshold (0.04008) for the normalised fluorescence intensity in the linear range of the semi-log plot of the PCR reaction (Fig. 33). $\Delta\Delta C_t$ method of analysis was used and further analyses were performed using Microsoft excel (spreadsheet package) and Origin 7.5.

$\Delta\Delta C_t$ for a given transcript t is calculated as follows (CS = wild type; GOI = genotype of interest)

$$\Delta C_{t,CS} = C_{t,CS} - C_{RpLP0,CS}$$

$$\Delta C_{t,GOI} = C_{t,GOI} - C_{RpLP0,GOI}$$

Log_2 fold change = $(\Delta C_{t,GOI} - \Delta C_{t,CS})$ if > 0 , down regulation

< 0 , up regulation

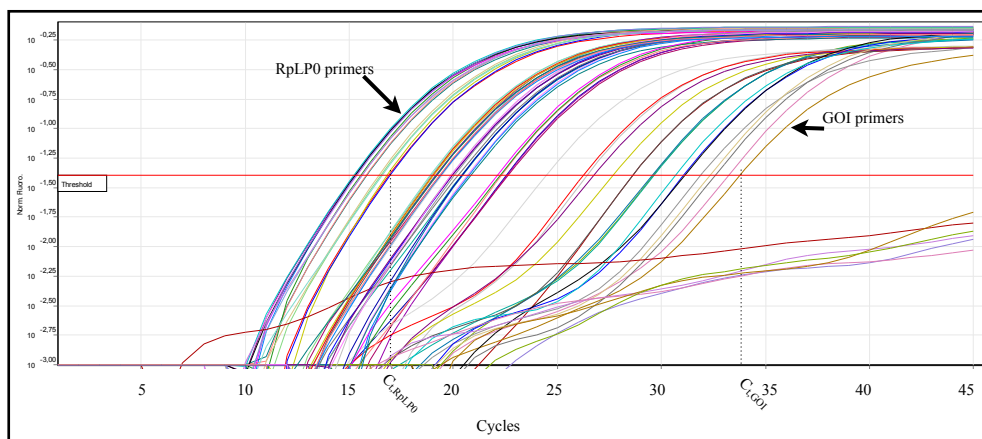


Fig. 33: An example qPCR traces and C_t values.

3.7 Behavioural assays

3.7.1 Negative geotaxis

Males of the required genotype were collected 3-5 days after eclosion. The animals were anaesthetised on ice and their wings were clipped. An empty food vial with scale drawn was used for the experiment. A single fly was taken in a vial of 10 cm height and tapped to the bottom by banging the vial to the table. As soon as the fly recovered and started climbing up the wall of the vial, the stopwatch was started. The time taken by the fly to cross the first centimetre from the bottom was recorded. The assay was repeated three times for each animal.

3.7.2 Longevity assay

Approximately 500 male flies (divided into 11 large sized vials) of a given genotype were tested. The flies were transferred to fresh food vials on every third or fourth day and the number of dead flies in the old vials were noted. This procedure continued until all the flies in the vials were dead. The time (days) taken for 50% of the total number of flies to be dead was calculated.

3.7.3 Fertility assay

10 mass crosses (10 males and 10 females) of 3-5 days old flies in medium sized food vials were made and transferred on every second day (Three times). The total number of progenies were counted from each vials and statistical analysis were performed using Origin 7.5.

4. RESULTS

4.1 Analysis of SAP47 and Synapsin protein interactions

4.1.1 Higher levels of phospho-synapsin in *Sap47* null mutant flies but no obvious change in synapsin distribution

Drosophila SAP47 is a synaptic vesicle associated presynaptic protein (Funk et al., 2004) and is enriched in brain and synaptic boutons. In a Western blot of head homogenate from *Sap47* null mutant (*Sap47¹⁵⁶*) flies an extra band not seen in wild-type homogenate is detected by anti-synapsin antibody 3C11 (Fig. 34) (also observed by N. Funk, unpublished).

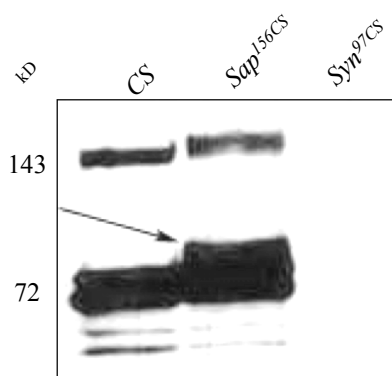


Fig. 34: Presence of shifted synapsin band in *Sap47¹⁵⁶CS* flies. Western blot of head homogenates (equivalent of 2 heads per lane) of the indicated genotypes was developed with anti-synapsin monoclonal antibody (MAB 3C11, dilution 1:50) and an extra upper shifted band for synapsin was detected in *Sap47* null mutants, *Sap47¹⁵⁶CS* (indicated by arrow).

The shifted band (arrow in Fig. 34) for synapsin is unique to *Sap47* null mutants. Such a shift could be due to altered posttranslational modification, like phosphorylation and/or due to increased expression of a larger synapsin isoform in *Sap47* null mutants.

To determine if the shift is due to altered phosphorylation of synapsin, aliquots of fresh head homogenates of wild-type *CS* and three different alleles of *Sap47* null mutants

were treated with shrimp alkaline phosphatase (AP) (Promega) prior to SDS-PAGE, corresponding aliquots were sham treated (only buffer). The shifted band observed in sham treated samples (Fig. 35, AP- lanes) was absent in AP treated samples (Fig. 35, AP+ lanes) and thus the result is suggestive that the shifted band is alkaline phosphatase sensitive and represents phospho-synapsin (Fig. 35). This effect was independent of the genetic background of the null mutants (w^{1118} in the original jump-out mutants, *CS* in the outcrossed lines (Funk et al., 2004)).

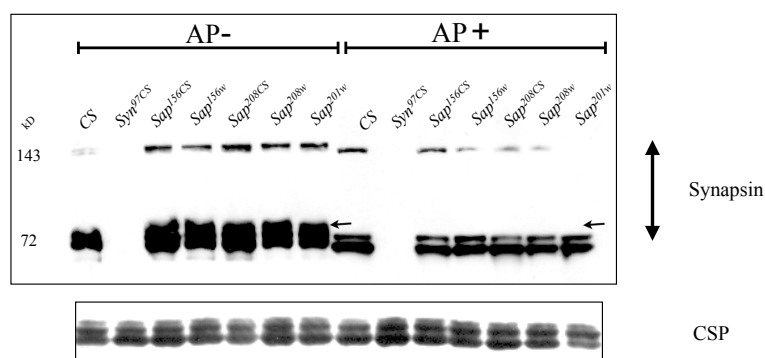


Fig. 35: Presence of phosphorylated synapsin in different alleles of *Sap47* null mutants. Western blot of head homogenates (2 head of each genotype was homogenised and divided into two groups alkaline phosphatase (40U of SAP) treated (AP+) and sham treated with buffer only (AP-), equivalent to 1 head per lane). The arrow indicates the presence of phospho-synapsin on the left and on the right it points to the loss of phosphorylation by alkaline phosphatase treatment. (Blot was cut horizontally and the upper part was incubated with anti-synapsin (MAB 3C11, 1:50), and the bottom part was incubated with anti-CSP (MAB ab49, 1:50) as loading control)

To test any changes in synapsin localization in *Sap47^{156CS}* mutant, sections of brain from WT, *Sap47^{156CS}*, and *Syn^{97CS}* mutants were immunohistochemically stained with anti-SAP47 and anti-SYN antibodies (Fig. 36). No obvious differences were detected.

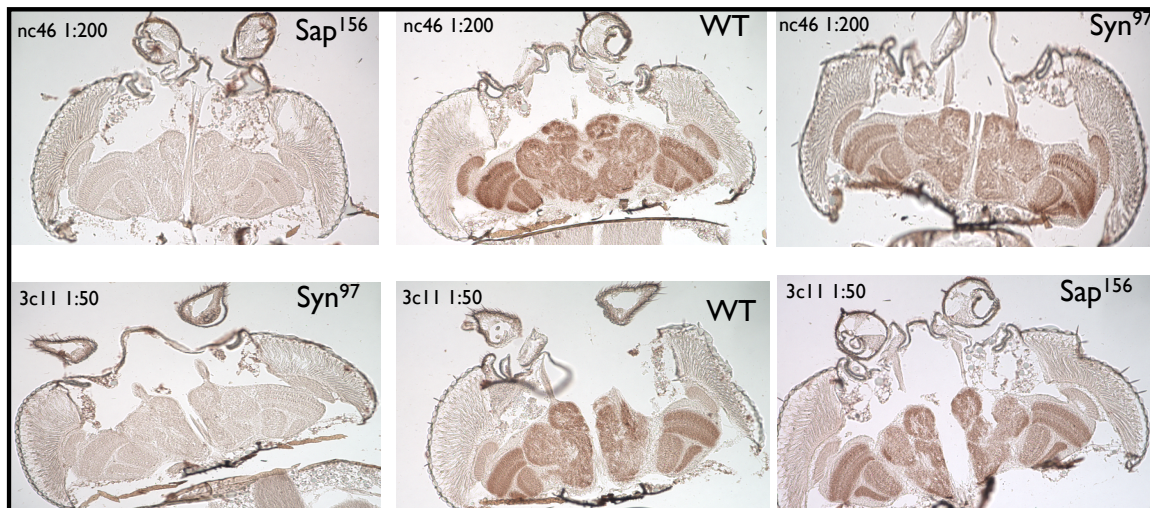


Fig. 36: No obvious differences in the staining pattern of synapsin between *Sap47*¹⁵⁶ and *CS* flies. Cryosections of frozen heads of indicated genotypes were stained with anti-SAP47 (MAB nc46, 1:200, upper row) and anti-SYN (MAB 3C11, 1:50, bottom row).

The Western blots also suggest that the total amount of synapsin is increased in the *Sap47* null mutants. To verify that, the amount of synapsin was altered along with the phosphorylation state in *Sap47* null mutants, the levels of synapsin in *CS* and *Sap47*^{156CS} were quantified using enzyme linked immunosorbent assay (ELISA). The results (Fig. 37) demonstrate that the levels of synapsin were about 2.5 folds higher in *Sap47*^{156CS} when compared to *CS* while the amount of SAP47 in *Syn*^{97CS} flies is unaltered in comparison to *CS*.

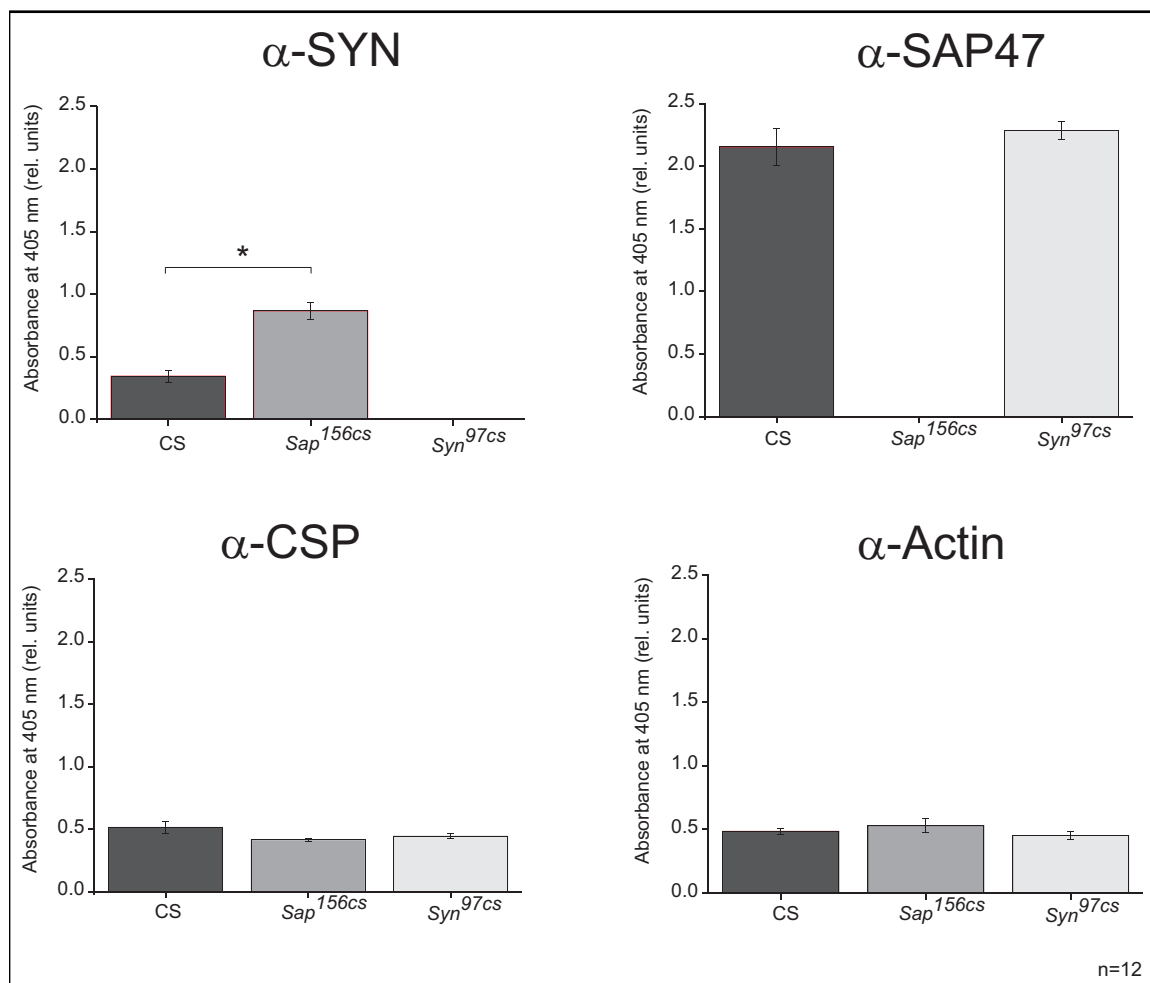


Fig. 37: The amount of SAP47 and SYN present in mutant and wild-type flies. The ELISA reading of the null mutants (*Syn*^{97CS} in α -SYN and *Sap47*^{156CS} in α -SAP47) due to unspecific reaction (background) has been subtracted from the data. (n=12, students t-test, $p < 0.05$). Actin and CSP are used as controls.

Since the levels of the control proteins actin and CSP are approximately the same in all the genotypes tested, these results suggest that there is an up-regulation of synapsin in *Sap47* null mutants and this increased amount of synapsin is largely present in phosphorylated form (see Discussion).

4.1.2 Partial rescue of synapsin phosphorylation in *Sap47* null mutants

To confirm that the higher levels of phospho-synapsin in *Sap47* null mutants are due to the absence of SAP47, a “rescue” experiment was performed. SAP47 protein was expressed pan-neuronally in the *Sap47^{156CS}* null mutant using the UAS-Gal4 system. The UAS-*Sap47* cDNA line (only the 47 kD isoform is expressed by this line) was kindly provided by T. Saumweber, *elav-gal4* was used as the driver line.

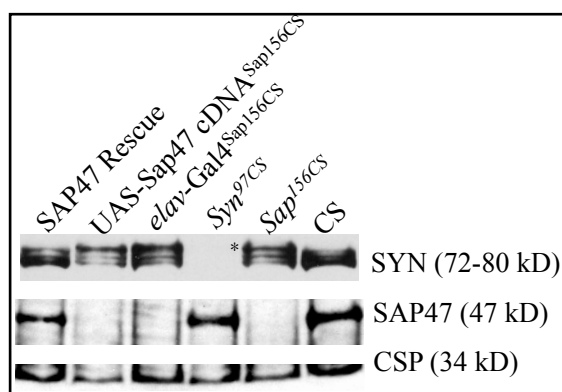


Fig. 38: Synapsin hyperphosphorylation in *Sap47* null mutants is partially abolished upon pan-neuronal expression of the 47 kDa SAP47 isoform (rescue). A partial rescue of synapsin hyperphosphorylation (compared to band marked with asterisk) is observed in *elav-gal4* driven UAS-*Sap47* cDNA (Loading: 2 heads per lane, blot developed with anti-SYN (MAB 3C11, dilution 1:50), anti-SAP47 (MAB nc46, dilution 1:200) and anti-CSP (MAB ab49, dilution 1:50) as loading control.

In the Western blot of the rescue flies (Fig. 38), the shifted band for synapsin in *Sap47^{156CS}* null mutants is present at reduced intensity when compared to the levels in driver (*elav-gal4*) and the effector (UAS-*Sap47* cDNA) fly lines, both of which are in *Sap47^{156CS}* background. The rescue of SAP47 in *Sap47^{156CS}* null mutants partially restored the wild type synapsin signal as seen in *CS*. The total amount of SYN protein in the rescue flies was quantified by an ELISA experiment (Fig. 39).

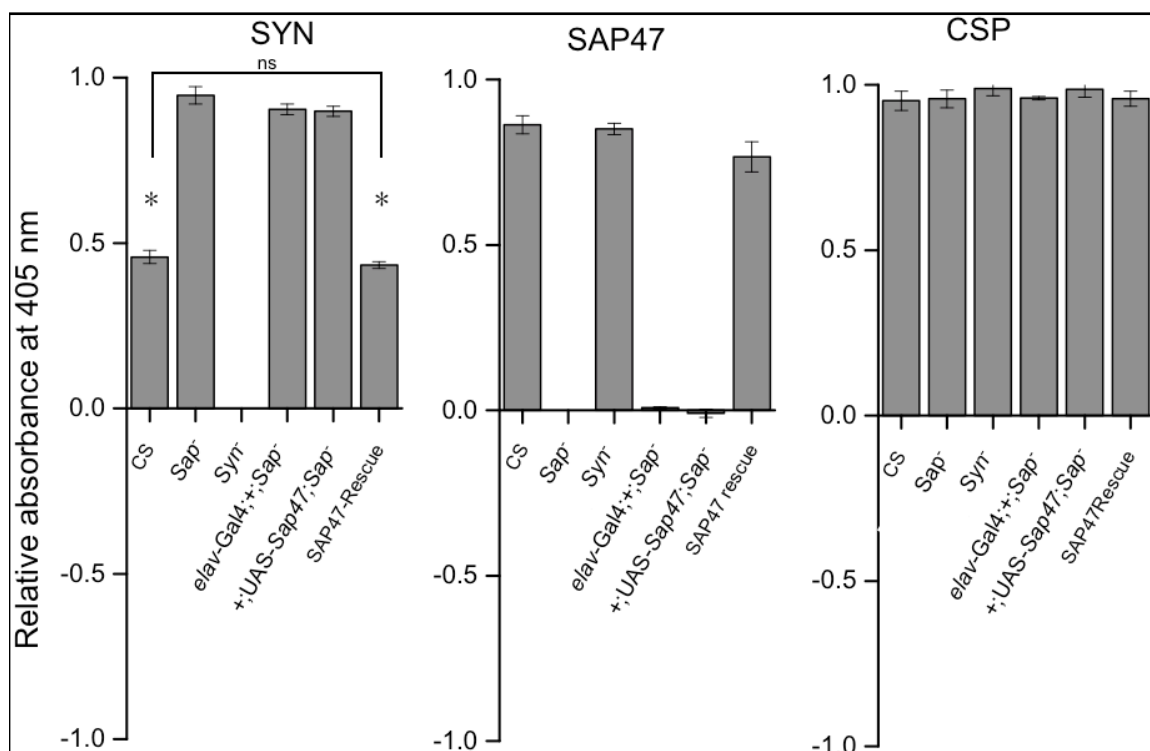


Fig. 39: Synapsin up-regulation in *Sap47* null mutants is abolished upon pan-neuronal expression of the 47 kDa SAP47 isoform (rescue). The ELISA reading of the null mutants (*Syn*^{97CS} in α -SYN and *Sap47*^{156CS} in α -SAP47) due to unspecific binding (background) has been subtracted from the data. CSP levels served as a control (detection by anti-CSP (MAB ab49, dilution 1:200)). (n=10, students t-test, *: p< 0.05).

In the rescue flies which express near-WT levels of SAP47 (Fig. 38 and 39), the increased levels of synapsin in *Sap47*^{156CS} null mutants, as also seen in the driver (*elav-gal4*) and the effector (*UAS-Sap47* cDNA) fly lines, both of which are in *Sap47*^{156CS} background, are reverted to levels comparable to *CS*. Again, there is no effect of the *Syn*^{97CS} mutation on the SAP47 levels. Thus, the results of Western blot and ELISA show that the higher levels of synapsin in *Sap47* null mutants are due to the lack of SAP47 and is independent of genetic background and the *Sap47* null allele under investigation. This phenomenon can be due to several reasons (see Discussion), the most obvious possibility being relatively higher transcript levels of *Syn* in *Sap47*^{156CS} null mutants when compared

to wild-type *CS*. To test this hypothesis we determined the mRNA levels for *Syn* in *Sap47^{156CS}* mutants.

4.1.3 Synapsin transcript levels in *Sap47^{156CS}* mutant and wild-type *CS* flies

Semi-quantitative polymerase chain reactions of reverse transcribed cDNAs (SQ-RT-PCRs) were performed to determine the relative levels of *Syn* transcript in *Sap^{156CS}* and *CS* flies. The experiment is designed to determine the levels of *Syn* transcript relative to the housekeeping reference gene coding for *Zwischenferment (Zw)* also known as glucose-6-phosphate dehydrogenase.

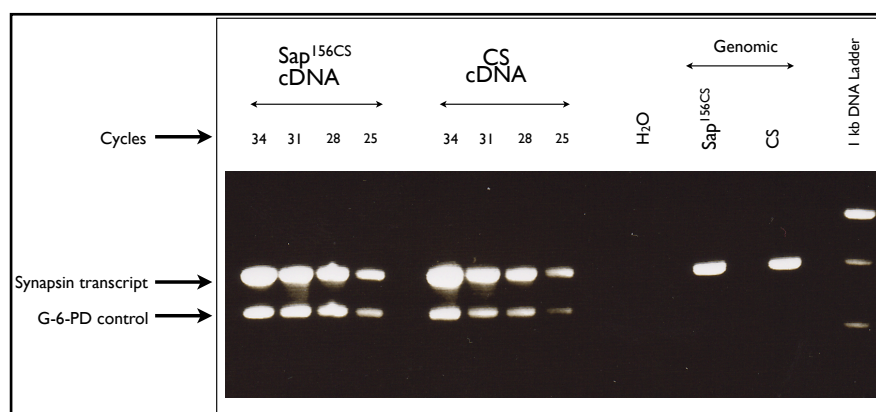


Fig. 40: Content of *Syn* transcript is comparable in *CS* and *Sap47* null mutants. 4 replicate PCR reactions each of *CS* and *Sap47* null mutants were used to perform the PCR for different numbers of cycles (25, 28, 31 and 34 cycles). The product of the reference gene PCR was mixed with the experimental PCR product prior to loading the gel. Transcript levels of *G6PD* served as control.

Syn transcript content was not dramatically different in *Sap47^{156CS}* from wild-type *CS* level (Fig. 40). However, a 2.5 fold increase in transcript content (to account for the 2.5 fold in protein content) might have escaped detection in our experimental design. Therefore, transcript levels in *Sap47^{156CS}* and *Syn^{97CS}* null mutants were quantified by microarray analysis (see 4.5, refer to PhD thesis of N. Nuwal, 2010).

4.1.4 Investigating direct protein interactions of SAP47 and synapsin by co-immunoprecipitation experiments

The increased levels of synapsin in *Sap47* null mutants suggests an interaction between the two proteins. The interactions can be direct or indirect involving a multitude of proteins. The interaction can also be genetic (this possibility has also been investigated in section 4.2).

Immunoprecipitation (IP) of SAP47 and synapsin was performed as described in the methods section. The precipitated proteins were eluted under denaturing and reducing conditions and tested by SDS-PAGE and Western blotting (Fig. 41).

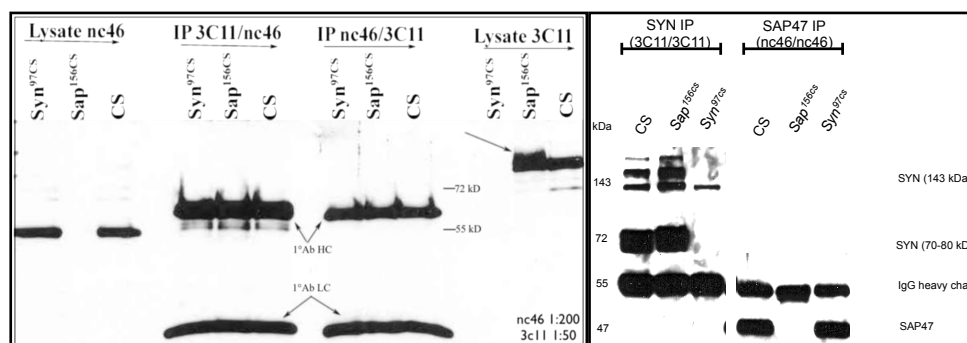


Fig. 41: IP of SAP47 and synapsin. In the left panel, the lysates/input for IP were positive for SAP47 (detection with MAB nc46, dilution 1:200) and synapsin (detection with MAB 3C11, dilution 1:50) but no co-IP of SAP47 with synapsin or vice-versa was observed. The shifted band for synapsin in *Sap47* null mutant is shown (arrow, lysate 3C11). The faint bands beneath the heavy chain of MAB 3C11 in IP 3C11/nc46 are probably the proteins from foetal calf serum (FCS) in the MAB supernatant. The panel on the right shows the IP of SYN (IP and blot development using MAB 3C11) and SAP47 (IP and blot development using MAB nc46) under these conditions.

To determine if SAP47 and synapsin bind to each other or are part of the same molecular complex, proteins precipitated from CS head lysate with anti-SAP47 (MAB

nc46) were probed with anti-SYN (MAB 3C11). In the reciprocal experiment the precipitate obtained with 3C11 was probed with nc46. Only the precipitated proteins (Fig. 41, right panel) and immunoglobulin chains were detected in the IP sample lanes but no co-immunoprecipitation of SAP47 with SYN or vice versa was observed (Fig. 41, left panel). The failure of this co-immunoprecipitation experiment suggests that SAP47 and synapsin under the IP conditions used do not interact in a stoichiometric manner (see Discussion). Different experimental approaches were tried and are mentioned below.

4.1.4.1 Competitive elution of immunoprecipitated synapsin by peptides containing the 3C11 epitope and analysis by 1D-SDS-PAGE

When a monoclonal antibody is used for IP an alternative to denaturing buffers for eluting the immunoprecipitated samples from the beads can be employed. For competitive elution the beads are incubated with excess of a peptide containing the epitope of the MAB in order to displace the antigen from the beads. This strategy has several advantages including the recovery of the beads due to the mild elution conditions and the specificity of elution which reduces or eliminates co-elution of the antibody and other components unspecifically bound to the solid matrix.

The MAB 3C11 epitope had been determined earlier by spotting sequential synapsin decapeptides on nitrocellulose membranes (Munch et al., 1999; Godenschwege et al., 2004). The peptide used for the elution therefore had the sequence:



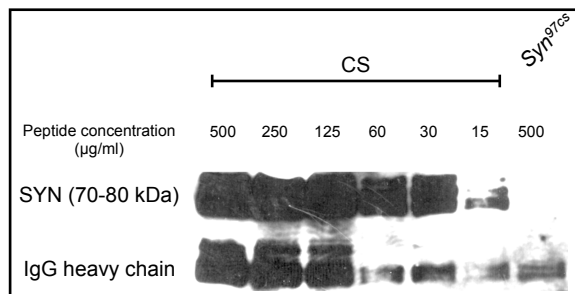


Fig. 42: Competitive elution of SYN from an IP with a peptide containing the 3C11 epitope. Peptide concentrations ranging from 15-500 µg/ml were used. The optimal peptide concentration was concluded to be 60 µg/ml due to minimal contamination of antibody proteins in the eluted sample and a strong signal for SYN (detection by anti-SYN (MAB 3C11, dilution 1:50)).

Immunoprecipitation from head homogenates of 50 *CS*, or 50 *Syn^{97CS}* flies was performed using anti-SYN monoclonal antibody (MAB 3C11). The sample was eluted by incubating the loaded beads with different concentrations of the peptide containing the 3C11 epitope. The eluted samples were tested by SDS-PAGE and subsequent detection by Western blotting. The optimal peptide concentration at which the level of non-specific signal (from antibody heavy/light chains and serum proteins) is minimal and the specific signal (MAB 3C11, synapsin) is maximal was found to be at 60 µg/ml (Fig. 42). This elution protocol was used for SYN isolation for mass spectrometric analysis of posttranslational modifications (see 4.4).

4.1.5 Blue Native-PAGE analysis of synapsins

An interaction between synapsin and SAP47 was not observed by conventional co-immunoprecipitation (co-IP) technique. A possible reason for this could be a weak interaction (see Discussion). To overcome the limitation of co-IP in case of weak interactions between proteins, the Blue Native Polyacrylamide Gel Electrophoresis (BN-PAGE) technique for the separation of protein complexes under mild conditions was used. BN-PAGE is useful for analysing and characterising protein complexes (Schagger and von Jagow, 1991).

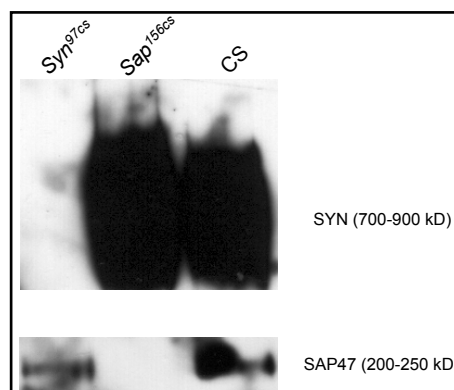


Fig. 43: Western blot after BN-PAGE. Synapsin protein is observed at a molecular weight around 700-900 kD and SAP47 is observed around 200-250 kD in fresh head homogenates of the genotypes mentioned. SAP47 and SYN are observed at different molecular weights and are not part of the same complex. (Loading: 10 heads/lane, detection with anti-SYN, MAB 3C11 (dilution 1:50) and anti-SAP47, MAB nc46 (dilution 1:200)).

In a Western blot following BN-PAGE (Fig. 43) the synapsin signal was detected at around 700-900 kD suggesting an involvement of synapsin in a multi-protein complex. SAP47 was not detected in the same molecular weight range as synapsin, suggesting that SAP47 and synapsin are not components of a common stable protein complex. However, this does not exclude the possibility that they interact transiently (see Discussion).

In order to further characterise the synapsin complex observed in Figure 43, BN-SDS-2D-PAGE technique was used (see Methods section). Briefly, after the first dimension of native electrophoresis is complete, the *CS* and *Syn^{97CS}* lanes were cut out with a sharp knife, equilibrated in SDS solution, and used as input for a second dimension discontinuous SDS gel. During this process the synapsin complexes fell apart into their components (subunits) to form protein-SDS micelles that separated in the SDS gel according to their molecular weight. The gels were analysed by Western blotting and silver staining (Fig. 44).

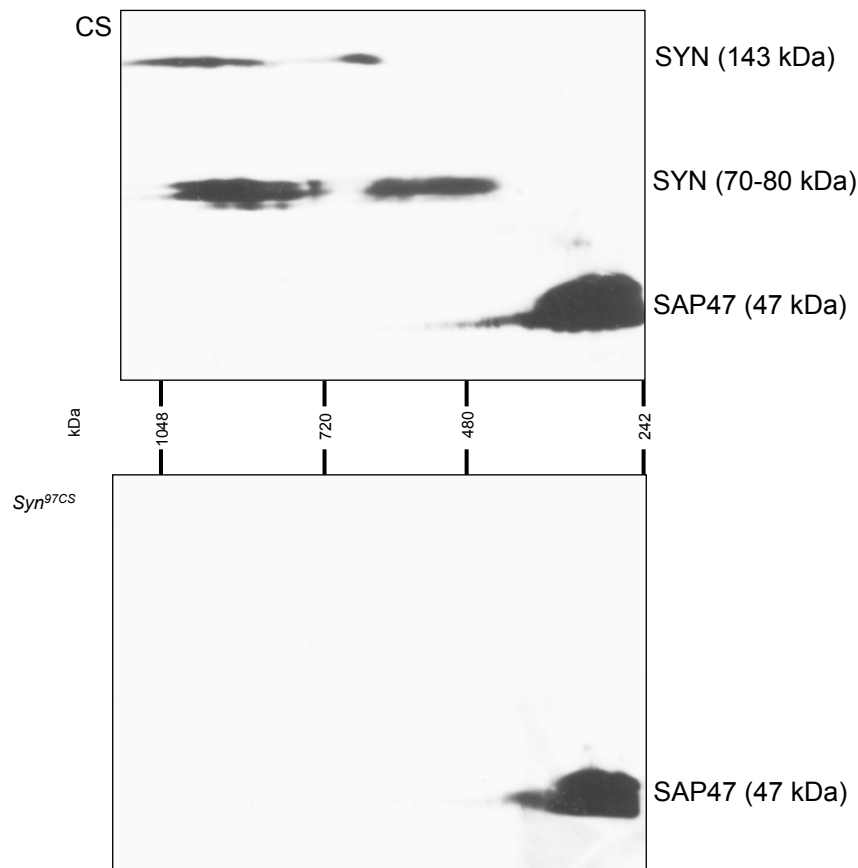


Fig. 44: BN-SDS-2D-PAGE and Western blot of fresh head homogenates of *CS* and *Syn^{97CS}* flies. SAP47 and synapsin are not found in the same complex as they are detected at different vertical axes. (Loading: 10 heads equivalent; detection by anti-SYN, MAB 3C11 (dilution 1:50) and anti-SAP47, MAB nc46 (dilution 1:200)).

The interpretation of 2D-BN-SDS-PAGE results is different from conventional 2D-SDS gels. Vertically aligned spots indicate that the proteins could be components of a larger protein complex. Larger complexes are located on the left hand side of the image.

Synapsin and SAP47 signals are detected at two different horizontal axes (Fig. 44). The control experiment using *Syn^{97CS}* mutants demonstrate the specificity of the MAB 3C11 signal in the *CS* blot. This result confirms that SAP47 and synapsin are not part of a same stable complex (see Discussion). It was also observed that in the first dimension both synapsin and SAP47 are located in the higher molecular weight range suggesting that they are individually involved in protein complexes (see Discussion). Our

experiments revealed no direct protein-protein interaction of SAP47 and synapsin. However, an interaction could also be indirect involving other proteins, dissociating the interactions spatially and/or temporally. We attempted to identify the unknown co-IPed proteins by mass spectrometry (see 4.4.3).

4.2 Functional interaction between *Sap47* and *Syn* genes

A possible mechanism that might explain the up-regulated phospho-synapsin in *Sap47* null mutants could be a functional interaction between *Sap47* and *Syn* at genetic level.

4.2.1 Generation of the *Sap47* and *Syn* double null mutants *NS17* and *NS62*

A first step to look into the possibility of a genetic interaction of the *Sap47* and *Syn* genes was taken by generating a *Sap47*^{156CS}, *Syn*^{97CS} double mutant in homozygous condition (Fig. 45). Two such double mutants, *Sap47*¹⁵⁶, *Syn*⁹⁷, *l(3) blp/TM3* and *Sap47*¹⁵⁶, *Syn*⁹⁷, *l(3) (NF)/TM3* had already been generated (S. Becker and N. Funk, unpublished). In both stocks only balanced flies and the trans-heterozygotes *Sap47*¹⁵⁶, *Syn*⁹⁷, *l(3) blp/Sap47*¹⁵⁶, *Syn*⁹⁷, *l(3) (NF)* were viable, indicating that both recombinant chromosomes contained a homozygous lethal mutation independent of the *Sap47* and *Syn* genes.

In an attempt to obtain double mutants without lethal mutation flies of cantonised *Sap47* null mutants (*Sap47*^{156CS}) and *Syn* null mutants (*Syn*^{97CS}) were used to generate independent double mutants by homologous recombination as both genes *Sap47* and *Syn* are present on the third chromosome at 3R (flybase). A mass cross of *Sap47*^{156CS} (9 virgin females) and *Syn*^{97CS} (12 males) flies was performed. Virgin females from the F₁ generation were crossed to males (in a ratio of 1:3) of *TM3Sb/TM6Tb* (cantonised stock provided by V. Albertowa). The progenies of the above cross were sorted on the basis of Tubby (Tb) and Stubble (Sb) phenotypes.

Only the virgin females were selected in order to obtain 3rd chromosomes that had received both the *Sap47^{156CS}* and *Syn^{97CS}* mutant alleles due to homologous recombination during meiosis. Each individual female was crossed to males of the stock of *Sap47^{156CSNF}*, *Syn^{97CSNF}*, *l(3)* (NF)/*TM3Sb* (short: *Sap⁻*, *Syn⁻*, *l(3)*NF (N. Funk, unpublished) which is homozygous lethal. The non balanced progeny of this cross was analysed using ELISA (see Methods).

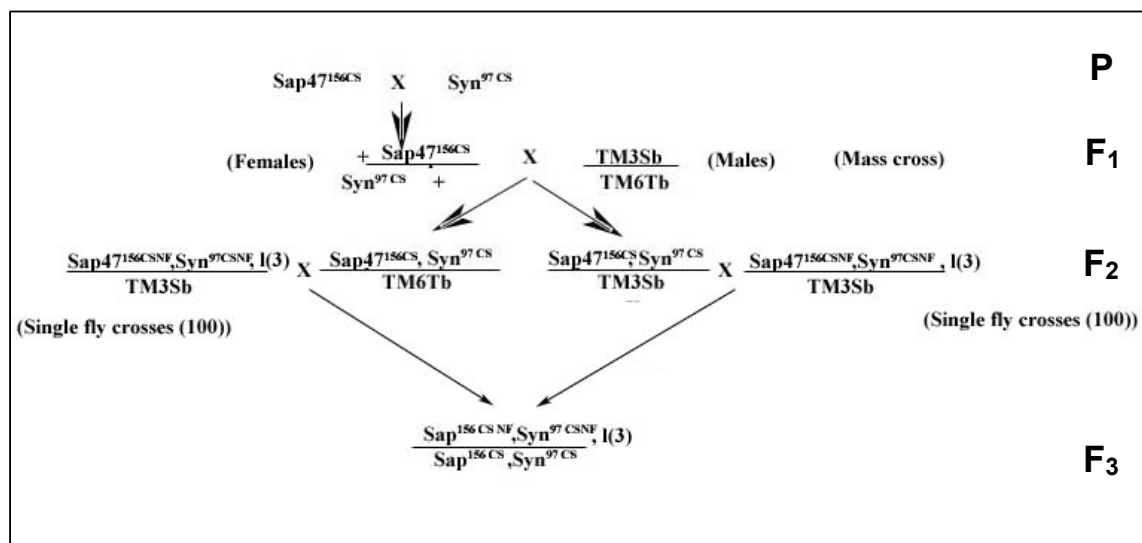


Fig. 45: Crossing strategy for generating *Sap47* and *Syn* double null mutant.

The ELISA was performed using both the monoclonal antibodies 3C11 and nc46 simultaneously on a single ELISA plate. From each of the 200 F₃ vials a non-balanced progeny was anaesthetised and the head was severed from the body using a surgical blade. The head was homogenised in PBS buffer and the homogenate was divided into two aliquots and loaded into separate wells of the ELISA plate. One set of wells was assayed with MAB nc46 to test for the absence of SAP47 and the other set of wells was assayed with 3C11 to test for the absence of synapsin. The lines *NS17* and *NS62* were found to be double null mutants, a result that was verified by Western blot (see Fig. 46). Interestingly, the parental lines of *NS17* and *NS62* were also homozygous lethal. The recombination chromosomes are therefore designated as *Sap⁻*, *Syn⁻*, *l(3)NS17* and *Sap⁻*, *Syn⁻*, *l(3)NS62*.

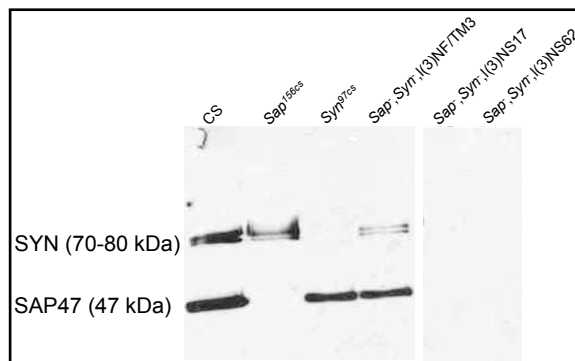


Fig. 46: Confirmation of absence of SAP47 and SYN for *Sap47*^{156CS}, *Syn*^{97CS} double mutants (two lanes at the right most). Coomassie staining of the gel after transfer showed the presence of other protein bands and this served as a loading control.

NS17 and *NS62* double mutants are homozygous for *Sap*⁻, *Syn*⁻ but are still trans-heterozygous for third site lethality.

NS17: *Sap*⁻, *Syn*⁻, *l(3)*^{NS17}/*Sap*⁻, *Syn*⁻, *l(3)*^{NF}

NS62: *Sap*⁻, *Syn*⁻, *l(3)*^{NS62}/*Sap*⁻, *Syn*⁻, *l(3)*^{NF}

In a similar manner as described above, yet another homozygous double mutant of *Sap47* and *Syn* was generated by V. Albertowa. Again the recombinant chromosomes carried a third site lethality. Three homozygous viable stocks (*SapSyn*^{V1}, *SapSyn*^{V2} and *SapSyn*^{V3}) were established after outcrossing the balanced lines for 6 generations with *CS*. Apparently, in these stocks the lethality had been removed by recombination (V. Albertowa, unpublished, see Discussion).

The next step after the generation of homozygous double mutants was to investigate and compare the phenotypes of the double mutants with those of the individual null mutants and *CS*. If the double mutants showed an additive phenotype this would suggest that SAP47 and synapsin might be functional in different pathways whereas a phenotype comparable to that of each individual mutants would suggest that the two proteins could be functional in a single pathway.

4.3 Behavioural analysis of *Syn*^{97CS}, *Sap47*^{156CS} and double null mutants

4.3.1 Locomotor assays

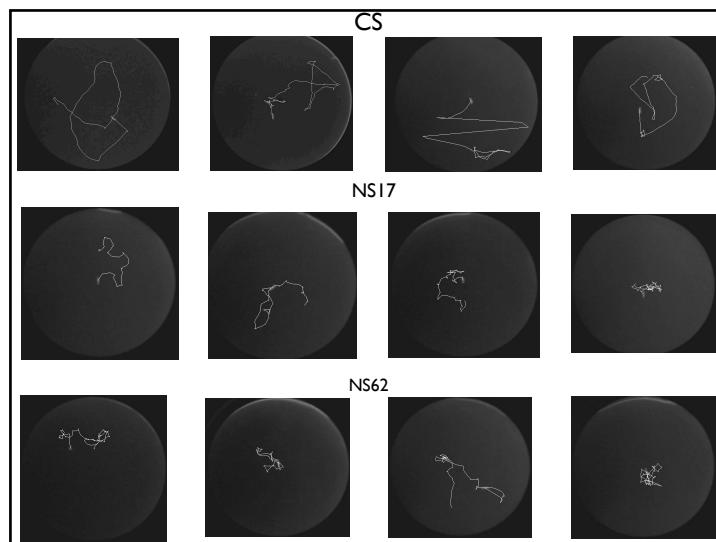


Fig. 47: Reduced locomotion in 3rd instar larvae of *NS17* and *NS62* (*Sap47-Syn* double null mutants). The larvae were placed at the centre of 1% agarose filled 9 cm \varnothing petri-dishes and after an acclimatization period of 3 minutes the larvae was again placed at the centre of the plate and a video of their activity was recorded for the next 3 minutes. The whole experiment was done under red light (for the camera to function). n=4 for each genotype.

In a preliminary crawling test 3rd instar larvae of *NS17* and *NS62* double null mutants were found to have reduced locomotor activity as they moved less from their original position on an agarose filled petri-dish. The activity was not quantified and would need further investigation (Fig. 47).

The negative geotaxis assay as previously described (Benzer, 1967) was modified to calculate the time taken by the fly to climb the first centimetre from the bottom of the vial (see Methods).

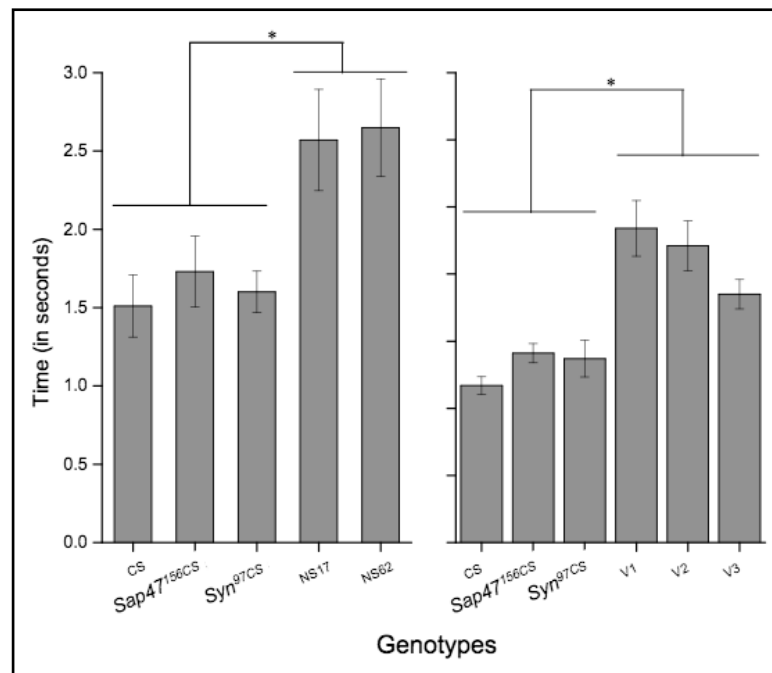


Fig. 48: Modified negative geotaxis. The double null mutants *NS17*, *NS62* (left panel), *V1*, *V2* and *V3* (right panel) take longer to climb the first one centimetre. Two-sample students t-test and Bonferroni correction was performed (n=15 for left panel and n=10 for right panel). (*: p<0.05) (Diploma thesis A. Schneider, 2008).

All tested double mutants (*NS17*, *NS62*, *V1*, *V2* and *V3*) were found to have a defect in their negative geotaxis (Fig. 48). However, this defect was restricted to the first few seconds of the response as the total distance climbed by the double null mutants in 30 s was not significantly different from *CS* and the single mutants *Sap47^{156CS}* and *Syn^{97CS}* (see Discussion, Diploma thesis A. Schneider, 2008).

4.3.2 Longevity assay

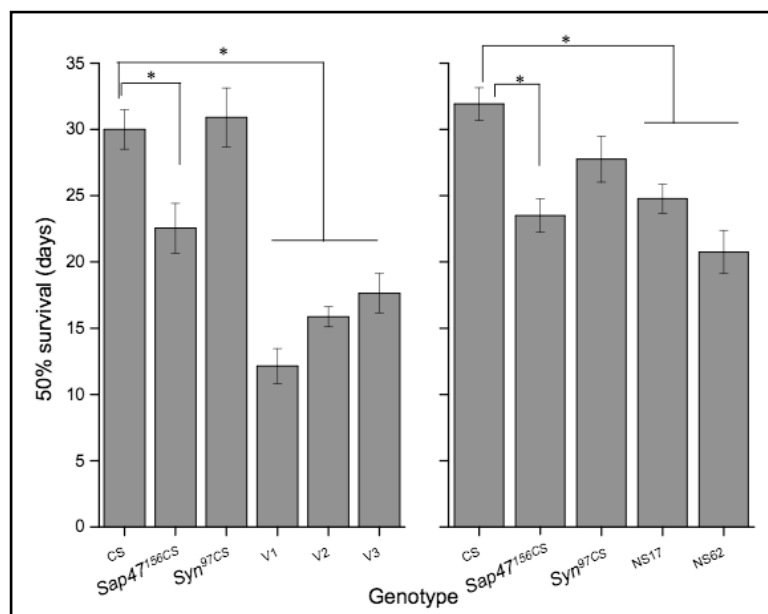


Fig. 49: Life expectancy (t_{50} , in days). Homozygous double mutants *V1*, *V2*, *V3*, *NS17* and *NS62* have reduced life span. Life expectancy of 500 males of *CS*, *Sap47^{186CS}*, *Syn^{97CS}*, *NS17*, *NS62*, *V1*, *V2* and *V3* flies was determined by calculating the time taken for half the initial number of flies to be dead. Two-sample students t-test and Bonferroni correction was performed (n=15 for left panel and n=10 for right panel). (*: $p < 0.05$) (Diploma thesis A. Schneider, 2008).

The double null mutants *V1*, *V2* and *V3* (provided by V. Albertowa) and *NS17* and *NS62* were found to have reduced life span (Diploma thesis A. Schneider, 2008). The number of double mutant flies reduces to half the initial number in significantly shorter time when compared to the wild type flies as observed in *CS*. Interestingly, only *Sap47* null mutant flies show a significant defect in life expectancy whereas the *Syn* null mutants are comparable to wild-type *CS* (Fig. 49).

On the other hand, if left undisturbed the double mutants appear to be more lethargic and having reduced locomotion, they prefer to stay at the bottom of vial and do not make efforts to climb the walls.

4.4 Characterization of synapsin posttranslational modifications (PTMs)

2D-PAGE is a standard method to obtain information about PTMs of any protein. In order to characterise the PTMs of SYN, we performed 2D-PAGE of immunoprecipitated SYN samples (using MAB 3C11). The aim of this experiment was to immunoprecipitate SYN isoforms and separate them using the 2D-PAGE to produce series of spots and then analyse each spot by mass spectrometry (MS). In order to detect the proteins from the gel spot by MS, we loaded a large amount of SYN protein on the gel. We standardised the conditions for IP in order to have minimal contamination from serum proteins and the monoclonal antibody (3C11). The first dimension of the 2D-PAGE (isoelectric focussing) produces best results only at optimal protein concentration (less than 50 µg of crude protein for broad range strip, pH 3-10 and less than 200 µg of crude protein for narrow range strips). The loading can be increased (to 400 µg) if the sample is highly enriched by fractionation or by IP.

4.4.1 Analysis of synapsins by 2D-PAGE

Characterization of *Drosophila* synapsins by 2D-PAGE of head homogenates and Western blotting (Fig. 50A) had indicated that the three short isoforms of 70, 74 and 80 kDa observed in 1D-SDS gels actually consist of multiple isoforms differing by isoelectric point. In agreement with this result several synapsin spots were identified by silver staining of a second dimension gel from 2D-PAGE analysis of synapsin IP samples (competitive elution protocol with DSS (see Methods), Fig. 50B). The spots were excised from the gel and an analysis by nano-LC-ESI MS/MS technique was attempted. However, the protein content in the gel pieces was too low such that no significant hits were obtained from MS/MS analysis (see Discussion, in collaboration with S. Heo).

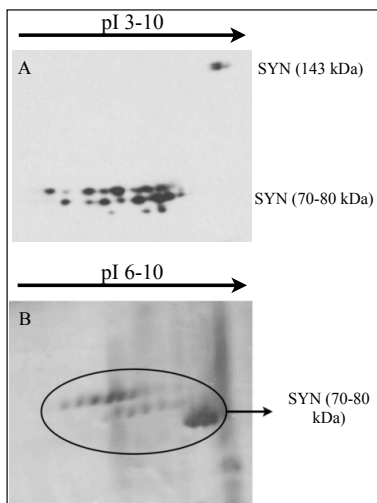


Fig. 50: (A) 2D-PAGE and Western blot of fresh head homogenates of w^{1118} by anti-SYN antibody (MAB 3C11, dilution (1:50), Loading: ~12 heads per gel strip) (Diploma thesis S. Racic, 2009) (B) Silver stained gel of synapsin competitively eluted after IP with wild-type head homogenate (see Methods). A parallel experiment using the synapsin null mutant (Syn^{97CS}) did not show comparable spots (gel image not shown).

Due to this failure, we performed 1D-SDS-PAGE of the IP sample. 1D-SDS-PAGE is less efficient in the separation of isoforms with different PTMs but protein content in gel pieces is higher (due to higher loading) compared to 2D-SDS-PAGE.

4.4.2 Immunoprecipitation of synapsin from head homogenates and detection by MS compatible silver staining

In order to detect PTMs of *Drosophila* synapsin, and possibly co-immunoprecipitated binding partners of synapsin, an IP of synapsin was performed from 180 mg (~2500 *Drosophila* heads) of brain tissue (IP protocol without DSS). Eluted wild-type (*CS*) and null mutant (Syn^{97CS}) samples were separated by SDS-PAGE and visualized by MS compatible silver staining (Mortz et al., 2001) (see Materials and Methods).

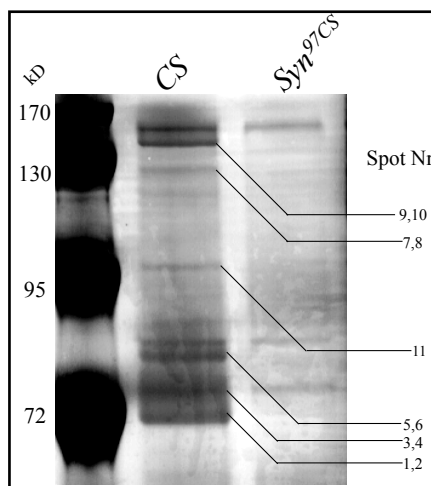


Fig. 51: Silver stained SDS gel after immunoprecipitation using anti-SYN monoclonal antibody (MAB 3C11). MS compatible silver staining revealed several bands in the *CS* lane out of which only 5 (those numbered) were unique (3 similar bands between *CS* and *Syn*^{97CS} lane). In total 11 gel pieces were picked from unique bands in the *CS* lane (numbered 1-11). Gel pieces 1-10 showed the presence of SYN. On MS analysis, protein from gel piece 11 did not produce a significant hit.

Several bands unique to *CS* and absent in *Syn*^{97CS} lane were observed. On analysis by nano-LC-ESI-MS-MS (see 4.4.3, MS analysis of synapsin) only synapsin proteins were detected from all the bands except band 11. Under the IP conditions used, we were able to precipitate large amount of SYN but no stable interaction partner was co-precipitated. This supports the finding of BN-SDS-PAGE analysis that synapsins are possibly present in the form of stable homo-multimers (see Discussion).

4.4.3 nano-LC-ESI-MS-MS analysis of synapsin (in collaboration with S. Heo and G. Lubec)

Gel pieces were excised from the bands observed in Figure 51 and were subjected to MS analysis (in collaboration with S. Heo and G. Lubec). Proteins trapped in the gel pieces were digested by the indicated enzymes (see Table 2) and subsequently extracted peptides were analysed by nano-LC-ESI-MS/MS. MS/MS spectra were interpreted and peak lists were generated by DataAnalysis 4.0. Data searches were performed via

MASCOT and Modiro against latest UniProtKB and NCBI database for protein identification and PTM search.

Tables 2: Enzyme conditions used and the synapsin sequence coverage obtained by collision-induced dissociation (CID) and electron-transfer dissociation (ETD) based MS/MS fragmentation and MASCOT or MODIRO based data analysis. Trypsin digestion produced the highest sequence coverage by CID method and MASCOT (uses mass spectrometry data to identify proteins from primary sequence databases) analysis (in collaboration with S. Heo).

A. CID/ETD based fragmentation and MASCOT/MODIRO based sequence analysis

Enzyme	Conditions	Identified protein (Swissprot Nr.)	Mascot v2.2.06		Modiro™ v1.1 (Min. Sig. 90 / 80)	
			CID	ETD	CID	ETD
Trypsin	25mM NH ₄ HCO ₃ (pH 7.8). 37°C overnight.	Synapsin (Q24546)	80.00	71.22	73.07 / 78.63	62.24 / 70.15
Chymotrypsin	25mM NH ₄ HCO ₃ (pH 7.8). 25°C overnight.		52.78	40.78	45.56 / 43.70	22.92 / 25.85
AspN	25mM NH ₄ HCO ₃ (pH 7.8). 37°C overnight.		52.39	26.83	18.34 / 22.73	6.82 / 12.29
Subtilisin	50mM NH ₄ HCO ₃ (pH 7.8). 37°C for 1h.		26.44	25.46	36.29 / 30.24	3.51 / 2.44
ProteinaseK	50mM NH ₄ HCO ₃ (pH 7.8). 37°C for 1h.		21.27	Not identified	12.20 / 11.22	1.46 / 1.46
Pepsin	100 mM HCl. 37°C for 4 h.		33.85	Not identified	40.20 / 34.93	3.02 / 10.24

B. Sequence data pooled from two different enzymatic digestions to obtain higher sequence coverage.

Enzyme		Identified protein (Swissprot number)	Mascot v2.2.06 (%)		Modiro™ v1.1 [Min. Sig. 90 / 80] (%)	
			CID	ETD	CID	ETD
Trypsin	Chymotrypsin	Synapsin (Q24546)	85.17	75.02	81.17 / 83.71	71.12 / 78.83
Trypsin	AspN		90.83	76.49	75.32 / 85.66	63.41 / 72.20
Trypsin	Subtilisin		84.29	78.73	81.76 / 84.59	62.54 / 70.15
Chymotrypsin	AspN		77.17	47.32	54.73 / 56.68	27.90 / 35.61
Chymotrypsin	Subtilisin		63.41	58.83	66.63 / 66.05	24.98 / 28.10

C. Sequence data pooled from MASCOT and MODIRO analysis to obtain higher sequence coverage.

Identified protein (Swissprot number)	Enzyme	Analyzing condition	Sequence coverage (%)
---------------------------------------	--------	---------------------	-----------------------

Synapsin (Q24546)	Trypsin	MASCOT CID + Modiro CID (Min. Sig. 90)	84.68
		MASCOT CID + Modiro CID (Min. Sig. 80)	85.95
	Chymotrypsin	MASCOT CID + Modiro CID (Min. Sig. 90)	55.71
		MASCOT CID + Modiro CID (Min. Sig. 80)	58.93
	AspN	MASCOT CID + Modiro CID (Min. Sig. 90)	58.83
		MASCOT CID + Modiro CID (Min. Sig. 80)	57.46
	Subtilisin	MASCOT CID + Modiro CID (Min. Sig. 90)	51.80
		MASCOT CID + Modiro CID (Min. Sig. 80)	47.22

A maximum sequence coverage of 90.83% was obtained from combinations of different endopeptidases. The largest coverage was obtained from peptides generated by Trypsin and AspN enzymes. The sequences deduced from the peptides revealed methionine as the N-terminal amino acid encoded by CUG (Fig. 54) and lysine substituted for the in-frame *amber* codon (Fig. 52A), which is read through during translation with about 20-25% efficiency (Klagges et al., 1996).

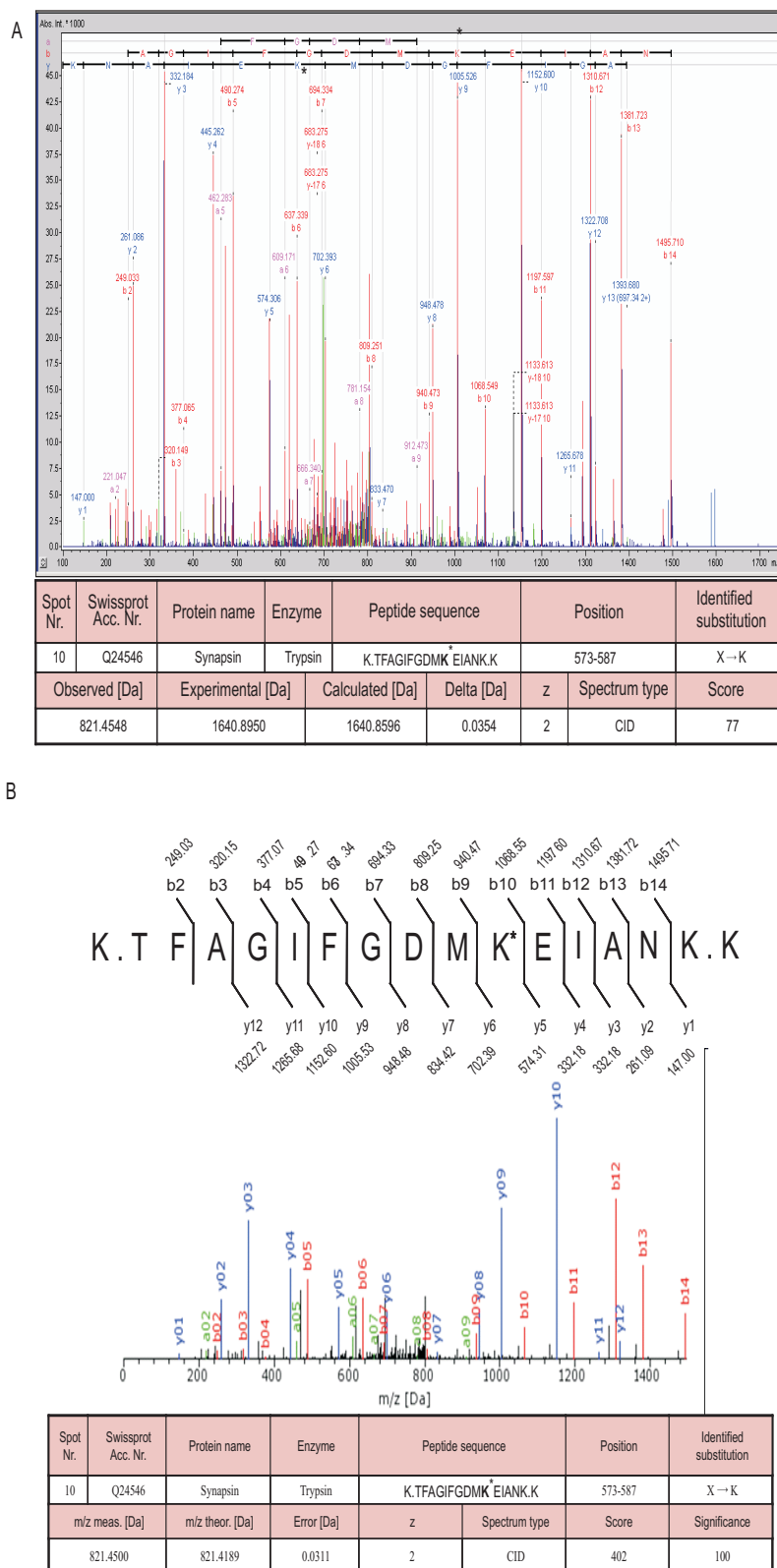
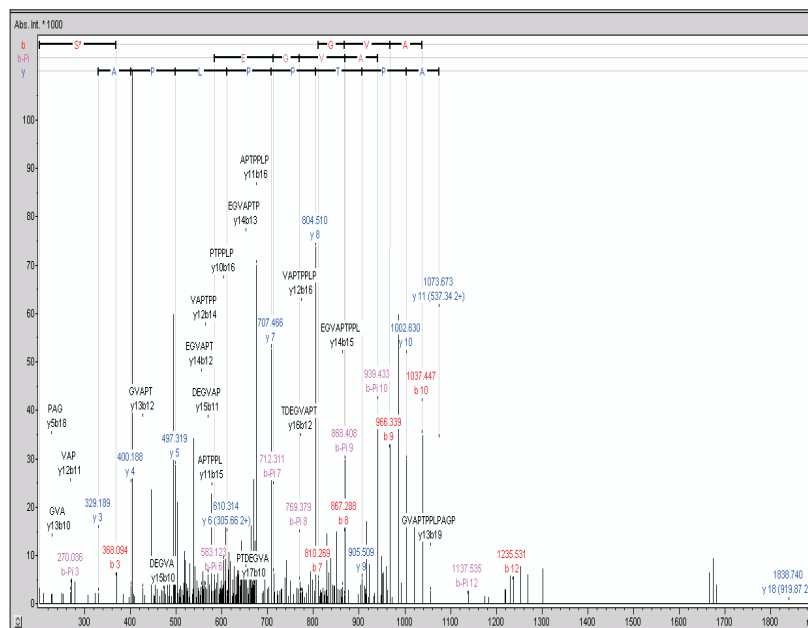


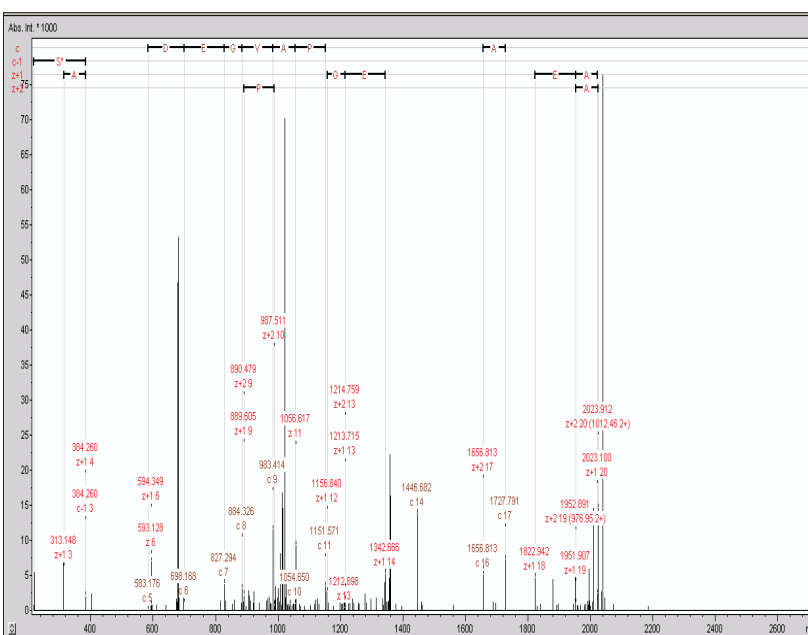
Fig. 52: Mass spectrometric determination of the sequence of synapsin peptide fragments with a lysine (MASCOT v2.2.06 (A) and MODIRO v1.1 analysis (B)) residue at the position corresponding to the *amber* stop codon. The substitution by lysine (K) is highly significant based on the ion score (in collaboration with S. Heo).

A



Spot Nr.	Swissprot Acc. Nr.	Protein name	Enzyme	Peptide sequence	Position	Identified PTMs
10	Q24546	Synapsin	Trypsin	R.AES*PTDEGVAPTPLPAGPR.P	462-481	Phosphorylation
Observed [Da]	Experimental [Da]	Calculated [Da]	Delta [Da]	z	Spectrum type	Score
680.37	2038.09	2037.94	0.1476	3	CID	42

B



Spot Nr.	Swissprot Acc. Nr.	Protein name	Enzyme	Peptide sequence	Position	Identified PTMs
10	Q24546	Synapsin	Trypsin	R.AES*PTDEGVAPTPLPAGPR.P	462-481	Phosphorylation
m/z meas. [Da]	m/z theor. [Da]	Error [Da]	z	Spectrum type	Score	Significance
680.37	680.3209	0.491	3	ETD	309	100

Fig. 52C: Representative mass spectra demonstrating S464 phosphorylation of *Drosophila* synapsin. Proteins from silver stained SDS-PAGE bands marked in Figure 51 were digested by the indicated enzymes and extracted peptides were analyzed by nano-LC-ESI-MS/MS (high capacity ion trap). MS/MS spectra were interpreted and peak lists were generated by DataAnalysis 4.0. Data searches were performed via MASCOT v2.2.06 (A) and ModiroTM v1.1 (B) against latest UniProtKB database for protein identification and PTM search. An asterisk marks the phosphorylated serine (in collaboration with S. Heo).

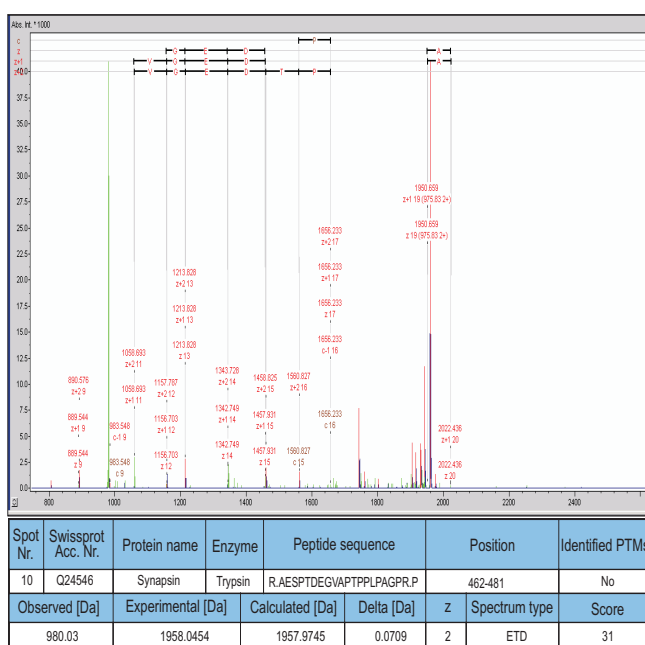


Fig. 52D: Representative mass spectra demonstrating S464 dephosphorylation of *Drosophila* synapsin. Samples were treated with alkaline phosphatase resulting in dephosphorylated peptides.

Several PTMs were detected after analysing the MS/MS spectra with MASCOT and Modiro software. Most of the PTMs identified were phosphorylation, methylation, deamidation, hydroxylation, methionine oxidation, sulfonation etc. Only the phosphorylation sites were confirmed by alkaline phosphatase treatment of corresponding gel pieces and re-analysis by nano-LC-ESI-MS-MS. Mass spectra of untreated and phosphatase treated samples are shown in Fig. 52C and D, respectively. A total of five

phosphorylation sites were detected and verified by phosphatase treatment (Table 3). The positions of these sites with respect to the domain structure of *Drosophila* synapsins is shown in Fig. 53. The PTMs apart from phosphorylation were not verified as they frequently are predicted based on mass shifts caused by artifacts of sample preparation and handling (Table 4). Figure 54 summarizes sequence coverage (indicated in red), methionine at N-terminal, domain structure (highlighted) and PTMs of the present analysis. The complete data set of this analysis can be found in Nuwal et al. (submitted).

Table 3: Identified and verified phosphorylations in synapsin (in collaboration with S. Heo). Coloured residues are the identified phosphorylated residues

Type of modification	Residue	Position
Phosphorylation	RGVSAPT*SPAKS	86
Phosphorylation	RAES*PTDEGVAPTPLPAGPRP	464
Phosphorylation	RRDSQTSQS*STISSVSRA	538
Phosphorylation	KS*MSMTSGGVGSGNGSGSGLGGYKI	961
Phosphorylation	KSMSMTSGGVGSGNGSGSGLGGY*KI	982

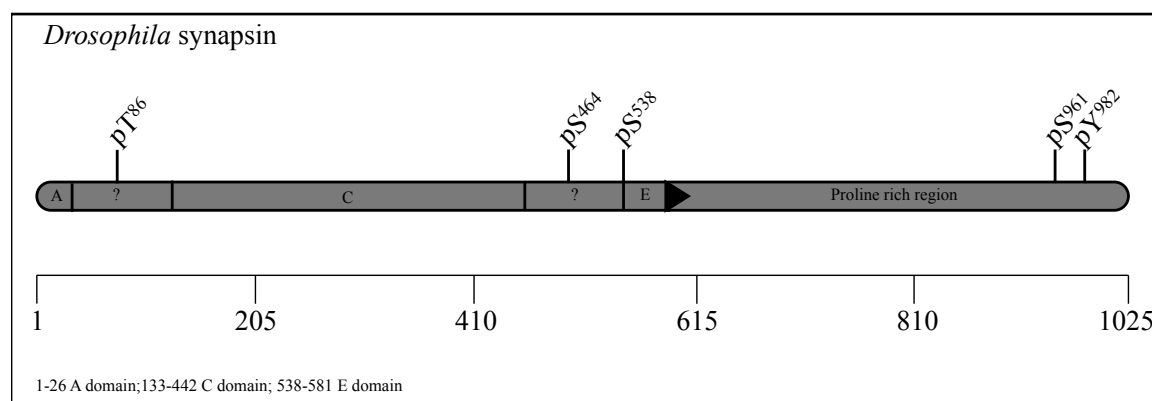


Fig. 53: Domains and identified phosphorylation sites in synapsin. The black arrow head refers to the *amber* stop codon read-through with efficiency of 20-25% (Klagges et al., 1996). The scale drawn below the domain structure with the phosphorylation sites refers to the amino acid residues.

Table 4: Several PTMs were identified in *Drosophila* synapsin. The PTMs marked in **red are significant (score greater than 200 and significance above 80), PTMs marked in **blue** have low scores less than 200 and or significance less than 80 (in collaboration with S. Heo).**

Type of modification	Residue	Position
Sulfonation	RGVSAPT*SPAKS	86
Hydroxylation	RDITVVSSAD*TGPVVTMAAYRS	178
Dioxidation (Sulfones)	KTNQGSAM*LEQITLTEKY	365
Triple oxidation (Kynurenin)	KYKSW*VDEISELFGGMEVCGLSVVAKD	378
Methylation	RMQ*NVCRPSMAQTGPGKLPSRS	437
Methylation	RMQNVCRPS*MAQTGPGKLPSRS	443
Methylation	RMQNVCRPSMAQ*TGPGKLPSR.S	446
Pyrophosphorylation	RPSMAQT*GPGKLPSRS	447
Pyrophosphorylation	R.PSMAQTGPGKLPS*R.S	454
Hydroxylation	RPAP*MGGPPPIPERT	484
Deamidation	RAGQRPPQTQ*NSVVEDAEDTMKN	556
Methylation	KGEGVIS*TQPTQRP	635
Methylation	KGEGVISTQPT*QRP	639
Methylation	RPSYSR*SESNASKH	900
Methylation	RPSYSRSESNAS*KH	906
Methylation	RFGAS*KS	959
Triple oxidation (Kynurenin)	RW*SASKE	1012

1	MKRGFSSGDL	SSEVDDVDPN	SLPPAARPIQ	DQPTKPPVAG	GPPNMPPPPA
51	PGQPAGAAPE	LSLSFAGAKT	PATAAPAPPR	GVSAPT [*] SPAK	SRESLLQQRVQ
101	SLTGAARDQG	ASILGAAVQS	ATQRAPAFSK	DKYFTLLVLD	DQNTDWSKYF
151	RGRRLHGDFD	IRVEQAEFRD	ITVVSSADTG	PVVTMAAYRS	GTRVAR [↓] SFRP
201	DFVLIRQPPR	DGSSDYRSTI	LGLKYGGVPS	INSLHSIYQF	QDKPWVFSHL
251	LQLQRRLLGRD	GFPLIEQTFE	PNPRDLFQFT	KFPSVLKAGH	CHGGVATARL
301	ENQSALQDAA	GLVSGAGNDS	HCYCTIEPYI	DAKFSVHIQK	IGNNYKAFMR
351	KSITGNWKTN	QGSAMLEQIT	LTEKYKSWVD	EISELFGGME	VCGLSVVVAK
401	DGREYIISAC	DSTFALIGDT	QEEDRRQIAD	LVSGRMQNVK	RPSMAQTGPG
451	KLPSRSSVSS	RAES [*] PTDEGV	APTPLPAGP	RPAPMGPPP	IPERTSPA [↓] VG
501	SIGRLSSRSS	ISEVPEEPSS	SGPSTVGGVR	RDSQTSQ [*] SST	ISSSVSRAGQ
551	RPPQTQNSVV	EDAEDTMKNL	RKTFAGIFGD	MXEIANKKRG	RTASETSSGS
601	GPGSVPSAG	PGSGFSSSFL	GKQFSFAGKG	EGVISTQPTQ	RPSEPPAIP
651	TTASSAVRPE	SSVSVD [↓] SRN	TDTLTERAGA	GYQPV [↓] TNYEQ	QERNV [↓] PF [↓] DK [↓] E
701	PSKSGSAASI	HTSSSSSISS	SSISSRINRN	GNAIQSPPPP	AGPPPPPTN
751	VTAVGSNANS	SSGYRNSFSS	SLSKDKTSYG	NYGSTTSVET	ITRMDTNTN
801	IGATATEAGE	ASGVTAITNI	SNSDGIVAPT	TGTITTSVTT	NDWRS [↓] AI [↓] GMR
851	SASVYSAPAA	VTTVLPGDTS	GYDSNSIASQ	GGLN [↓] NP [↓] SDL	PSYTR [↓] PSY [↓] SR
901	SESNA [↓] SKHSD	LDVIFGDSKT	TPASYNGNKY	TRAAGSISDA	DMIFGGPPSN
951	YKTDRF [↓] GASK	[*] SMSMTSGGVG	SGNGSGSGLG	[*] G [↓] KIYDSIQN	AAFSD [↓] FS [↓] DSG
1001	SMSSIGSHTK	RWSASKEEDD	ELDLK		




	Domain A	*	Phosphorylation (verified)
	Domain C	Δ	Sulfonation
	Domain E	▼	Methylation
		↓	Pyrophosphorylation
		↑	Triple oxidation (Kynurenin)
		↓	Dioxidation (Sulfones)
		↓	Hydroxylation

Fig. 54: Sequence coverage of synapsin by multi-enzyme digestion and nano-LC-ESI-MS/MS. MASCOT and Modiro analysis identified the N-terminal methionine, and revealed that the stop codon at position 582 is read through and in most cases is represented by lysine (K) in the protein, and determined PTMs (in collaboration with S. Heo).

4.5 Genome wide transcript analysis of *Sap47^{156CS}*, *Syn^{97CS}* and *Sap47-Syn* double mutants (in collaboration with N. Nuwal, and S. Kneitz)

The total mRNA (poly A⁺) of *Sap47^{156CS}*, *Syn^{97CS}* and double mutants *V2* and *V3* were analysed and compared to total mRNA of two different wild-types (*CS^{NF}* and *CS^V*) using microarray technique. The aim of this experiment was to determine the genes which have significantly altered gene expression in the mutants when compared to the wild-types. The identified genes could be the functional interaction partners of the mutants and could compensate for the loss of function in null mutant lines *Sap47^{156CS}*, *Syn^{97CS}* and double mutants (*V2* and *V3*) as they do not show obvious defects (in collaboration with N. Nuwal, and S. Kneitz).

Prior to starting with microarray analysis, the transcripts of *Sap47* and *Syn* in the null mutants was verified by RT-PCR and it was found that the 5' end of *Sap47* and *Syn* gene was absent whereas the 3' end was intact in the respective individual and double mutants (Fig. 55 A and C, refer to PhD thesis of N. Nuwal, 2010). An essential step in the analysis of any microarray data was to check the quality of the data from the arrays and this was checked by plotting log₂ (intensity ratio) vs mean (log₂ intensities). Long comet-like pattern of non-differentially expressed probes and a small proportion of highly differentially expressed probes were obtained (data not shown, refer to PhD thesis of N. Nuwal, 2010). The genes which were significantly altered in the mutants (p<0.01) were selected and verified by quantitative real time PCR (refer to PhD thesis of N. Nuwal, 2010).

Microarray analysis and qPCR results showed that the transcript levels of *Cir1* (calcium independent receptor for α -latrotoxin) gene was found to be consistently altered (down-regulated) only in the *Syn^{97CS}* mutant (Fig. 55 B, refer to PhD thesis of N. Nuwal, 2010). The transcripts of *Sap47* and *Syn* in the null mutants *Sap47^{156CS}*, *Syn^{97CS}*, *V2* and *V3* were verified by qPCR (Fig. 55 A and C). The 3' end of the transcripts of *Sap47* in *Sap47^{156CS}*, *V2* and *V3*, and *Syn* in *Syn^{97CS}*, *V2* and *V3* were detected at lower levels in qPCR and microarray, this is because the probes in microarray are designed against the 3' region of the gene and this region is intact in the null mutants. The 5' end of the transcript

was absent in the *Syn*^{97CS}, *V2* and *V3* mutants and this served as a negative control for our experiments (refer to PhD thesis of N. Nuwal, 2010).

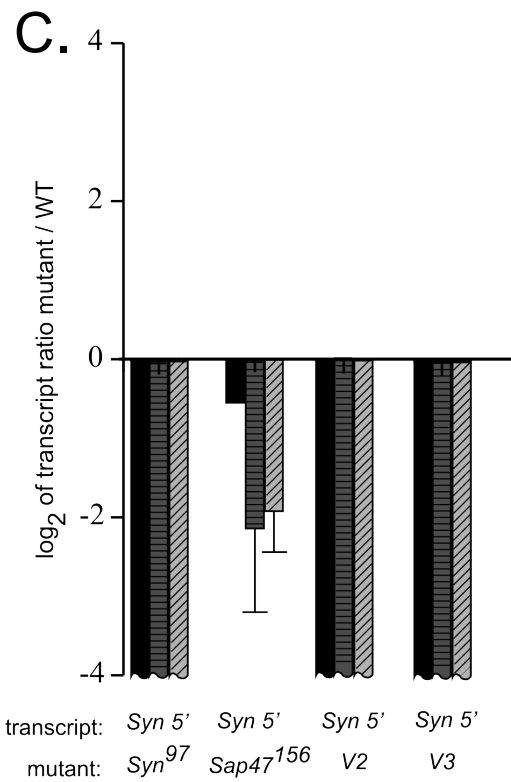
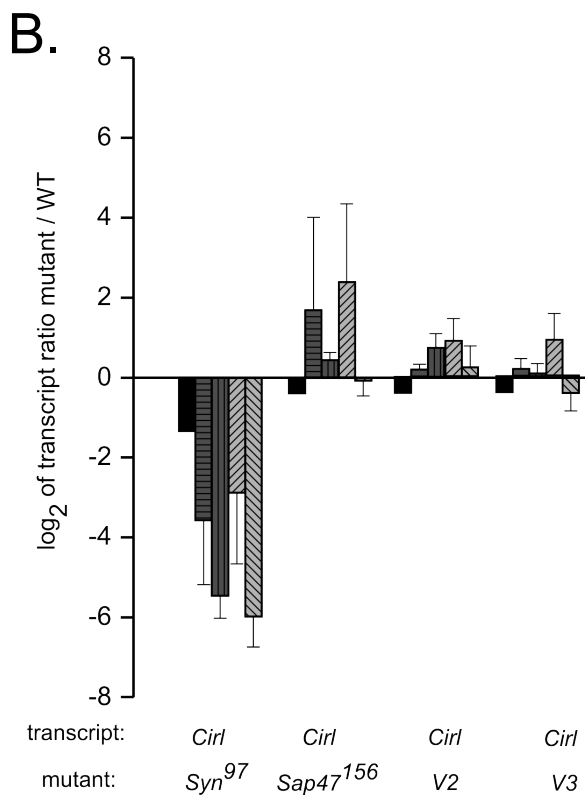
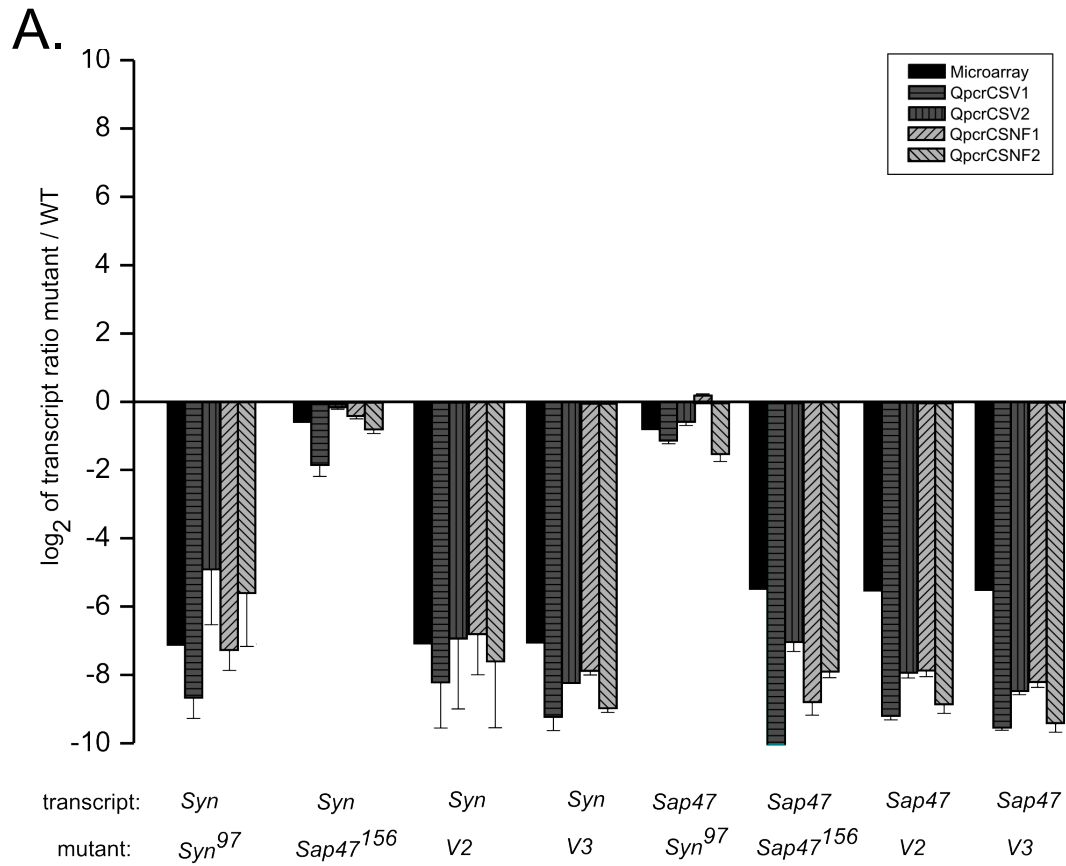


Fig. 55: Transcript analysis of *Sap47*, *Syn* and *Sap-Syn* double mutants (*V2* and *V3*). (A) The 3' transcripts of *Sap47* and *Syn* are present at lower levels in the respective individual and double mutants (*V2* and *V3*) when compared to two different wild-types (*CS^{NF}* and *CS^V*). (B) *Cirtl* is significantly down-regulated only in *Syn^{97CS}* and unchanged in *Sap^{156CS}*, *V2* and *V3* mutants. (C) 5' end of *Syn* transcript is absent in *Syn^{97CS}*, *V2* and *V3* mutants thus the columns for these genotypes are broken in the plot. Note: Average intensities of *V2* and *V3* were used for microarray analysis (black bars are identical for *V2* and *V3* in all panels) (Standard deviations of means are shown for qPCR results, refer to PhD thesis of N. Nuwal, 2010).

The microarray analysis and the qPCR results as shown above also verified our previous observation that *Syn* transcript is not altered in *Sap47* null mutants (see 4.1.3)

4.6 Analysis of Tubulin binding chaperone E-like

The *Drosophila* *Tbce*-like or *Tbcel* (*CG12214*) gene is located on the chromosome arm 2R (www.flybase.org). It has only one exon and is nested in an intron of the *KCNQ* gene (*CG33135*). *Tbcel* has two different transcripts RA and RB due to alternative transcription start sites (see Fig. 56) and is highly expressed in brain and other tissues (Table 5, flybase.org). In a yeast-two-hybrid screen performed by N. Funk to identify interacting partners of *Drosophila* SAP47, TBCEL was the only interacting partner obtained (PhD thesis N. Funk, 2003).

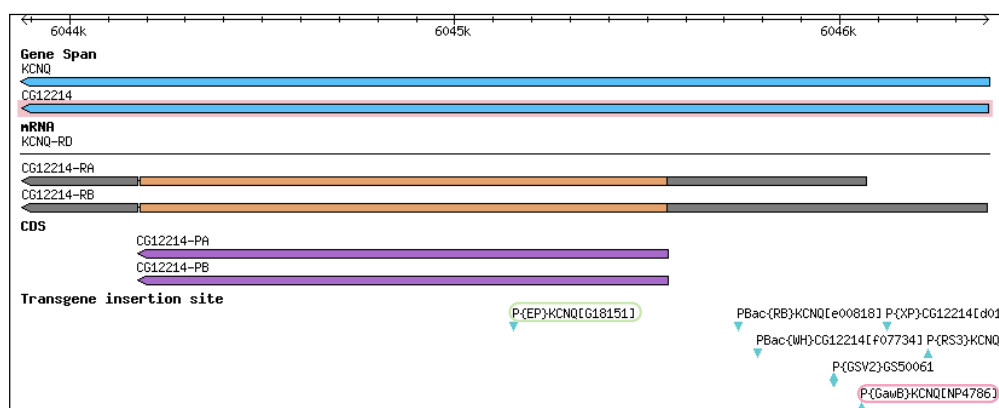


Fig. 56: *Drosophila* *Tbcel* (*CG12214*) gene structure. The gene is nested in an intron of the *KCNQ* gene and codes for two transcripts RA and RB. The coding region of two transcripts are identical. The G18151 insertion (P-element, highlighted in green) is located 403 bp downstream of the ATG (translation start site), NP4786 (P-element, highlighted in pink) is inserted 504 bp upstream of the ATG. (Source: Flybase).

4.6.1 TBCE and TBCEL have conserved domains

Amino acid sequences of TBCE and TBCEL proteins of *Drosophila* (Flybase, genes *CG7861* and *CG12214*, respectively), human (TBCE: GenBank accession AAH08654.1; TBCEL: GenBank accession AAI20990.1) and mouse (TBCE: GenBank accession AAL92570.1; TBCEL: GenBank accession AAI39388.1) were obtained from NCBI database. The sequences were aligned using ClustalW 2.0 software available online

(see Appendix). Two major domains identified in *Drosophila* TBCEL protein were leucine rich repeats (LRRs) and ubiquitin-like domain (UBL). A schematic of the domain structure of TBCE and TBCEL is shown in Fig. 57.

TBCEL is not predicted to have a glycine-rich cytoskeletal attached domain (CAP-Gly) (see Discussion).

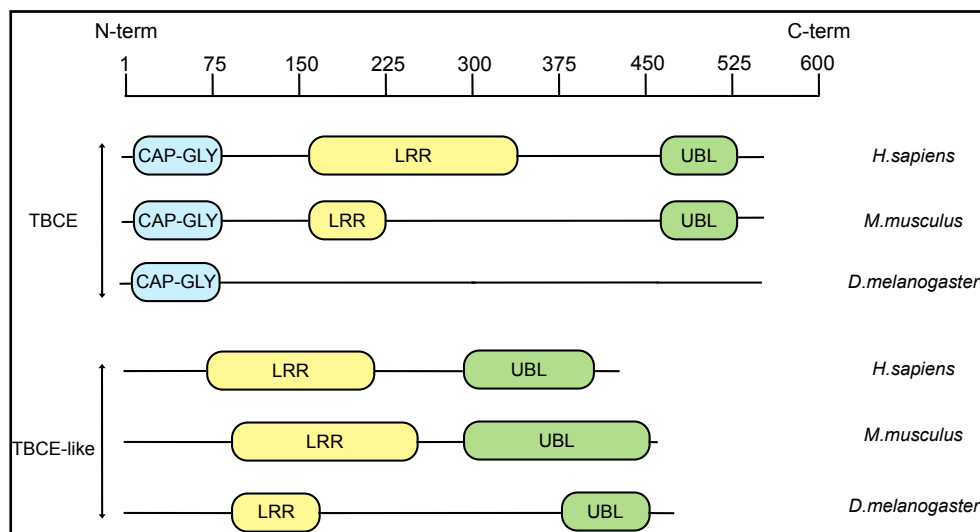


Fig. 57: TBCE and TBCEL domain homology. CAP-Gly is a glycine-rich cytoskeleton-associated protein domain involved in interactions with the cytoskeletal structure; LRR are leucine-rich repeat sequences involved in protein-protein interactions; UBL is a ubiquitin-like domain that may play a role in proteosomal mediated degradation. The CAP-Gly domain is not present in TBCEL. Coloured boxes indicate amino acid sequence homology. Prediction by fold recognition algorithm (<http://motif.genome.jp/>).

Table 5: Expression of *Tbcel* transcript in different tissues of adult *Drosophila*. The enrichment score defines the tissue-specificity of *Tbcel*, scores above 1.4 indicate high enrichment in particular tissue (Source: <http://flyatlas.org/>, (Chintapalli et al., 2007)).

Tissue	Enrichment
Brain	2.60
Head	1.40
Eye	1.66
Thoracic ganglion	2.10
Crop	2.70
Ovary	0.80
Testis	1.90
Salivary gland	1.73
Mated spermatheca	1.06
Virgin spermatheca	1.05

In order to investigate further the TBCEL protein and its functions, we generated a polyclonal antiserum (in collaboration with G. Krohne) against His-tagged TBCEL in Guinea pig.

4.6.2 Generation of anti-TBCEL antiserum

Cloning and expression of the *Tbcel* cDNA in the His-tag plasmid and purification of the protein has been described in Methods section. TBCEL antiserum was obtained from the final bleed of a Guinea pig immunised with 1 µg of bacterially expressed *Drosophila* His-tagged TBCEL. The antiserum was tested on Western blots of fresh head homogenate from adult *CS* flies and purified His-tagged TBCEL and was found to recognise a band at around 55-59 kD in both the bacterially expressed His-tagged TBCEL and the endogenous TBCEL in wild-type (*CS*) flies (see Fig. 58).

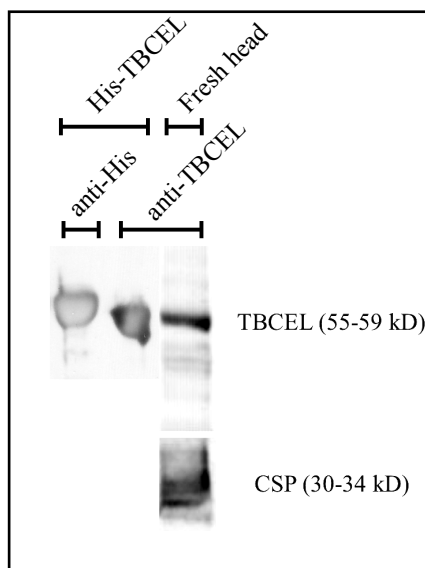


Fig. 58: *Drosophila* TBCEL is a 55-59 kD protein. Western blot of lysate from bacteria expressing His-tagged TBCEL (left two lanes) and of homogenate from 2 wild type fly heads (rightmost lane, Note: The image is taken from a different blot with anti-CSP as loading control (Diploma thesis S. Racic, 2009)). The anti-TBCEL antiserum recognises the induced His-tagged TBCEL (also recognised by anti-His antibody) and the endogenous TBCEL at around the same size (55-59 kDa). (antibody dilutions, anti-His 1:400, anti-TBCEL 1:4000, anti-CSP 1:50).

The generation of anti-TBCEL antibody was important for our investigation of TBCEL protein localization and expression in *Drosophila*. The availability of a null mutant for TBCEL would serve as a negative control for our qualitative and quantitative studies of TBCEL.

4.6.3 Analysis of NP4786 and G18151 P-insertion stocks

In order obtain a null mutant for the *Tbcel* gene we checked the list of available transposon insertion stocks for the *Tbcel* gene (*CG12214*) in flybase. When we started our experiments no insertion in the coding region of the gene was available. We therefore chose the NP4786 line which at that time represented the P-element insertion in the 5' UTR closest to the translation start site. This insertion may disrupt transcription and is very likely to affect the transcription efficiency of the coding region. With this line we

started an extensive P-element jump-out mutagenesis described below (4.6.6) in order to generate a deletion in the gene as a reliable null mutant. More recently, however, the G18151 insertion stock has been added to the flybase repository. The G18151 P-element is inserted in the open reading frame (ORF) and is putatively a null mutant for the *Tbcel* gene (Fig. 56).

The NP4786 stock (short name: NP) is homozygous lethal (maintained over *CyO* balancer). Its P-element cassette contains a weak promoter in front of the yeast transcription factor *gal4* encoding cDNA. Thus, the NP4786 line can reflect the expression pattern of a neighbouring enhancer (enhancer trap) when crossed to flies having a UAS (upstream activating sequence) construct with a reporter gene (e.g GFP).

To determine if the lethality is due to the insertion in *Tbcel* gene we crossed the *NP/CyO* flies to a deficiency stock, *Df(2R)BSC281/CyO* (short name: *Df/CyO*). The F_1 progenies (NP/Df) of this cross were viable, suggesting that the lethality is most likely due to a second site mutation on the 2nd chromosome outside the Df region.

The NP4786 insertion was verified by PCR using primer pair 1 (inverted repeats of the the P-element) and 2 (3' flanking genomic region) and pair 1 and 4 (5' flanking genomic region) and the G18151 insertion was verified by using primer pairs 1 and 4 (5' flanking genomic region) Figure 59, respectively, and sequencing of the PCR products (Diploma thesis I. Montalban, in preparation). The insertions were found to be as reported in the database (www.flybase.org).

4.6.3.1 Transcript analysis of the NP4786 line

Prior to beginning with the P-element mutagenesis we investigated whether the NP insertion line by itself was a null/strong hypomorph mutant. The 5' UTR of a gene can play several regulatory roles like modifying mRNA stability (Oliveira and McCarthy, 1995) and localization (see review Jansen, 2001). Efficiency of translation can also be affected by disruption of the 5' UTR of the gene (see review Gray and Wickens, 1998; van der Velden and Thomas, 1999; Pesole et al., 2001). The NP4786 line has a P-element

insertion in the 5' UTR region of *Tbcel* gene such that it could be a null mutant or a hypomorph for the gene function. We determined the presence and level of transcripts in *NP/Df* flies by RT-PCR (Fig. 59 and 60).

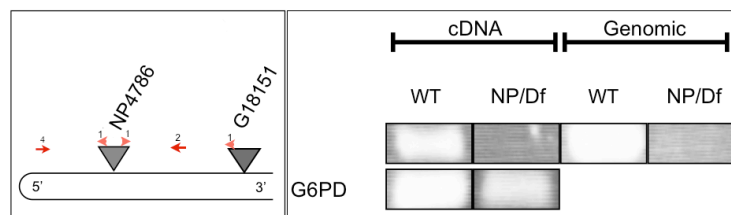


Fig. 59: The primers (pair 2 and 4) across the P-element produced no signal from reverse transcribed template and from the genomic template from *NP/Df* flies. *G6PD* transcript levels served as an internal control and WT as a positive control. The genomic region including the P-element was too large to be amplified under the conditions used and no detectable product was formed.

PCR with primer pair 2 and 4 (Fig. 59) across the P-element produced no detectable product from reverse transcribed cDNA. As an internal control, the *G6PD* transcript was detected from the same cDNA samples of WT and *NP/Df* and was found to be normal.

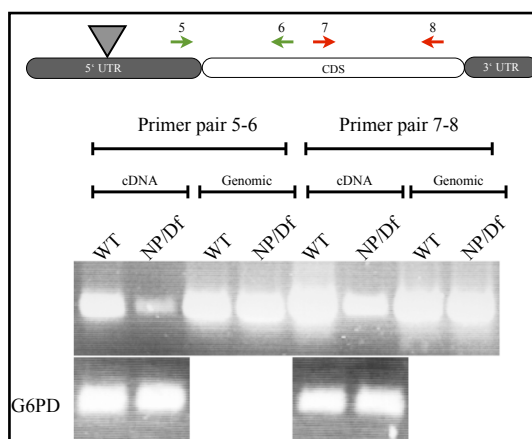


Fig. 60: Presence of reduced transcript downstream of the NP4786 P-element. *G6PD* transcript levels served as an internal control and WT as a positive control.

PCR with two different primer pairs downstream of the P-element produced normal genomic product and reduced but detectable product from reverse transcribed cDNA from *NP/Df* flies. As an internal control, *G6PD* transcript was detected from the same cDNA samples of WT and *NP/Df* and was found to be normal (Fig. 60).

The results in Figure 59 and 60 prove that the P(GawB) element in the NP4786 line disrupts the *Tbcel* transcript. The reduced amount of transcripts observed with primer pairs downstream of the NP4786 has not been further characterised but it may lead to reduction or complete loss of TBCEL protein. The absence/down-regulation of TBCEL protein in *NP/CyO* flies was verified by Western blotting using the anti-TBCEL antiserum.

4.6.3.2 Protein analysis of the NP4786 and G18151 stocks

In a semi-quantitative Western blot of adult head homogenates *NP/CyO* flies were found to have approximately half the amount of protein when compared to *CS* flies (Fig. 61 compare the WT lane with 1 head loading to 2 head loading of *NP/CyO*). Since the *CyO* chromosome can be assumed to produce normal amounts of TBCEL,

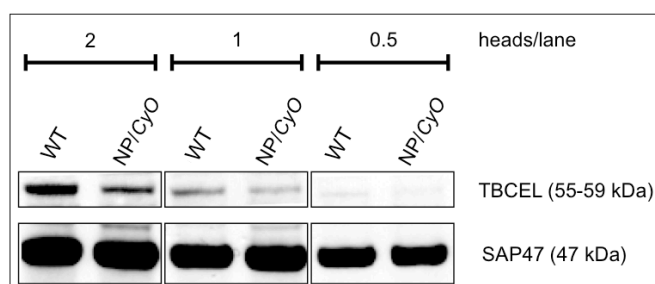


Fig. 61: Semi quantitative Western blot of NP4786 line. TBCEL protein is approximately reduced to half the expression in wild type *CS*. SAP47 protein levels served as loading control (anti-SAP47, MAB nc46 (dilution, 1:200), anti-TBCEL, (dilution, 1:4000)).

this result suggests that the NP insertion results in a null mutation or a strong hypomorph for the *Tbcel* gene. To confirm this finding we tested the *NP/Df* flies on a Western blot. The result (Fig. 62) shows that the NP line, the line e00818 (see Fig. 56) and the line G18151 are null mutants or strong hypomorphs for the *Tbcel* gene.

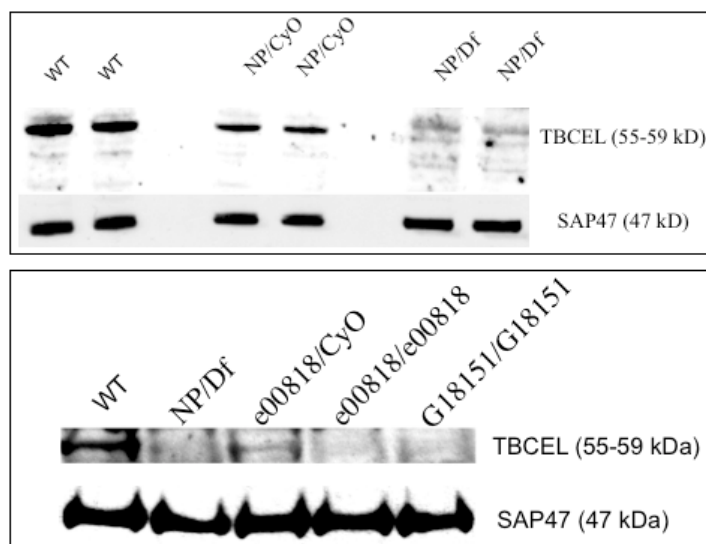


Fig. 62: Western blots for different insertion mutants of the *Tbcel* gene. In the upper blot, the bands detected in the *NP/Df* lane at about the same position as the signal in WT and *NP/CyO* are due to unspecific cross-reactivity of the anti-TBCEL antiserum. The bottom blot demonstrates that *NP/Df*, e00818 and G18151 homozygous flies are null mutants or strong hypomorphs for the *Tbcel* gene. SAP47 protein levels served as loading control (anti-SAP47, MAB nc46 (dilution, 1:200), polyclonal antiserum, anti-TBCEL, (dilution, 1:4000))

As mentioned above, the G18151 fly line was not listed in the flybase when we started with our P-element mutagenesis using the NP4786 line (the obvious choice would have been to use the G18151 stock). The G18151 line is homozygous viable and has a P-element insertion in the coding region of the gene such that an intact TBCEL protein cannot be formed. Thus, this line can safely be assumed to represent a true null mutant for the *Tbcel* gene. We tested G18151 line on a Western blot and found no detectable TBCEL protein in homozygous flies (Fig. 62 and 63). No TBCEL was detected in males or

females of this line whereas in wild-type *CS*, TBCEL was detected in heads and bodies (Fig. 63).

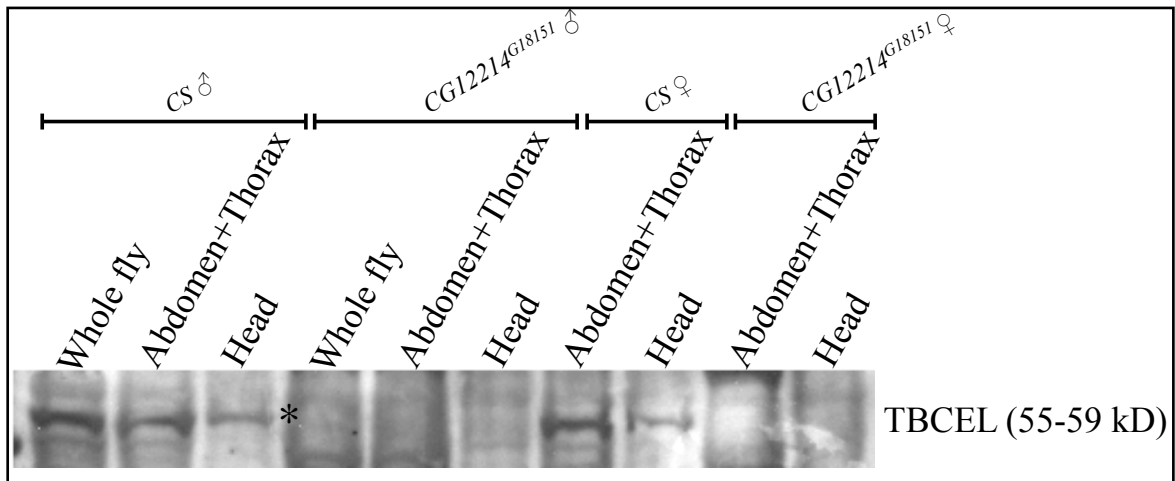


Fig. 63: Loss of TBCEL in G18151 insertion mutants, asterisk marks the TBCEL signal. Note: From the abdomen of males the gut had been removed (Anti-TBCEL, (dilution, 1:4000)). (Diploma thesis I. Montalban, in preparation)

Since *NP/Df* and G18151 homozygous flies are viable this confirms our finding that the lethality in NP line is due to a second site mutation. The *NP/Df* and G18151 lines will serve as null mutants for further experiments.

4.6.4 Expression of TBCEL in *Drosophila* testes

The expression analysis for TBCEL was concentrated on adult testes because it has been reported that the human homologue of TBCEL is highly enriched in testis (Bartolini et al., 2005) and also *Drosophila Tbccl* transcript is enriched in testis (see Table 5). Since the null mutants required to demonstrate specificity of immunohistochemical staining became available only towards the end of the thesis, this study requires further analysis.

A schematic of *Drosophila* spermatogenesis is shown in Fig. 64 for better understanding of results that follow:

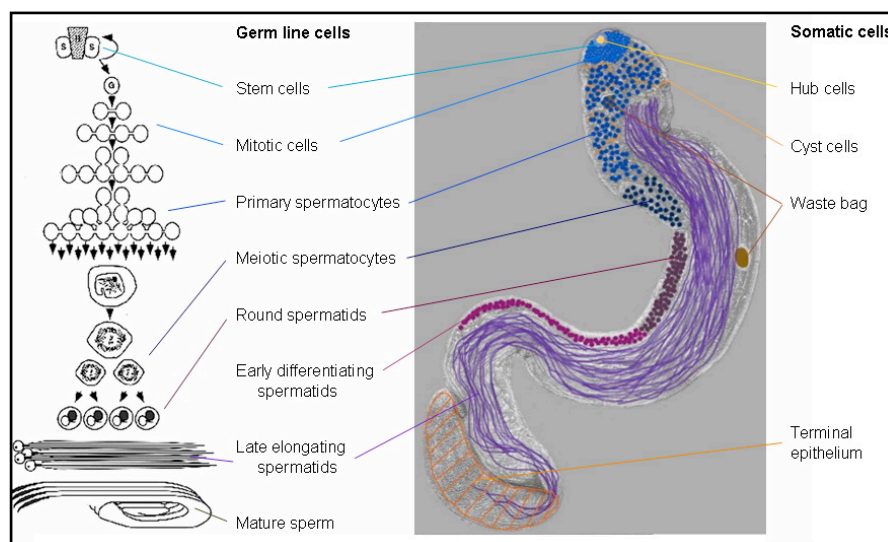


Fig. 64: Spermatogenesis in *Drosophila melanogaster* (Source: http://www.fly-ted.org/images/Spermatogenesis_diagram.png).

4.6.4.1 Expression and localization of TBCEL in adult testis

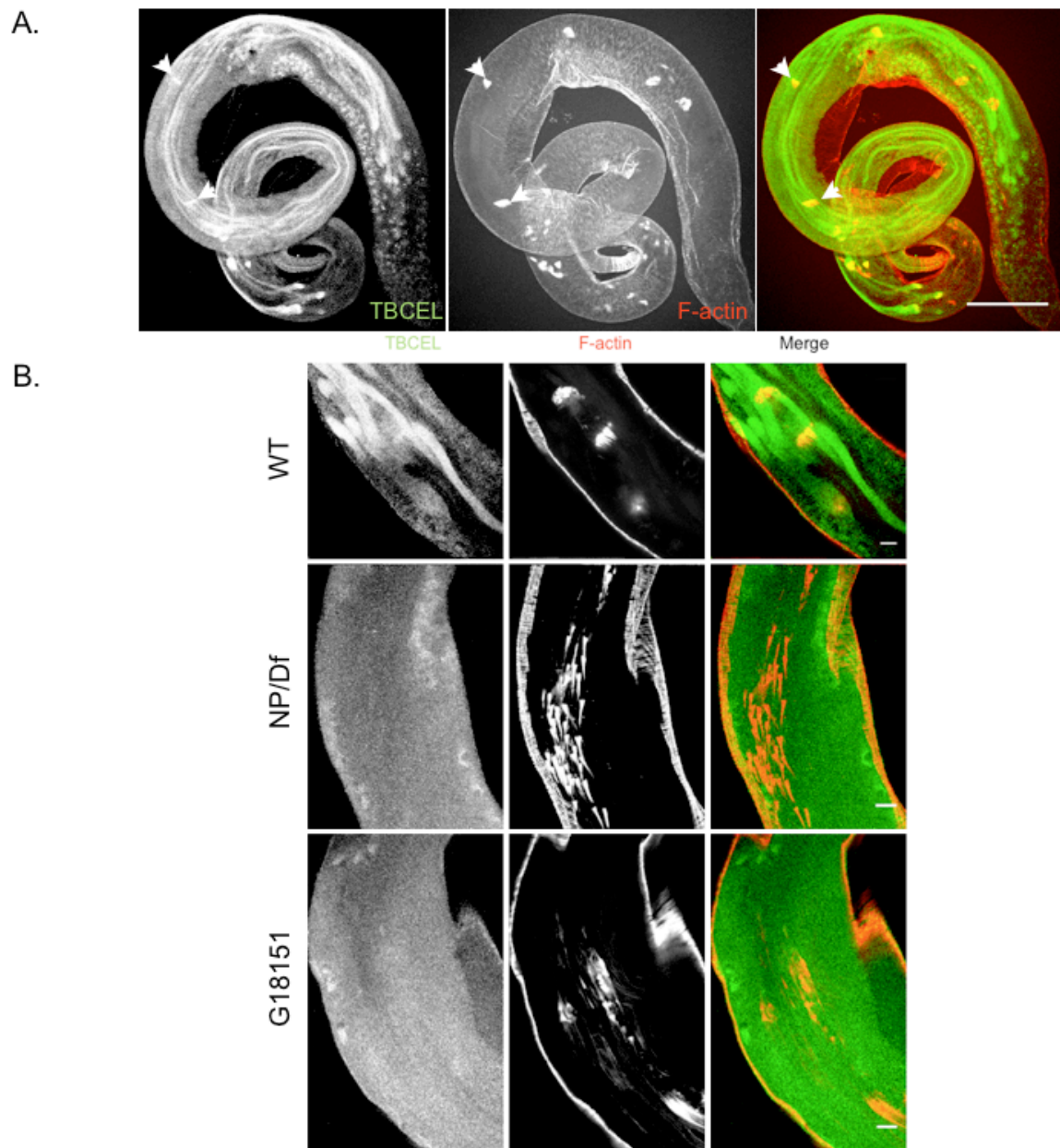


Fig. 65: (A) An overview of TBCEL detection in testis (10X objective). The TBCEL protein is enriched in the investment cone (arrow heads) (B) Details at higher resolution (40X objective). NP/Df and G18151 testes show only background staining. In WT (wild-type, w^{1118}) TBCEL staining is present in spermatid bundles (see also Fig. 66). The actin-rich investment cones are stained with phalloidin. Investment cones are dispersed in NP/Df and G18151 testes (Phalloidin 1:200; anti-TBCEL 1:1000).

In wild-type flies, uniform staining with anti-TBCEL antiserum was observed in the spermatid bundles enclosed by the cyst cells. This reflects the TBCEL expression because it was not seen in the null mutants *NP/Df* and G18151. We observed an enrichment of TBCEL staining at the actin cones (investment cones) of wild-type flies (Fig. 66) suggesting that TBCEL is present in the cytoplasm or the investment cone complex, these details need to be investigated further (Fig. 66).

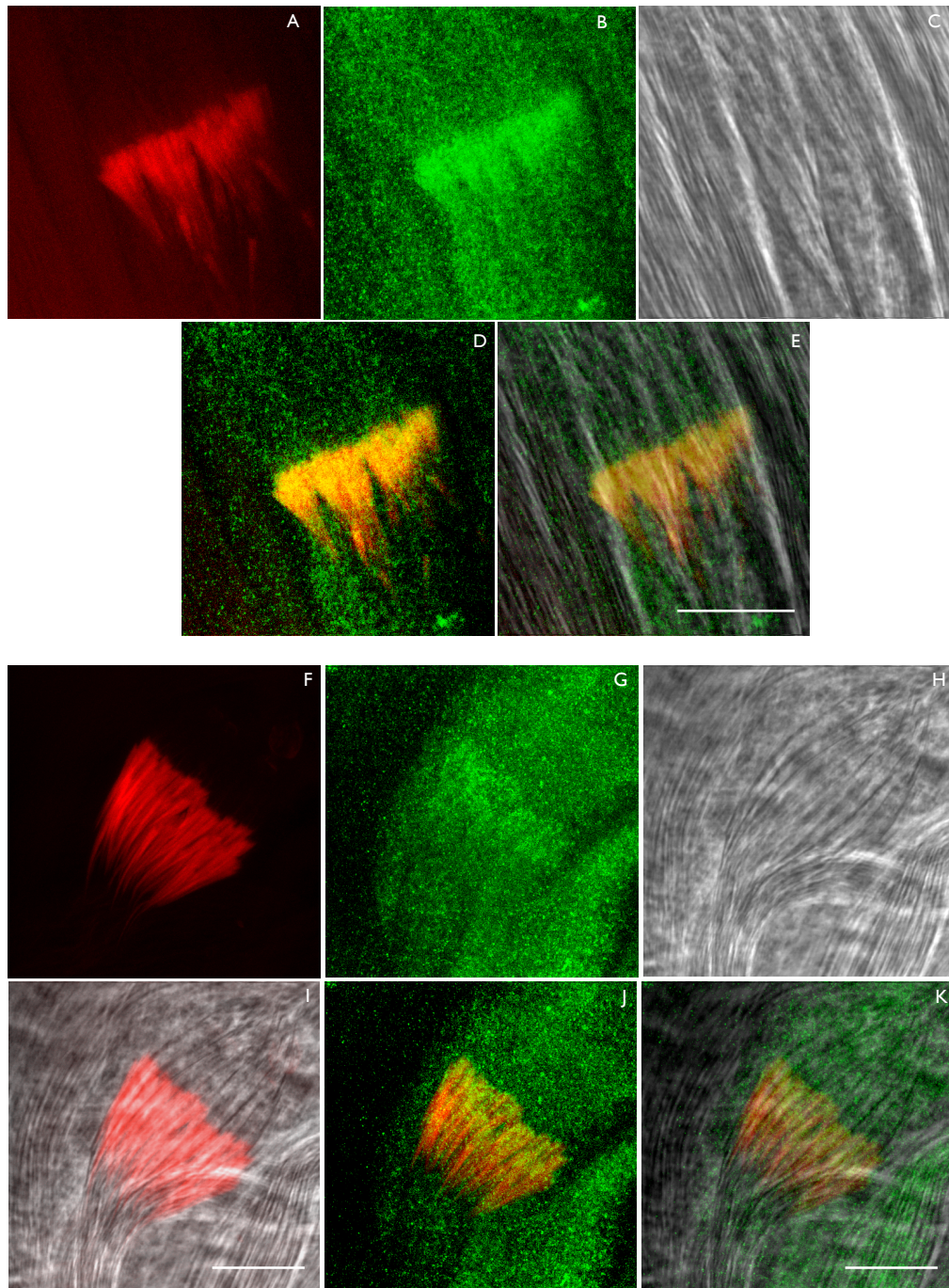


Fig. 66: TBCEL is enriched around the actin cones. Actin cones were stained by Phalloidin (in red, A and F), TBCEL was detected by anti-TBCEL (in green, B and G), the phase contrast images (C and H) were obtained using Leica confocal microscope with 40X phase contrast objective. Actin and TBCEL colocalize at the investment cones (shown in J and D). The phase contrast images provide the structural information. NP/Df and G18151 stocks have no detectable TBCEL staining (see Fig. 65) (Phalloidin 1:200; anti-TBCEL 1:1000). Scale bar 10 μ m

4.6.4.2 Overexpression of TBCEL in testis

The Gal4 expression of the NP4786 enhancer trap line was revealed by crossing the NP line to the UAS-*Tbcel* line generated by S. Wegener (see Master thesis S. Wegener, 2008). Dissected testes were co-stained with TBCEL and propidium iodide (nuclear stain). It was observed that the two signals do not co localize and thus TBCEL is not a nuclear protein (see Fig. 67). The expression pattern of enhancer trap line and endogenous protein was identical and more intense in over-expression flies when compared to the endogenous levels.

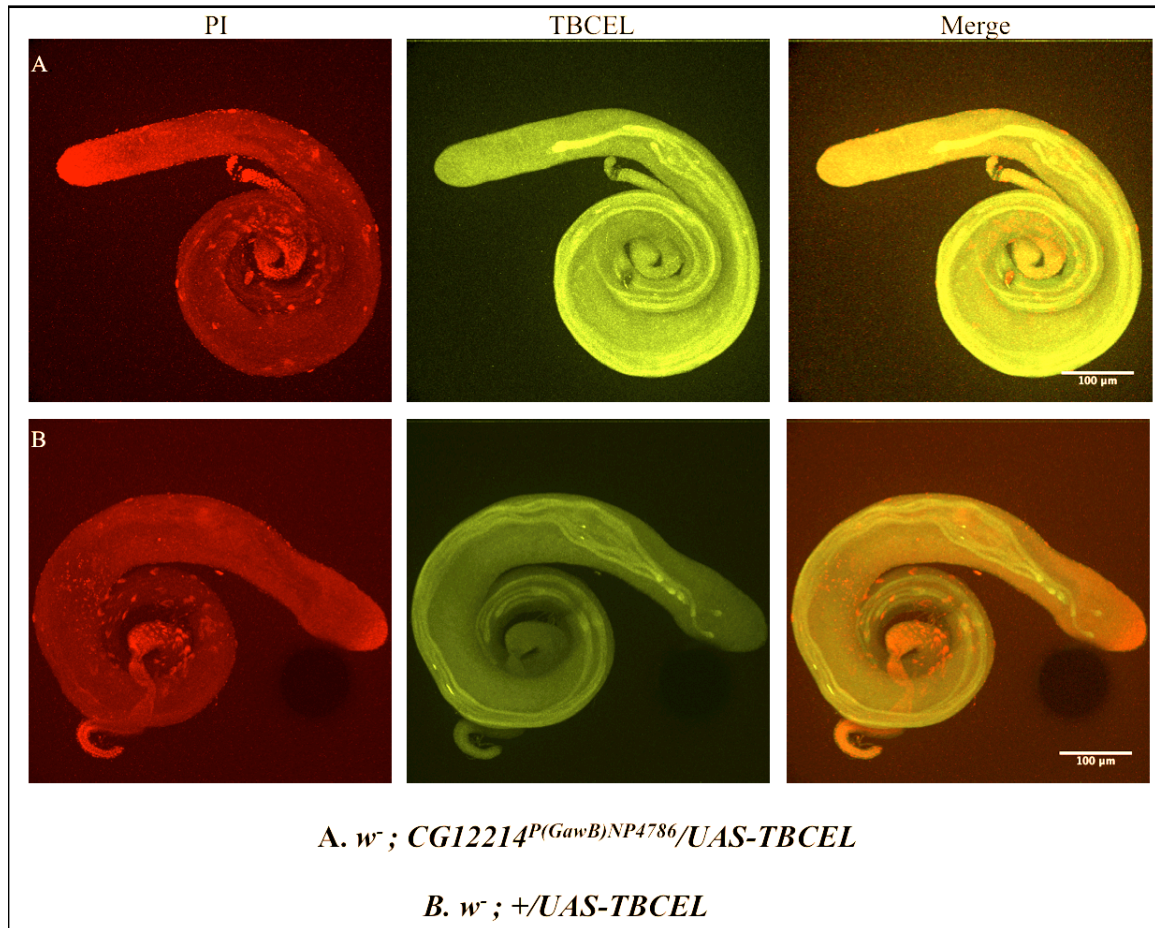


Fig. 67: TBCEL is absent in nuclei. Nuclear stain propidium iodide (PI, red) and TBCEL (green) do not overlap. Enhancer trap expression of NP4786 revealed by detecting TBCEL (Panel A). Enhancer trap expression and the endogenous TBCEL is detected around the spermatid bundle (compare panel A and B) (PI was present in the mounting medium; anti-TBCEL 1:1000).

4.6.4.3 Expression of *gal4* in adult brain and testis of the NP enhancer trap line

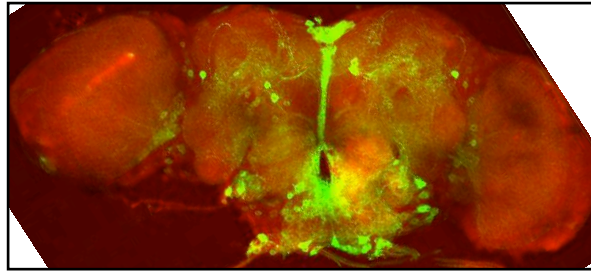
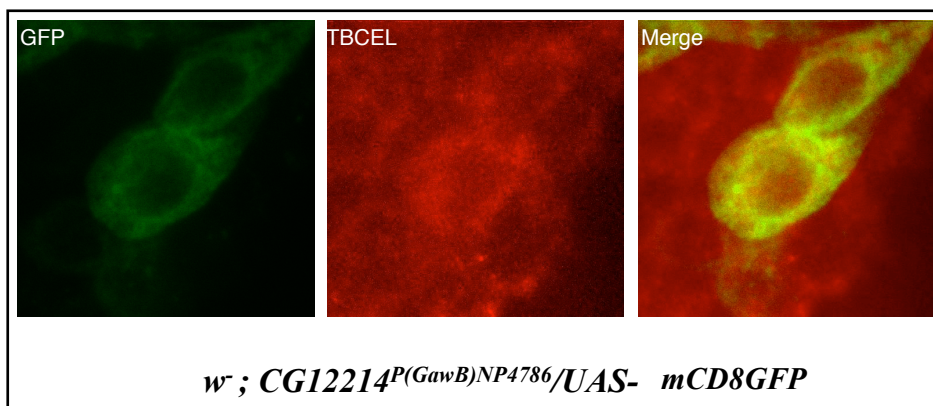


Fig. 68: NP4786 enhancer trap expression revealed by crossing P(GawB)NP4786 line to UAS-mCD8::GFP. The median cells along with the bundle and the subesophageal ganglion are strongly stained (mouse anti-GFP, dilution (1:1000), anti-mouse alexa 488, dilution (1:1000); anti-HRP Cy3 coupled (cross-reacts to Na⁺/K⁺ ATPase in the plasma membrane), dilution (1:1000)).

The enhancer trap expression of the NP4786 line on crossed to UAS-mCD8::GFP (cell surface GFP reporter) showed strong and selective GFP expression in the brain (Fig. 68). In some brain cells, the enhancer trap expression seems to co-localize with the endogenous TBCEL (Fig. 69, upper panel), suggesting that the NP line reflects at least partially the expression pattern of TBCEL by trapping the enhancer acting on *Tbcel* gene (Fig. 69).



NP4786/UAS-mCD8::GFP

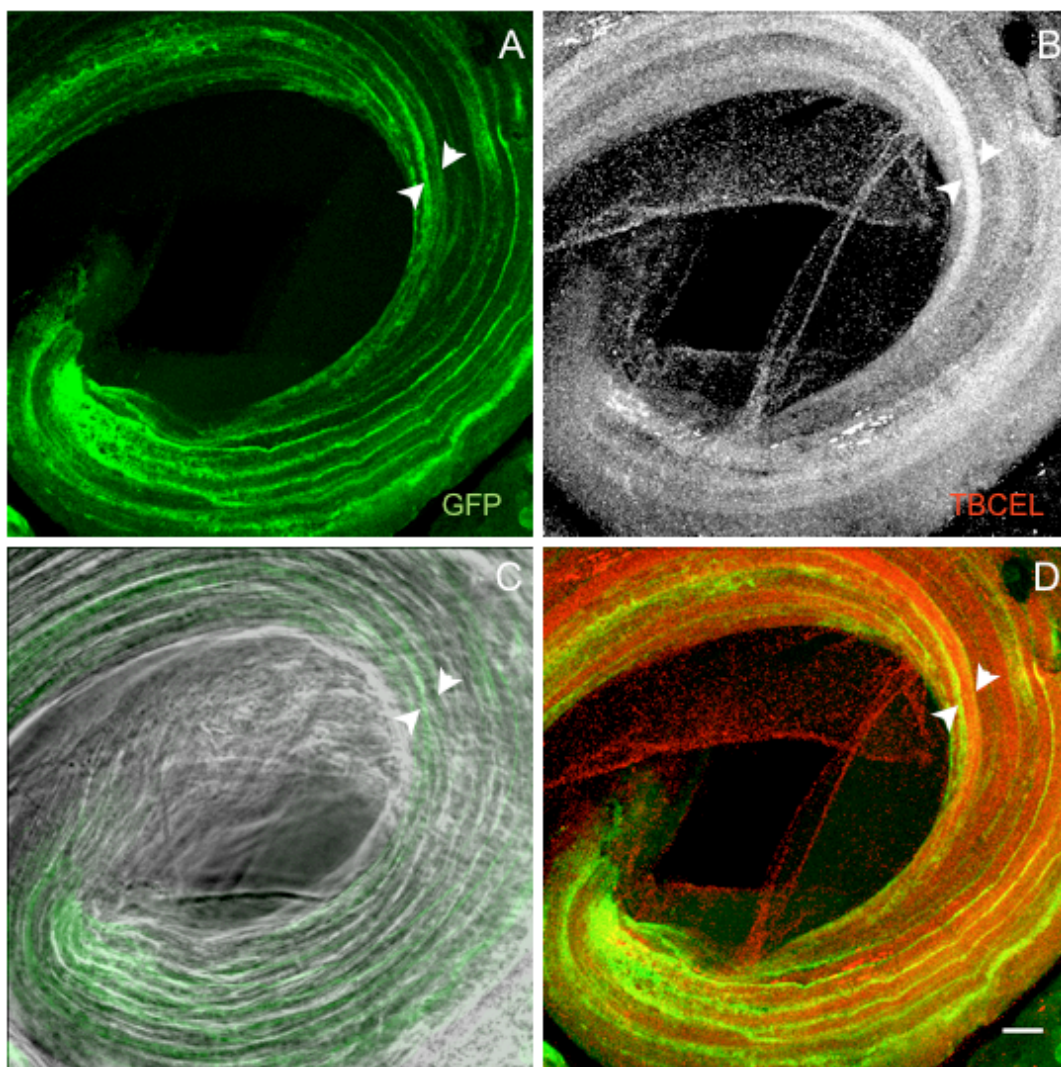


Fig. 69: NP4786 enhancer trap expression revealed by crossing P(GawB)NP4786 line to UAS-mCD8::GFP and co-localization with endogenous TBCEL in the brain (top panel) and in the cyst cells of testis (A-D, white arrow heads mark the cyst cells). Panel C is a merge of phase contrast image and GFP signal (Panel A) (mouse anti-GFP, dilution (1:1000), anti-mouse alexa 488, dilution (1:1000); anti-TBCEL, dilution (1:1200), anti-guinea pig Cy3, dilution (1:1000)).

4.6.5 Fertility assay

The human homologue of TBCEL is highly expressed in testis (Bartolini et al., 2005). In *Drosophila* we found TBCEL also to be expressed in testis (see 4.6.4). The presence of TBCEL in testis could indicate its involvement in spermatogenesis. A defect in qualitative or quantitative aspects of spermatogenesis could lead to sterility in males (for e.g., oligospermia- few spermatozoa in semen; aspermia- complete lack of semen; azoospermia- absence of living sperm cells in semen; teratospermia- sperm with abnormal morphology; asthenozoospermia- reduced sperm motility).

Males of NP/Df and G18151 were found to be sterile when mated with WT (w^{1118}) virgin females (Fig. 70A)

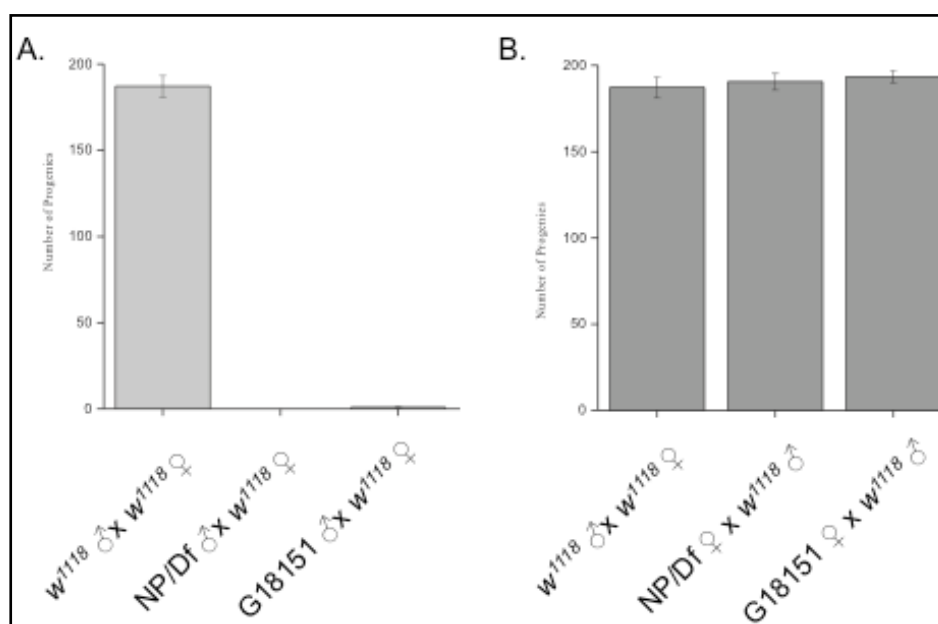


Fig. 70: (A) Males of *NP/Df* and G18151 are sterile when crossed to *w¹¹¹⁸* females. 10 males (2-3 days old) of *w¹¹¹⁸*, *NP/Df* and G18151 were crossed to 10 virgin females (2-3 days old) of *w¹¹¹⁸* in individual medium sized vials (10 vials for each cross). The parents were transferred after sufficient egg laying (5 days). Progenies were counted in each vial until no more flies emerged. (B) Females of *NP/Df* and G18151 in the reciprocal cross were fertile. The average number of flies from each vial is plotted and S.E.M is marked.

4.6.6 P-element mutagenesis of *Tbcel* gene

In parallel to the characterization of NP4786 and G18151 line we performed a P-element jump-out mutagenesis of *Tbcel* gene using the NP4786 line in order to generate a deletion mutant for the *Tbcel* gene (see Fig. 56 and 71).

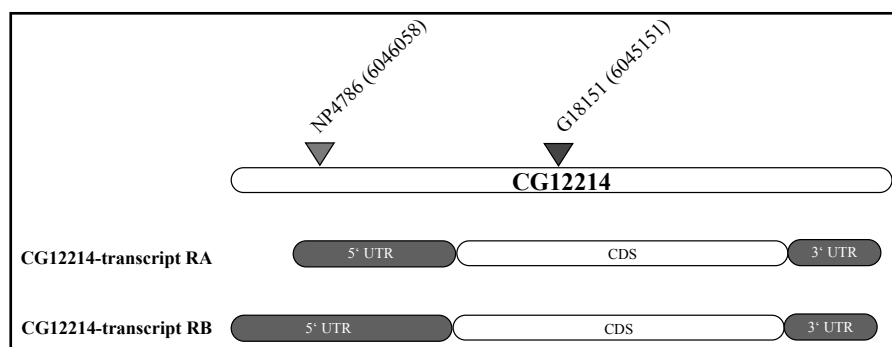


Fig. 71: NP4786 P-element insertion is in 5' UTR and G18151 has P insertion in the ORF region of the gene (Source: flybase.org)

The crossing scheme is shown in Figure 72. The progenies from the single fly crossings were tested by PCR for presence of deletions in the *Tbcel* gene. As a first step the transposase and the P-element had to be brought together in the same fly for transposition to occur. 245 mass crosses between 25 virgin females of the NP line and 25 males of the transposase line ($\Delta 2-3^{Ki}$) were set up (Stage II in Fig. 72). The male progenies of the cross with red eye colour and kinked bristles (to select the $\Delta 2-3^{Ki}$ chromosome) were selected (*NP/CyO*; $\Delta 2-3^{Ki}$) and crossed to *Sco/CyO* virgin females in

612 mass crosses (Stage III in Fig. 72). Non-*Sco*, *CyO* flies with white eyes were selected (absence of mini-*white* gene indicate jump-out of the P-element) and 273 fly lines were established by crossing them individually to *Sco/CyO* flies (Stage IV and V in Fig. 72). The white eyes could also result from a deletion in the mini-*white* gene during transposition, leaving the rest of the P-element intact. To confirm the presence of any deletions, PCRs were performed in two stages. In stage 1, the absence of the P-element was determined by having primers in the P-element and the flanking genomic region (primer pair 1f/1r, see Materials).

4.6.6.1 First attempt

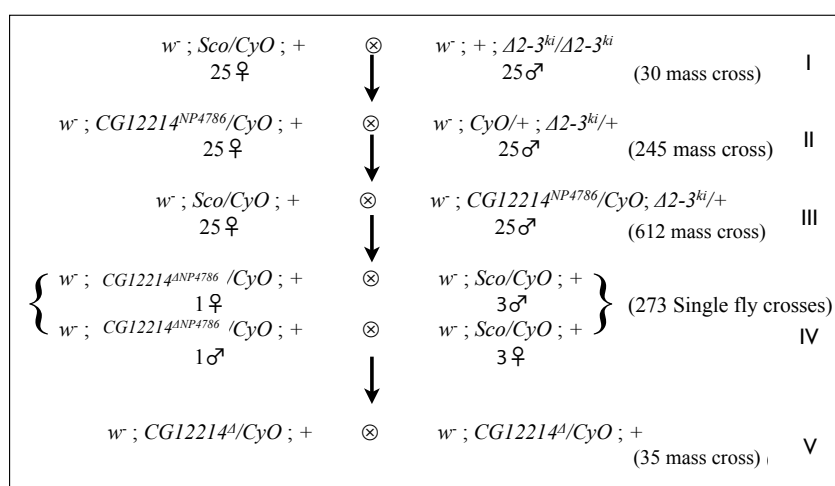


Fig. 72: Crossing scheme for P-element jump-out mutagenesis (First trial).

Single fly crosses in total	273
Total single fly lines screened (white eyes)	135
Dead/Infertile	138
Total lines with P-element Jump out	35

Only 35 lines were obtained in which the P-element had jumped out. The rest (100, as 138 were dead/infertile) which had suffered an internal deletion within the P-element disrupting the mini-*white* gene were discarded. These 35 flies were subjected to a second round of PCR with primer pairs around the P-element (primer pair 1f/5r, see Materials).

Homozygous viable flies	11
Homozygous lethal flies	24
Revertants	35

All the 35 fly lines were revertants as PCR with genomic DNA from neither the homozygous viable flies nor the homozygous lethal flies produced a shorter product when compared to the wild-type flies (a shorter product would correspond to a deletion). The reason for homozygous lethality could be the presence of the second site lethality in the original NP4786 line described above (4.6.3).

Since we failed to obtain any deletion mutants from this first mutagenesis we performed the mutagenesis for the second time with a larger number of singly fly crossings and using a modified technique involving a deficiency chromosome to prevent recombination mediated repair of any deleted segment (within the deficiency region).

The NP4786 line was backcrossed to *w¹¹¹⁸* flies for 2 generations to clear the background of lethal mutations. The backcrossed flies were still homozygous lethal and were used for P-element mutagenesis.

4.6.6.2 Second mutagenesis (with kind help from B. Muehlbauer, G. Gramlich and I. Montalban)

In the second attempt, the NP4786 line was used for the mutagenesis and the crossing scheme is as shown in Figure 73 and 74. The jump-out was induced in flies heterozygous for the deficiency chromosome (*Df*) which lacks the region of the *Tbcel* gene. In these flies recombination mediated repair of deletions generated by P-element jump-out was less likely.

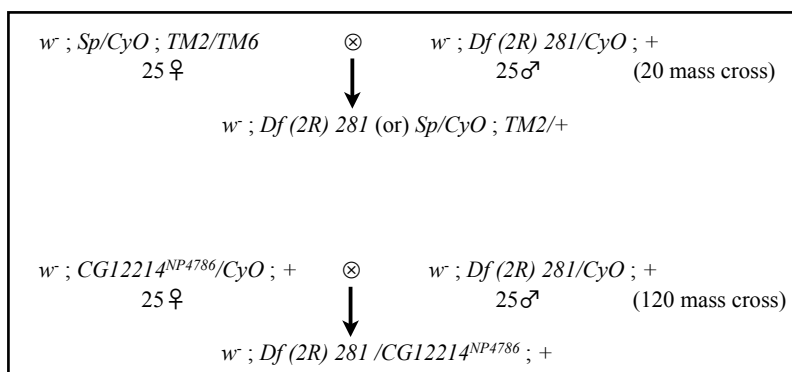


Fig. 73: Fly crossings to obtain the NP4786 line in *Df* background.

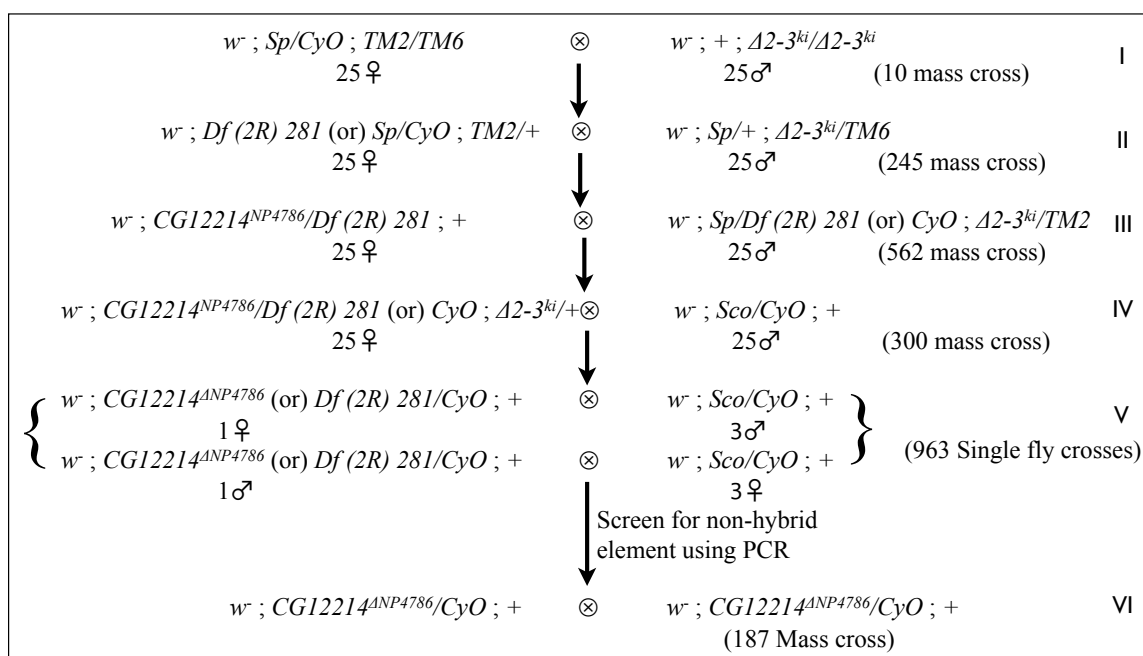


Fig. 74: Crossing scheme for P-element jump-out mutagenesis (Second trial).

The parents of the single fly crosses from the second mutagenesis attempt (Fig. 74) were first tested by PCR (Primers XP5' and RB3', see Materials) for presence of the hybrid element (see Fig. 75a) which is characteristic for the *Df* chromosome (flybase.org). A positive signal in this PCR implies that the white eyes are from the *Df* chromosome and not from a jump-out event.

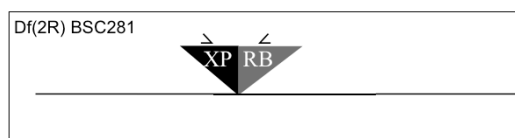


Fig. 75a: Screen for presence of hybrid element from deficiency line.

The flies that tested positive for the presence of this hybrid element were discarded.

Total single fly lines screened (white eyes)	923
Positive for hybrid element and P-element	204
Total lines screened for deletion	719

The flies which were white eyed but did not have the hybrid element were either flies which had suffered an internal deletion of the mini-*white* gene in the P-element or had experienced a jump-out of the P-element from the locus. In order to select only the flies with a P-element jump-out event we performed two PCRs with primer pairs 1f/1r and 2f/2r (Fig. 75b). The lines with positive signals from both the PCRs indicated the presence of the P-element (both ends intact) and were discarded.

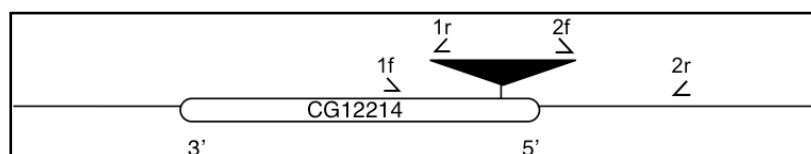


Fig. 75b: Screen for absence of P-element (5' and 3' ends of the P-element)

Total lines screened for presence of P-element (Stage 2 and 3)	719
--	-----

Positive for P-element (intact 5' and 3' ends) or dead	523
Total lines screened for deletion (Stage 4)	196

The absence of both signals implies that the lines are either revertants or have suffered a deletion in the flanking region of the P-element. The 22 homozygous viable lines were tested by PCR with primer pair 3f/3r. A signal similar to wild-type indicates that the coding region is not affected or that the lines are revertants.

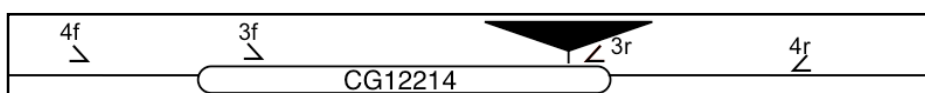


Fig. 75c: Screen for absence of P-element and deletions in the gene

The homozygous flies (22 in number) were all revertants. The rest 174 flies were tested by PCR using primer pair 4f/4r (Fig. 75c) and only 2 fly lines produced a signal larger than the wild-type signal indicating the presence of a residual part of the P-element. These two lines need to be characterised further to determine the extent of *Tbcel* gene disruption. The rest 172 fly lines were discarded.

5. DISCUSSION

5.1 Up-regulated and hyper-phosphorylated synapsin in *Sap47* null mutants

In section 4.1 we verified earlier observations (N. Funk, unpublished) that the synapsin protein is present at higher levels and hyper-phosphorylated in *Sap47* null mutants. We quantified this observation using ELISA and found synapsin levels in *Sap47* mutants to be ~2 fold increased when compared to wild-type *CS* flies. The hyper-phosphorylation and up-regulation was independent of the particular *Sap47* null allele tested and was partially rescued by pan-neuronal expression of *Sap47*-cDNA using *elav-gal4* (rescue flies generated by T. Saumweber). The rescue was only partial, possibly due to the following reasons:

- The expression of SAP47 in the *Sap47* null mutant under the control of *elav-gal4* is somewhat weaker than in WT, as suggested by the Western blot of Fig. 38.
- The expression profile by *elav-Gal4* is not the same as that of SAP47. For example, *elav-gal4* drives expression of UAS constructs in almost all neurons and additionally in embryonic glial cells (Berger et al., 2007) whereas SAP47 is expressed in most but not all neurons (Reichmuth et al., 1995). Also, mis- and over- expression could cause SAP47 to be targeted for degradation (see review Hershko and Ciechanover, 1982).

The results from section 4.1 suggests that:

- either the *Syn* gene in WT is down regulated by SAP47 (SAP47 has a transcription factor like BSD domain (Doerks et al., 2002)). Thus when the *Sap47* gene is mutated the down regulation is lost. No biochemical evidence exists for an interaction between SAP47 and DNA or RNA.
- or synapsin and SAP47 are involved in a co-regulated pathway and the absence of SAP47 protein is compensated by increased levels of synapsin. The possible cause of this increase might be as follows:
 1. Due to an increase in the transcription rate of the *Syn* gene. However, the transcript levels of *Syn* were determined by semi-quantitative RT-PCR (see Fig. 40), qPCR and microarray technique (see Fig. 55). No significant difference was observed between

WT and *Sap47* null mutants with respect to *Syn* transcript. It is known that mRNA levels and protein levels do not always correlate (Gygi et al., 1999).

2. Up-regulation of *Syn* expression without changes in *Syn* transcript levels can occur if synapsin half-life is decreased due to SAP47 in wild-type conditions. However, there are no reports so far about such an inhibitory effect, and to substantiate this speculation would require further investigations.
3. Synapsin is destabilized through protein-protein interaction with SAP47. It is known that in vertebrates the synapsin III isoform is stabilized by interaction with synapsin I and II isoforms (Hosaka and Sudhof, 1999). In wild-type conditions, synapsins might be prevented by SAP47 from forming large and stable homo-multimers and in the absence of SAP47 (in *Sap47* null mutants) these stable interactions are predominant. Interactions between SAP47 and synapsin were investigated by co-immunoprecipitation (co-IP) experiments (see Fig. 41) but a stable interaction was not detected. The interaction, if it exists, is not very stable as was evident from the BN-SDS-PAGE analysis of native complexes (see Fig. 43 and 44). Also, elution of IP sample competitively with an epitopic peptide and analysis by Western blot and mass spectrometry did not reveal an interaction between SAP47 and synapsin.

There is a possibility that the interaction could be transient and could not be captured with our experimental procedure (see Fig. 41). An interesting observation from the BN-SDS-PAGE analysis was that *Drosophila* synapsins under non-denaturing conditions are part of a large complex detected around 700-900 kDa. The fact that no interaction partner at stoichiometric concentration was found by immunoprecipitation and MS/MS suggests that *Drosophila* synapsins may be involved in formation of homo-multimers which is also observed in vertebrates (Hosaka and Sudhof, 1999).

The ELISA data obtained with MAB ab49 directed against the integral SV membrane protein cysteine-string protein (CSP) indicates that the concentration of synaptic vesicles in the brain probably is not altered by either the *Sap47*^{156CS} or the *Syn*^{97CS} null mutations. The actin control in addition show that head sizes are not significantly different for the genotypes studied. Also, the expression pattern of synapsin in *Sap*^{156CS} is not different from in wild-type (see Fig. 36).

5.2 Functional genetic interaction between *Sap47* and *Syn* genes

Sap47-Syn double null mutants *NS17* and *NS62* were generated by homologous recombination (see 4.2.1). These mutant lines are homozygous lethal but are viable as trans-heterozygotes with other homozygous lethal *Sap47-Syn* double mutation. Also, in another independent homologous recombination experiment by V. Albertowa, a homozygous lethal double mutant was generated. After backcrossing this line to *CS* flies for six generations in order to cantonise (homogeneous wild-type background) the stock, *Sap47-Syn* double mutant fly lines *V1*, *V2* and *V3* were obtained which were homozygous viable. Both groups of viable double mutants are weak and have reduced locomotor activity and life expectancy (see Fig. 48 and 49).

The behavioral experiments clearly suggest that the phenotype of double mutants (*NS17* and *NS62* or *V1*, *V2* and *V3*) is different or more severe (negative geotaxis, life expectancy, larval locomotion) when compared to individual null mutants. Thus, there is a genetic interaction between the two genes or there are different polymorphisms in the double mutants selected during the recombination experiment or accumulated over the subsequent several generations of inbreeding. It has been demonstrated in different species that alleles of a gene may have different phenotypes in different inbred strains or genetic backgrounds (Threadgill et al., 1995; Frankel and Schork, 1996; Gibson et al., 1999).

The different effects of combining *Sap47* and *Syn* mutations on locomotion and learning/memory could lead to the hypothesis that the synapses governing locomotion have a parallel mode of action for the two genes, i.e. they act in two parallel pathways involved in neurotransmission. At synapses which are involved in learning, the two proteins possibly have a linear mode of action, i.e. one acts upstream or downstream of the other. Different isoforms of SAP47 could be present in different types of synapses and these isoforms will probably serve different functions. Pan-neuronal expression (by *elav-gal4*) does not completely rescue the *Sap47* null mutant learning defect in an appetitive learning paradigm using 3rd instar larvae (Saumweber T. et al., submitted). The rescue experiment with the longer isoform needs to be performed to verify the hypothesis of

isoform specific functions (in progress T. Saumweber). Similarly, *Syn* cDNA rescues the learning defect (PhD thesis B. Michels, 2009).

Suppressor or enhancer type of genetic interaction can serve as a model for *Sap47-Syn* interaction in the double null mutants at the synapses involved in locomotor behavior. The two individual null mutants have wild-type levels of locomotor activity whereas the double mutants are impaired in locomotion (enhancement of phenotype).

5.3 Posttranslational modifications of synapsin and their implications

The availability of a monoclonal antibody (3C11) specific for *Drosophila* synapsin and a null mutant (*Syn^{97CS}*) provided the basis for detection of synapsin by nano-LC-ESI-MS/MS in immunoprecipitated samples from adult head homogenates of wild-type (WT) *Drosophila* (CS) (see Fig. 51). To obtain high sequence coverage and identify posttranslational modifications and the amino acid/s at the position X582 (stop codon), immunoprecipitated proteins were separated by SDS-PAGE and bands differing between wild type and *Syn* null mutant lanes were excised as shown in Figure 51. The gel pieces were subjected to a combination of multi-enzyme digestion (trypsin, chymotrypsin, Asp-N, proteinase-K, pepsin and nonspecific enzyme subtilisin) summarized in Table 2. Mass spectrometric analysis showed the presence of synapsin protein in 5 bands from WT but not from *Syn^{97CS}* null mutant lanes of silver stained 1D-SDS gels. We isolated and detected the shorter (~72 kD) and the read-through isoforms (~143 kD). We also detected few peptides of the longer isoform from the band around 72 kD, which could possibly be the degraded products of the longer isoform.

It is surprising to note that only synapsin proteins were immunoprecipitated and detected and no other protein was co-precipitated, as it is known that synapsin interacts with cytoskeletal and synaptic vesicle associated proteins (Cesca et al., 2010). This observation suggests that different isoforms of *Drosophila* synapsins form homomultimers *in vivo* as discussed above.

So far most published experiments in proteomics depend on affordable “high sequence coverage” for many purposes, such as identification of splice variants, isoforms, amino acid substitutions, and PTM analysis. To achieve high sequence coverage of *Drosophila* synapsin we applied multi-enzyme digestion and used different analyzing tools called MASCOT and Modiro to complement each other. By summing up the peptides identified from different enzyme applications and analyzing tools, the total synapsin sequence coverage obtained via combination of all conditions was 90.83% (see Table 2). A series of sequence conflicts were identified in *Drosophila* synapsin (see Table 6 below) from the two different search engines. Some of these sequence conflicts may be due to mutations or single nucleotide polymorphisms. An interesting observation was made, the first amino acid was found to be a methionine in spite of the fact that the start codon is CUG and not AUG. Use of different start sites on the basis of context and the presence of certain sequence features (Touriol et al., 2003) or by a leaky-scanning process (Kozak, 1995, 1997) for generating several isoforms of a given protein has been reported earlier with first reports from studies in Sendai (Curran and Kolakofsky, 1988) and Moloney murine leukaemia viruses (Prats et al., 1989). This process can be responsible for generating different isoforms of *Drosophila* synapsin with possibly different functions. The conserved PKA site in the N-terminal domain A is upstream of the first methionine encoded by the transcript (Klagges et al., 1996; Godenschwege et al., 2004) and thus isoforms initiated at this downstream methionine would not contain this PKA site and would not have the same conserved function as reported for vertebrate synapsin. It has been observed in mammals that under in-vitro and in-vivo conditions non-AUG codons can initiate translation with methionine (Peabody, 1987, 1989). In certain cases like MHC class I presented peptides and the murine leukemia virus-coded group-specific antigen gp85gag, a CUG codon can initiate translation with leucine (Prats et al., 1989; Malarkannan et al., 1999).

Table 6: Sequence conflicts in *Drosophila* synapsin, identified using MASCOT and Modiro search softwares.

Protein name (Swissprot accession number)	Spot	Sequence conflict Identified with MASCOT v2.2.06		Sequence conflict Identified with Modiro™ v1.1	
		CID	ETD	CID	ETD
Synapsin (Q24546)	1	D178V, A364S, R461K, R589H, R1011D, S1015D	D108H, Y188F, D178V, A364S, R461K, I847F, A1014D, S1015N	G81R, D178H, L221V, D260N, H290Q, N360I, I502N, S617R	G81C, N143D, R955C, S975A
	2	D131G, D178V, D178H, P181L, Y188F, N360I, S363A, A364S, E902G, S903G, A958D, A1014P	D131G, D170H, D178V, Y188F, A364S, E902G, S903G, A958D, A1014P	T122K, D170N, I171N, D178H, S190I, L221V, D260N, N360I, E367K, I502N, E513K, S542G, T786S, I791K, L884R, S971P,	D170N, D178H, E913K, S949G
	3	R210P, N360I, D430N, R504S, N904I, R955M	R210P, D430N, N904I, R955M	G68R, A72P, G81R, T122K, Q123P, I171N, G191R, N360D, N360I, Y405N, S459R, I502N, I511N, S538G, I723K, F956C, L979M, G981C, D1023G	N360I, T447P, I511N, S903Y, D912N, F956S,
	4	Y188F, S363A, E367K, R461G, E902G, S903N, S903W, A958S, G957D, W1012G	Y188F, R461G, E902G, S903N, G957D, A958S, Q1012G	T73K, T73N, T184S, S213P, L221V, L223V, E367K, D380G, I502N, S709N, S971A,	R98S, I231K, N360I, I502N, Y982C
	5	S363A, E902G, S903R, N904I, S1013A	R461K, E902G, S903R, N904I	N20D, V99E, L186R, L221V, F247C, D260N, I265N, N343S, L385R, D401V, D401G, S443G, S496C, I502N T673K, N750K, L979P	Q119H, I353F, D380G, I943S, S897W, S903Y, S938G
	6	S903C, S904N	S903N	P71R, D108V, F128C, L136R, L221V, S363R, E367K, S454Y, I502N, E564A, T818K, L884R	S112P, Q691E, Y898S
	7	L96M, N360I, R504S, E902K, S903A, S1013N	S903A	Q119E, E167Q, L221V, F247C, E367K, S456G, I502N, F993C	A75P, Q123H, N360I, P917R, N990T
	8	P200A, L221V, N360I, E902D, S903P, S903G, A958E, S1013I	S903C, A958Q	I171N, L221V, L223V, N360I, T447A, T473N, A478E, I502N, S506N, Q556E, G590E, V605G, S607C, I710N, S906A, V969G, S975R	N360I, P602R, I710N, T921R, R955C
	9	D108N, D108H, E164K, L221V, D260N, E266K, N360I, S363A, A364S, L366Q, D430N, D532N, D580V, N586I, S903A, S903N, G957D, K919Q, A1014D, S1015N	N586I, E902D, E902G, S903N, S903G, G957D, A1014D	G81R, Q119E, I171N, T172P, D178N, V194D, E266K, N360I, S383G, L385H, V432A, L476R, G479E, I502N, S543F, S546N, Q735K, G972C, G974C, Q989R	S112P, R124K, D260N, N360I, T447M, T495S, I541K, Q735K, P896S, S903C, S903Y, R955S, L979R, G981R,

	10	S363A, D430N, R504S, D580N, D580V, S903G, E902G, A1014D	D430N, D580N, S903G	G81R, D108N, I171N, F386C, I502N, L505M, N557K, I634T, S971R	I171N, D430N, N557K, S558A, S899W
--	----	---	---------------------	--	--------------------------------------

Single use of MASCOT or Modiro MS data analysis software was not able to reveal higher sequence coverage. This is because representative amino acid sequence must be uploaded to the Modiro program. Thus, if there are sequence conflicts in the peptides (e.g. a stop codon), Modiro will ignore these peptides. In addition, Modiro would have accepted peptides with a mass (MS) and fragment (MS/MS) tolerance higher than ± 0.2 Da. The use of two different analyzing tools was also helpful in identifying several PTMs which would have been missed from a single search engine application.

Our findings support the hypothesis that the in-frame *amber* (UAG) stop codon of the *Syn*-RA transcript is read-through to produce the higher isoform of *Drosophila* synapsins. Our mass spectrometric analysis reveals that this *amber* stop codon is translated to lysine with a high ion score (see Fig. 52). Other amino acids, such as asparagine, glutamic acid, histidine, threonine and serine, were also identified at the position X582 but with lower ion scores. The function of nonsense suppressor tRNAs (*sup*⁺ tRNAs) has been well characterized in bacteria (Steege, 1983) and yeast (Capecchi et al., 1975). We have previously demonstrated that GST-synapsin fusion proteins generated from the RA isoform cDNA in *sup*⁻ and *sup*⁺ *E. coli* strains have different read-through efficiencies of the in-frame stop codon (X582) (Klagges et al., 1996). There are possibilities of suppression of stop codon by the presence of secondary structure in the vicinity, upstream or downstream that may directly interfere with the ribosome, release factors and tRNAs and facilitate suppression of the termination process (Bossi, 1983). Alternative hypothesis for eliminating the stop codon by duplicate translational frame-shifting or differential splicing (Godenschwege et al., 2004) are not supported by the present findings.

Vertebrate synapsins are substrate for several protein kinases like PKA, CaMKs, Src, cdk and MAPK/Erk, which modulate their biochemical properties. In mammals and

other vertebrates the domain 'A' of synapsin contains the P-site 1 (RRXS) that has been identified as a target site for cAMP-dependent protein kinase (PKA) and calcium/calmodulin dependent protein kinase I/IV. In *Drosophila*, this motif is conserved in the genome, but at the transcript level, the enzyme adenosine deaminase acting on RNA (ADAR) edits the genomic site (RRFS) to RGFS (Diegelmann et al., 2006) in the majority of transcripts. The edited site is not phosphorylated significantly *in vitro* by bovine PKA (Diegelmann et al., 2006). There is a second RRXS site (S533, according to the cDNA sequence) in *Drosophila* synapsin (Klagges et al., 1996; Diegelmann et al., 2006). The accessibility of this site to PKA, or to other kinases, is not known and needs to be investigated further. In the current study we did not observe phosphorylation at either of these PKA sites. The reason for the absence of phosphorylation at these sites could be low abundance of these phosphorylations when compared to the phosphorylation events we identified. The phosphorylation could be an activity dependent phenomenon occurring only at higher levels of activity. As a first step towards understanding the roles of PKA sites I and II in *Drosophila*, UAS-*Syn* cDNA (PKA I and II mutated; PKA I mutated and II wild-type; PKA I non-edited and II mutated; PKA I non-edited and II wild-type) transgenic flies (in *Syn*⁹⁷ mutant background) were generated (PhD thesis B. Michels, 2009). Under the control of *elav-gal4*, these transgenes express synapsin pan-neuronally with modified sites (I and II) for PKA (see Fig. 76). In associative learning experiments with 3rd instar larvae having ectopic expression of UAS-*Syn* cDNA (PKA I and II mutated), they have significantly reduced learning when compared to the wild-type and is comparable to the learning in *Syn* null mutants (*Syn*^{97CS}) (PhD thesis B. Michels, 2009).

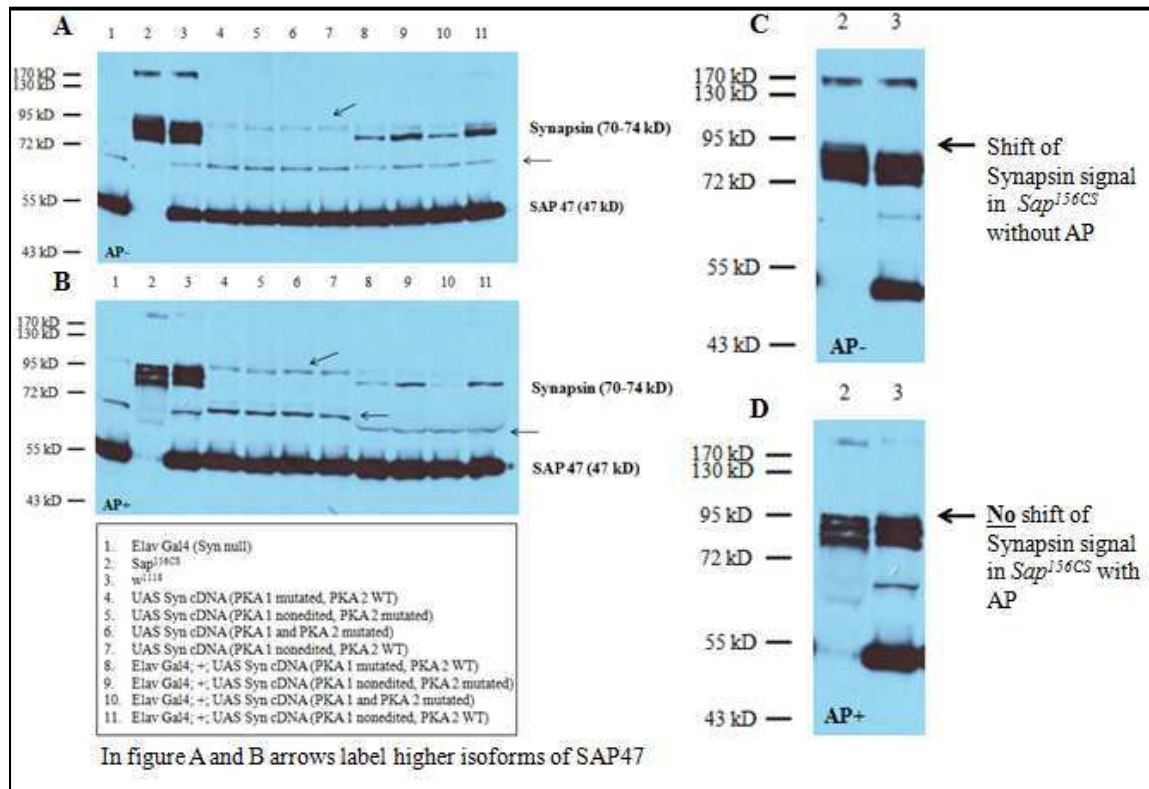


Fig. 76: Expression of mutated synapsin revealed by Western blots of head homogenates from transgenic flies of the indicated genotypes. A clear effect of dephosphorylating the homogenate by alkaline phosphatase (AP) treatment in B and D is seen only in lane 2 (compare with Fig. 35). C and D are enlarged images of lanes 1 and 2 from A and B respectively. In lanes 8-11 of B the shift in SAP47 signal (arrow around 60 kDa) is due to the presence of high amount alkaline phosphatase enzyme at that position (Diploma thesis S. Racic, 2009).

In a phosphoproteome analysis, Zhai et al. reported synapsin phosphorylation at serine 509, 510 and 539 in *Drosophila* embryos (Zhai et al., 2008). From the present study, five novel phosphorylation sites were identified and verified via phosphatase treatment, T86 near the domain A, S464 and S538 near the domain E, S961 and Y982 in the read-through proline rich region. In vertebrate synapsin I, phosphorylation at the PKA site in domain A leads to a slight loss of affinity to vesicles. The domains C and E are involved in direct interactions with cytoskeletal components like actin and thus enable synapsins to maintain a synaptic vesicle pool in the periphery of the plasma membrane in

a phosphorylation dependent manner (Cesca et al., 2010). The detection of phosphorylation sites near domain E of *Drosophila* synapsin suggests that they could be involved in regulating the binding of synapsin to vesicles or components of cytoskeleton. However, this requires further in-depth analysis.

We have obtained large sequence coverage for *Drosophila* synapsin and the analysis indicated a number of sequence conflicts. Novel phosphorylation sites were identified and verified. A Lysine tRNA specific suppression of *amber* stop codon to produce a read-through isoform of synapsin was determined. These findings provide a basis for further characterization of *Drosophila* synapsins. Knowledge about kinases involved in phosphorylation of synapsin will shed light on its role at the synapse and its function like learning and memory which so far remain elusive.

5.4 Whole genome microarray analysis of *Sap*^{156CS}, *Syn*^{97CS} and *V2* and *V3* null mutants (the experiments were performed by S. Kneitz and N. Nuwal, and were evaluated in collaboration with N. Nuwal, refer to PhD thesis of N. Nuwal, 2010)

The 3' transcript of *Sap47* and *Syn* are intact in the null mutants *Sap*^{156CS} and *Syn*^{97CS}, respectively and are detected at low levels in the microarray and qPCR analysis (see PhD thesis of N. Nuwal, 2010). This suggests that the mutants have an internal transcription start site. The presence of a functional protein albeit truncated could account for a weak phenotype associated with the respective null mutants (Godenschwege et al., 2004; Michels et al., 2005) but this is highly unlikely. On detection, absence of the 5' end of the *Syn* transcript served as a negative control for our experiment as the P-element mutagenesis disrupted the first exon and intron of the *Syn* gene (Godenschwege et al., 2004).

The *Cirl* gene was down-regulated specifically in *Syn* null mutants by at least 2 fold but was not significantly altered in other genotypes tested by microarray and qPCR (see 4.5). CIRL protein is reported to be a G-protein coupled receptor for α -latrotoxin (Krasnoperov et al., 1997; Bittner et al., 1998; Brody and Cravchik, 2000). On application of α -latrotoxin at synapses, CIRL interacts with neuexins (Tobaben et al., 2002) and

other synaptic proteins like synaptotagmin and syntaxin (Krasnoperov et al., 1997) leading to vesicle exocytosis in a Ca^{2+} independent manner. *Drosophila* mutants of *Cir1* have 50% reduced locomotor activity and reduced evoked potentials at NMJs (Song et al., 2003). Application of α -latrotoxin and measuring the evoked release at the NMJs would be an intuitive experiment to study defects in latrotoxin mediated vesicle release in the *Syn^{97CS}* mutants. The double mutants do not show a reduction of *Cir1* transcript possibly because of polymorphisms masking the gene effect. An alternative explanation would be the suppression of the phenotype by the *Sap47* mutation. Both these hypotheses need further investigation and validation by using *Cir1* mutants and RNAi lines. Kindly refer to the PhD thesis of N. Nuwal, 2010 for the list of genes which are significantly altered in the individual and the double mutants.

5.5 *Tbcel* expression in *Drosophila* testis and brain

The *Drosophila Tbcel* gene (*CG12214*) was identified in a yeast-two-hybrid screen as a potential interaction partner of SAP47 (N. Funk, unpublished). Based on the high sequence similarity to its vertebrate homologue it was named *Tbce-like (Tbcel)*. *Drosophila* TBCE functions at the NMJs and is involved in MT assembly (Jin et al., 2009). Vertebrate TBCEL is involved in destabilisation of MTs, targeting them for degradation via a ubiquitin mediated pathway (Bartolini et al., 2005).

The *Tbcel* gene is nested in a large intron of the *KCNQ* gene (source: Flybase). Two completely sequenced cDNAs (GH13040 and MIP04546) are known and reported in flybase. The GH13040 clone was used for the generation of UAS-*Tbcel* flies (Master thesis S. Wegener, 2008) and the anti-his-tagged-TBCEL antiserum (this thesis). Flybase reports several expressed sequence tags (ESTs) for the *Tbcel* gene, and based on these ESTs a gene model was predicted and is shown below (see Fig. 77). The correctness of the gene model (Fig. 56) was verified by performing an RT-PCR which provided no evidence for the model DMG2 or DMG4 of Fig. 77 (data not shown).

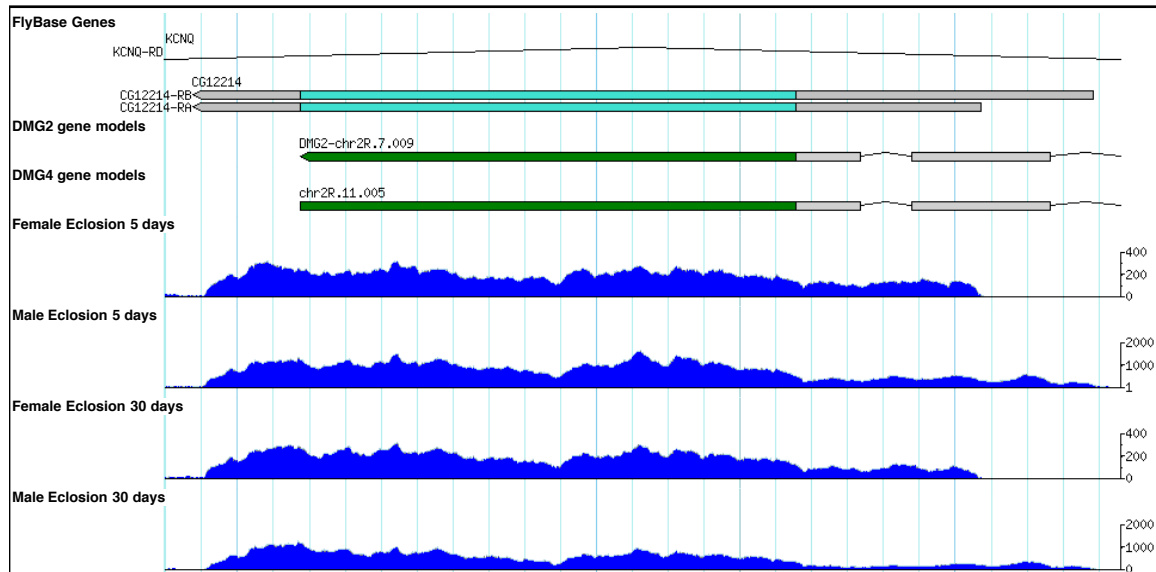


Fig. 77: The *CG12214*-RB transcript is specific for or highly enriched in males when compared to females (Source: RNA-seq data from flybase). The intron shown in the DMG 2 and 4 gene models is not detected by RT-PCR from adult flies (data not shown).

NP/CyO flies have a P-element insertion in the 5' UTR of the *Tbcel* gene and are homozygous lethal due to second site lethality on the second chromosome outside the deficiency regions of *Df(2R)BSC281* and *Df(2R)BSC350* as they are viable over these deficiencies spanning the gene. Another fly line *NP6285/CyO* with a P-element insertion upstream of *NP4786* is also homozygous lethal but again is viable over the deficiency. RT-PCR for *NP/Df* with two primer pairs downstream of the P-element insertion demonstrates that the mRNAs containing the intact coding region of the gene is present in these flies, albeit at reduced concentration (Fig. 60). In the P-element insertion line *G18151*, the insertion is downstream of the translation start and thus disrupts the ORF. In a Western blot of fresh head and testis homogenates of *NP/Df* and *G18151* flies, TBCEL protein is not detected by an anti-TBCEL antiserum suggesting that these lines are indeed null mutants for *Tbcel*. The two insertions *NP6285* and *NP4786* over the deficiency chromosome are male sterile. This suggests that the correct amount of RB-transcript and possibly the 5' UTR region is crucial for functioning of TBCEL in males.

It is known that UTRs may play a role in mRNA stability, localisation and translational efficiency. Insertions in the coding region as in the G18151 usually are assumed to eliminate the functioning of the encoded protein. Surprisingly, however, the G18151 homozygous males have only severely impaired fertility whereas *NP/Df* males are sterile. This leads to the speculation that the G18151 insertion possibly causes an interrupted transcript to be made which could produce a truncated protein, with partial functions. Thus in the G18151 stock, the flies could generate an intact N-terminal domain of the protein which codes for the CAP-Gly domain and might be able to rescue the phenotype. Alternatively, transcription might be initiated downstream of the mini-*white* gene in the P-element and lead to a transcript which is producing a truncated protein containing the C-terminal domains of TBCEL. Although there is no predicted ATG start site downstream of the G18151 insertion, suggesting that such a downstream translation is unlikely, it still could occur using an unconventional start site. As a third hypothesis, the G18151 stock could have acquired a polymorphism that prevents complete male sterility. All three hypotheses need to be tested by further investigations.

Spermatogenesis is a well studied developmental process (reviewed in Fuller, 1993). The primary hub cells undergo mitotic division to produce several spermatogonia. Each spermatogonium undergoes 4 mitotic divisions to produce 16 premature spermatocytes in each cyst, and these spermatocytes undergo 2 more meiotic divisions to form 64 syncytial spermatids in each cyst. The nuclei of the premature spermatids are aligned with mitochondrial derivatives which fuse to form the major and minor derivative. These derivatives coalesce together to form a dense structure which is encapsulated in several layers of mitochondrial membrane, also known as the Nebenkern stage. In the elongation stage, the cysts move towards the basal end, the sperm tails or the axonemes elongate along with the associated Nebenkern structure in a polarised manner with the head of the sperm containing the nucleus positioned at the basal end and the tail growing towards the apical end. The nucleus also undergoes dramatic change in shape becoming thin and flattened (Cross and Shellenbarger, 1979). After the completion of axoneme elongation and the change in nuclear morphology, the disruption of the syncytial organisation and the individualisation of each of the spermatid in the cysts begins. The Individualisation complex (IC) with an actin cone is assembled at the basal end of the

spermatid (Fabrizio et al., 1998). The IC moves towards the apical end in the form of a cystic bulge and eliminates excess cytoplasm in spermatids at the apical tip in the form of a waste bag. The individualised mature spermatids are coiled and transferred to the seminal vesicle (see Fig. 64 and 78).

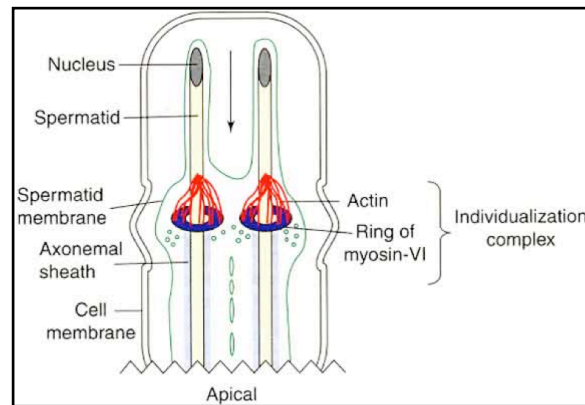


Fig. 78: Spermatid bundle organisation in testis of adult *Drosophila* male (Source: http://www.bio.umass.edu/vidali/web/cell_motil/myosin_vi_6.jpg)

In *Drosophila* spermatogenesis, different structures utilise different forms of β -tubulins but the same α -tubulin. The head of the spermatid (basal region) has β 1-tubulin, the cyst cell has β 3-tubulin and the axoneme has β 2-tubulin (Kemphues et al., 1982; Kimble et al., 1989). We checked for the expression of TBCEL protein in *Drosophila* by immunocytochemistry and found specific staining of spermatid bundles in the testes of adult males which was localised within the β -tubulin staining (data not shown). The staining was not observed in the null mutants (see Results section) though spermatids were present and observed under a dark-field microscope. The presence of spermatids in the null mutants G18151 and *NP/Df* testes was verified by staining for actin in the ICs. The phalloidin staining was dispersed in null mutants and not tightly bundled as seen in wild-type testis (Fig. 65 and 66). Our results also show that the assembly of investment cones is intact in the null mutant testes but as the IC complex proceeds along the testis walls the investment cones get dispersed as observed by dispersed actin staining. Proper IC organisation at the nucleus but dispersed IC along the testis walls is also observed in male sterile mutants *mulet* (*mlt*) (Fabrizio et al., 1998). The chromosomal location of *mlt*

mutation has been reported as 46F but the gene has not been identified and characterised (Fabrizio et al., 1998). Our complementation experiments and sequencing of the *mlt* P-element insertions have now demonstrated that *mlt* is an allele of the *Tbcel* gene.

The expression pattern of *Tbcel* transcript in embryonic central nervous system and testis is shown in the online databases fly-ted.org by in-situ hybridisation (ISH) (see Fig. 79).

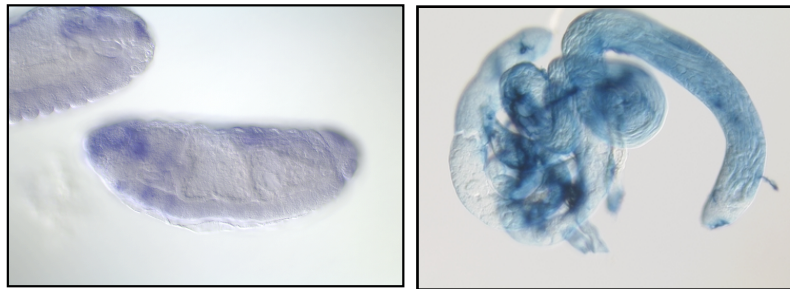


Fig. 79: TBCEL expression in embryonic ventral nerve cord, and adult testis detected by in situ hybridisation. (Source: ISH database, Fly-ted.org)

5.6 P-element mutagenesis of *Tbcel* gene

We performed two jump-out mutageneses of *Tbcel* gene using the NP4786 line which has a P-element insertion in the 5' UTR of the *Tbcel* gene. In the first attempt the jump-out was induced in flies carrying the P-element over the *CyO* balancer chromosome. This attempt to generate deletion mutants of the gene failed, only flies with a presumably precise jump-out (revertants) or carrying a P-element with intact inverted repeats but a disrupted mini-*white* gene were obtained. Possible reasons for the failure to obtain deletion mutants are :

- Homologous recombination mediated repair of the double stranded DNA break caused by the P-element excision. Thus, the mutant is reverted to wild-type. Apart from the homologous chromosome acting as repair template, it has been shown that the repair can be mediated by the sister chromatid during the S-phase of the cell cycle if the jump occurs after DNA replication (Engels et al., 1990).

- It is likely that the *Tbcel* gene locus is highly critical and is thus efficiently repaired to wild-type condition (revertant) or not highly accessible to the transposase.
- The deletions caused by the jump-out are large enough to cause dominant lethality. However, this is not very likely as deficiencies spanning this region are viable over a balancer.
- The excised P-element re-integrates elsewhere in the genome which causes dominant lethality.

We did not obtain any deletion mutants from our first jump-out screen so we performed the second mutagenesis in flies with P-element (NP4786) over a deficiency chromosome (Df(2R)BSC281) to prevent homologous recombination mediated repair. In this situation only the sister chromatid mediated repair was possible in case the jump-out occurred after the DNA replication. This mutagenesis has produced a single jump-out line which has to be verified and investigated further. The results of P-element mutageneses suggest that the locus is under the control of high fidelity repair mechanisms.

6. SUMMARY

In this thesis we have used *Drosophila melanogaster* as a model organism to investigate proteins and their putative interacting partners that are directly or indirectly involved in the release of neurotransmitters at the synapse. We have used molecular techniques to investigate conserved synaptic proteins, synapsin and synapse associated protein of 47 kD (SAP47), and a putative interaction partner of SAP47, tubulin binding chaperone E-like (TBCEL).

SAP47 and synapsins are highly conserved synaptic vesicle associated proteins in *Drosophila melanogaster*. To further investigate the role and function of *Sap47* and *Syn* genes, we had earlier generated the null mutants by P-element mutagenesis (Funk et al., 2004; Godenschwege et al., 2004). Western blots and ELISA of brain homogenates from *Sap47¹⁵⁶* null mutants showed the presence of up-regulated phospho-synapsin in comparison to wild-type (*CS*) and the presence of up-regulated phospho-synapsin was partially abolished when a pan-neuronal rescue of SAP47 was performed by the Gal4-UAS technique. Thus, the results suggest a qualitative and quantitative modulation of synapsin by SAP47. At the transcript level, we did not observe any difference in content of *Syn* transcript in *Sap47¹⁵⁶* and wild-type *CS* flies. The question of a direct molecular interaction between SAP47 and synapsin was investigated by co-immunoprecipitation (Co-IP) experiments and we did not find any stable interactions under the several IP conditions we tested. The possibility of *Sap47* as a modifier of *Syn* at the genetic level was investigated by generating and testing homozygous double null mutants of *Sap47* and *Syn*. The *Syn⁹⁷*, *Sap47¹⁵⁶* double mutants are viable but have a reduced life span and decreased locomotion when compared to *CS*.

In 2D-PAGE analysis of synapsins we identified trains of spots corresponding to synapsins, suggesting that synapsin has several isoforms and each one of them is posttranslationally modified. In an analysis by Blue native-SDS-PAGE (BN-SDS-2D-PAGE) and Western blot we observed synapsin and SAP47 signals to be present at 700-900 kDa and 200-250 kDa, respectively, suggesting that they are part of large but

different complexes. We also report the possibility of *Drosophila* synapsin forming homo- and heteromultimers, which has also been reported for synapsins of vertebrates.

In parallel to the above experiments, phosphorylation of synapsins in *Drosophila* was studied by IP techniques followed by 1D-SDS gel electrophoresis and mass spectrometry (in collaboration with S. Heo and G. Lubec). We identified and verified 5 unique phosphorylation sites in *Drosophila* synapsin from our MS analysis. Apart from phosphorylation modifications we identified several other PTMs which have not been verified. The significance of these phosphorylations and other identified PTMs needs to be investigated further and their implications for synapsin function and *Drosophila* behavior has to be elucidated by further experiments.

In a collaborative project with S. Kneitz and N. Nuwal, we investigated the effects of *Sap*¹⁵⁶ and *Syn*⁹⁷ mutations by performing a whole *Drosophila* transcriptome microarray analysis of the individual null mutants and the double mutants (*V2* and *V3*). We obtained several candidates which were significantly altered in the mutants. These genes need to be investigated further to elucidate their interactions with *Sap47* and *Syn*.

In another project, we investigated the role and function of *Drosophila* tubulin-binding chaperone E-like (*Tbcel*, *CG12214*). The TBCEL protein has high homology to vertebrate TBCE-like (or E-like) which has high sequence similarity to tubulin-binding chaperone E (TBCE) (hence the name TBCE-Like). We generated an anti-TBCEL polyclonal antiserum (in collaboration with G. Krohne). According to flybase, the *Tbcel* gene has only one exon and codes for two different transcripts by alternative transcription start sites. The longer transcript RB is present only in males whereas the shorter transcript RA is present only in females. In order to study the gene function we performed P-element jump-out mutagenesis to generate deletion mutants. We used the NP4786 (NP) stock which has a P(GawB) insertion in the 5' UTR of the *Tbcel* gene. NP4786 flies are homozygous lethal due to a second-site lethality as the flies are viable over a deficiency (*Df*) chromosome (a deletion of genomic region spanning the *Tbcel* gene and other upstream and downstream genes). We performed the P-element mutagenesis twice. In the first trial we obtained only revertants and the second experiment is still in progress. In the

second attempt, jump-out was performed over the deficiency chromosome to prevent homologous chromosome mediated double stranded DNA repair.

During the second mutagenesis an insertion stock G18151 became available. These flies had a P-element insertion in the open reading frame (ORF) of the *Tbcel* gene but was homozygous viable. Western blots of fresh tissue homogenates of *NP/Df* and G18151 flies probed with anti-TBCEL antiserum showed no TBCEL signal, suggesting that these flies are *Tbcel* null mutants. We used these flies for further immunohistochemical analyses and found that TBCEL is specifically expressed in the cytoplasm of cyst cells of the testes and is associated with the tubulin of spermatid tails in wild-type *CS*, whereas in *NP/Df* and G18151 flies the TBCEL staining in the cyst cells was absent and there was a disruption of actin investment cones. We also found enrichment of TBCEL staining around the actin investment cone. These results are also supported by the observation that the enhancer trap expression of the NP4786 line is localised to the cyst cells, similar to TBCEL expression. Also, male fertility of *NP/Df* and G18151 flies was tested and they were found to be sterile with few escapers. Thus, these results suggest that TBCEL is involved in *Drosophila* spermatogenesis with a possible role in the spermatid elongation and individualisation process.

7. ZUSAMMENFASSUNG

In dieser Arbeit benutzte ich *Drosophila melanogaster* als Modellorganismus für die Untersuchung von Proteinen und ihren möglichen Interaktionspartnern, die direkt oder indirekt an der Freisetzung von Neurotransmittern an der Synapse beteiligt sind. Für die Untersuchung der konservierten synaptischen Proteine Synapsin (SYN) und Synapsen-assoziiertes Protein von 47 kDa (SAP47), sowie ihrer möglichen Interaktionspartner, bediente ich mich molekularer Methoden.

SAP47 und SYN sind hoch konservierte Proteine von *Drosophila melanogaster*, die mit synaptischen Vesikeln assoziiert sind. Um die Rolle und Funktion der *Sap47*- und *Syn*-Gene näher zu beleuchten, wurden bereits früher mit Hilfe von P-Element Mutagenesen Null Mutanten generiert (Funk et al., 2004; Godenschwege et al., 2004). Western Blots und ELISA der Gehirnhomogenate der *Sap47¹⁵⁶* Nullmutanten zeigten im Vergleich zum Wildtyp (*CS*) das Vorhandensein von hochreguliertem phospho-Synapsin. Dieser Effekt ließ sich durch ein panneuronales Rescue wieder partiell rückgängig machen. Diese Ergebnisse lassen eine qualitative sowie quantitative Modulation von SYN durch SAP47 vermuten. Auf der Transkriptebene konnte ich keinen Unterschied im Gehalt von *Syn* Transkript zwischen den *Sap47¹⁵⁶* und wildtypischen *CS* Fliegen feststellen. Das Vorhandensein einer direkten molekularen Interaktion zwischen SAP47 und SYN wurde in Co-Immunopräzipitations-Experimenten (CO-IP) untersucht. Ich konnte unter diversen getesteten IP Bedingungen keine stabilen Interaktionen finden. Die Möglichkeit, dass *Sap47* auf der molekularen Ebene modifizierend auf das *Syn*-Gen wirkt, wurde durch das Erzeugen und Testen homozygoter doppelter Nullmutanten für *Sap47* und *Syn* untersucht. *Syn⁹⁷*, *Sap47¹⁵⁶* Doppelmutanten sind lebensfähig, zeigen jedoch eine im Vergleich zu *CS* reduzierte Lebensspanne und Lokomotion.

In einer 2D-SDS-PAGE Analyse der Synapsine identifizierte ich Reihen von Synapsin-Signalen, die darauf schließen ließen, dass Synapsin über mehrere Isoformen verfügt, von denen jede mehrfach posttranslational modifiziert ist. In einer Blue native-SDS-PAGE (BN-SDS-2D-PAGE) mit anschließendem Western Blot konnte ich Synapsin und SAP47 Signale bei 700-900 kDa beziehungsweise 200-250 kDa feststellen, was

darauf schließen ließ, dass sie als Komponenten von unterschiedlichen größeren Komplexen fungieren. Ich zeigte außerdem die Möglichkeit auf, dass *Drosophila* Synapsin Homo- und Heteromultimere bilden kann, was bereits für Synapsine von Wirbeltieren gezeigt wurde.

Gleichzeitig mit den obigen Experimenten untersuchte ich durch IP Methoden, gefolgt von 1D SDS Gelelektrophorese und Massenspektroskopie (in Zusammenarbeit mit S. Heo und G. Lubec), die Phosphorylierung der Synapsine in *Drosophila*. In der MS Analyse konnte ich 5 distinkte Phosphorylierungs-Stellen des *Drosophila* Synapsins identifizieren und verifizieren. Zusätzlich zu den Modifikationen durch Phosphorylierung konnte ich einige andere posttranslationale Modifikationen zeigen, die jedoch nicht verifiziert wurden. Die Bedeutung dieser Phosphorylierung, sowie anderer identifizierter Modifikationen, sollte durch weitere Experimente beleuchtet werden.

In einem Kollaborationsprojekt mit S. Kneitz und N. Nuwal untersuchte ich die Auswirkungen der *Sap47*¹⁵⁶ und *Syn*⁹⁷ Mutationen mithilfe einer Microarray Analyse des gesamten *Drosophila* Transkriptoms der individuellen Nullmutanten sowie Doppelmutanten (*V2* und *V3*). Es wurden einige Kandidaten gefunden, die in den Mutanten signifikante Änderungen aufweisen. Diese Gene sollten weiterhin auf ihre Interaktionen mit *Sap47* und *Syn* untersucht werden.

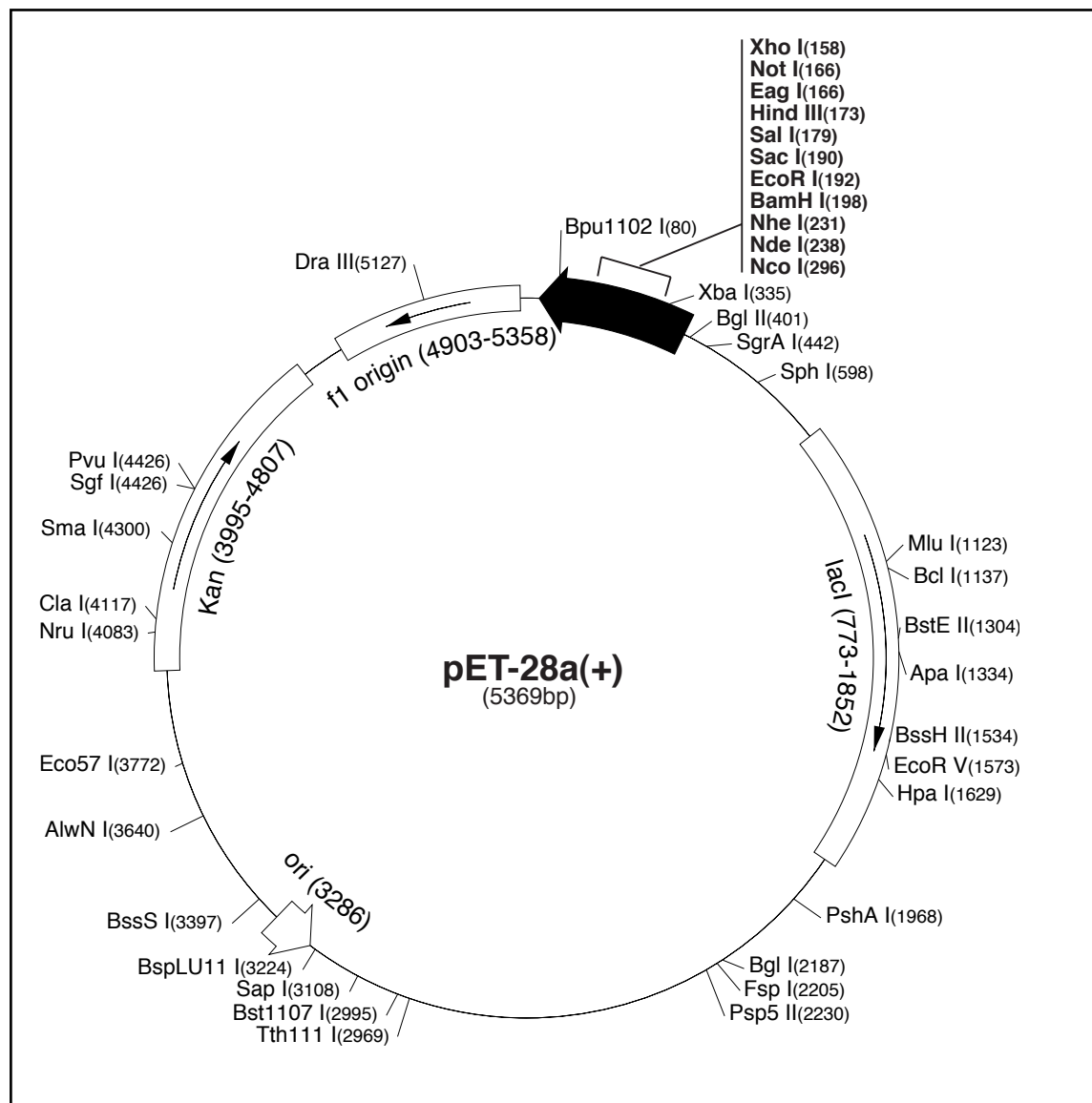
In einem weiteren Projekt untersuchte ich die Rolle und Funktion des *Drosophila* tubulin binding chaperon E-like-Gens (*Tbcel*, *CG12214*). Das TBCEL Protein weist eine hohe Homologie zum Vertebraten TBCE-like (oder E-like) auf, welches über eine namensgebende hohe Sequenzähnlichkeit zum Tubulin bindenden Chaperon E (TBCE) verfügt. Ich erzeugte ein polyklonales anti-TBCEL Antiserum (in Kollaboration mit G. Krohne). Laut Flybase besitzt das *Tbcel*-Gen nur ein Exon und kodiert für zwei unterschiedliche Transkripte durch alternative Orte des Transkriptionsstarts. Das längere Transkript RB ist nur in Männchen vorhanden, während das kürzere Transkript RA sich nur in Weibchen finden lässt. Um eine Untersuchung der Genfunktion zu ermöglichen, führte ich eine P-Element jump-out-Mutagenese durch, mit der Deletions-Mutanten generiert werden sollten. Ich benutzte dazu den Stamm NP4786 (NP), welches eine P (GawB) Insertion in der 5' UTR des *Tbcel*-Gens aufweist. NP4786 Fliegen sind aufgrund

einer second-site Lethalität homozygot letal, da sie über einer chromosomalen Defizienz (*Df*) (einer Deletion der genomischen Region, die das *Tbcel*-Gen sowie benachbarte Gene umfasst) lebensfähig sind. Die P-Element jump-out-Mutagenese wurde von mir zweimal durchgeführt, wobei ich beim ersten Mal nur Revertanten erhielt, während der zweite Durchgang sich momentan noch in Arbeit befindet. Beim zweiten Versuch wurde der jump-out über dem Defizienz-Chromosom durchgeführt, um eine doppelsträngige DNA Reparatur durch das homologe Chromosom zu verhindern.

Während der zweiten Mutagenese wurde ein Stamm G18151 verfügbar, bei welchem die P-Element Insertion im offenen Leseraster (Open reading frame: ORF) des *Tbcel*-Gens erfolgt war. Western Blots von frischem Gewebehomogenat der *NP/Df* und G18151 Fliegen zeigten nach dem Testen mit anti-TBCEL Antiserum kein Signal, was darauf schließen lässt, dass diese Fliegen *Tbcel* Nullmutanten sind. Ich verwendete diese Fliegen für weitere immunhistochemische Analysen und fand heraus, dass TBCEL im Wildtyp spezifisch im Zytoplasma der Cysten-Zellen der Hoden exprimiert wird, sowie mit dem Tubulin der Spermatidenschwänze assoziiert ist, während es in den *NP/Df* und G18151 Fliegen keine TBCEL-Färbung der Cysten-Zellen gab. Des Weiteren konnte eine Störung der Actin Kegel und eine Anreicherung von TBCEL um diese herum gezeigt werden. Diese Ergebnisse werden zusätzlich durch die Beobachtung unterstützt, dass die Enhancer-trap Expression der NP4786 Linie analog zu dem TBCEL in den Cysten-Zellen lokalisiert ist. Zusätzlich wurde die Fertilität der *NP/Df* und G18151 Männchen getestet und gezeigt, dass diese Tiere nahezu vollständig steril sind. Die Ergebnisse lassen daher vermuten, dass TBCEL an der Spermatogenese bei *Drosophila* beteiligt ist, sowie eine mögliche Rolle bei der Elongation und Individualisierung der Spermatiden spielt.

8. APPENDIX

8.1 pET 28a vector map for expression of His-Tagged proteins



8.2 Alignment of 6 different types of tubulin- α , β , γ , δ , ϵ and ζ (modified from Vaughan et al., 2000) from protozoan parasite *Trypanosoma brucei*.

alpha	-MREAICIHIGQAGCQVGNACWELFCLEHGIQPDGAMP SDKTIGVEDDA-----F	49
beta	-MREIVCVQAGQCGNIGSKFWEVISDEHGVDPTGT YQGDSLQLER-----I	47
gamma	MPREIITLQVQCGNQGSEFWRLCAEHGIRHDG VVESFASGGDDR-----K	48
epsilon	MPREVTVQVQCGNQLGLKWWVDLLQEHKANPQFTDARDALFDVSGSAP-----LA	52
delta	--MACVHVLVGQCGNQLGAHFLTALTD EARRCSEDEYASQISADHFRPAPTQKGI RRGV	58
zeta	--MAIVVQVQCGNQLGEELWRQLSIATDKG-----	30
	: : **.* *:* :	
alpha	NFFFSETGAGKHVPRAVFLDLEPTVVD EVRTGTYR---QLFHPEQLISGKED--AANNYA	104
beta	NVYFDEATGGRYVPRSVLIDLEPGTMDSVRAGPYG---QIFRPDNFIFGQSG--AGNNA	102
gamma	DVFFYQADDDHYIPRALLVDLEPRVINAIQRGSMQ---RLFNPENVIHSEGGGAGNNA	105
epsilon	SVGDKACRAGSLKARCVAVDMEEGVLRAML RGPLG---HLFDATFFVSDVSG--AGNNA	107
delta	SNGNSGHHDEPPLPRVMIDMEPKVVESVVTGVNDGGAFQVRAEQCVTRDEG--SGNNA	116
zeta	-AVRSPFFTSNRKARCMVDSEPKVQTVYNYAD----IMRAENVVCGHSG--RGNHWA	83
	.*.: :* * .: : . . .*::*	
alpha	RGHYTIGKEIVDLCLDRIRK-----LADNCTGLQG	134
beta	KGHYTEGAELIDSVLVDCCK-----EAESCDCLQG	132
gamma	HG-YEMGDTVQETLFDMIER-----EAENSDSLEG	134
epsilon	VGHMEYGDKYIDSITETVRE-----QVERCDSIQS	137
delta	FGYYEQGSR-CDEIVESLRR-----QSEARGAAHS	145
zeta	LGYYGLNPKSSRCAEKAAASRPFQVTKDQRRGDNFVVRDALRAIYAETRRDTEEFEA	143
	* . . : : :	
alpha	FLVYHAVGGGTGSGLGALLLERLSVDYGK KSKLGYTVYPSPO---VSTAVVEPYNSVLST	191
beta	FQICHSLGGGTGSGMGTLLISKREQYPDRIMM TFSIIPSPK---VSDTVVEPYNTTLSV	189
gamma	FVLTHSIAGGTGSGMGSYLLENLNDRFPKKLIQ TYSVFPNQSRGSDSVIQPYNSLLAI	194
epsilon	FLIMHSLSGGTGAGLGT RVLGMLDEFPHVFRICPVVMPSAI---DDVVTAPYNTAFAV	193
delta	FHIVHSVAGGTGSGVGLVSDAIRVEFP RALLLHTAVWPFAT---GEVVTQWYNCVLAM	201
zeta	ILVLHSLAGGTGSGMASLLEKIRYFIEPT EDELANADEKA---EADMMWNDGLDGLMLM	200
	: : *:.*****:*. : : :	
alpha	HSLLEHTDVAAML DNEAIYDLTRRLDIERP-----	222
beta	HQLVENSDESMCIDNEALYDICFRTLKLTTP-----	220
gamma	KRLTLHADCVVLDNTALNRIATDNLHISSP-----	225
epsilon	RELIEHADAVLPLDNDALARMADSALGQKTIGQAAGERKEPQTTLGAPAAARGYSVAQPTQ	253
delta	SALRESADAVFVAHNDDFDVSARPLQKAVNG-----RT	234
zeta	HKRRALFLISIAVAPOSIGEISTQSLNAALT-----	231
	:	
alpha	---TYTNLNLRLIGQVVSLSLTASLRFD-----GALNVDLTEFQTNLVYPYRIHFV	268
beta	---TFGDLNHLVSAVSGVTCCLEFP-----GQLNSDLRKLAVNLVFPRLHFF	266
gamma	---TVEQMNLVSTVMAASTATLRYP-----GYMNDLMSMLASLIPTPRCHFV	271
epsilon	TKLPYDSMNALVAQLLSNLT CAMRFP-----GPLNMDINEITNLVYPYRLLFL	302
delta	SEVSFD TINHEIGRLLDLHLPKKLYPV-----PSTAPEKKPHQPSTFPASRTTSS	285
zeta	----LHALRIVDAVLLLRNDCLRRDDRAAGPRGAGGKETISSSSSLSLKPCATFTEV	287
	:. . : : :	
alpha	LTSYAPVISAEK---AYHEQLS-----VSEISNAVFEPAS-MMTKCDP---RHGKYMAC	315
beta	MMGFAPLTSRGS---QYRGLS-----VPELTQQMFDAKN-MMQAADP---RHGRYLTA	313
gamma	CTGYTPTTLDTSNIQSSVQKTS-----VHDVMRLLMPKN-MMVSTSM---KSGCYISL	321
epsilon	TSAIAPLSVARHAAASAPRSVDTMIAACLDKNHQFVDVSNGLSSALH---EAGTCLAT	358
delta	TGAMASLRCCGLTDVVEAVALDPALKFFSGLALPVT PPDNRVVVAPEAT---SWYPLLCE	341
zeta	NEVFVTLMPVLLYGVGESPICNLVLS CSPSHRKMNNILTVPTPQRHYLRFKESSILSR	347
	.. . : :	
alpha	CLMYRG-DVVPKDVNAAVATIKTKRTIQFVDW SPTGFKCGINYPPTVVPGGD--LAKVQ	372
beta	SALFRG-RMSTKEVDEQMLNVQKNSSYFIEWIPNNIKSSVCDIPP-----KGLK	362
gamma	LNLIQG-DVDPAQVHRSLEIR-ERSPNFIPWGPASIQVILSKKSP-----YL--DTRHR	372
epsilon	AIVARGPQITVGDLTRNIPRIR--ERQKLVYWNEDGCKTALCSVSP-----LGHR	406
delta	ASRRTGELFVPAPSGDNNTSNN--LSTAFIEQRP--LLWSLRGPAACSEGLAH--LREVL	395

alpha	RAVCMIANSTAIAEV FARIDHKFDLMYSKRAFVHWYV GEGMEEG---EFSEAREDLAALE	429
beta	MAVTFIGNNTCIQEMFRRVGEQFTLMFRRKAFLHWYTGEGMDEM---EFTEAESNMNDLV	419
gamma	VSGLVMANHTSISSLFQRTLKQFDLLFN RGVFLEQYKRYGPIKDNLDEFKHSRDVVESLV	432
epsilon	NSVLMLANHCSIAQKLQSAHERFMRLYSVRSHVHHYEPYLEQAY---FDDTCDTVLTVV	462
delta	SRSTPTHGRELIVPPSALLLHEERLLGRRAHVSVFGPTHNIGLRLASALERAEDLLRVS	455
zeta	PAATLLTEIEGVLVMNQARELNAQLLFP LLRTAAVKVKAGAFMS---TFLDSGVAAERIQ	464
	: : . :	. :
alpha	KDYEEVGAESADMDGEEDVEEY-----	451
beta	SEYQQYQDATIEEEGEFDEEEQY-----	442
gamma	SEYKACESSDYIRNF-----	447
epsilon	DDYNYLNTVQMPADVPRSMRDLVYF-----	487
delta	AYVHHFSRYGVGEEELRDVVRMWDTAAAYGAA	488
zeta	LAIKSVALKLADAED-----	480

8.3 Alignment of TBCEL from different species

Protein Acc.	Gene	Organism
NP_689928.3	TBCEL	Homo sapiens
XP_001166986.1	TBCEL	Pan troglodytes
XP_546476.2	TBCEL	Canis lupus familiaris
XP_001253382.1	TBCEL	Bos taurus
NP_766626.1	Tbcel	Mus musculus
NP_001014111.1	Tbcel	Rattus norvegicus
XP_427094.2	TBCEL	Gallus gallus
XP_001919357.1	LOC561554	Danio rerio
NP_610562.1	CG12214	Drosophila melanogaster
XP_309507.4	AgaP_AGAP011141	Anopheles gambiae
NP_741764.1	coel-1	Caenorhabditis elegans

NP_689928.3		-----	
XP_001166986.1		-----	
XP_546476.2	1	MPSGYQVEQRVIKQEDKKARDETKGFSRVPDQESLEEHVNHCGFTLREKK	50
XP_001253382.1		-----	
NP_766626.1		-----	
NP_001014111.1		-----	
XP_427094.2		-----	
XP_001919357.1	1	-----ME	2
NP_610562.1		-----	
XP_309507.4		-----	
NP_741764.1		-----	
NP_689928.3	1	MDQPSGRSFMQVLCEKYSPE-NFPYRRGPG-----	29
XP_001166986.1	1	MDQPSGRSFMQVLCEKYSPE-NFPYRRGPG-----	29
XP_546476.2	51	MDQPSGRSFMQVLCEKYSPE-NFPYRRGPG-----	79
XP_001253382.1	1	MDQPSGRSFMQVLCEKYSPE-NFPYRRGPG-----	29
NP_766626.1	1	MDQPSGRSFMQVLCEKYSPE-NFPYRRGPG-----	29
NP_001014111.1	1	MDQPSGRSFMQVLCEKYSPE-NFPYRRGPG-----	29
XP_427094.2	1	MDQPSGRSFMQVLCEKYSPE-NFPYRRGPG-----	29
XP_001919357.1	3	SEETEGRTLQVISEKYSPE-NFPYCRGPG-----	31
NP_610562.1	1	----MPSLLEALERKYFAECEFENAHQPELHKRSDLPNDFTVTKCGGRM	45
XP_309507.4	1	----MPTLLEALEEKYGMPEDEKEEHVEE-----EV	27
NP_741764.1	1	-MEEGCSTLVRSLQKYLDD-DEDIVQ-----DI	27
NP_689928.3	30	-MGVHVPATPQGSMPKDRNLNPSVLVLNSCGITCAGDEKEIAAFAHAVSE	78
XP_001166986.1	30	-MGVHVPATPQGSMPKDRNLNPSVLVLNSCGITCAGDEKEIAAFAHAVSE	78
XP_546476.2	80	-MGVHVPATPQGSMPKDRNLNPSVLVLNSCGITRAGDEKEIAAFAHAVSE	128
XP_001253382.1	30	-MGVHVPATPQGSMPKDRNLNPSVLVLNSCGITCAGDEKEIAAFAHAVSE	78
NP_766626.1	30	-VGVHVPATPQGSMPKDRNLNPSVLVLNSCGITCAGDEREIAAFAHAVSE	78
NP_001014111.1	30	-MGVHVPATPQGSMPKDRNLNPSVLVLNSCGITCAGDEREIAAFAHAVSE	78
XP_427094.2	30	-MGVHVPATPQGSMPKDRNLNPSVLVLNSCGITCAGDENEIAAFAHAVSE	78
XP_001919357.1	32	-VGVVIRSSPQGSVPKDRNLNPSILVLDGCGITEAGDEEEVATFCAHVSE	80
NP_610562.1	46	EFSEIFIPRLSP-----LTSVPALLVLNDCDIDSAGDFDSIREKQQRVRE	89
XP_309507.4	28	LVSIFVPKLPP-----RQSTPQLLILNDCNIDRAGEPEDLKKKCRIVKE	71
NP_741764.1	28	IFTGFTGCSFCKMA---SQRALELLVLNMMNIDTIGDSEKILATLASHVSE	74
NP_689928.3	79	LDLSDNKLEDWHEVSKIIVSNVPQLEFLNLSSNPLNLSVLERTCAGSFSGV	128
XP_001166986.1	79	LDLSDNKLEDWHEVSKIIVSNVPQLEFLNLSSNPLNLSVLERTCAGSFSGV	128
XP_546476.2	129	LDLSDNKLEDWHEVSKIIVSNVPQLEFLNLSSNPLNLSVLERTCAGSFSGV	178
XP_001253382.1	79	LDLSDNKLEDWHEVSKIIVSNVPQLEFLNLSSNPLNLSVLERTCAGSFSGV	128
NP_766626.1	79	LDLSDNKLDQWHEVSKIIVSNVPQLEFLNLSSNPLSLSVLERTCAGSFSGV	128
NP_001014111.1	79	LDLSDNKLDQWHEVSKIIVSNVPQLEFLNLSSNPLSLSVLERTCAGSFSGV	128
XP_427094.2	79	LDLSDNKLEDWHEVSKIIVSNVPHLEFLNLSSNPLSLSVLERRCAGSFAGV	128
XP_001919357.1	81	LDLSHNQLKDWGEISKILSNIPNLDFLNLMSNPLHGSSLEPCLAEAFSGL	130
NP_610562.1	90	LDLAQNKLSDWSEVFSILEHMPRIEFLNLNLSKNQLASPIGTLPTA-PTINL	138
XP_309507.4	72	LDLAQNKLNNWNEVFVILSHMPRVEFVNLSLNHLTGPIQKPPVT-RMDHL	120
NP_741764.1	75	ADLGNWQISKWSDIACILKNLPHLRVLNIGHNPLN-PVIDHEL--PVSTL	121

NP 689928.3	129	RKLVLNNSKASWETVHMILQELPDLEELFLCLNDY-ETVSCPSI-----	171
XP 001166986.1	129	RKLVLNNSKASWETVHTIILQELPDLEELFLCLNDY-ETVSCPSI-----	171
XP 546476.2	179	RKLVLNNSKASWETVHTIILQELPDLEELFLCLNDY-ETVSCPSI-----	221
XP 001253382.1	129	RKLVLNNSKASWETVHTIILQELPDLEELFLCLNDY-ETVSCPSI-----	171
NP 766626.1	129	RKLVLNNSKASWETVHTIILQELPELEELFLCLNDY-ETVSCPSV-----	171
NP 001014111.1	129	RKLVLNNSKASWETVHTIILQELPDLEELFLCLNDY-ETVSCPSV-----	171
XP 427094.2	129	RKLVLNNSKASWETVHTIILQELPDLEELFLCLNDY-ETVSCPSV-----	171
XP 001919357.1	131	RRLVLNNTHTVTDWMVHTLTREIPDLEELFLCLNEY-ESVNASSM-----	173
NP 610562.1	139	KSLVLNGTYLDWACVDTLTKNLPVLQELHLSLNNY-RQVLIDAEAEQRL	187
XP 309507.4	121	RNLVLNNTKLEWCSVEKLLRLLPALEELHLSLNEY-THVLIDTVNPTDRS	169
NP 741764.1	122	HTIILNGTHLPFKTLQSFLSVLPKVTLEHMSDNQFNDDDCDEP-----	165
NP 689928.3	172	-----CCHSL	176
XP 001166986.1	172	-----CCHSL	176
XP 546476.2	222	-----CCHSL	226
XP 001253382.1	172	-----CCHSL	176
NP 766626.1	172	-----CCHSL	176
NP 001014111.1	172	-----CCHSL	176
XP 427094.2	172	-----CCQSL	176
XP 001919357.1	174	-----PCPSL	178
NP 610562.1	188	QE-----TETPEETERRITKAHPAL	207
XP 309507.4	170	NSANSERGSTDEGSQGTATDASSNNNTHDGSATSQTKEQQKETDPHGGV	219
NP 741764.1	166	-----ISTTV	170
NP 689928.3	177	KLLHITDNNLQDWTEIRKLGVMFPSLDTLVLANNHLNAIE-----	216
XP 001166986.1	177	KLLHITDNNLQDWTEIRKLGVMFPSLDTLVLANNHLNAIE-----	216
XP 546476.2	227	KLLHITDNNLQDWTEIRKLGVMFPSLDTLVLANNHLNAIE-----	266
XP 001253382.1	177	KLLHITDNNLQDWTEIRKLGVMFPSLDTLVLANNHLNAIE-----	216
NP 766626.1	177	KLLHITDNNLQDWTEIRKLGVMFPSLDTLVLANNHLNAIE-----	216
NP 001014111.1	177	KLLHITDNNLQEWTEIRKLGVMFPSLDTLVLANNHVNAIE-----	216
XP 427094.2	177	KLLHITDNNLQDWTEIRKLGIMFPSLDTLILANNLTTIE-----	216
XP 001919357.1	179	RLLHITDNQLQDWVEVRKLLGLMYPGLVSLILSNNSLSSIH-----	218
NP 610562.1	208	KTLHFTGNPVEHWQEICRLGRLEALVLAADCPKSLQ-----	247
XP 309507.4	220	RKLHLTGNYISEWGEICRIGRVFPQLEALVLAADCPPLRYVDYMDHTKGTES	269
NP 741764.1	171	RTVHLNRCGFLKWSVMNVVVRFPNVCSVFCENPLKDVT-----	210
NP 689928.3	217	-----EPDDSLARLFNLRSLSLHKSGLQSWEDIDKLNSEFPKLEEVRL	260
XP 001166986.1	217	-----EPDDSLARLFNLRSLSLHKSGLQSWEDIDKLNSEFPKLEEVRL	260
XP 546476.2	267	-----EPDDSLARLFNLRSLSLHKSGLQSWEDIDKLNSEFPKLEEVRL	310
XP 001253382.1	217	-----EPDDSLARLFNLRSLSLHKSGLQSWEDIDKLNSEFPKLEEVRL	260
NP 766626.1	217	-----EPADSLARLFNLRSLSLHKSGLQSWEDIDKLNSEFPKLEEVRL	260
NP 001014111.1	217	-----EPADSLARLFNLRSLSLHKSGLQSWEDIDKLNSEFPKLEEVRL	260
XP 427094.2	217	-----ESEDSLARLFNLRSLSLHKSGLHGWEDIDKLNSEFPKLEEVKLL	260
XP 001919357.1	219	-----EPEDSLHRLFNLRSLSLHKSGLSRWEDVEKLNFFPKLQEVVRM	262
NP 610562.1	248	-----AESSETHRYFPSLRLLNLSAQLDWAAIDELAKFSELNLRVK	292
XP 309507.4	270	PATSCNESEESHKYFQNLKLLNLSNAKIDSWEDIDRLAEFPLCNVRLQ	319
NP 741764.1	211	-----HCKHFEQLPWFNFLNLAKTSIDSWDSLQDLNRMTSISDLRVP	252
NP 689928.3	261	GIPLLQPY---TTEERRKLVARLPSVSKLNGS-VVTDGEREDSERFFIR	306
XP 001166986.1	261	GIPLLQPY---TTEERRKLVARLPSVSKLNGS-VVTDGEREDSERFFIR	306
XP 546476.2	311	GIPLLQPY---TTEERRKLVARLPSVSKLNGS-VVTDGEREDSERFFIR	356
XP 001253382.1	261	GIPLLQPY---TTEERRKLVARLPSVSKLNGS-VVTDGEREDSERFFIR	306
NP 766626.1	261	GIPLLQPY---TTEERRKLVVARLPSVSKLNGS-VVTDGEREDSERFFIR	306
NP 001014111.1	261	GIPLLQPY---TTEERRKLVVARLPSVSKLNGS-VVTDGEREDSERFFIR	306
XP 427094.2	261	GIPLLQSY---TTEERRKLLIARLPSIKLNGS-IVGDGEREDSERFFIR	306
XP 001919357.1	263	GIPLLQPY---TDQERRCLMVAQLPHVTVLNGS-VVTDGEREDAERFFIR	308

<u>NP 610562.1</u>	293	HWPLWESLEC-TEHERRQLLIARLPNVEMLNCGGKISSDERVDSERAFVR	341
<u>XP 309507.4</u>	320	YWPLWARTDSTTEHERRQLLIARLPNISILNCGDTIGAVEREDAERSFIR	369
<u>NP 741764.1</u>	253	NIPLLDAL---TNEERLHLIIIGRLHHLRVLNGS-KISSEQREQSERFFIR	298
<u>NP 689928.3</u>	307	YYVDVPQEEVPFRYHELITKYGKLEPLAEVDLRPQSS--AKVEVHFNDQV	354
<u>XP 001166986.1</u>	307	YYVDVPQEEVPFRYHELITKYGKLEPLAEVDLRPQSS--AKVEVHFNDQV	354
<u>XP 546476.2</u>	357	YYVDVPQEEVPFRYHELITKYGKLEPLAEVDLRPQSS--AKVEVHFNDQV	404
<u>XP 001253382.1</u>	307	YYVDVPQEEVPFRYHELITKYGKLEPLAEVDLRPQSS--AKVEVHFNDQV	354
<u>NP 766626.1</u>	307	YYVDVPQEEVPFRYHELITKYGKLEPLAEVDLRPQSS--AKVEVHFNDQV	354
<u>NP 001014111.1</u>	307	YYVDVPQEEVPFRYHELITKYGKLEPLAEVDLRPQSS--AKVEVHFNDQV	354
<u>XP 427094.2</u>	307	YYMEFPEEEVPFRYHELITKYGKLEPLAVVDLRPQSS--VKVEVHFQDKV	354
<u>XP 001919357.1</u>	309	YHLDCPEDELPQ-----	320
<u>NP 610562.1</u>	342	YYMDKPEEERPARYQELLQIHGKLDPLVNVSLKPKDKR--VKVLFYNDVS	389
<u>XP 309507.4</u>	370	HYLDKPDATERPRRYELIGVHGQLDPLVNIIDLPERK--VKVRFTEFEDKA	417
<u>NP 741764.1</u>	299	YYQE--QKEKPLQYKTLIDKHGNLEKLVITIDLTPKKEAVVKILCEEKEVN	346
<u>NP 689928.3</u>	355	EEMSIRLDQTVAELEKQKTLVQLPSTNMLLYYFDHEAPF--GPEEMKYS	402
<u>XP 001166986.1</u>	355	EEMSIRLDQTVAELEKQKTLVQLPSTNMLLYYFDHEAPF--GPEEMKYS	402
<u>XP 546476.2</u>	405	EEMSIRLDQTVAELEKQKTLVQLPSTNMLLYYFDHEAPF--GPEEMKYS	452
<u>XP 001253382.1</u>	355	EEMSIRLDQTVAELEKQKTLVQLPSTNMLLYYFDHEAPF--GPEEMKYS	402
<u>NP 766626.1</u>	355	EEMSIRLDQTVAELEKQKTLVQLPSTNMLLYYFDHEAPF--GPEEMKYS	402
<u>NP 001014111.1</u>	355	EEVSIRLDQTVAELEKQKTLVQLPSTNMLLYYFDHEAPF--GPEEMKYS	402
<u>XP 427094.2</u>	355	EEMSIRLDQTVAELEKHLKTVVQLSTNMLLYYFDHEAPF--GPEEMKYS	402
<u>XP 001919357.1</u>		-----	
<u>NP 610562.1</u>	390	ESRFVDIYLTVNDLKVKLEKLVGLAPNKMRLYYLDQDYKEF-GPEEMRYP	438
<u>XP 309507.4</u>	418	IERTVDVNRTVSDLKSRLELFDVPAARMRLYYVDQDFRDQGLEEMKYP	467
<u>NP 741764.1</u>	347	QEITISLEPTVLDPMKILDPKVGKFTRMKFLLLREDGRTD-DFSSSDY-	394
<u>NP 689928.3</u>	403	SRALHSFGIRDGDKIYVESKTK-----	424
<u>XP 001166986.1</u>	403	SRALHSFGIRDGDKIYVESKTK-----	424
<u>XP 546476.2</u>	453	SRALHSFGIRDGDKIYVESKTK-----	474
<u>XP 001253382.1</u>	403	SRALHSFGIRDGDKIFVESKTK-----	424
<u>NP 766626.1</u>	403	SRALHSFGIRDGDKIFVESKTK-----	424
<u>NP 001014111.1</u>	403	SRALHSFGIRDGDKIFVESKTK-----	424
<u>XP 427094.2</u>	403	SRALHSYGIRDGDKIYVEPRMK-----	424
<u>XP 001919357.1</u>		-----	
<u>NP 610562.1</u>	439	NKQLYSYNIQSGDEIIIDAKK-----	459
<u>XP 309507.4</u>	468	HKVLYSYNIRSGDEIIIERKVKS-----	490
<u>NP 741764.1</u>	395	NMPLHYFKIEDGDSFLVQEKIIVTRRRRPPSSSTSSSSS	432

8.4 Sequence alignment of TBCE (mouse, human, flies) and TBCEL (mouse, human, flies)

CLUSTAL 2.0.12 multiple sequence alignment

```

Mouse_TBCE      -----MSDILPLDVIGRRVEVNGEYATVRFVCGAVPPVAGLWLGVEWDNPERGKHDGSHEGT 56
Human_TBCE      -----MSDTLTADVIGRRVEVNGEHATVRFVAGVPPVAGPWLGVEWDNPERGKHDGSHEGT 56
Drosophila_TBCE MVGIIIDEVQLFYPLGTRIKIGDNYGTVRYVGEVSGHMGSWLGIEWDDGLRGKHNGIVDGK 60
Mouse_TBCEL     -----
Human_TBCEL     -----
Drosophila_TBCEL -----

Mouse_TBCE      MYFKCRHPTGGSFVRPSKVNFGDDFLTALKKRYVLEDGPDDE---NSCSLVGSKQVQT 113
Human_TBCE      VYFKCRHPTGGSFIRPNKVNFGTDFLTAIKNRYVLEDGPEEDR---KEQIVTIGNKPVET 113
Drosophila_TBCE RYFQTQPTPTGGSFIRPGKVGPCATLEDAARERYLNYDSSNVDESILREAQASLQASLFEV 120
Mouse_TBCEL     -----MDQPSGRSFMQVLCCKYSPENFPYRRG---PGVGVHVPATP--- 38
Human_TBCEL     -----MDQPSGRSFMQVLCCKYSPENFPYRRG---PGMGVHVPATP--- 38
Drosophila_TBCEL -----MPSLLEALERKYFAECEFEFENAHQPELHKRSD---LPNDFTVTKCGGRM 45
                .      :      :.      :      :

Mouse_TBCE      IGFEHITKKQSQLRALQDISLWNCVAVSHAGEQGRIAEACPNIRVVNLSKNLLSTWDEVVL 173
Human_TBCE      IGFDSIMKQQSQLSKLQEVSLRNCVAVSCAGEKGGVAEACPNIRKVDLSKNLLSSWDEVIH 173
Drosophila_TBCE VGMDKIARKQSKFEQLEEVSDQTPVNAAG---YLKELTHLTTLVNVSHTLIWNWEIVAS 176
Mouse_TBCEL     QGSPMKDRLN---LPSVLVLNSCGITCAGDEREIAAFCAHVSELDLSDNKLDQWHEVSK 94
Human_TBCEL     QGSPMKDRLN---LPSVLVLNSCGITCAGDEKEIAAFCAHVSELDLSDNKLEDWHEVSK 94
Drosophila_TBCEL EFSIFIPRLSPLTSPALLVLNDCDIDSAGDFDSIREKQQRVRELDLAQNKLDWSEVFS 105
                : .      : : .      : : * *      : : : : : : * *

Mouse_TBCE      IAEQLKDLEALDLSENKLFPP--SDSPTLTRTFSTLTKTLVLNKTGIT-WTEVLHCAPSWP 230
Human_TBCE      IADQLRHLEVLNVSENLKFP--SGS-VLTGTVLKVVLVNLQTVGIT-WAEVLRVAVGCP 229
Drosophila_TBCE IAQQLPSLTNLNLSNRLVLPVSSQITELEPSFRQLKRINLRSCGFSWDKDVMTALLWP 236
Mouse_TBCEL     IVSNVPQLEFLNLSNPLSLS--VLERTCAGSFGVRKLVLNNSKAS-WETVHTILQELP 151
Human_TBCEL     IVSNVPQLEFLNLSNPLNLS--VLERTCAGSFGVRKLVLNNSKAS-WETVHMILQELP 151
Drosophila_TBCEL ILEHMPRIEFLNLSKNQLASP--IGTLPTAPTIN-LKSLVLNGTYLD-WACVDTLKLNLP 161
* . : : * : * * * .      : : : : * .      * *      *

Mouse_TBCE      VLEELYLKS-----NISISERPNNVLQKMRLLDLSNPNIDES 269
Human_TBCE      GLEELYLES-----NIFISERPNDVLQTVKLLDLSNQLIDEN 268
Drosophila_TBCE NILSLGLQENSL-----GQLAEVDRTKIFKQLHELDLHRTNIMDFD 277
Mouse_TBCEL     ELEELFLCLNDY-----ETVSCPSVCCSHSLKLLHITDNNLQDWT 190
Human_TBCEL     DLEELFLCLNDY-----ETVSCPSICCHSLKLLHITDNNLQDWT 190
Drosophila_TBCEL VLQELHLSLNNYRQVLIDAEAEAEQRLQETETPEETERRITKAHPALKTLHFTGNPVEHWQ 221
: . * * *      : : * : . .

Mouse_TBCE      QLSLIADLPR-LEHLVLSDIGLSSIHFPDAEIGCKTSMFPALKYLIVNDNQIS-EWSFIN 327
Human_TBCE      QLYLIAHLPR-LEQLILSDTGISSLHFPDAGIGCKTSMFPALKYLIVNDNQIS-QWSFFN 326
Drosophila_TBCE QVTKLGNLTT-LRLLNIMENGIEEIKLPDCDSQEKLNIFVSLEQLNLLHNPWNEDAFN 336
Mouse_TBCEL     EIRKLGVMFPLDITLVANNHLNAIEEPADS---LARLFPNLRISLHKSGLQ-SWEDID 246
Human_TBCEL     EIRKLGVMFPLDITLVANNHLNAIEEPADS---LARLFPNLRISLHKSGLQ-SWEDID 246
Drosophila_TBCEL EICRLGRLFPNLEALVLADCPKSLQAEESSE--THRYFPLRLLNLSAQLD-SWAAID 278
: : . : * * : : : . : :      * * . : : : . : :

Mouse_TBCE      ELDKLQSLQALSCTRNPISKADK-----AEEIIIAKIAQLRTLNRQILPEERRGAELDY 382
Human_TBCE      ELEKLPSLRALSCLRNPLTKEDKEAET-ARLLIIASIGQLKTLNKCEILPEERRRAELDY 385
Drosophila_TBCE ELDKLPQLKRLSKTPHLKSNDNFDEFS-----KAVASIASLQFINKAQVTAQRRGAEYDI 391
Mouse_TBCEL     KLNSFPKLEEVRLGIPLLQP--YTTEERRKLVVARLPSVSKLNG-SVVTDGEREDSERF 303
Human_TBCEL     KLNSFPKLEEVRLGIPLLQP--YTTEERRKLVVARLPSVSKLNG-SVVTDGEREDSERF 303
Drosophila_TBCEL ELAKFSELNRNRVKKHWPLWESLECTEHEHRRQLLIARLPNVEMLNGGKISSDERVDSERA 338
* * . : * . : :      :      : * : : : * . . * .

Mouse_TBCE      RKAFGNEWKAGGHPDPDKNRPNAAFLSAHPRYQLLCKYGAPEDEELKTOQPFMLKQQL 442
Human_TBCE      RKAFGNEWKAGGHPDPDKNRPNAAFLSAHPRYQLLCKYGAPEDEELKTOQPFMLKQQL 445
Drosophila_TBCE WKYALDWMQATQG---GTDSLREFCRHRTYPLLVKYGSPADFPVRSQ---AKQS 442
Mouse_TBCEL     FIRYYVDVPEEVP-----FRYHELITKYGKLEPLAEVDLRPQS----- 342
Human_TBCEL     FIRYYVDVPEEVP-----FRYHELITKYGKLEPLAEVDLRPQS----- 342
Drosophila_TBCEL FVRYMDKPEEER-----ARYQELLIHGKLDPLVNVSLPKDK----- 377
: : :      : :      : * * .

```



```

Mouse_TBCE      LTLKIKCSNQPERQILEKQLPDSMTVQVKGLLSRLLKVPVSELLLSYESSKMP-GREIE 501
Human_TBCE      LTLKIKYPHQLDQKVLEKQLPGSMTIQVKGLLSRLLKVPVSDLLLSYESPKKP-GREIE 504
Drosophila_TBCE NLINVSIRHQLTGETWEKKVPRMITVQTLQGLVMKRFRLSGDVPQLCYVDALHP-DLVVP 501
Mouse_TBCEL     ---SAKVEVHFNDQVEEMSIRLDQTVAELEKQKTLVQLPTSMLLYYFDHEAP-FGPEE 398
Human_TBCEL     ---SAKVEVHFNDQVEEMSIRLDQTVAELEKQKTLVQLPTSMLLYYFDHEAP-FGPEE 398
Drosophila_TBCEL ---RVKVLFTYNDVSESRFVDIYLTVNDLKVKLEKLVGLAPNKMRLYYLDQYKEFGPEE 434
                .           .   :   * :   ::   :   . : . .   * * .

Mouse_TBCE      LENDLQPLQFYSVENGDCLLVRW--- 524
Human_TBCE      LENDLKSLQFYSVENGDCLLVRW--- 527
Drosophila_TBCE LDNNAKTLDYFYSVQEHDTVLVQ---- 523
Mouse_TBCEL     MKYSSRALHSFGIRDGDKIFVESKTK 424
Human_TBCEL     MKYSSRALHSFGIRDGDKIYVESKTK 424
Drosophila_TBCEL MRYPNKQLYSYNIQSGDEIIIDAKK- 459
                :           : *   : : : . * : :

```

9. BIBLIOGRAPHY

- Adams MD et al. (2000) The genome sequence of *Drosophila melanogaster*. *Science* 287:2185-2195.
- Akbergenova Y, Bykhovskaia M (2007) Synapsin maintains the reserve vesicle pool and spatial segregation of the recycling pool in *Drosophila* presynaptic boutons. *Brain Res* 1178:52-64.
- Akkad DA, Godde R, Epplen JT (2006) No association between synapsin III gene promoter polymorphisms and multiple sclerosis in German patients. *J Neurol* 253:1365-1366.
- Annan RS, Huddleston MJ, Verma R, Deshaies RJ, Carr SA (2001) A multidimensional electrospray MS-based approach to phosphopeptide mapping. *Anal Chem* 73:393-404.
- Bahler M, Greengard P (1987) Synapsin I bundles F-actin in a phosphorylation-dependent manner. *Nature* 326:704-707.
- Baines AJ, Bennett V (1985) Synapsin I is a spectrin-binding protein immunologically related to erythrocyte protein 4.1. *Nature* 315:410-413.
- Baines AJ, Bennett V (1986) Synapsin I is a microtubule-bundling protein. *Nature* 319:145-147.
- Bajjalieh SM, Peterson K, Shinghal R, Scheller RH (1992) SV2, a brain synaptic vesicle protein homologous to bacterial transporters. *Science* 257:1271-1273.
- Ballif BA, Carey GR, Sunyaev SR, Gygi SP (2008) Large-scale identification and evolution indexing of tyrosine phosphorylation sites from murine brain. *J Proteome Res* 7:311-318.
- Ballif BA, Villen J, Beausoleil SA, Schwartz D, Gygi SP (2004) Phosphoproteomic analysis of the developing mouse brain. *Mol Cell Proteomics* 3:1093-1101.

- Ballif BA, Cao Z, Schwartz D, Carraway KL, 3rd, Gygi SP (2006) Identification of 14-3-3epsilon substrates from embryonic murine brain. *J Proteome Res* 5:2372-2379.
- Bartolini F, Tian G, Piehl M, Cassimeris L, Lewis SA, Cowan NJ (2005) Identification of a novel tubulin-destabilizing protein related to the chaperone cofactor E. *J Cell Sci* 118:1197-1207.
- Beers MF, Johnson RG, Scarpa A (1986) Evidence for an ascorbate shuttle for the transfer of reducing equivalents across chromaffin granule membranes. *J Biol Chem* 261:2529-2535.
- Belmont L, Mitchison T, Deacon HW (1996) Catastrophic revelations about Op18/stathmin. *Trends Biochem Sci* 21:197-198.
- Belmont LD, Mitchison TJ (1996) Identification of a protein that interacts with tubulin dimers and increases the catastrophe rate of microtubules. *Cell* 84:623-631.
- Benfenati F, Greengard P, Brunner J, Bahler M (1989a) Electrostatic and hydrophobic interactions of synapsin I and synapsin I fragments with phospholipid bilayers. *J Cell Biol* 108:1851-1862.
- Benfenati F, Bahler M, Jahn R, Greengard P (1989b) Interactions of synapsin I with small synaptic vesicles: distinct sites in synapsin I bind to vesicle phospholipids and vesicle proteins. *J Cell Biol* 108:1863-1872.
- Benfenati F, Valtorta F, Chiergatti E, Greengard P (1992) Interaction of free and synaptic vesicle-bound synapsin I with F-actin. *Neuron* 8:377-386.
- Benfenati F, Neyroz P, Bahler M, Masotti L, Greengard P (1990) Time-resolved fluorescence study of the neuron-specific phosphoprotein synapsin I. Evidence for phosphorylation-dependent conformational changes. *J Biol Chem* 265:12584-12595.
- Bennett MV, Crain SM, Grundfest H (1959) Electrophysiology of supramedullary neurons in *Spheroides maculatus*. I. Orthodromic and antidromic responses. *J Gen Physiol* 43:159-188.

- Bennett V, Baines AJ, Davis JQ (1985) Ankyrin and synapsin: spectrin-binding proteins associated with brain membranes. *J Cell Biochem* 29:157-169.
- Bennett V, Baines AJ, Davis J (1986) Purification of brain analogs of red blood cell membrane skeletal proteins: ankyrin, protein 4.1 (synapsin), spectrin, and spectrin subunits. *Methods Enzymol* 134:55-69.
- Benzer S (1967) BEHAVIORAL MUTANTS OF *Drosophila* ISOLATED BY COUNTERCURRENT DISTRIBUTION. *Proc Natl Acad Sci U S A* 58:1112-1119.
- Bergada I, Schiffrin A, Abu Srair H, Kaplan P, Dornan J, Goltzman D, Hendy GN (1988) Kenny syndrome: description of additional abnormalities and molecular studies. *Hum Genet* 80:39-42.
- Berger C, Renner S, Luer K, Technau GM (2007) The commonly used marker ELAV is transiently expressed in neuroblasts and glial cells in the *Drosophila* embryonic CNS. *Dev Dyn* 236:3562-3568.
- Bhamidipati A, Lewis SA, Cowan NJ (2000) ADP ribosylation factor-like protein 2 (Arl2) regulates the interaction of tubulin-folding cofactor D with native tubulin. *J Cell Biol* 149:1087-1096.
- Bittner MA, Krasnoperov VG, Stuenkel EL, Petrenko AG, Holz RW (1998) A Ca²⁺-independent receptor for alpha-latrotoxin, CIRL, mediates effects on secretion via multiple mechanisms. *J Neurosci* 18:2914-2922.
- Bommel H, Xie G, Rossoll W, Wiese S, Jablonka S, Boehm T, Sendtner M (2002) Missense mutation in the tubulin-specific chaperone E (Tbce) gene in the mouse mutant progressive motor neuronopathy, a model of human motoneuron disease. *J Cell Biol* 159:563-569.
- Bossi L (1983) Context effects: Translation of UAG codon by suppressor tRNA is affected by the sequence following UAG in the message. *Journal of Molecular Biology* 164:73-87.

- Brand AH, Perrimon N (1993) Targeted gene expression as a means of altering cell fates and generating dominant phenotypes. *Development* 118:401-415.
- Brody T, Cravchik A (2000) *Drosophila melanogaster* G protein-coupled receptors. *J Cell Biol* 150:F83-88.
- Bruzzone R, Dermietzel R (2006) Structure and function of gap junctions in the developing brain. *Cell Tissue Res* 326:239-248.
- Buckley K, Kelly RB (1985) Identification of a transmembrane glycoprotein specific for secretory vesicles of neural and endocrine cells. *J Cell Biol* 100:1284-1294.
- Campo R, Fontalba A, Sanchez LM, Zabala JC (1994) A 14 kDa release factor is involved in GTP-dependent beta-tubulin folding. *FEBS Lett* 353:162-166.
- Capecchi MR, Hughes SH, Wahl GM (1975) Yeast super-suppressors are altered tRNAs capable of translating a nonsense codon in vitro. *Cell* 6:269-277.
- Cassimeris L, Spittle C (2001) Regulation of microtubule-associated proteins. *Int Rev Cytol* 210:163-226.
- Catterall WA (2000) Structure and regulation of voltage-gated Ca²⁺ channels. *Annu Rev Cell Dev Biol* 16:521-555.
- Cavalleri GL et al. (2007) Multicentre search for genetic susceptibility loci in sporadic epilepsy syndrome and seizure types: a case-control study. *Lancet Neurol* 6:970-980.
- Ceccaldi P, Grohovaz F, Benfenati F, Chiergatti E, Greengard P, Valtorta F (1995) Dephosphorylated synapsin I anchors synaptic vesicles to actin cytoskeleton: an analysis by videomicroscopy. *J Cell Biol* 128:905-912.
- Cesca F, Baldelli P, Valtorta F, Benfenati F (2010) The synapsins: Key actors of synapse function and plasticity. *Progress in Neurobiology* 91:313-348.
- Chi P, Greengard P, Ryan TA (2001) Synapsin dispersion and recluster during synaptic activity. *Nat Neurosci* 4:1187-1193.

- Chintapalli VR, Wang J, Dow JA (2007) Using FlyAtlas to identify better *Drosophila melanogaster* models of human disease. *Nat Genet* 39:715-720.
- Cohen MW, Jones OT, Angelides KJ (1991) Distribution of Ca²⁺ channels on frog motor nerve terminals revealed by fluorescent omega-conotoxin. *J Neurosci* 11:1032-1039.
- Coleman WL, Bykhovskaia M Cooperative regulation of neurotransmitter release by Rab3a and synapsin II. *Mol Cell Neurosci*.
- Cross D, Vial C, Maccioni RB (1993) A tau-like protein interacts with stress fibers and microtubules in human and rodent cultured cell lines. *J Cell Sci* 105 (Pt 1): 51-60.
- Cross DP, Shellenbarger DL (1979) The dynamics of *Drosophila melanogaster* spermatogenesis in in vitro cultures. *J Embryol Exp Morphol* 53:345-351.
- Curran J, Kolakofsky D (1988) Ribosomal initiation from an ACG codon in the Sendai virus P/C mRNA. *EMBO J* 7:245-251.
- Czernik AJ, Pang DT, Greengard P (1987) Amino acid sequences surrounding the cAMP-dependent and calcium/calmodulin-dependent phosphorylation sites in rat and bovine synapsin I. *Proc Natl Acad Sci U S A* 84:7518-7522.
- Danowski BA (1989) Fibroblast contractility and actin organization are stimulated by microtubule inhibitors. *J Cell Sci* 93 (Pt 2):255-266.
- De Camilli P, Greengard P (1986) Synapsin I: a synaptic vesicle-associated neuronal phosphoprotein. *Biochem Pharmacol* 35:4349-4357.
- De Camilli P, Cameron R, Greengard P (1983a) Synapsin I (protein I), a nerve terminal-specific phosphoprotein. I. Its general distribution in synapses of the central and peripheral nervous system demonstrated by immunofluorescence in frozen and plastic sections. *J Cell Biol* 96:1337-1354.
- De Camilli P, Harris SM, Jr., Huttner WB, Greengard P (1983b) Synapsin I (Protein I), a nerve terminal-specific phosphoprotein. II. Its specific association with synaptic

vesicles demonstrated by immunocytochemistry in agarose-embedded synaptosomes. *J Cell Biol* 96:1355-1373.

- De Camilli P, Benfenati F, Valtorta F, Greengard P (1990) The synapsins. *Annu Rev Cell Biol* 6:433-460.
- Desai A, Mitchison TJ (1997) Microtubule polymerization dynamics. *Annu Rev Cell Dev Biol* 13:83-117.
- Desai A, Verma S, Mitchison TJ, Walczak CE (1999) Kin I kinesins are microtubule-destabilizing enzymes. *Cell* 96:69-78.
- Diaz GA, Khan KT, Gelb BD (1998) The autosomal recessive Kenny-Caffey syndrome locus maps to chromosome 1q42-q43. *Genomics* 54:13-18.
- Diegelmann S, Nieratschker V, Werner U, Hoppe J, Zars T, Buchner E (2006) The conserved protein kinase-A target motif in synapsin of *Drosophila* is effectively modified by pre-mRNA editing. *BMC Neurosci* 7:76.
- Dittman J, Ryan TA (2009) Molecular circuitry of endocytosis at nerve terminals. *Annu Rev Cell Dev Biol* 25:133-160.
- Doerks T, Huber S, Buchner E, Bork P (2002) BSD: a novel domain in transcription factors and synapse-associated proteins. *Trends Biochem Sci* 27:168-170.
- Dunlap K, Luebke JI, Turner TJ (1995) Exocytotic Ca²⁺ channels in mammalian central neurons. *Trends Neurosci* 18:89-98.
- Engels WR, Johnson-Schlitz DM, Eggleston WB, Sved J (1990) High-frequency P element loss in *Drosophila* is homolog dependent. *Cell* 62:515-525.
- Esser L, Wang CR, Hosaka M, Smagula CS, Sudhof TC, Deisenhofer J (1998) Synapsin I is structurally similar to ATP-utilizing enzymes. *EMBO J* 17:977-984.
- Eubel H, Braun HP, Millar AH (2005) Blue-native PAGE in plants: a tool in analysis of protein-protein interactions. *Plant Methods* 1:11.
- Evans WH, Martin PE (2002) Gap junctions: structure and function (Review). *Mol Membr Biol* 19:121-136.

- Fabrizio JJ, Hime G, Lemmon SK, Bazinet C (1998) Genetic dissection of sperm individualization in *Drosophila melanogaster*. *Development* 125:1833-1843.
- Fanarraga ML, Parraga M, Aloria K, del Mazo J, Avila J, Zabala JC (1999) Regulated expression of p14 (cofactor A) during spermatogenesis. *Cell Motil Cytoskeleton* 43:243-254.
- Feierbach B, Nogales E, Downing KH, Stearns T (1999) Alf1p, a CLIP-170 domain-containing protein, is functionally and physically associated with alpha-tubulin. *J Cell Biol* 144:113-124.
- Fiumara F, Milanese C, Corradi A, Giovedi S, Leitinger G, Menegon A, Montarolo PG, Benfenati F, Ghirardi M (2007) Phosphorylation of synapsin domain A is required for post-tetanic potentiation. *J Cell Sci* 120:3228-3237.
- Fontalba A, Paciucci R, Avila J, Zabala JC (1993) Incorporation of tubulin subunits into dimers requires GTP hydrolysis. *J Cell Sci* 106 (Pt 2):627-632.
- Franceschini P, Testa A, Bogetti G, Girardo E, Guala A, Lopez-Bell G, Buzio G, Ferrario E, Piccato E (1992) Kenny-Caffey syndrome in two sibs born to consanguineous parents: evidence for an autosomal recessive variant. *Am J Med Genet* 42:112-116.
- Frankel WN, Schork NJ (1996) Who's afraid of epistasis? *Nat Genet* 14:371-373.
- Fuller M (1993) Spermatogenesis. In: *The Development of Drosophila melanogaster* (Bate M, Arias AM, eds), pp 71-147. NY: Cold Spring Harbor Laboratory Press.
- Funk N, Becker S, Huber S, Brunner M, Buchner E (2004) Targeted mutagenesis of the Sap47 gene of *Drosophila*: flies lacking the synapse associated protein of 47 kDa are viable and fertile. *BMC Neurosci* 5:16.
- Furshpan EJ, Potter DD (1957) Mechanism of nerve-impulse transmission at a crayfish synapse. *Nature* 180:342-343.
- Fykse EM, Fonnum F (1988) Uptake of gamma-aminobutyric acid by a synaptic vesicle fraction isolated from rat brain. *J Neurochem* 50:1237-1242.

- Gao Y, Vainberg IE, Chow RL, Cowan NJ (1993) Two cofactors and cytoplasmic chaperonin are required for the folding of alpha- and beta-tubulin. *Mol Cell Biol* 13:2478-2485.
- Gao Y, Thomas JO, Chow RL, Lee GH, Cowan NJ (1992) A cytoplasmic chaperonin that catalyzes beta-actin folding. *Cell* 69:1043-1050.
- Gao Y, Melki R, Walden PD, Lewis SA, Ampe C, Rommelaere H, Vandekerckhove J, Cowan NJ (1994) A novel cochaperonin that modulates the ATPase activity of cytoplasmic chaperonin. *J Cell Biol* 125:989-996.
- Garcia CC, Blair HJ, Seager M, Coulthard A, Tennant S, Buddles M, Curtis A, Goodship JA (2004) Identification of a mutation in synapsin I, a synaptic vesicle protein, in a family with epilepsy. *J Med Genet* 41:183-186.
- Geissler S, Siegers K, Schiebel E (1998) A novel protein complex promoting formation of functional alpha- and gamma-tubulin. *EMBO J* 17:952-966.
- Gibson G, Wemple M, van Helden S (1999) Potential variance affecting homeotic Ultrabithorax and Antennapedia phenotypes in *Drosophila melanogaster*. *Genetics* 151:1081-1091.
- Giovedi S, Darchen F, Valtorta F, Greengard P, Benfenati F (2004a) Synapsin is a novel Rab3 effector protein on small synaptic vesicles. II. Functional effects of the Rab3A-synapsin I interaction. *J Biol Chem* 279:43769-43779.
- Giovedi S, Vaccaro P, Valtorta F, Darchen F, Greengard P, Cesareni G, Benfenati F (2004b) Synapsin is a novel Rab3 effector protein on small synaptic vesicles. I. Identification and characterization of the synapsin I-Rab3 interactions in vitro and in intact nerve terminals. *J Biol Chem* 279:43760-43768.
- Gitler D, Cheng Q, Greengard P, Augustine GJ (2008) Synapsin IIa controls the reserve pool of glutamatergic synaptic vesicles. *J Neurosci* 28:10835-10843.
- Godenschwege TA et al. (2004) Flies lacking all synapsins are unexpectedly healthy but are impaired in complex behaviour. *Eur J Neurosci* 20:611-622.

- Goelz SE, Nestler EJ, Chehrazi B, Greengard P (1981) Distribution of protein I in mammalian brain as determined by a detergent-based radioimmunoassay. *Proc Natl Acad Sci U S A* 78:2130-2134.
- Gray NK, Wickens M (1998) Control of translation initiation in animals. *Annu Rev Cell Dev Biol* 14:399-458.
- Greengard P, Valtorta F, Czernik AJ, Benfenati F (1993) Synaptic vesicle phosphoproteins and regulation of synaptic function. *Science* 259:780-785.
- Griffith LM, Pollard TD (1978) Evidence for actin filament-microtubule interaction mediated by microtubule-associated proteins. *J Cell Biol* 78:958-965.
- Grynberg M, Jaroszewski L, Godzik A (2003) Domain analysis of the tubulin cofactor system: a model for tubulin folding and dimerization. *BMC Bioinformatics* 4:46.
- Guillaud L, Setou M, Hirokawa N (2003) KIF17 dynamics and regulation of NR2B trafficking in hippocampal neurons. *J Neurosci* 23:131-140.
- Gygi SP, Rochon Y, Franz BR, Aebersold R (1999) Correlation between protein and mRNA abundance in yeast. *Mol Cell Biol* 19:1720-1730.
- Hell JW, Maycox PR, Stadler H, Jahn R (1988) Uptake of GABA by rat brain synaptic vesicles isolated by a new procedure. *EMBO J* 7:3023-3029.
- Hershko A, Ciechanover A (1982) Mechanisms of intracellular protein breakdown. *Annu Rev Biochem* 51:335-364.
- Hershkovitz E, Shalitin S, Levy J, Leiberman E, Weinshtock A, Varsano I, Gorodischer R (1995) The new syndrome of congenital hypoparathyroidism associated with dysmorphism, growth retardation, and developmental delay--a report of six patients. *Isr J Med Sci* 31:293-297.
- Hilfiker S, Schweizer FE, Kao HT, Czernik AJ, Greengard P, Augustine GJ (1998) Two sites of action for synapsin domain E in regulating neurotransmitter release. *Nat Neurosci* 1:29-35.

- Hilfiker S, Benfenati F, Doussau F, Nairn AC, Czernik AJ, Augustine GJ, Greengard P (2005) Structural domains involved in the regulation of transmitter release by synapsins. *J Neurosci* 25:2658-2669.
- Hofbauer A, Ebel T, Waltenspiel B, Oswald P, Chen YC, Halder P, Biskup S, Lewandrowski U, Winkler C, Sickmann A, Buchner S, Buchner E (2009) The Wuerzburg hybridoma library against Drosophila brain. *J Neurogenet* 23:78-91.
- Hosaka M, Sudhof TC (1998a) Synapsins I and II are ATP-binding proteins with differential Ca²⁺ regulation. *J Biol Chem* 273:1425-1429.
- Hosaka M, Sudhof TC (1998b) Synapsin III, a novel synapsin with an unusual regulation by Ca²⁺. *J Biol Chem* 273:13371-13374.
- Hosaka M, Sudhof TC (1999) Homo- and heterodimerization of synapsins. *J Biol Chem* 274:16747-16753.
- Hosaka M, Hammer RE, Sudhof TC (1999) A phospho-switch controls the dynamic association of synapsins with synaptic vesicles. *Neuron* 24:377-387.
- Humeau Y, Doussau F, Vitiello F, Greengard P, Benfenati F, Poulain B (2001) Synapsin controls both reserve and releasable synaptic vesicle pools during neuronal activity and short-term plasticity in *Aplysia*. *J Neurosci* 21:4195-4206.
- Hurley SL, Brown DL, Cheetham JJ (2004) Cytoskeletal interactions of synapsin I in non-neuronal cells. *Biochem Biophys Res Commun* 317:16-23.
- Huttner WB, Schiebler W, Greengard P, De Camilli P (1983) Synapsin I (protein I), a nerve terminal-specific phosphoprotein. III. Its association with synaptic vesicles studied in a highly purified synaptic vesicle preparation. *J Cell Biol* 96:1374-1388.
- Jansen RP (2001) mRNA localization: message on the move. *Nat Rev Mol Cell Biol* 2:247-256.
- Jin S, Pan L, Liu Z, Wang Q, Xu Z, Zhang YQ (2009) Drosophila Tubulin-specific chaperone E functions at neuromuscular synapses and is required for microtubule network formation. *Development* 136:1571-1581.

- John JP, Chen WQ, Pollak A, Lubec G (2007) Mass spectrometric studies on mouse hippocampal synapsins Ia, IIa, and IIb and identification of a novel phosphorylation site at serine-546. *J Proteome Res* 6:2695-2710.
- Jovanovic JN, Benfenati F, Siow YL, Sihra TS, Sanghera JS, Pelech SL, Greengard P, Czernik AJ (1996) Neurotrophins stimulate phosphorylation of synapsin I by MAP kinase and regulate synapsin I-actin interactions. *Proc Natl Acad Sci U S A* 93:3679-3683.
- Kang SU, Zhang M, Burgos M, Lubec G (2009) Mass spectrometrical characterisation of mouse and rat synapsin isoforms 2a and 2b. *Amino Acids*.
- Kao HT, Porton B, Hilfiker S, Stefani G, Pieribone VA, DeSalle R, Greengard P (1999) Molecular evolution of the synapsin gene family. *J Exp Zool* 285:360-377.
- Kao HT, Porton B, Czernik AJ, Feng J, Yiu G, Haring M, Benfenati F, Greengard P (1998) A third member of the synapsin gene family. *Proc Natl Acad Sci U S A* 95:4667-4672.
- Kelly TE, Blanton S, Saif R, Sanjad SA, Sakati NA (2000) Confirmation of the assignment of the Sanjad-Sakati (congenital hypoparathyroidism) syndrome (OMIM 241410) locus to chromosome 1q42-43. *J Med Genet* 37:63-64.
- Kempfues KJ, Kaufman TC, Raff RA, Raff EC (1982) The testis-specific beta-tubulin subunit in *Drosophila melanogaster* has multiple functions in spermatogenesis. *Cell* 31:655-670.
- Kimble M, Incardona JP, Raff EC (1989) A variant beta-tubulin isoform of *Drosophila melanogaster* (beta 3) is expressed primarily in tissues of mesodermal origin in embryos and pupae, and is utilized in populations of transient microtubules. *Dev Biol* 131:415-429.
- Klagges BR, Heimbeck G, Godenschwege TA, Hofbauer A, Pflugfelder GO, Reifegerste R, Reisch D, Schaupp M, Buchner S, Buchner E (1996) Invertebrate synapsins: a single gene codes for several isoforms in *Drosophila*. *J Neurosci* 16:3154-3165.

- Kline-Smith SL, Walczak CE (2002) The microtubule-destabilizing kinesin XKCM1 regulates microtubule dynamic instability in cells. *Mol Biol Cell* 13:2718-2731.
- Knapek S, Gerber B, Tanimoto H Synapsin is selectively required for anesthesia-sensitive memory. *Learn Mem* 17:76-79.
- Kozak M (1995) Adherence to the first-AUG rule when a second AUG codon follows closely upon the first. *Proc Natl Acad Sci U S A* 92:7134.
- Kozak M (1997) Recognition of AUG and alternative initiator codons is augmented by G in position +4 but is not generally affected by the nucleotides in positions +5 and +6. *EMBO J* 16:2482-2492.
- Krasnoperov VG, Bittner MA, Beavis R, Kuang Y, Salnikow KV, Chepurny OG, Little AR, Plotnikov AN, Wu D, Holz RW, Petrenko AG (1997) alpha-Latrotoxin stimulates exocytosis by the interaction with a neuronal G-protein-coupled receptor. *Neuron* 18:925-937.
- Kubota H, Hynes G, Carne A, Ashworth A, Willison K (1994) Identification of six Tcp-1-related genes encoding divergent subunits of the TCP-1-containing chaperonin. *Curr Biol* 4:89-99.
- Lakhan R, Kalita J, Misra UK, Kumari R, Mittal B Association of intronic polymorphism rs3773364 A>G in synapsin-2 gene with idiopathic epilepsy. *Synapse* 64:403-408.
- Landesman Y, White TW, Starich TA, Shaw JE, Goodenough DA, Paul DL (1999) Innexin-3 forms connexin-like intercellular channels. *J Cell Sci* 112 (Pt 14): 2391-2396.
- Lashkari DA, DeRisi JL, McCusker JH, Namath AF, Gentile C, Hwang SY, Brown PO, Davis RW (1997) Yeast microarrays for genome wide parallel genetic and gene expression analysis. *Proc Natl Acad Sci U S A* 94:13057-13062.
- Leroy Q, Raoult D Review of microarray studies for host-intracellular pathogen interactions. *J Microbiol Methods* 81:81-95.
- Lewis SA, Cowan NJ (2002) Bad chaperone. *Nat Med* 8:1202-1203.

- Lewis SA, Tian G, Cowan NJ (1997) The alpha- and beta-tubulin folding pathways. *Trends Cell Biol* 7:479-484.
- Lewis SA, Tian G, Vainberg IE, Cowan NJ (1996) Chaperonin-mediated folding of actin and tubulin. *J Cell Biol* 132:1-4.
- Li J, Han YR, Plummer MR, Herrup K (2009) Cytoplasmic ATM in neurons modulates synaptic function. *Curr Biol* 19:2091-2096.
- Li L, Chin LS, Shupliakov O, Brodin L, Sihra TS, Hvalby O, Jensen V, Zheng D, McNamara JO, Greengard P, et al. (1995) Impairment of synaptic vesicle clustering and of synaptic transmission, and increased seizure propensity, in synapsin I-deficient mice. *Proc Natl Acad Sci U S A* 92:9235-9239.
- Liguori M, Cittadella R, Manna I, Valentino P, La Russa A, Serra P, Trojano M, Messina D, Ruscica F, Andreoli V, Romeo N, Livrea P, Quattrone A (2004) Association between Synapsin III gene promoter polymorphisms and multiple sclerosis. *J Neurol* 251:165-170.
- Lin RC, Scheller RH (2000) Mechanisms of synaptic vesicle exocytosis. *Annu Rev Cell Dev Biol* 16:19-49.
- Llinas R, Sugimori M, Silver RB (1992) Microdomains of high calcium concentration in a presynaptic terminal. *Science* 256:677-679.
- Maccioni RB (1986) Molecular cytology of microtubules. *Revis Biol Celular* 8:1-124.
- Malarkannan S, Horng T, Shih PP, Schwab S, Shastri N (1999) Presentation of out-of-frame peptide/MHC class I complexes by a novel translation initiation mechanism. *Immunity* 10:681-690.
- Mandell JW, Czernik AJ, De Camilli P, Greengard P, Townes-Anderson E (1992) Differential expression of synapsins I and II among rat retinal synapses. *J Neurosci* 12:1736-1749.
- Margolis RL, Wilson L (1978) Opposite end assembly and disassembly of microtubules at steady state in vitro. *Cell* 13:1-8.

- Margolis RL, Wilson L, Keifer BI (1978) Mitotic mechanism based on intrinsic microtubule behaviour. *Nature* 272:450-452.
- Martin L, Fanarraga ML, Aloria K, Zabala JC (2000) Tubulin folding cofactor D is a microtubule destabilizing protein. *FEBS Lett* 470:93-95.
- Martin N, Jaubert J, Gounon P, Salido E, Haase G, Szatanik M, Guenet JL (2002) A missense mutation in *Tbce* causes progressive motor neuronopathy in mice. *Nat Genet* 32:443-447.
- McNally FJ (1996) Modulation of microtubule dynamics during the cell cycle. *Curr Opin Cell Biol* 8:23-29.
- Melki R, Rommelaere H, Leguy R, Vandekerckhove J, Ampe C (1996) Cofactor A is a molecular chaperone required for beta-tubulin folding: functional and structural characterization. *Biochemistry* 35:10422-10435.
- Mese G, Richard G, White TW (2007) Gap junctions: basic structure and function. *J Invest Dermatol* 127:2516-2524.
- Messa M, Congia S, Defranchi E, Valtorta F, Fassio A, Onofri F, Benfenati F Tyrosine phosphorylation of synapsin I by Src regulates synaptic-vesicle trafficking. *J Cell Sci*.
- Michels B, Diegelmann S, Tanimoto H, Schwenkert I, Buchner E, Gerber B (2005) A role for Synapsin in associative learning: the *Drosophila* larva as a study case. *Learn Mem* 12:224-231.
- Mitchison T, Kirschner M (1984a) Microtubule assembly nucleated by isolated centrosomes. *Nature* 312:232-237.
- Mitchison T, Kirschner M (1984b) Dynamic instability of microtubule growth. *Nature* 312:237-242.
- Monaldi I, Vassalli M, Bachi A, Giovedi S, Millo E, Valtorta F, Raiteri R, Benfenati F, Fassio A (2009) The highly conserved synapsin domain E mediates synapsin dimerization and phospholipid vesicle clustering. *Biochem J*.

- Monaldi I, Vassalli M, Bachi A, Giovedi S, Millo E, Valtorta F, Raiteri R, Benfenati F, Fassio A (2010) The highly conserved synapsin domain E mediates synapsin dimerization and phospholipid vesicle clustering. *Biochem J*.
- Mortz E, Krogh TN, Vorum H, Gorg A (2001) Improved silver staining protocols for high sensitivity protein identification using matrix-assisted laser desorption/ionization-time of flight analysis. *Proteomics* 1:1359-1363.
- Munch G, Schickanz D, Behme A, Gerlach M, Riederer P, Palm D, Schinzel R (1999) Amino acid specificity of glycation and protein-AGE crosslinking reactivities determined with a dipeptide SPOT library. *Nat Biotechnol* 17:1006-1010.
- Munton RP, Tweedie-Cullen R, Livingstone-Zatchej M, Weinandy F, Waidelich M, Longo D, Gehrig P, Potthast F, Rutishauser D, Gerrits B, Panse C, Schlapbach R, Mansuy IM (2007) Qualitative and quantitative analyses of protein phosphorylation in naive and stimulated mouse synaptosomal preparations. *Mol Cell Proteomics* 6:283-293.
- Navone F, Greengard P, De Camilli P (1984) Synapsin I in nerve terminals: selective association with small synaptic vesicles. *Science* 226:1209-1211.
- Nogales E (2000) Structural insights into microtubule function. *Annu Rev Biochem* 69:277-302.
- Okada Y, Yamazaki H, Sekine-Aizawa Y, Hirokawa N (1995) The neuron-specific kinesin superfamily protein KIF1A is a unique monomeric motor for anterograde axonal transport of synaptic vesicle precursors. *Cell* 81:769-780.
- Oliveira CC, McCarthy JE (1995) The relationship between eukaryotic translation and mRNA stability. A short upstream open reading frame strongly inhibits translational initiation and greatly accelerates mRNA degradation in the yeast *Saccharomyces cerevisiae*. *J Biol Chem* 270:8936-8943.
- Olivera BM, Miljanich GP, Ramachandran J, Adams ME (1994) Calcium channel diversity and neurotransmitter release: the omega-conotoxins and omega-agatoxins. *Annu Rev Biochem* 63:823-867.

- Onofri F, Messa M, Matafora V, Bonanno G, Corradi A, Bachi A, Valtorta F, Benfenati F (2007) Synapsin phosphorylation by SRC tyrosine kinase enhances SRC activity in synaptic vesicles. *J Biol Chem* 282:15754-15767.
- Panchin Y, Kelmanson I, Matz M, Lukyanov K, Usman N, Lukyanov S (2000) A ubiquitous family of putative gap junction molecules. *Curr Biol* 10:R473-474.
- Parsons SM, Prior C, Marshall IG (1993) Acetylcholine transport, storage, and release. *Int Rev Neurobiol* 35:279-390.
- Parvari R et al. (2002) Mutation of TBCE causes hypoparathyroidism-retardation-dysmorphism and autosomal recessive Kenny-Caffey syndrome. *Nat Genet* 32:448-452.
- Peabody DS (1987) Translation initiation at an ACG triplet in mammalian cells. *J Biol Chem* 262:11847-11851.
- Peabody DS (1989) Translation initiation at non-AUG triplets in mammalian cells. *J Biol Chem* 264:5031-5035.
- Perdahl E, Adolfsson R, Alafuzoff I, Albert KA, Nestler EJ, Greengard P, Winblad B (1984) Synapsin I (protein I) in different brain regions in senile dementia of Alzheimer type and in multi-infarct dementia. *J Neural Transm* 60:133-141.
- Pesole G, Mignone F, Gissi C, Grillo G, Licciulli F, Liuni S (2001) Structural and functional features of eukaryotic mRNA untranslated regions. *Gene* 276:73-81.
- Petrucci TC, Morrow JS (1987) Synapsin I: an actin-bundling protein under phosphorylation control. *J Cell Biol* 105:1355-1363.
- Petrucci TC, Morrow JS (1991) Actin and tubulin binding domains of synapsins Ia and Ib. *Biochemistry* 30:413-422.
- Phelan P, Starich TA (2001) Innexins get into the gap. *Bioessays* 23:388-396.
- Pieribone VA, Shupliakov O, Brodin L, Hilfiker-Rothenfluh S, Czernik AJ, Greengard P (1995) Distinct pools of synaptic vesicles in neurotransmitter release. *Nature* 375:493-497.

- Porter ME, Scholey JM, Stemple DL, Vigers GP, Vale RD, Sheetz MP, McIntosh JR (1987) Characterization of the microtubule movement produced by sea urchin egg kinesin. *J Biol Chem* 262:2794-2802.
- Porton B, Kao HT, Greengard P (1999) Characterization of transcripts from the synapsin III gene locus. *J Neurochem* 73:2266-2271.
- Prats AC, De Billy G, Wang P, Darlix JL (1989) CUG initiation codon used for the synthesis of a cell surface antigen coded by the murine leukemia virus. *J Mol Biol* 205:363-372.
- Qin S, Hu XY, Xu H, Zhou JN (2004) Regional alteration of synapsin I in the hippocampal formation of Alzheimer's disease patients. *Acta Neuropathol* 107:209-215.
- Quarumby L (2000) Cellular Samurai: katanin and the severing of microtubules. *J Cell Sci* 113 (Pt 16):2821-2827.
- Radcliffe PA, Garcia MA, Toda T (2000a) The cofactor-dependent pathways for alpha- and beta-tubulins in microtubule biogenesis are functionally different in fission yeast. *Genetics* 156:93-103.
- Radcliffe PA, Vardy L, Toda T (2000b) A conserved small GTP-binding protein Alp41 is essential for the cofactor-dependent biogenesis of microtubules in fission yeast. *FEBS Lett* 468:84-88.
- Rahamimoff R, DeRiemer SA, Sakmann B, Stadler H, Yakir N (1988) Ion channels in synaptic vesicles from Torpedo electric organ. *Proc Natl Acad Sci U S A* 85:5310-5314.
- Reichmuth C, Becker S, Benz M, Debel K, Reisch D, Heimbeck G, Hofbauer A, Klagges B, Pflugfelder GO, Buchner E (1995) The sap47 gene of *Drosophila melanogaster* codes for a novel conserved neuronal protein associated with synaptic terminals. *Brain Res Mol Brain Res* 32:45-54.
- Reinders J, Sickmann A (2005) State-of-the-art in phosphoproteomics. *Proteomics* 5:4052-4061.

- Richardson RJ, Kirk JM (1990) Short stature, mental retardation, and hypoparathyroidism: a new syndrome. *Arch Dis Child* 65:1113-1117.
- Richardson RJ, Kirk J (1991) A new syndrome of congenital hypoparathyroidism, severe growth failure, and dysmorphic features. *Arch Dis Child* 66:1365.
- Riehemann K, Sorg C (1993) Sequence homologies between four cytoskeleton-associated proteins. *Trends Biochem Sci* 18:82-83.
- Rizzoli SO, Betz WJ (2005) Synaptic vesicle pools. *Nat Rev Neurosci* 6:57-69.
- Rosahl TW, Spillane D, Missler M, Herz J, Selig DK, Wolff JR, Hammer RE, Malenka RC, Sudhof TC (1995) Essential functions of synapsins I and II in synaptic vesicle regulation. *Nature* 375:488-493.
- Rose MD, Biggins S, Satterwhite LL (1993) Unravelling the tangled web at the microtubule-organizing center. *Curr Opin Cell Biol* 5:105-115.
- Sanjad SA, Sakati NA, Abu-Osba YK, Kaddoura R, Milner RD (1991) A new syndrome of congenital hypoparathyroidism, severe growth failure, and dysmorphic features. *Arch Dis Child* 66:193-196.
- Schaefer MK, Schmalbruch H, Buhler E, Lopez C, Martin N, Guenet JL, Haase G (2007) Progressive motor neuronopathy: a critical role of the tubulin chaperone TBCE in axonal tubulin routing from the Golgi apparatus. *J Neurosci* 27:8779-8789.
- Schagger H, von Jagow G (1991) Blue native electrophoresis for isolation of membrane protein complexes in enzymatically active form. *Anal Biochem* 199:223-231.
- Schena M, Shalon D, Davis RW, Brown PO (1995) Quantitative monitoring of gene expression patterns with a complementary DNA microarray. *Science* 270:467-470.
- Schiebler W, Jahn R, Doucet JP, Rothlein J, Greengard P (1986) Characterization of synapsin I binding to small synaptic vesicles. *J Biol Chem* 261:8383-8390.

- Schmalbruch H, Jensen HJ, Bjaerg M, Kamieniecka Z, Kurland L (1991) A new mouse mutant with progressive motor neuronopathy. *J Neuropathol Exp Neurol* 50:192-204.
- Schnapp BJ, Vale RD, Sheetz MP, Reese TS (1986) Microtubules and the mechanism of directed organelle movement. *Ann N Y Acad Sci* 466:909-918.
- Schneggenburger R, Neher E (2000) Intracellular calcium dependence of transmitter release rates at a fast central synapse. *Nature* 406:889-893.
- Schoenfeld TA, Obar RA (1994) Diverse distribution and function of fibrous microtubule-associated proteins in the nervous system. *Int Rev Cytol* 151:67-137.
- Schulman H, Greengard P (1978) Stimulation of brain membrane protein phosphorylation by calcium and an endogenous heat-stable protein. *Nature* 271:478-479.
- Setou M, Nakagawa T, Seog DH, Hirokawa N (2000) Kinesin superfamily motor protein KIF17 and mLin-10 in NMDA receptor-containing vesicle transport. *Science* 288:1796-1802.
- Sheetz MP, Vale R, Schnapp B, Schroer T, Reese T (1987) Movements of vesicles on microtubules. *Ann N Y Acad Sci* 493:409-416.
- Sheng ZH, Yokoyama CT, Catterall WA (1997) Interaction of the synprint site of N-type Ca²⁺ channels with the C2B domain of synaptotagmin I. *Proc Natl Acad Sci U S A* 94:5405-5410.
- Sheng ZH, Rettig J, Takahashi M, Catterall WA (1994) Identification of a syntaxin-binding site on N-type calcium channels. *Neuron* 13:1303-1313.
- Sheng ZH, Rettig J, Cook T, Catterall WA (1996) Calcium-dependent interaction of N-type calcium channels with the synaptic core complex. *Nature* 379:451-454.
- Silva AJ, Rosahl TW, Chapman PF, Marowitz Z, Friedman E, Frankland PW, Cestari V, Cioffi D, Sudhof TC, Bourtschuladze R (1996) Impaired learning in mice with abnormal short-lived plasticity. *Curr Biol* 6:1509-1518.

- Smith SJ, Buchanan J, Osses LR, Charlton MP, Augustine GJ (1993) The spatial distribution of calcium signals in squid presynaptic terminals. *J Physiol* 472:573-593.
- Song W, Nie Z, Petrenko AG, Zinsmaier KE (2003) The G protein-coupled receptor *Drosophila* CIRL regulates synaptic transmission. Program and Abstracts 44th Annual *Drosophila* Research Conference, Chicago, 2003:33.
- Stanley EF (1997) The calcium channel and the organization of the presynaptic transmitter release face. *Trends Neurosci* 20:404-409.
- Steege DA (1983) A nucleotide change in the anticodon of an *Escherichia coli* serine transfer RNA results in supD-amber suppression. *Nucleic Acids Res* 11:3823-3832.
- Steen H, Kuster B, Mann M (2001) Quadrupole time-of-flight versus triple-quadrupole mass spectrometry for the determination of phosphopeptides by precursor ion scanning. *J Mass Spectrom* 36:782-790.
- Sudhof TC (2004) The synaptic vesicle cycle. *Annu Rev Neurosci* 27:509-547.
- Sudhof TC, Czernik AJ, Kao HT, Takei K, Johnston PA, Horiuchi A, Kanazir SD, Wagner MA, Perin MS, De Camilli P, et al. (1989) Synapsins: mosaics of shared and individual domains in a family of synaptic vesicle phosphoproteins. *Science* 245:1474-1480.
- Swamy M, Kulathu Y, Ernst S, Reth M, Schamel WW (2006) Two dimensional Blue Native-/SDS-PAGE analysis of SLP family adaptor protein complexes. *Immunol Lett* 104:131-137.
- Takei Y, Harada A, Takeda S, Kobayashi K, Terada S, Noda T, Takahashi T, Hirokawa N (1995) Synapsin I deficiency results in the structural change in the presynaptic terminals in the murine nervous system. *J Cell Biol* 131:1789-1800.
- Threadgill DW, Dlugosz AA, Hansen LA, Tennenbaum T, Lichti U, Yee D, LaMantia C, Mourton T, Herrup K, Harris RC, et al. (1995) Targeted disruption of mouse

EGF receptor: effect of genetic background on mutant phenotype. *Science* 269:230-234.

- Tian G, Huang MC, Parvari R, Diaz GA, Cowan NJ (2006) Cryptic out-of-frame translational initiation of TBCE rescues tubulin formation in compound heterozygous HRD. *Proc Natl Acad Sci U S A* 103:13491-13496.
- Tian G, Huang Y, Rommelaere H, Vandekerckhove J, Ampe C, Cowan NJ (1996) Pathway leading to correctly folded beta-tubulin. *Cell* 86:287-296.
- Tian G, Lewis SA, Feierbach B, Stearns T, Rommelaere H, Ampe C, Cowan NJ (1997) Tubulin subunits exist in an activated conformational state generated and maintained by protein cofactors. *J Cell Biol* 138:821-832.
- Tobaben S, Sudhof TC, Stahl B (2002) Genetic analysis of alpha-latrotoxin receptors reveals functional interdependence of CIRL/latrophilin 1 and neurexin 1 alpha. *J Biol Chem* 277:6359-6365.
- Touriol C, Bornes S, Bonnal S, Audigier S, Prats H, Prats AC, Vagner S (2003) Generation of protein isoform diversity by alternative initiation of translation at non-AUG codons. *Biol Cell* 95:169-178.
- Trinidad JC, Thalhammer A, Specht CG, Schoepfer R, Burlingame AL (2005) Phosphorylation state of postsynaptic density proteins. *J Neurochem* 92:1306-1316.
- Trinidad JC, Specht CG, Thalhammer A, Schoepfer R, Burlingame AL (2006) Comprehensive identification of phosphorylation sites in postsynaptic density preparations. *Mol Cell Proteomics* 5:914-922.
- Trinidad JC, Thalhammer A, Specht CG, Lynn AJ, Baker PR, Schoepfer R, Burlingame AL (2008) Quantitative analysis of synaptic phosphorylation and protein expression. *Mol Cell Proteomics* 7:684-696.
- Tweedie-Cullen RY, Reck JM, Mansuy IM (2009) Comprehensive mapping of post-translational modifications on synaptic, nuclear, and histone proteins in the adult mouse brain. *J Proteome Res* 8:4966-4982.

- Vainberg IE, Lewis SA, Rommelaere H, Ampe C, Vandekerckhove J, Klein HL, Cowan NJ (1998) Prefoldin, a chaperone that delivers unfolded proteins to cytosolic chaperonin. *Cell* 93:863-873.
- Vale RD (1987) Intracellular transport using microtubule-based motors. *Annu Rev Cell Biol* 3:347-378.
- Vale RD, Reese TS, Sheetz MP (1985a) Identification of a novel force-generating protein, kinesin, involved in microtubule-based motility. *Cell* 42:39-50.
- Vale RD, Schnapp BJ, Mitchison T, Steuer E, Reese TS, Sheetz MP (1985b) Different axoplasmic proteins generate movement in opposite directions along microtubules in vitro. *Cell* 43:623-632.
- van der Velden AW, Thomas AA (1999) The role of the 5' untranslated region of an mRNA in translation regulation during development. *Int J Biochem Cell Biol* 31:87-106.
- Vaughan S, Attwood T, Navarro M, Scott V, McKean P, Gull K (2000) New tubulins in protozoal parasites. *Curr Biol* 10:R258-259.
- Vawter MP, Thatcher L, Usen N, Hyde TM, Kleinman JE, Freed WJ (2002) Reduction of synapsin in the hippocampus of patients with bipolar disorder and schizophrenia. *Mol Psychiatry* 7:571-578.
- Verma R, Chen S, Feldman R, Schieltz D, Yates J, Dohmen J, Deshaies RJ (2000) Proteasomal proteomics: identification of nucleotide-sensitive proteasome-interacting proteins by mass spectrometric analysis of affinity-purified proteasomes. *Mol Biol Cell* 11:3425-3439.
- Voloshin O, Gocheva Y, Gutnick M, Movshovich N, Bakhrat A, Baranes-Bachar K, Bar-Zvi D, Parvari R, Gheber L, Raveh D Tubulin chaperone E binds microtubules and proteasomes and protects against misfolded protein stress. *Cell Mol Life Sci.*
- Walczak CE, Mitchison TJ (1996) Kinesin-related proteins at mitotic spindle poles: function and regulation. *Cell* 85:943-946.

- Walczak CE, Mitchison TJ, Desai A (1996) XKCM1: a *Xenopus* kinesin-related protein that regulates microtubule dynamics during mitotic spindle assembly. *Cell* 84:37-47.
- Watanabe A (1958) The interaction of electrical activity among neurons of lobster cardiac ganglion. *Jpn J Physiol* 8:305-318.
- Westenbroek RE, Hell JW, Warner C, Dubel SJ, Snutch TP, Catterall WA (1992) Biochemical properties and subcellular distribution of an N-type calcium channel alpha 1 subunit. *Neuron* 9:1099-1115.
- Westenbroek RE, Sakurai T, Elliott EM, Hell JW, Starr TV, Snutch TP, Catterall WA (1995) Immunochemical identification and subcellular distribution of the alpha 1A subunits of brain calcium channels. *J Neurosci* 15:6403-6418.
- Wittig I, Schagger H (2008) Features and applications of blue-native and clear-native electrophoresis. *Proteomics* 8:3974-3990.
- Wolburg H, Rohlmann A (1995) Structure--function relationships in gap junctions. *Int Rev Cytol* 157:315-373.
- Wong RW, Setou M, Teng J, Takei Y, Hirokawa N (2002) Overexpression of motor protein KIF17 enhances spatial and working memory in transgenic mice. *Proc Natl Acad Sci U S A* 99:14500-14505.
- Yokokawa R, Tarhan MC, Kon T, Fujita H (2008) Simultaneous and bidirectional transport of kinesin-coated microspheres and dynein-coated microspheres on polarity-oriented microtubules. *Biotechnol Bioeng* 101:1-8.
- Yokokawa RT, T.; Kon, M.; Nishiura, R.; Ohkura, M.; Edamatsu, K.; Sutoh; Fujita, H. (2004) Hybrid Nano Transport System by Biomolecular Linear Motors. *Journal of Microelectromechanical Systems* 13:612-619.
- Zabala JC, Cowan NJ (1992) Tubulin dimer formation via the release of alpha- and beta-tubulin monomers from multimolecular complexes. *Cell Motil Cytoskeleton* 23:222-230.

- Zappacosta F, Huddleston MJ, Karcher RL, Gelfand VI, Carr SA, Annan RS (2002) Improved sensitivity for phosphopeptide mapping using capillary column HPLC and microionspray mass spectrometry: comparative phosphorylation site mapping from gel-derived proteins. *Anal Chem* 74:3221-3231.
- Zhai B, Villen J, Beausoleil SA, Mintseris J, Gygi SP (2008) Phosphoproteome analysis of *Drosophila melanogaster* embryos. *J Proteome Res* 7:1675-1682.
- Zhao C, Takita J, Tanaka Y, Setou M, Nakagawa T, Takeda S, Yang HW, Terada S, Nakata T, Takei Y, Saito M, Tsuji S, Hayashi Y, Hirokawa N (2001) Charcot-Marie-Tooth disease type 2A caused by mutation in a microtubule motor KIF1Bbeta. *Cell* 105:587-597.

ACKNOWLEDGEMENTS

I thank my supervisor Prof. Dr. Erich Buchner for motivating, guiding and giving me an opportunity to work with him and also providing the right atmosphere for doing productive research. I thank my second supervisor and collaborator Prof. Dr. Georg Krohne and members of his lab for the excellent collaboration on the TBCE-Like project. I sincerely acknowledge and thank Prof. Dr. Gert Lubec, and his lab members, especially Seok Heo for their collaboration and co-operation on the Synapsin phosphorylation project. I thank Dr. Susanne Kneitz, Margarethe Göbel (Technical Assistant) and Nidhi Nuwal for their collaboration and co-operation on the Microarray project.

I thank Dr. Burkhard Poeck and Prof. Dr. André Fiala for helping me in troubleshooting with my experiments. I thank Prof. Dr. Martin Heisenberg, Dr. Henrike Scholz, Dr. Birgit Michels and Timo Saumweber for their insightful discussions and all the help from time to time.

I also thank the F2 student Monazza Ahmad; Diploma students, Sonja Racic, Itsaso Montalban and Andrea Schneider and Technical assistants Dieter Dudaczek (for wonderful cryosections), Barbara Muehlbauer and Gertrud Gramlich (for P-element mutagenesis) for their excellent work and enthusiasm. I also thank Margarete Mohr and Irina Stahl for their help with most of the administrative work. I also thank Konrad Öchsner and Andreas Eckart for helping with the hardware and software related issues. I thank Alexander Kapustjanskij, Mandy Jauch and Alice Schubert for their help with ordering chemicals and reagents. I am grateful to all my colleagues in the Department of Genetics and Neurobiology for their constant help, assistance and also for providing a cheerful working environment.

I wish to thank my family for providing me with an opportunity to pursue my goals and for constant inspiration and support.

Wuerzburg

.....
Tulip Nuwal

PUBLICATIONS

1. Nuwal T, Heo S, Lubec G, Buchner E: Mass Spectrometric Analysis of Synapsins in *Drosophila melanogaster* and Identification of Novel Phosphorylation Sites (2010, submitted)
2. Nuwal T, Racic S, Funk N, Buchner E: Quantitative and qualitative modulation of synapsins by SAP47 in *Drosophila* (Abstract and poster presentation, 32nd Goettingen neurobiology conference, Goettingen, Germany, T7-8C).
3. Nuwal T, Buchner E: Analysis of Synapsin, SAP47 and TBCE-like function in *Drosophila melanogaster* (Abstract and poster presentation, 12th European Drosophila Neurobiology Conference. September 6-10, 2008. Wuerzburg, Germany, Journal of Neurogenetics 2009 ,23 Suppl 1, pp V.35).
4. Buchner E, Asan E, Bucher D, Diegelmann S, Funk N, Nieratschker V, Nuwal T, Wagh DA, Sigrist S, Rasse T: Synapsin, SAP47, Bruchpilot: Functional analysis of presynaptic proteins in *Drosophila* (Abstract and poster presentation, 31st Goettingen neurobiology conference, Goettingen, Germany, T6-9C).

ERKLÄRUNG

Erklärung gemäß § 4 Absatz 3 der Promotionsordnung der Fakultät für Biologie der Bayerischen Julius-Maximilians-Universität zu Würzburg vom 15. März 1999.

Hiermit erkläre ich, die vorgelegte Dissertation selbständig angefertigt zu haben und keine anderen als die von mir angegebenen Quellen und Hilfsmittel benutzt zu haben. Alle aus der Literatur entnommenen Stellen sind als solche kenntlich gemacht. Des Weiteren erkläre ich, dass die vorliegende Arbeit weder in gleicher noch in ähnlicher Form bereits in einem anderen Prüfungsverfahren vorgelegen hat. Zuvor habe ich keine akademischen Grade erworben oder zu erwerben versucht.

Wuerzburg, den

.....

Tulip Nuwal